Post-Translational Regulation of the Tumour Suppressor IRF-1

Alexander Garvin BSc.

Supervisors: Dr Nicole Clarke
& Prof. David Heery

Thesis submitted to the University of Nottingham
for the degree of Doctor of Philosophy

June 2010

Abstract

IRF-1 (Interferon Regulatory Factor 1) is a transcription factor first identified as a regulator of Interferon expression. Two decades after its discovery, IRF-1 has been shown to be involved in numerous other pathways including apoptosis, cell cycle regulation, DNA damage/repair, immune cell development and inflammation. Transcriptional regulation of IRF-1 by a number of external agents has been extensively studied, however almost nothing is known about the post-translational regulation of IRF-1 activity. In this study IRF-1 is shown to be phosphorylated at Thr^{180} by GSK3β (Glycogen Synthase Kinase 3β). Phosphorylated Thr^{180} promotes interaction with the ubiquitin E3 ligase $SCF^{Fbxw7\alpha,}$ (Skp1-Cul1-Fbxw7α) which increases turnover of IRF-1 protein. Phosphorylation dependent ubiquitination of IRF-1 was confirmed, as substitution of Thr^{180} to alanine reduced IRF-1 ubiquitination and increased stability. Enhanced phosphorylation of IRF-1 (by increasing GSK3β expression) promotes increased ubiquitination/degradation. Transactivation of the TRAIL (TNFα Related Apoptosis Inducing Ligand) promoter by IRF-1 was found to be dependent on GSK3β phosphorylation of Thr^{180} by use of reporter assays and inducible expression of IRF-1 in breast cancer cell lines. Importantly IRF-1 activity on the TRAIL promoter is dependent on proper turnover by the UPS (Ubiquitin Proteasome System), as chemical inhibition of the proteasome, or reduction in IRF-1 ubiquitination reduced activity in reporter assays. This suggests that phosphorylation of IRF-1 by GSK3β acts as a destruction signal through association with $SCF^{Fbxw7\alpha}$. This signal dependent turnover of IRF-1 is required for proper transcriptional activation of the TRAIL promoter.

Acknowledgments

First and foremost I would like to thank my supervisor Nicole Clarke. I'm very appreciative for her excellent guidance while also being given enough freedom to organise my own research. My gratitude to the School of Pharmacy for funding my studentship. Many thanks to Bas Winkler and David Heery for helpful guidance throughout my PhD. In addition I am grateful to several members of David's lab who put up with my incessant questions in the first few months of my PhD. Particularly, Hilary Collins who was unfortunate enough to sit opposite me in the old lab, and to whom most of my questions were directed. Surely enough Hilary chose the bench furthest away from mine once we moved into the new lab. I still "borrow" reagents from her shelf. I'm ever indebted to Karin Kindle for her advice and friendship throughout my PhD. Cristina and Ta were also always on hand with helpful advice for which I'm very thankful. Thank you also to Fran for convincing me to do my first half marathon and to Chun for letting me bully him into running it with me. Many thanks also to everyone in C50 (Sian, Joel, Rachel etc etc) write up for stimulating (non scientific) conversation. Also thanks to everyone in the Gene Regulation Group and RNA Biology group. I am also hugely grateful to our technician Debs for answering all of my ordering enquiries and putting up with my unreasonably urgent requests. Most importantly thank you to Debs and Jane Doughty for listening to my early morning whinges throughout my time in Nottingham. My thanks also to Jerome for the GST pulldown and Alessandro for the QPCR which are included in this thesis. My family also deserve huge thanks for their support throughout my PhD particularly for driving backwards and forwards over the years to help me move. Thank you mum for finally learning what IRF-1 stands for (after three years).

Contents

CHAPTER 1. INTRODUCTION

CHAPTER 4. PHOSPHORYLATION OF THREONINE 180 / SERINE 184 REGULATES IRF-1 TRANSCRIPTIONAL ACTIVITY

CHAPTER 5. IRF-1 TURNOVER IS REGULATED BY PHOSPHORYLATION

CHAPTER 6. PHOSPHORYLATION OF IRF-1 PROMOTES INTERACTION WITH THE UBIQUITIN LIGASE SCF^{FBXW7}

CHAPTER 7. CONCLUSIONS

CHAPTER 8. SUPPLEMENTARY DATA

FIGURES

Tables

Abbreviations

Ab	Antibody
AML	Acute Myeloid Leukaemia
APL	Acute Promyelocytic Leukaemia
βGAL	β Galactosidase
BSA	Bovine Serum Albumin
C-MYC	Cellular Myelocytomatosis Oncogene
CDK	Cyclin Dependent Kinase
ChIP	Chromatin Immunoprecipitation
CHX	Cycloheximide
CK1/2	Casein Kinase 1/2
Co-IP	Co-immunoprecipitate
DBD	DNA Binding Domain
DMEM	Dulbecco's Modified Essential Medium
DOX	Doxycycline
DUB	De-Ubiquitinases
ECL	Enhanced Chemiluminescence
eYFP	Enhanced Yellow Fluorescent Protein
FBS	Foetal Bovine Serum
FBXL	F-box and LRR protein
FBXO	F-box and other domain protein
FBXW	F-box and WD40 protein
GAS	IFNγ activated sequence
GSK3α/β	Glycogen Synthase Kinase 3 α/β
GSH	Glutathione
GST	Glutathione S transferase
HEK293	Human Embryonic Kidney 293
HSP	Heat Shock Protein
IAD	Interferon Association Domain
IP	Immunoprecipitate
IRF	Interferon Regulatory Factor
IRF-E	IRF Element
IFN	Interferon
IL	Interleukin
iNOS	Inducible Nitric Oxide Synthase
ISG	Interferon Stimulated Gene
ISRE	Interferon Stimulated Response Element
KAT	Lysine Acetyltransferases
KDAC	Lysine De-Acetylases
LB	Luria-Bertani Broth
LPS	Lipopolysaccharide
MDS	Myelodysplastic Syndrome
MEF	Murine Embryonic Fibroblast
MHC	Major Histocompatability Complex

Abbreviations (cont)

MYND	MTG8-Nervy and DEAF-1 domain
NFkB	Nuclear Factor κB family members
NLS	Nuclear Localisation Signal
PBS	Phosphate Buffered Saline
PEI	Polyethylene imine
PIAS	Protein Inhibitor of Activated STAT
PKA/B/C	Protein Kinase A/B/C
PMSF	Phenylmethylsulphonyl Fluoride
PTM	Post-Translational Modification
RA	Retinoic Acid
RIPA	Radioimmunoprecipitation Buffer
RNA Pol II	RNA Polymerase 2
SCF	Skp1-Cul-1-Fbox complex
SDS PAGE	SDS-Polyacrylamide Gel Electrophoresis
STAT	Signal Transducer and Activator of Transcription
SUMO	Small Ubiquitin Like Modifier
TAD	Transcriptional Activation Domain
TBST	Tris buffered Saline – TWEEN
TET	Tetracycline
TetR	Tetracycline Repressor
TF	Transcription Factor
TLR	Toll Like Receptor
TNFα	Tumour Necrosis Factor α
TRAIL	TNFα Related Apoptosis Inducing Ligand
Ubq	Ubiquitin
UPS	Ubiquitin-Proteasome System
WB	Western Blot
ZEO	Zeocin

Chapter 1. Introduction

1.1.1. Transcription

The cells ability to control the expression of its genes in an orderly fashion is a fundamental process. In order to activate expression of a particular gene transcription is employed. Transcription is the process by which DNA is converted to RNA, and is the first step in gene expression. Every gene in a cell genome contains the regulatory sequences required to control its expression. Often (although not always) these regulatory elements are found in the promoter region which is often found close to the transcriptional start site of the coding gene. Promoters contain binding elements for the basal transcription factors as well as for specific transcription factors. Transcription factors (TFs) are proteins that are able to recognise specific DNA sequences. A huge number of TFs are present in eukaryotic cells, which imparts specificity to gene expression, as different combination of TF binding sites are present on each gene promoter. Protein coding gene transcription is regulated by RNA Polymerase II (RNA Pol II), while RNA Pol I is involved in generating ribosomal RNA transcripts and RNA Pol III is involved in the transcription of transfer RNA molecules. RNA Pol II cannot initiate transcription alone, but numerous other factors including TFs, coactivators, kinases and chromatin remodelling complexes are also needed this conglomeration of proteins can be defined as a pre-initation complex (PIC). To initate transcription, the RNA Pol II complex must gain access to the template strand of DNA; this is aided by a helicase enzyme recruited by RNA Pol II which partially unwinds the DNA. RNA Pol II is phosphorylated and disengages from the other proteins in the PIC. The RNA Pol II enzyme then elongates through the the gene, generating an RNA copy. Upon reaching the 3' end of the template, the RNA Pol II disengages from the DNA, and the released RNA is polyadenylated.

Polyadenylation is required for the stability of the mRNA (messanger RNA) and for its export to the cytosol for translation into a protein. In addition to polyadenylation, the 5' end of the mRNA is chemically modified (capped) which is important for its ability to be translated. Introns are spliced out of the RNA by the splicesome complex to yield a mature mRNA. The mRNA is exported out of the nucleus to enable translation into a protein (Alberts *et al.* 2002).

1.1.2 Post translational modification (PTM)

At least two remarkable processes have enabled eukaryotes to expand the functions of their genes. First, each gene can encode multiple transcripts through the use of alternative splicing, secondly via chemical modifications of proteins leading to changes in their physical characteristics. These modifications are termed post-translational modifications. PTMs include addition of functional groups such as phosphate, addition of polypeptides (for example ubiquitin), chemical modifications of amino acids (isomerisation of proline) or structural changes involving disulphide bridges. Of the twenty amino acids that make up proteins, 15 can be modified by PTMs (Hunter 2007). A selection of PTMs is given in table 1.1.

Modification	Residue modified	Addition enzymes	Chemical Group
Acetylation	Lysine	Lysine acetyltransferases (addition) Lysine de-acetylases (removal)	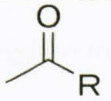
Methylation	Lysine Arginine	Methyltransferases. Arginine may be mono, di or tri methylated. Demethylases (removal)	
Phosphorylation	Serine Threonine Tyrosine	Kinases (addition) Phosphatases (removal)	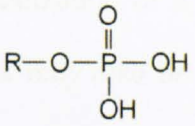
O-Glycosylation	Serine Threonine	Acetylgalactosaminyltransferase.	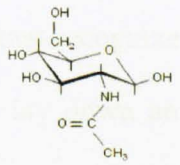
Sulfation	Tyrosine	Sulfotransferases	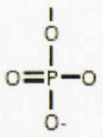
ADP-Ribosylation	Arginine, Glutamic acid, Aspartic acid	ADP Ribosyltransferases (addition) ADP Ribosyl-Arginine hydrolases (removal)	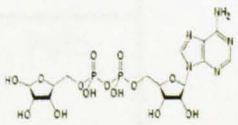
Isomerisation	Proline	Proline isomerases	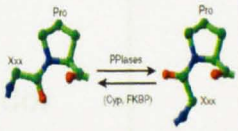
Ubiquitination, **SUMO-ylation,** **NEDDylation** **ISG-15ylation**	Lysine	E3 enzymes (specific for Ubiquitin, SUMO-1/2/3, NEDD, ISG-15 etc). Removal enzymes include de-ubiquitinases and de-SUMOylases.	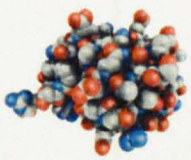

Table 1.1. PTMs. A selection of PTMs are listed along with the residues modified, the enzymes involved, and the structure of the functional groups. The protein in the ubiquitination column is human ubiquitin, SUMO, NEDD8 and ISG-15 are not illustrated.

1.1.3. Crosstalk between PTMs

An emerging theme of PTM study is the concept of "crosstalk" in which one modification modulates another. This effect can be on the same, neighbouring or a distant residue. Crosstalk can be agonistic or antagonistic and can have drastic effects on the activity of the protein. Crosstalk between modifications can be brought about by one modification altering the subcellular localization of a protein exposing the protein to new PTM enzymes. PTM crosstalk may also be due to changes in the structure of the protein exposing or preventing residues from being modified by a second PTM. In addition specialized domains that recognize residues that have been modified can "read" a specific PTM and lay down an additional modification on the substrate protein. Some of the better studied PTM binding modules are listed in table 1.2 (Seet *et al.* 2006).

PTM	Domain
Phospho-serine	14-3-3, MH2, WW, BRCT, Polo Box, FF
Phospho-threonine	FHA, WD40
Phospho-tyrosine	PTB, SH2
Methyl-lysine	Chromodomain, PHD, Tudor
Acetyl-lysine	Bromodomain
Ubiquityl-lysine	UIM, UBA
Sumoyl-lysine	SIM
Glycosyl-asparagine	FBA

Table 1.2. PTM binding modules. A selection of PTM binding modules is shown for each modified amino acid. Abbreviations **MH2** (MAD Homology 2), **BRCT** (BRCA domain), **FHA** (Forkhead Associated), **PTB** (Phospho-Tyrosine Binding), **SH2** (Src Homology), **PHD** (Plant Homeodomain), **UIM** (Ubiquitin Interacting Motif), **UBA** (Ubiquitin Associated), **SIM** (SUMO Interaction Motif), **FBA** (Fbox Associated).

1.1.4. Negative crosstalk

Some amino acids can be modified by more than one PTM. Different PTMs cannot co-occupy the same amino acid, and as such there is direct competition for different PTMs on single amino acids. Ser (serine) and Thr (threonine) residues can be both phosphorylated and O-glycosylated, and as such these two modifications compete. Thr^{58} of c-Myc can be both phosphorylated and O-glycosylated, although it is believed that should Thr^{58} be unavailable for O-Glycosylation a neighbouring residue will be O-glycosylated instead (Chou *et al.* 1995). Sulfation and phosphorylation compete for the hydroxyl group of Tyr, while nitration of the aromatic ring of Tyr prevents phosphorylation (Reinehr *et al.* 2004). The most striking example of direct competition is for lysine, in which acetylation, methylation, hydroxylation, ubiquitination, SUMOylation and NEDDylation can occur (Yang and Seto 2008). Consequently there are numerous examples in which one modification excludes another. Acetylation prevents ubiquitination in p53, SUMOylation in Sp3 and methylation in histone 3 (Hunter 2007).

Neighbouring amino acids can influence the addition of PTMs. The O-GlcNAc modification on Ser^{149} of p53 reduces phosphorylation of Thr^{155}, which then prevents ubiquitination and proteasome dependent degradation (Yang *et al.* 2006). Methylation of arginine within a PKB (Protein Kinase B) consensus site of FOXO1 (Forkhead Box O1) prevents phosphorylation, which consequently prevents cytoplasmic re-localisation and degradation (Yamagata *et al.* 2008). Lys^{9} of histone 3 can be acetylated, which enables interaction with the HP1

(Heterochromatin Protein 1) protein. Should the adjacent Ser^{10} be phosphorylated however, this interaction is blocked (Berger 2002).

1.1.5. Positive crosstalk

Addition of a single PTM may promote the addition of other distinct PTMs. Phosphorylation of one Ser or Thr residue can promote the phosphorylation of another Ser/Thr by GSK3 (Glycogen Synthase Kinase 3) enzymes, as this group of kinases often requires phosphorylated "primed" residues to interact with their substrates (see section 1.6.2). Some ubiquitin ligases contain domains which recognise SUMO (Small Ubiquitin like Modifier) chains. Consequently these ligases promote ubiquitination and degradation of SUMOylated proteins (Perry *et al.* 2008). Phosphorylation can promote SUMOylation, this so called phospho-sumoyl switch is found in a number of proteins, including HSF1 (Heat Shock Factor 1), and PPARγ (Peroxisome Proliferator Activated Receptor γ). The phosphorylated residue is found within the consensus site (Ψ-K-x-E-xx-S) needed for substrate recognition by the SUMOylation machinery. It has been suggested that since many SUMOylated substrates contain a negatively charged amino acids at a +5 position relative to the recognition site, the phosphorylated residues mimic this effect (Mohideen *et al.* 2009).

1.1.6. Ubiquitination

Ubiquitin (Ubq) is an extremely well conserved 76 amino acid protein that, as the name suggests is ubiquitously expressed. Ubiquitin serves as a protein tag for destruction by the 26S proteasome. Ubiquitination has since been shown to be involved in numerous other processes that are quite distinct from protein turnover, including the DNA damage response, mediation of protein-protein interactions and altering subcellular localisation (Schwartz and Ciechanover 2009). Addition of ubiquitin proteins to their substrates requires an enzymatic cascade of three enzymes. The E1 enzyme (ubiquitin activating enzyme) activates the C terminal glycine residue of ubiquitin by conversion into a high energy thioester. There are two known E1 enzymes in the human genome, with the second enzyme only recently being characterised (Pelzer *et al.* 2007). E2 enzymes are involved in ubiquitin transfer, and E3 enzymes recognise substrates for ubiquitination by E2 enzymes. There are approximately thirty seven E2 enzymes and up to six hundred E3 enzymes encoded in the human genome. There are two main classes of E2 enzymes, HECT (Homologous to E6-AP C terminus) and RING (Really Interesting New Gene) fingers (Deshaies and Joazeiro 2009). Ubiquitin is transferred to the ε-NH2 group of an internal lysine residue in the substrate protein. E3 enzymes can recognise their substrates through specific amino acid motifs called degrons. A degron can be defined as the minimal element sufficient for recognition and degradation by the proteasome pathway. Some degrons can be modified by phosphorylation, which greatly enhances the interaction with the E3 protein. These degrons are called phospho-degrons (see section 1.1.8).

Ubiquitin itself can become a substrate for ubiquitination on any of the seven lysines in its structure (see figure 1.1). This leads to the formation of ubiquitin polymers. Various combinations of mono, multi-mono and poly-ubiquitination can occur on a single substrate. To be recognised as a substrate for degradation by the proteasome, the substrate must be poly-ubiquitinated with at least four ubiquitin proteins. Some forms of ubiquitination do not signal destruction for their substrates, for example K^{63} linked ubiquitination (Komander 2009). Further details of the different ubiquitin chain types are given in figure 1.1. Approximately 95 de-ubiquitinating enzymes (DUBs) are present within the human genome. These DUBs are involved in removing and editing ubiquitin chains from substrate molecules (Sowa *et al.* 2009). DUB enzymes recognise ubiquitinated substrates via specialised protein-protein interaction motifs that recognise ubiquitin. There are at least twenty ubiquitin interacting motifs in the proteome. These motifs are also found in other proteins and it is now apparent that ubiquitin can serve as a mediator of protein-protein interactions (Hurley *et al.* 2006).

A.

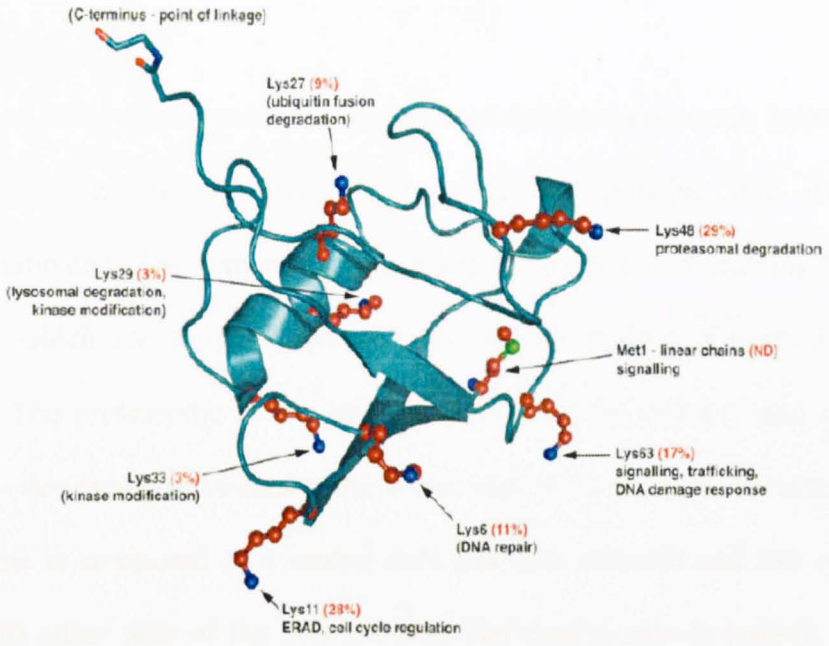

B.

Chain type	Comments
Met 1	Linear ubiquitin chains can be added to substrates of the NFkB signalling pathway. Linear ubiquitin chains are not thought to promote degradation of substrates.
Lys 6	Very little is known about Lys6 linked ubiquitin chains, possibly involved in DNA damage repair signalling.
Lys 11	Promotes proteasomal degradation of substrates. Involved in enodoplsamic reticulum associated degradation (ERAD). APC (Anaphase Promoting Complex) attaches Lys 11 Ubq chains to substrates suggesting a role in cell cycle regulation.
Lys 27	Function not yet established, possibly involved in proteasome mediated degradation.
Lys 29	Lysosomal degradation of substrates. May be involved in N end rule degradation of substrates.
Lys 33	Function not yet established, possibly involved in kinase inactivation.
Lys 48	Predominantly involved in proteasome mediated degradation. The most studied chain type.
Lys 63	Non degradative, involved in endocytosis, DNA damage signalling, chromatin regulation (H2A) and TNFα signalling.

Figure 1.1 Schematic of ubiquitin protein. A) Schematic of the seven lysine residues to which ubiquitin can conjugate to itself in addition to the position of Met 1 (methionine 1) which is used for generating linear chains of ubiquitin. The relative proportion of each chain type in *S.cerevisiae* is highlighted in red. **B)** Description of the known roles for each ubiquitin chain type. From Komander 2009.

1.1.7. The proteasome

The 26S proteasome is a large, evolutionary conserved, barrel shaped multi-subunit protein complex which recognises proteins that have been polyubiquitinated. The proteasome functions to break down proteins into short peptides, which are further processed into amino acids and re-used for new proteins. The proteasome is required for regulating the quantity and quality of proteins - destroying misfolded protein that may harm the cell. Structurally, the proteasome is composed of a central core (the 20S subunit) and two regulatory caps (19S) either side of the 20S subunit. The central core is hollow, allowing substrates to enter, with the 19S "lids" opening to allow entry (see figure 1.2). The substrate is partially unfolded and translocated through the 20S subunit. Three different proteolytic activities, a trypsin like, chymotrypsin like and peptidyl-glutamyl like proteases are responsible for degrading substrates (Murata *et al.* 2009). Several inhibitors of the proteasome have been developed, with MG132 and lactacystin being commonly used as tools to understand proteasome dependent regulation of proteins. Proteasome inhibitors are also being investigated for their therapeutic potential as anti cancer agents, with Bortezomib being licensed for use against multiple myeloma and mantle cell lymphoma (Schwartz and Ciechanover 2009). The proteasome can also be found within the nucleus, as several components contain nuclear localisation signals (von Mikecz 2006). Components of the 19S subunit have been shown to be recruited to transcriptionally active genes by TFs suggesting the proteasome is intimately involved in transcription (see section 1.1.10) (Reid *et al.* 2003).

It is not yet fully understood how the proteasome is able to recognise poly-ubiquitinated proteins. At least one component of the proteasome (S5a) can make direct contact with poly-Ubq chains via its UIM domain. Additional proteins (Rad23 and Dsk2) also interact with poly-Ubq chains through their UBA domains, however neither of these proteins are direct components of the proteasome. It is likely that a variety of accessory and chaperone proteins help to deliver polyubiquitinated proteins to the proteasome. It has also been suggested that ubiquitin E2 and E3 enzymes may associate with the proteasome, allowing efficient transfer of polyubiquitinated substrates (Hartmann-Petersen *et al.* 2003).

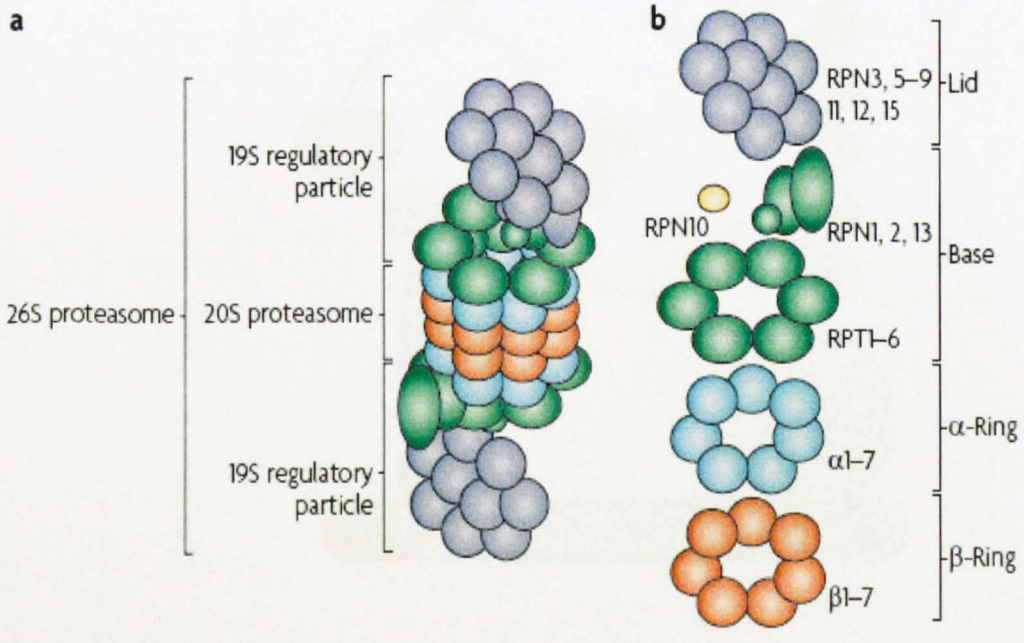

Figure 1.2. Schematic diagram of the human proteasome. The individual subunits that make up the proteasome are highlighted. From Murata *et al.* 2009.

1.1.8. The SCF E3 ubiquitin ligases

The SCF (Skp1-Cul1-Fbox) complex is a multimeric ubiquitin E3 ligase complex made up from four proteins. A scaffold protein called Cullin1 interacts with RBX1 (Ring Box-1) through its C terminus, while it interacts with SKP1 (S-phase kinase associated protein -1) through its N terminus. RBX1 is required for interaction with the E2 enzyme, and was discovered after the initial naming of the SCF complex. SKP1 in turn recruits the specificity module, known as Fbox proteins to the SCF complex (Jin *et al.* 2004).

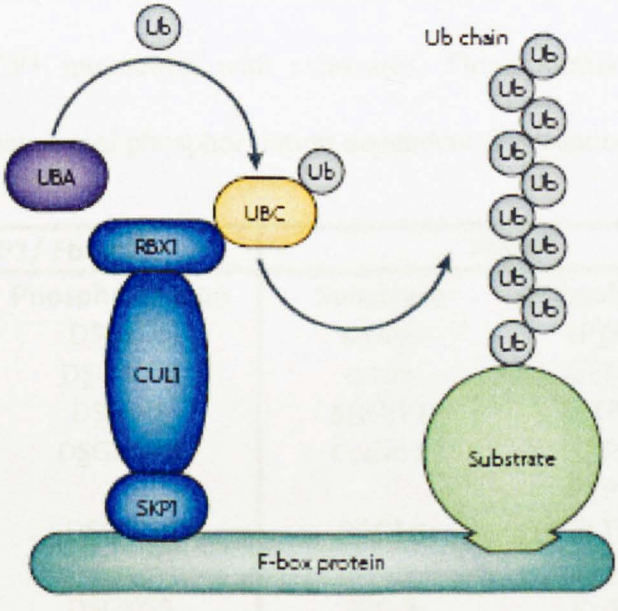

Figure 1.3. Schematic of the SCF complex. The schematic shows the Rbx1 protein interacting with the E2 enzyme (in the case of SCF complexes UbcH5), and the Cullin 1 scaffold, which interacts with the specificity module SKP1-Fbox. The Fbox protein makes protein-protein interactions with the substrate, bringing it into contact with the E2 enzyme and allowing transfer of ubiquitin. From Welcker and Clurman 2007.

The Fbox proteins interact with SKP1 through their Fbox domains. The Fbox domain is a 40 amino acid sequence first identified in Cyclin F (Bai *et al.* 1996). There are currently 68 known Fbox proteins in mammals, with other Fbox proteins being found in yeast and plants (Jin *et al.* 2004). The Fbox proteins contain other domains, which make contact with the SCF substrates. The presence of these domains is used to subdivide the Fbox family into three classes, Fbxw contain **WD40** motifs, Fbxl contain **LRR** motifs (Leucine Rich Repeats) while the third group Fbxo contain various **other** motifs and domains (Jin *et al.* 2004). Most Fbox proteins recognise phosphorylated substrates, although some recognise carbohydrate side chains (Glenn *et al.* 2008). Consensus motifs have been mapped for Fbxw7 and βTRCP1 interaction with substrates. These motifs are called phospho-degrons, as they signal phosphorylation dependent degradation.

βTRCP1/ Fbxw1		Fbxw7	
Substrate	**Phospho degron**	**Substrate**	**Phospho degron**
IKBβ	D**S**GLD**S**	**c-Myc**	LP**T**PPL**S**PS
p105	D**S**GVET**S**	**c-Jun**	GE**T**PPL**S**PI
Catenin	D**S**GIH**S**	**SREBP1**	TL**T**PPP**S**DA
PDCD4	D**S**GRGD**S**	**Cyclin E**	LL**T**PPQ**S**GK
			IP**T**PDK**E**DD
Claspin	D**S**GQG**S**	**PGC1α**	PL**T**PE**S**PN
			GL**T**PPT**T**P
ATF4	D**S**GKG**S**	**SRC-3**	VH**S**PMA**S**
SNAIL	D**S**GKG**S**	**SV40 T antigen**	FL**T**PSP**E**SP
Per1	T**S**GCS**S**		
Consensus	**D$\underline{S}$G$_{XX(X)}$$\underline{S}$**		**LL$\underline{T}$P$_{XX}$$\underline{D/T/S}$**

Table 1.3 Phospho-degrons. The phospho-degrons of βTRCP1 (β-Transducin repeats containing protein 1 /Fbxw1) and Fbxw7 (Fbox and WD40 containing 7). Data is adapted from Frescas & Pagano 2007 and Hunter 2007. Abbreviations **IKBβ** (Inhibitor of NFκB-β), **PDCD4** (Programmed Cell Death 4), **ATF4** (Activating Transcription Factor 4), **Per** (Period), **SREBP** (Sterol Regulatory Element Binding Protein), **PGC1α** (PPARγ Coactivator α), **SRC-3** (Steroid Receptor Coactivator 3).

1.1.9. Fbxw7

Fbxw7 (FBox WD40 containing 7) is one of the most studied Fbox proteins (after Skp2 and βTRCP1) and is proving to be a key node in several oncogenic signalling pathways. Fbxw7 was first identified in a yeast screen for proteins involved in cell cycle control. The yeast homolog of Fbxw7 was named Cdc4 (Cell Division 4) (Hartwell 1973).Various orthologues of Fbxw7 protein are found throughout the animal kingdom, in nematodes it is known as SEL-10 and in fruit flies as archipelago (Welcker and Clurman 2008). The Fbxw7 gene encodes three protein coding transcripts which are produced from alternative splicing. Each isoform has its own first exon, while the other ten exons are shared between all three. The α isoform is the largest and most highly expressed of the three isoforms. The β and γ isoforms exhibit some tissue specific expression patterns (Spruck *et al.* 2002). Each of the three isoforms localises to a different subcellular location, with the α isoform being nuclear, β cytoplasmic and γ nucleolar, see figure 1.4A (Welcker and Clurman 2007).

Fbxw7 contains three major domains, an N terminal Fbox, eight C terminal WD40 repeats which are required for the interaction with phosphorylated substrates and a D (dimerisation) domain (Orlicky *et al.* 2003). The D domain is required for Fbxw7 dimers to form (see figure 1.4B). Although not yet well understood, it is thought that dimerised Fbxw7 proteins are able to make contacts with more than one degron in a substrate. This allows Fbxw7 to promote degradation of its target substrates even if they do not carry the required phosphorylation mark (Tang *et al.* 2007).

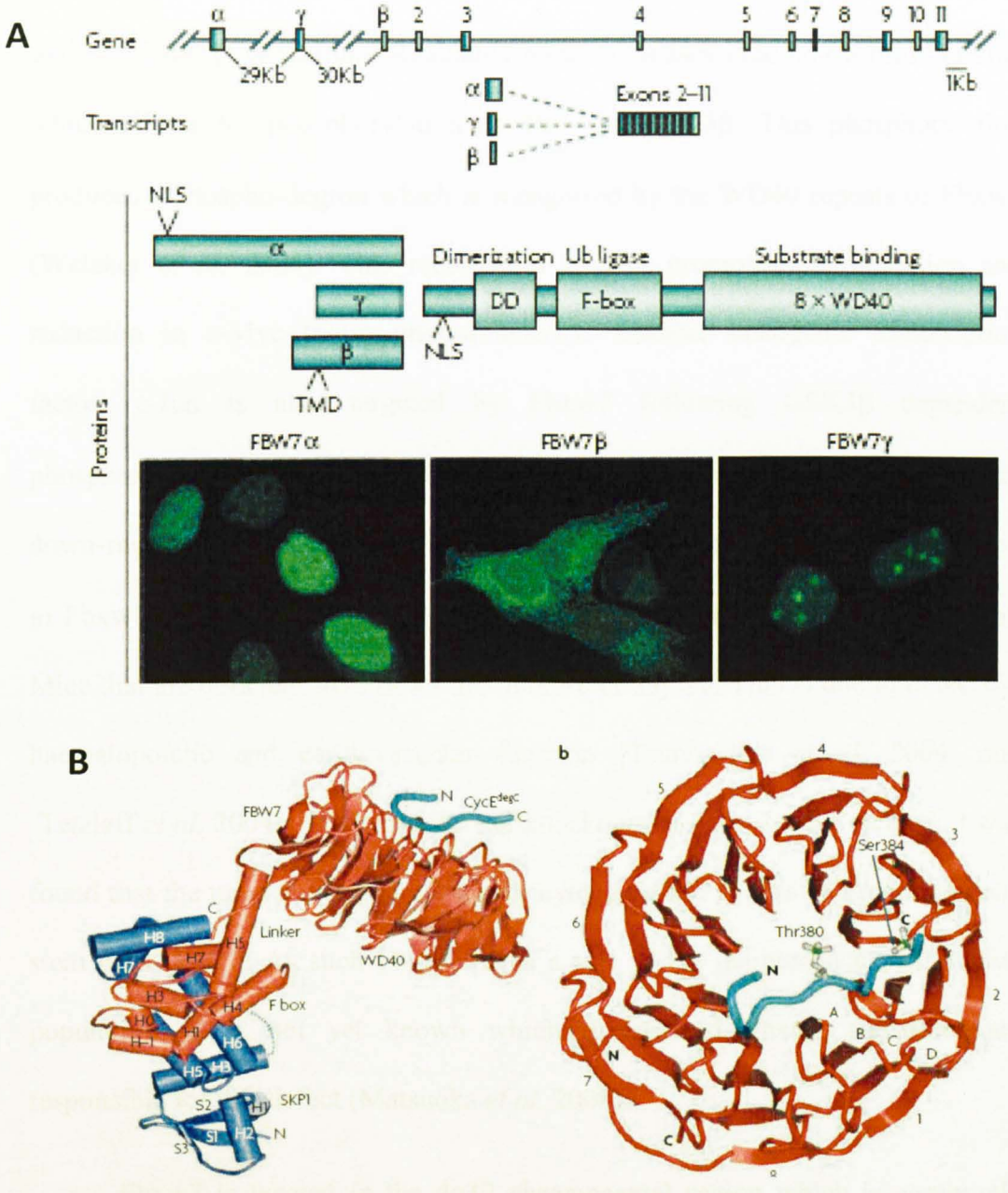

Figure 1.4 Structure of Fbxw7 A) Genomic organisation of the human Fbxw7 gene, showing the three alternative transcripts caused by differential use of the first exon. Cartoon of the domain organisation of Fbxw7 and localisation of the threeisoforms of Fbxw7 (Welcker & Clurman 2007). **B)** Cartoon structure of Fbxw7, the blue protein is SKP1, while the red protein is Fbxw7α. The eight bladed beta propeller WD40 domain of Fbxw7 is shown bound to the phospho-degron of Cyclin E (cyan). From Welcker and Clurman 2007.

One of the best studied Fbxw7 substrates is c-Myc. Phosphorylation of c-Myc at Ser^{62} by ERK (Extracellular Regulated Kinase) kinases produces a priming site, which allows for phosphorylation at Thr^{58} by GSK3β. This phosphorylation produces a phospho-degron which is recognised by the WD40 repeats of Fbxw7 (Welcker *et al.* 2004). This recognition in turn promotes ubiquitination and reduction in c-Myc transcriptional activity. Another oncogenic transcription factor; c-Jun is also targeted by Fbxw7 following GSK3β dependent phosphorylation (Wei *et al.* 2005). As such two of the most potent oncogenes are down-regulated by the activity of GSK3β and Fbxw7 working in unison. Studies in $Fbxw7^{-/-}$ mice have shed further light on the roles of Fbxw7 in development. Mice that are deficient for Fbxw7 die *in utero* at day 11. This is due to defects in haematopoietic and cardiovascular function (Tsunematsu *et al.* 2004 and Tetzlaff *et al.* 2004). When conditional knockouts of Fbxw7 were created, it was found that the mice developed severe pancytopenia due to loss of haematopoietic stem cells (HSC). As such Fbxw7 plays a role in the maintenance of the HSC population. It is not yet known which deregulated Fbxw7 substrates are responsible for this defect (Matsuoka *et al.* 2008).

Fbxw7 is located in the 4q32 chromosomal region which is commonly deleted in cancers. It has been reported that in some cancers 30% of samples harbour mutations in the Fbxw7 gene (Maser *et al.* 2007). The Fbxw7 gene is prone to truncating mutations, but more commonly point mutations within the WD40 motifs are found. Three arginine residues that are essential for substrate recognition are highly prone to mutation (Calhoun *et al.* 2003). In addition to mutations in the Fbxw7 gene, mutations in substrates can prevent Fbxw7 binding.

For example the T58A mutation of c-Myc found in Burkitts Lymphoma samples prevents Fbxw7 dependent ubiquitination (Bahram *et al.* 2000).

1.1.10 UPS and transcription.

Although long thought to be entirely separate biological processes, growing evidence suggests that the ubiquitin-proteasome system (UPS) is intimately involved in transcription. Quantitative, temporal and spatial regulation of TFs is essential for fine tuning of transcriptional responses and all of these processes can be controlled by the UPS. The first ubiquitinated protein described was the histone H2A. Other histones including H2B, H1 and H3 have also been shown to be ubiquitinated (Weake and Workman 2008). It is not fully understood how ubiquitination of histones affects transcription, although it has been suggested to act in both transcriptional activation and repression. It is possibly, that addition of bulky ubiquitin groups has an allosteric effect on chromatin structure, or that ubiquitin acts as a protein-protein interface with HDAC6, which posses an ubiquitin interacting domain (Hook *et al.* 2002). Mono-ubiquitination of histone 2B (ub-H2B) has been extensively studied in the context of transcription. Addition of ubiquitin to H2B occurs via the E3 ligases RNF20/40 in mammals. Ub-H2B is found to be enriched on chromatin of actively transcribed genes in both the 5' region and throughout the coding sequence, indeed there is evidence that ub-H2B plays a role in transcriptional elongation. Two histone marks associated with activate transcription (H3K4me and H3K79me) are also increased by ub-H2B suggesting complex PTM crosstalk is occurring. Conversely; in addition to acting as a mark for transcriptional activation, ub-H2B may also play a role in transcriptional silencing (Shema *et al.* 2008).

The UPS system also serves to keep TFs away from the nucleus. In the case of NFκB proteins, interaction with IκB (Inhibitor of NFκB) prevents translocation to the nucleus. Destruction of IκB liberates NFκB and allows its entry to the nucleus and the DNA within (Palombella *et al.* 1994). The UPS can also affect the abundance of a TF by targeting it for destruction. In the case of several TFs including p53, HIF1α (Hypoxia Inducible Protein 1α) and β-Catenin, constitutive turnover occurs in the absence of signal. The Wnt signalling TF β-Catenin is targeted for destruction through GSK3β dependent phosphorylation. Wnt signals lead to the inhibition of GSK3β which prevents β-Catenin destruction and allows it to bring about transcription of Wnt target genes (Yost *et al.* 1996). This enables the cell to keep a low amount of TF available, but if needed can rapidly increase the amount of TF and allow a transcriptional response. The UPS can re-programme transcriptional responses by regulating the availability of transcriptional coactivators. The ubiquitin ligase RLIM (RING finger LIM domain) recognises DNA bound TF LIM and its coactivator CLIM (Coactivator LIM). RLIM destroys CLIM, which allows LIM to interact with a different set of coactivators (Ostendorff *et al.* 2002).

Intriguingly transcriptional activation and destruction appear to be entwined. There is a significant overlap between TADs (the minimal region of a protein required for transcriptional activation) and degrons in unstable transcription factors (see figure 1.5), suggesting that the transcriptional activity of a TF is linked to its ability to be ubiquitinated and destroyed (Salghetti *et al.* 2000). It is possible that the UPS can mark active TFs for destruction during the process of transcriptional activation. In yeast the TF GCN4 (General Control

Nondepressible 4) is phosphorylated by Srb10, leading to UPS dependent destruction. The Srb10 kinase is a component of the Pol II holoenzyme suggesting that Pol II can eliminate the coactivators that recruited it, and prevent inappropriate transcriptional re-initiation. TFs regulated in this fashion have been dubbed Blackwidow (Tansey 2001) or Kamikaze factors (Thomas and Tyers 2000).

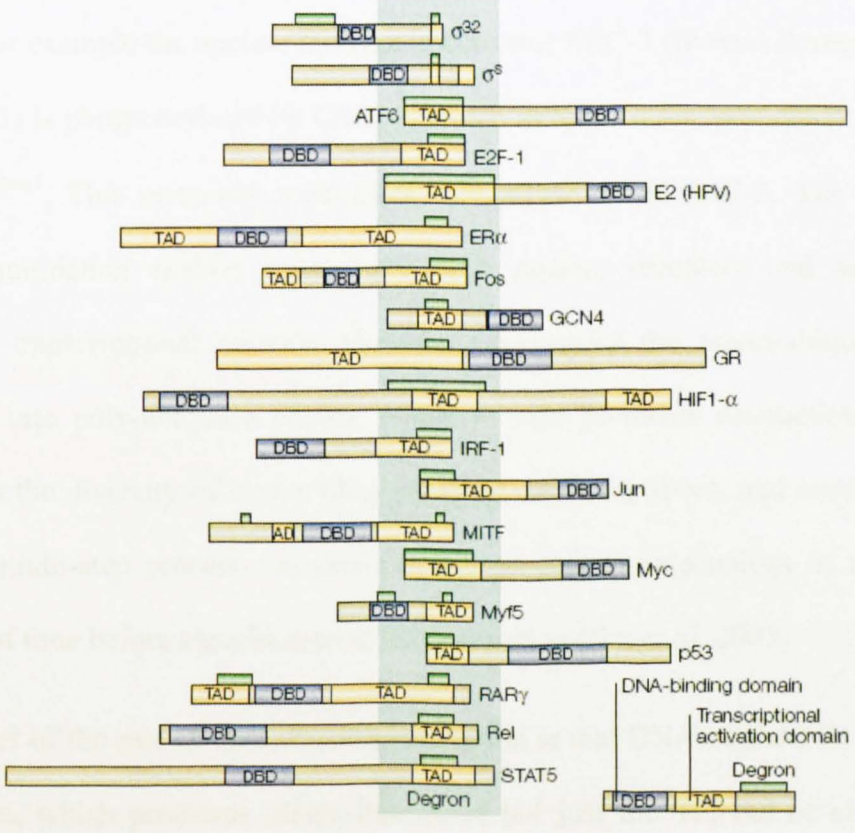

Figure 1.5. Overlap between the TADs and degrons of several unstable transcription factors. Here degrons are designated the regions which regulate ubiquitination, rather than the regions containing ubiquitinated lysines. The blue box highlights the overlap between the degrons and the TADs. From Muratani & Tansey 2003.

The role of the UPS in regulating TF activity may differ from protein to protein. Not all TFs respond in the same fashion to the UPS system. While some TFs are simply degraded by the UPS, which enables a dosage response, others require it

for activity. The UPS system is able to destroy some TFs that are bound to DNA. This could be a possible mechanism for PIC quality control. If a TF is able to bind a promoter, but does not recruit other proteins which shield it from the UPS, it is destroyed preventing aberrant transcription. This also allows for the one shot Blackwidow / Kamikaze response in which a TF can only initiate one round of transcription before being destroyed and new factors being needed for further rounds (Lipford and Deshaies 2003). TFs may also be activated by the UPS system, for example the nuclear receptor coactivator SRC-3 (Steroid Receptor Co activator 3) is phosphorylated by GSK3β, which in turn causes recruitment of the E3 SCF^{Fbxw7}. This promotes multi-mono ubiquitination of SRC-3. The multi-monoubiquitination enables interactions with nuclear receptors and as such increases transcriptional activity. However, eventually the mono-ubiquitin is extended into poly-ubiquitin chains, which in turn promotes destruction. This highlights the diversity of events ubiquitination can bring about, and reminds us that this multi-step process can promote protein-protein interactions in a short window of time before signalling proteins destruction (Wu *et al.* 2007).

One model of the role of the UPS in transcription is that DNA bound TFs recruit E3 ligases, which promotes ubiquitination of not just the TF, but of other co activators, Pol II and histones. This in turn recruits the proteasome, which destroys the proteins involved in assembly of the PIC (and thus prevents it spontaneously reforming), but also aids Pol II in elongation and promotes modification of the chromatin during transcription (Muratani and Tansey 2003).

1.2.1. The Interferon Regulatory Factor (IRF) family.

Currently the IRF family consists of nine members with the first members; IRF-1 and IRF-2 being identified in the 1980s (Miyamoto *et al.* 1988). All IRF family members contain a well conserved DNA binding domain, sometimes referred to as an IRF domain (see figure 1.6). This domain contains a pentad of tryptophan residues that are distinctive for the IRF family of transcription factors. Surprisingly, although IRF family members contain similar DBDs they act on disparate genes. This is likely due to the lack of conservation between IRF's C terminal regions. Consequently each IRF occupies its own transcriptional niche (Takaoka *et al.* 2008). The roles of **IRF-1** are discussed in detail in sections 1.2.2-1.3. IRF-1's closest relative in the IRF family is **IRF-2** (see figure 1.6). IRF-2 was originally described as an antagonistic repressor of IRF-1 activity (Harada *et al.* 1989) and an oncoprotein (Harada *et al.* 1993). IRF-2 also acts as a transcriptional activator (Vaughan *et al.* 1995). **IRF-3**, like IRF-1 and IRF-2 is constitutively expressed; however it is found predominantly in the cytoplasm (Au *et al.* 1995). Viral signalling leads to phosphorylation of IRF-3 promoting nuclear translocation and transcriptional activity. IRF-3 can homodimerise and heterodimerise with IRF-7. Both of these proteins are essential for type I interferon signalling (Au and Pitha 2001).

IRF-4 is predominantly expressed haematopoetically, and possesses little DNA binding affinity of its own. Partner factors, including other transcription factors such as Pu.1 or other IRFs such as IRF-8 are essential for IRF-4 DNA binding. IRF-4 is important in B cell development, and is found to be translocated in multiple myeloma samples (Shaffer *et al.* 2009). IRF-4 can act as a

transcriptional repressor, and is able to prevent IRF-1 transactivation of the TRAIL promoter (Yoshida *et al.* 2005). **IRF-5** is up-regulated in response to interferons, viral infection and DNA damaging agents and is critical in innate immune signalling and may have tumour suppressor activities (Takaoka *et al.* 2005). IRF-5 plays a role in the pathology of Systemic Lupus Erthyromatosis (Graham *et al.* 2006).

IRF-6 is unique among the IRF family as it is the only member whose knockout mice are not viable. IRF-$6^{-/-}$ mice have severe defects in craniofacial, skin and limb development (Kondo *et al.* 2002). Mutations in the IRF-6 gene are associated with van der Woude syndrome, which is characterised by cleft palate (Ingraham *et al.* 2006). **IRF-7** is required for type I IFN signalling in partnership with IRF-3. Levels of IRF-7 are lower than IRF-3 in most cell types (Sato *et al.* 2000). **IRF-8** – also known as ICSBP (Interferon Consensus Sequence Binding Protein) is similar to IRF-4 in its DNA binding and tissue distribution. IRF-8 may act as a tumour suppressor, as knockout IRF-8 mice develop a CML (Chronic Myeloid Leukaemia) like syndrome (Holtschke *et al.* 1996). **IRF-9** is a component of the trimeric ISGF3 (Interferon Stimulated Gene Factor 3) complex, which also contains STAT-1 (Signal Transducer and Activator of Transcription) and STAT-2. As such IRF-9 is best known for its role in directing the transcription of ISGs (Interferon Stimulated Genes) (Majumder *et al.* 1998).

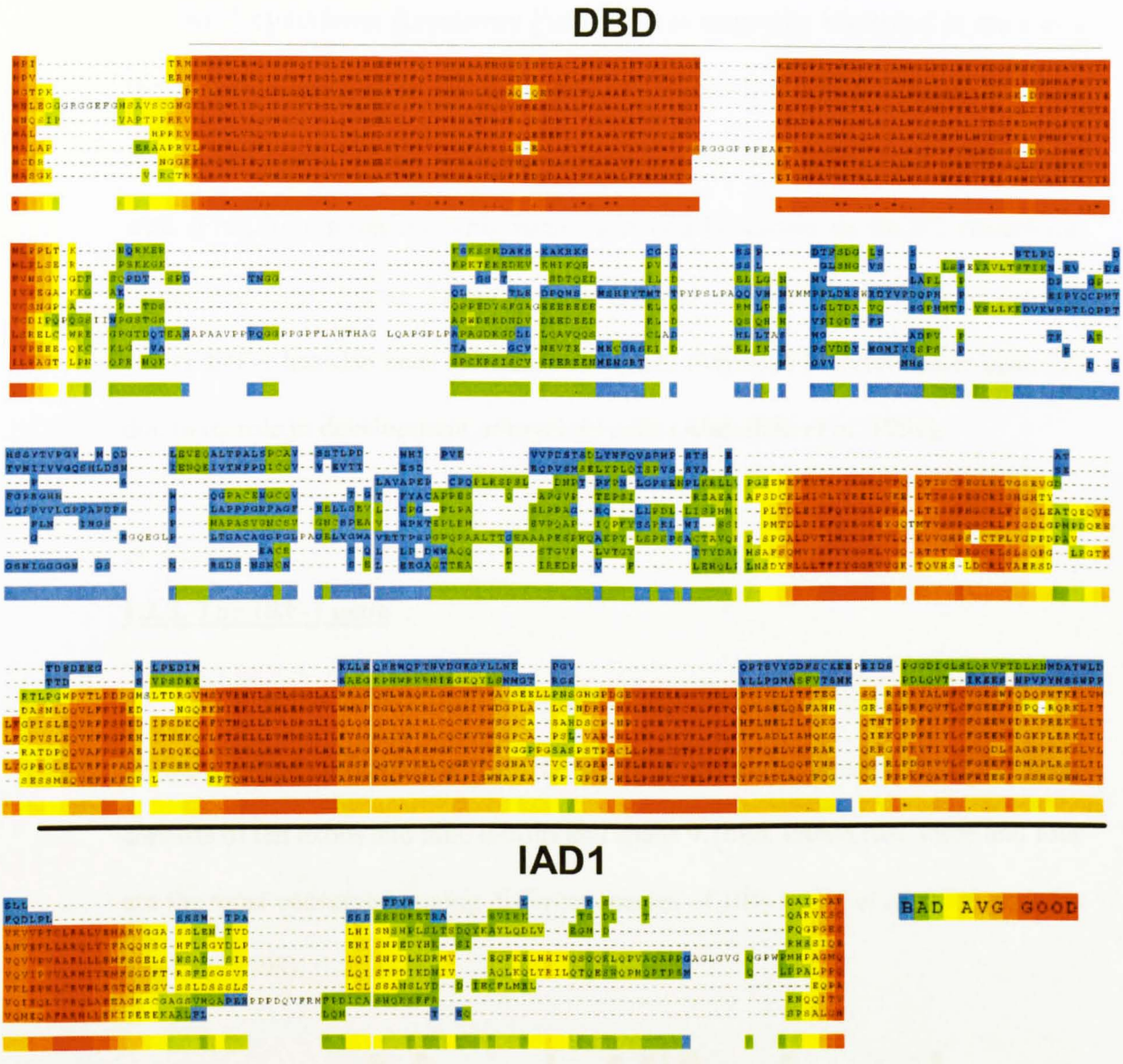

Figure 1.6. Alignment of human IRF family members, The amino acid sequences of human IRF-1 through IRF-9 where aligned against each other using the T-Coffee multiple alignment programme (http://www.ebi.ac.uk/Tools/t-coffee/index.html). The score of the amino acid alignment is represented as a heat map were red is the strongest alignment and blue the weakest. Conservation among the DNA binding domain is strong among IRF family members, while the C terminal regions are poorly conserved. The IAD1 region (IRF Association Domain 1) is only conserved between IRF-3 through IRF-9, with IRF-1 and IRF-2 possessing a variant of this domain.

1.2.2. IRF-1 discovery

IRF-1 (**I**nterferon **R**egulatory **F**actor **1**) was originally identified in mice as a factor that transactivates the promoters of Interferon α and β (Miyamoto *et al.* 1988). The human IRF-1 gene was cloned shortly after from HeLa cells treated with IFNα (Interferon α). This factor was briefly known as ISGF2 (Interferon Stimulated Gene Factor 2) but is now referred to as IRF-1 (Pine and Darnell 1989). IRF-1 has also been identified as Myd32 (Myeloid Differentiation gene 32) due to its role in development of myeloid cells (Abdollahi *et al.* 1991).

1.2.3. The IRF-1 gene

The human IRF-1 gene is located on chromosome five at position q.31.1 - the long arm of chromosome five (Harada *et al.* 1993). In humans, the IRF-1 gene consists of ten exons and nine introns and spans 9.16kb. Exons two, three and four are the most conserved among different species of IRF-1 (Shi *et al.* 2008 and Jia and Guo 2008).

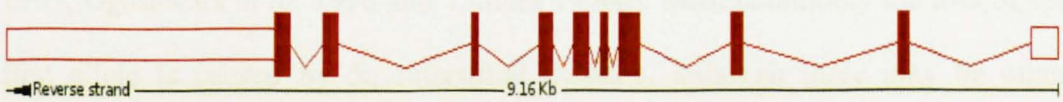

Figure 1.7 Exon distribution of human IRF-1. Protein coding exons are shown as filled bars, while exons that encode 5' and 3' UTR are shown unfilled. Source: http://www.ensembl.org/Homo_sapiens/Transcript/Summary?db=core;g=ENSG00000125347;r=5:131817302-131826469;t=ENST00000245414

1.2.4. 5q Syndrome and loss of heterozygosisty (LOH)

The localisation of IRF-1 on chromosome five led to the hypothesis that it may be involved in cancer, as this region is deleted in certain solid tumours, myelodysplastic syndrome (MDS) and is the sole karyotypic feature of 5q syndrome. 5q syndrome (also known as monosomy five) is characterised by refractory anaemia and megakaryocytic abnormalities. IRF-1 is one of the most commonly lost genes in this chromosomal deletion (Boultwood *et al.* 1993 and Willman *et al.* 1993). Loss of the IRF-1 gene as a feature of the 5q deletion has been reported in bladder cancer, colorectal carcinomas, esophageal cancer and pulmonary large cell neuroendocrine carcinomas (Ogasawara *et al.* 1996, Tamura *et al.* 1996a, Peralta *et al.* 1998, Kram *et al.* 2001 and Shin *et al.* 2005). Some studies on the 5q deletion have identified patients that retain the IRF-1 locus, suggesting that IRF-1 is not entirely responsible for the clinical manifestations of this deletion (Boultwood *et al.* 1993 and Kroef *et al.* 1994).

LOH (Loss of heterozygosity) of the IRF-1 locus has been observed in AML, MDS, gastric and esophageal tumours (Green *et al.* 1999, Willman *et al.* 1993, Ogasawara *et al.* 1996 and Tamura 1996a). Most commonly the loss of the first allele is caused by 5q interstitial deletion, although there may be other mechanisms by which one IRF-1 allele is lost. It is not yet clear if germ line mutations in the IRF-1 locus are involved in IRF-1 LOH. The remaining IRF-1 allele undergoes accelerated exon skipping leading to a complete loss of proper IRF-1 expression and LOH. In one case of gastric cancer the remaining IRF-1 allele contained a point mutation which severely reduced its transcriptional activity (Ogasawara *et al.* 1996).

1.2.5. IRF-1 Splicing.

Several splicing variants of IRF-1 have been identified. Most splicing variants occur in exons two and three which code for the DNA binding domain (DBD) (Harada *et al.* 1994). As expected these mutants have no transcriptional activity. These mutations have been found in patients with MDS, APL, AML and CML (Maratheftis *et al.* 2006, Green *et al.* 1999 and Tzoanopoulos *et al.* 2002). Five splice variants have been reported in cervical cancers. These splice variants involve exons seven, eight and nine (Lee *et al.* 2006).

1.2.6. IRF-1 mutations and polymorphisms

The protein coding region of human IRF-1 gene exhibits relatively few point mutations, with mechanisms of inactivation primarily occurring from deletions and exon skipping. Only two missense mutations in the IRF-1 coding sequence have been reported to date. M8L (Met^{8}→Leu) was identified in a gastric adenocarcinoma sample, and is reported to be less effective at inducing cell cycle arrest compared to wild type IRF-1 (wild type IRF-1) (Nozawa *et al.* 1998). A mutation producing IRF-1 W11R (Trp^{11}→Arg) was found in non small cell lung carcinoma cell lines. This mutation abolished DNA binding, as structural analysis of the IRF-1 DBD had previously shown that the Trp^{11} residue is important in making contact with DNA (Eason *et al.* 1999).

Some IRF-1 polymorphisms are associated with human diseases. Most of the polymorphisms are located in the untranslated or intronic regions of the IRF-1 gene. Among eleven promoter polymorphisms identified by Ji and coworkers

three modified a Sp1 binding site, suggesting a mechanism by which these polymorphism may affect IRF-1 induction (Ji *et al.* 2004). The A4396G polymorphism may alter the binding of certain transcription factors to the IRF-1 promoter. This polymorphism has been found to be associated with breast cancer and is more frequent in African Americans than in European populations (Bouker *et al.* 2007). IRF-1 promoter polymorphisms have also been correlated to clinical outcome in Hepatitis C and Bechets disease (Saito *et al.* 2002 and Lee *et al.* 2007).

1.3.1. DNA binding domain (DBD)

The IRF-1 DBD is located within the first 115 amino acids and constitutes the most conserved region of IRF-1 between different species (see figure 1.9). The DNA binding domain of IRF-1 is the only part of IRF-1 which has been crystallised and structurally studied (Escalante *et al.* 1998). Residues 1-113 of mouse IRF-1 were co-crystallised with 13bp of DNA corresponding to the IRF-E (IRF Element) found in the IFNβ promoter. The DBD consists of three α-helices flanked by mixed four stranded β sheets. In addition, three characteristic large loops emanate from the β-sheets and α-helices. The IRF-1 DBD has a unique helix-turn-helix structure (see figures 1.8 and 1.9).

IRF-1 recognises DNA via the major groove. Residues projecting from the last two turns of the recognition helix are responsible for interacting with the IRF-E. The DBD of IRF-1 also forms extensive contacts with residues outside of the core GAAA sequence. Residues within all of the α helices and loops one and three make contact with phosphate groups up to 6 bp away from GAAA.

IRF-1 is characterised by its tryptophan (Trp) pentad or tryptophan cluster, which is highly conserved in all members of the IRF family. Only three of the five residues interact with the DNA (Trp^{11}, Trp^{38} and Trp^{58}). These residues straddle the major groove and make hydrogen and van der-Waals interactions with the sugar phosphate backbone. The Trp residues are held in place by the hydrophobic core of the DBD including two absolutely conserved residues (Phe^{55} and Phe^{81}) found in α-helix two and α-helix three (Escalante *et al.* 1998).

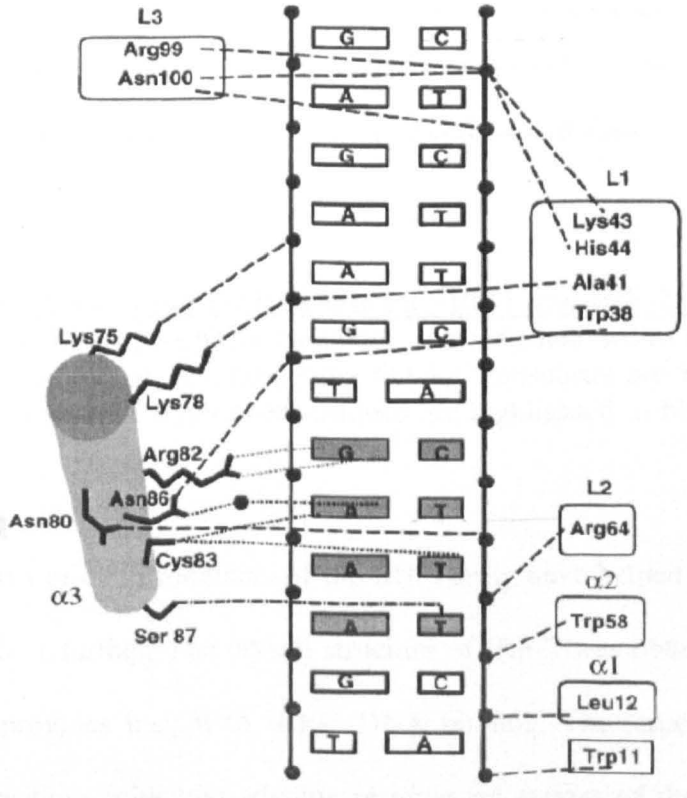

Figure 1.8 Schematic of residues involved in IRF-1 : DNA interactions. The core GAAA motif is shaded. The three loops are designated L1-L3 and the α helices as α1-α3. Hydrogen bonds to bases are drawn as dotted lines, while hydrogen bonds to the DNA backbone are shown as dashes. Diagram from Escalante *et al.* 1998.

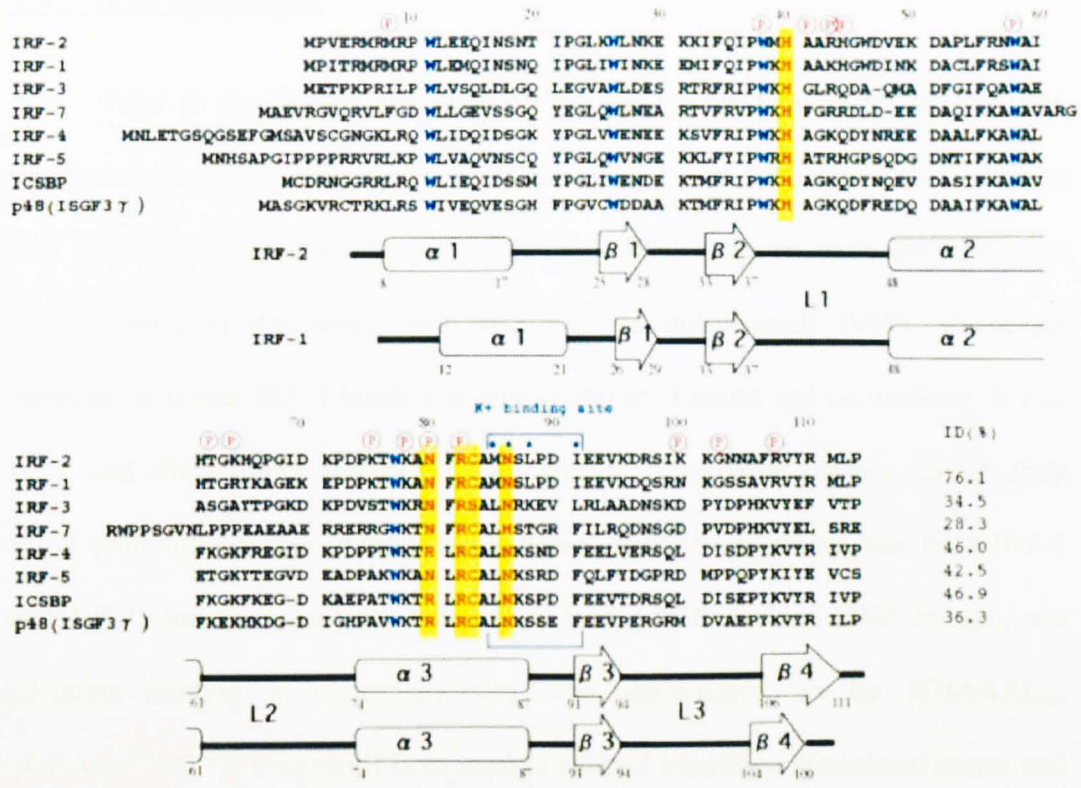

Figure 1.9 Alignment of the DBD of murine IRF-1 and IRF-2. Residues that make contacts with the phosphate backbone are indicated with circled pink P. Critical residues involved in binding the GAAA consensus are highlighted in yellow and the conserved tryptophan residues are highlighted in blue. From Fuji *et al.* 1999.

Crystal structures of other members of the IRF family have helped to understand the DBD of IRF-1 further. The crystal structure of IRF-2 was obtained at higher resolution, so provides insight to IRF-1 DNA binding. The structure of IRF-2 identified interactions with two adenine residues up stream of the core GAAA sequence; this is in agreement with the AA ($_{N1-4}$) GAAA IRF-E consensus site. This interaction involves the completely conserved His^{40} residue making contact with the minor groove. Although this was not as clearly demonstrated in the first study, it is likely that this interaction occurs in IRF-1 (Fujii *et al.* 1999).

1.3.2. DNA recognition

Prior to the crystal structure of the IRF-1 DBD being solved, an IRF consensus site had already been identified. IRF-1 was first shown to be able to bind Interferon Stimulated Response Element (ISRE) sequences in the promoters of the interferon stimulated gene ISG15 (Pine and Darnell 1989). The exact sequence to which IRF-1 binds was first found by Tanaka and co-workers. It was noted that since IRF-1 and IRF-2 have similar N terminal regions (DBD) they might bind similar sites. This was confirmed, and it was found that both IRF-1 and IRF-2 bind essentially the same sites. Using PCR assisted DNA binding site selection method a consensus site was determined to be (G)AAA($_{N2-3}$)GAAA($^{G/C}$)($^{T/C}$). This motif is located in several interferon stimulated genes and was named IRF-E (Interferon regulatory factor – element) (Tanaka *et al.* 1993). A selection of IRF-1 binding sites is given in table 1.4.

GENE	SEQUENCE	REFERENCE
Single site IRF-E		
IFNβ	AG**AA**GT **GAAA** GT	Neish *et al.* 1995
ODC	GG**AA**CT **GAAA** CT	Manzella *et al.* 2000
FoxP3	TA**AA**CGC **GAAA** TT	Fragale *et al.* 2008
IL-12Rβ1	CA**AA**GT **GAAA** GC	Kano *et al.* 2008
TLR9	AA**AA**CT **GAAA** ACA	Guo *et al.* 2005
IL-10	AA**AA**TT **GAAA** AC	Ziegler-Heitbrock *et al.* 2003
RIG-1	TC**AA** GTC **GAAA** GT	Su *et al.* 2007
ISRE or single site IRF-E		
OAS	AG **GAAA** C **GAAA** CC	Tanaka *et al.* 1993
XAF1	AA **GAAA** C **GAAA** CT	Wang *et al.* 2006
VCAM1	GT **GAAA** AC **GAAA** CC	Neish *et al.* 1995
RANTES	A T **GAAA** A **GAAA** AC	Liu and Ma 2006
iNOS	AT **GAAA** GT **GAAA** GA	Neish *et al.* 1995
Caspase-1	CT **GAAA** CT **GAAA** G	Casano *et al.* 1994
FasL	GA **GAAA** GA **GAAA** GA	Kirchhoff *et al.* 2002
IL27p28	CG **GAAA** GT **GAAA** CC	Pirhonen *et al.* 2007
Multiple sites (ISRE/IRF-E)		
ISG54	**AA**GG **GAAA** GT **GAAA** CT	Tanaka *et al.* 1993
CIITA	G**AA**A **GAAA** GT **GAAA** GG	Rahat *et al.* 2001
MECL1	A**AA**G**GAAA** GC **GAAA** GC	Foss and Prydz 1999
IL-7	A**AA**GTA **GAAA** CT **GAAA** GT	Oshima *et al.* 2004
IL-6	T**AA**AA **GAAA** AAA **GAAA** GT	Sanceau *et al.* 1995
INDO	GT**AA**G **GAAA** ACT **GAAA** CC	Konan and Taylor 1996
ISG15	G **GAAA** GG **GAAA** CC **GAAA** CT	Tanaka *et al.* 1993
IL-15	A **GAAA** AGT **GAAA** GA **GAAA** GA	Azimi *et al.* 2000

Table 1.4 IRF-1 binding sites. List of IRF-E and ISRE elements known to be bound by IRF-1 in target promoters. The IRF-E motif overlaps with ISRE motifs. The core GAAA motif is highlighted. Some genes contain multiple IRF-1 binding sites, which are not all described here. Abbreviations, **ODC** (Ornithine Decarboxylase), **FoxP3** (Forkhead P3), **IL-12Rβ1** (IL-12 receptor β1), **TLR9** (Toll Like Receptor 9), **OAS** (Oligoadenylates Synthetase), **XAF1** (XIAP Associated Factor 1), **RANTES** (Regulated upon Activation Normally T cell expressed and presumably secreted), **VCAM-1** (Vascular Cell Adhesion Molecule-1) **FasL** (Fas Ligand), **CIITA** (Class II Transactivator) **LMP2** (Low Molecular Weight Protein 2), **INDO** (Indoamine-2-3 dioxygenase), **H4** (histone 4), **RIG-1** (Retinoid Inducible Gene-1). Adapted from (Fujii *et al.* 1999).

1.3.3 Transactivation and repressor domains

The transactivation domain (TAD) resides within the central C terminal region of the IRF-1 protein. In mouse IRF-1, the TAD is mapped to amino acids 185-260 (Schaper *et al.* 1998 and Kirchhoff *et al.* 2000), while in humans it is located between amino acids 217-260 (Kim *et al.* 2003a). The IRF-1 TAD overlaps with the heterodimerisation domain (aa 124-219) used for interaction between IRF-1 and IRF-8 (Schaper *et al.* 1998).

Several short stretches of IRF-1 have been suggested as repressor domains. The region from amino acid 170-200 has a repressive effect on the IFNβ promoter reporter (Lin *et al.* 1994). Residues between amino acid 197 and 202 (IPVEVV) have a repressive effect on IRF-1 activity (Upreti *et al.* 2004). IRF-1 also contains an LxxLL motif in its C terminus (^{306}LDSLL^{310}). The LxxLL motif is a short α-helix domain involved in protein – protein interactions. This region has been implicated in recruitment of coactivators to nuclear receptors (Heery *et al.* 1997). This region is required for IRF-1 repression of the Cdk2 (Cyclin Dependent Kinase 2) promoter, and mutation of LxxLL residues reduces IRF-1's growth suppressor activities. This LxxLL motif does not modify IRF-1 protein-DNA interactions (Eckert *et al.* 2006). The chaperone protein Hsp70 (Heat Shock Protein 70) interacts through the IRF-1 LxxLL motif and is involved in the proteasome dependent turnover of IRF-1 (Narayan *et al.* 2009).

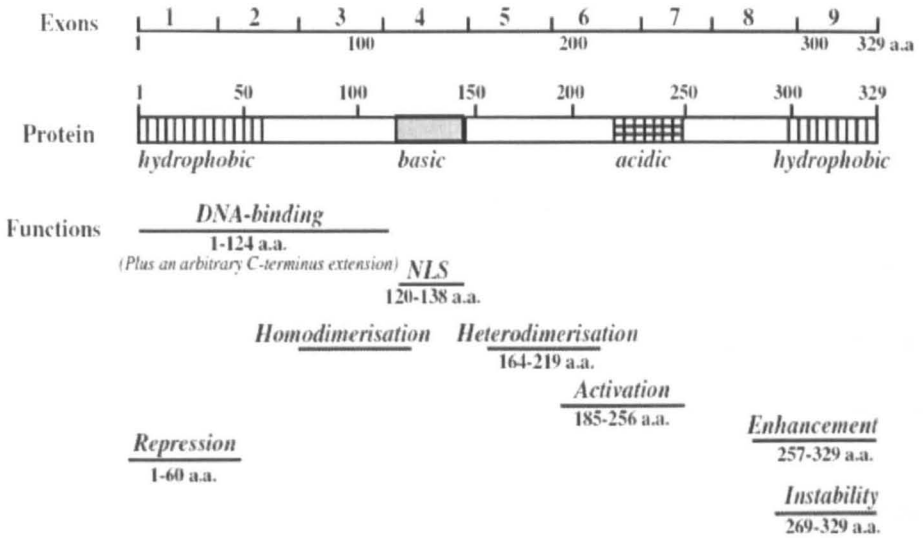

Figure 1.10 Domains of IRF-1. Schematic of murine IRF-1, with the locations of the variously described domains and motifs. Top (exons) illustrates the location of the exons in relation to the protein. The Activation domain is referred to as the TAD domain in the text. From Upreti and Rath 2005.

1.3.4. Nuclear localisation signal

IRF-1 is almost exclusively retained in the nucleoplasm. The nuclear localisation signals of IRF-1 have been mapped. Two distinct sequences (^{120}RKERKSK and ^{132}KSKTKRK) are both required for proper localisation. Epitope mapping suggests this region is exposed to the surface (Schaper *et al.* 1998). IRF-1 has been shown to physically interact with the nuclear import protein Karyopherin 2 (KPNA2) in normal human epidermal keratinocytes. Knockdown of KPNA2 causes IRF-1 to be exclusively localised in the cytosol (Umegaki *et al.* 2007).

Nuclear translocation of IRF-1 may also be brought about by interactions with the TLR (Toll Like Receptor) adaptor protein MyD88 (Myeloid Differentiation Gene 88) this "licensing" of IRF-1 by MyD88 into the nucleus is involved in transcription of a distinct set of IRF-1 targets involved in the immune response (Negishi *et al.* 2006 and Schmitz *et al.* 2007).

Cytosolic localisation of IRF-1 has been noted by immunohistochemistry in a number of tumours, including breast, melanoma, colon and endometrial tumours (Lowney *et al.* 1999, Kuroboshi *et al.* 2003, Zhu *et al.* 2006, Coppola *et al.* 2009 and Giatromanolaki *et al.* 2004).

1.3.5 IRF-1 protein turnover

IRF-1 is a relatively unstable protein with a half life of around 30 minutes (Watanabe *et al.* 1991 and Pion *et al.* 2009). IRF-1 is degraded by the ubiquitin-26S proteasome system. Evidence for this degradation comes from the stabilisation of IRF-1 by proteasome inhibitors (MG-132 and MG-115) and the presence of poly-ubiquitinated IRF-1 detected by immunoblot (Nakagawa and Yokosawa 2000 and Pion *et al.* 2009). Truncation studies suggested that the extreme C terminus of IRF-1 (aa 291-329) regulates IRF-1 stability (Nakagawa and Yokosawa 2000).

The cysteine protease inhibitor E64d (which blocks the activity of Calpains and lysosomal proteases) does not lead to accumulation of IRF-1 protein in HeLa cells, suggesting that neither of these enzyme classes are involved in IRF-1 degradation (Nakagawa and Yokosawa 2000). IRF-1 is primarily poly-ubiquitinated by K^{48} linked ubiquitin which is involved in degradation. The far C terminus of IRF-1 was found to be important for IRF-1 stability. Deletion of the last 25 amino acids of IRF-1 induced a stabilisation of the protein, although it did not affect the ubiquitination. Substitutions between lysine and arginine on residues 275 and 299 (singly and in combination) did not lead to a significant change in half life, or ubiquitination suggesting that these two residues are not involved in IRF-1 turnover. Rather the conclusion is that, the far C terminus of IRF-1 regulates protein interactions that regulate IRF-1 turnover instead of harbouring the lysines which are targeted by ubiquitin (Pion *et al.* 2009).

The same group identified an interaction between the LxxLL motif in the far C terminus of IRF-1 and Hsp70. This chaperone in turn interacts with Hsp90 which

is involved in protein stability. Inhibition of Hsp90 caused a de-stabilisation of IRF-1, while over-expression of Hsp90α/β increases the stability of IRF-1. It is suggested that IRF-1 is a "client" of the Hsp70/90 chaperone complex, which is required to prevent degradation of IRF-1 (Narayan *et al.* 2009).

1.3.6. IRF-1 protein-protein interactions

Approximately 35 proteins have been documented to interact with IRF-1. The majority of these interactions have not been extensively studied and the consequences of the interactions are not well understood. The largest group of interacting partners are those involved in transcription. IRF-1 can heterodimerise with two other members of the IRF family (IRF-8 and IRF-5). The interaction with IRF-5 has not been studied in detail (Barnes *et al.* 2003 and Meraro *et al.* 1999) although the importance of the interaction between IRF-1 and IRF-8 is well understood. IRF-8 requires other transcription factors in order to bind to promoters, and together IRF-1 and IRF-8 co-regulate a significant cohort of genes (Dror *et al.* 2007). Several TFs interact with IRF-1, many of these TFs occupy binding sites adjacent to IRF-1 binding sites (Hurgin *et al.* 2002, Tendler *et al.* 2001 and Drew *et al.* 1995a). IRF-1 also makes contact with several coactivators including KAT (lysine acetyltransferases) enzymes p300 and CBP, as well as components of the basal transcriptional machinery such as TFIIB and RNA Pol II (Merika *et al.* 1998 Ramsauer *et al.* 2007 and Kadam and Emerson 2003). The next largest group of interacting partners contains those that are related to IRF-1 post translational modifications, including the kinases CK2 and PKCα, as well as components of the SUMOylation machinery (Lin and Hiscott 1999, Giroux *et al.* 2003 and Kim *et al.* 2008). A number of viral proteins have been identified as interacting partners of IRF-1. Most of these proteins inhibit IRF-1 transcriptional activity through as yet unknown mechanisms. All of the published IRF-1 interacting partners are listed in table 1.5.

Protein	Interaction domain	Outcome	Reference
IRF-5	*Unknown*	*Unknown*	Barnes *et al.* 2003
IRF-8	IAD	Transactivation of promoters	Meraro *et al.* 1999 and Dror *et al.* 2007
p50, p65, RelA	*Unknown*	Transactivation of iNOS and other promoters.	Saura *et al.* 1999, Drew *et al.* 1995b and Liu and Khachigian 2009
C/EBPβ	*Unknown*	Transactivation of IL18BP promoter	Hurgin *et al.* 2002
HIF1α	*Unknown*	Hypoxic activation of iNOS promoter	Tendler *et al.* 2001
GRα	*Unknown*	Increased activity of IRF-1 in reporter assays.	Jiang *et al.* 2004
p53	*Unknown*	Transactivation of p21 and GBP promoters	Dornan *et al.* 2004 and Guimaraes *et al.* 2009
STAT-1	200-300	Transactivation of LMP2 promoter	Chatterjee-Kishore *et al.* 2000a
CBP	C terminus	Interacts on IFNβ enhancesome	Merika *et al.* 1998
p300	271-290	Interaction enhances acetylation of p53	Dornan *et al.* 2004
hGCN5	DBD	*Unknown*	Masumi *et al.* 1999
PCAF	DBD	Increases IRF-1 reporter activity	Masumi *et al.* 1999
SRC-2	*Unknown*	Increases IRF-1 reporter activity	Bhandare *et al.* 2009
TFIIB	N terminus	Transcription	Wang *et al.* 1996
RNA Pol II	*Unknown*	Transcription	Ramsauer *et al.* 2007
HMG1	*Unknown*	Interacts on IFNβ enhancesome	Yie *et al.* 1999
NPM	*Unknown*	Prevents DNA binding	Kondo *et al.* 1997
HDAC1	*Unknown*	Repression of PDGF-D promoter	Liu and Khachigian 2009
CK2	*Unknown*	Phosphorylation, increases IRF-1 activity	Lin and Hiscott 1999
PKCα	*Unknown*	In vitro phosphorylation	Giroux *et al.* 2003
ULK2	*Unknown*	*Unknown*	Ewing *et al.* 2007
SUMO-1	233-255	Decreases transcriptional activity	Kim *et al.* 2008
PIASγ	1-190	SUMO-1ylation of IRF-1	Nakagawa and Yokosawa 2002
Ubc9	1-190	SUMO-1ylation of IRF-1	Nakagawa and Yokosawa 2002, Kim *et al.* 2008
E6	*Unknown*	*Unknown*	Ronco *et al.* 1998
E7	167-325	Decreases IRF-1 activity in reporter assay.	Park *et al.* 2000
vIRF-1	C terminus	Decreases IRF-1 activity	Burysek *et al.* 1999
Tat	C terminus	Promotes transcription of the HIV genome.	Sgarbanti *et al.* 2002
MyD88	*Unknown*	Increases shuttling into nucleus, increasing transcriptional activity	Negishi *et al.* 2006 and Schmitz *et al.* 2007
VEGFR 2	*Unknown*	*Unknown*	Lee *et al.* 2008
KPNA2	*Unknown*	Nuclear translocation of IRF-1	Umegaki *et al.* 2007
GAGE	*Unknown*	Reduces IRF-1 transcriptional activity	Kular *et al.* 2009
Hsp70/90	301-325	Regulates IRF-1 stability	Narayan *et al.* 2009

Table 1.5 Interacting partners of IRF-1. Table summarising the known interacting partners of human and mouse IRF-1 and the site of interaction on IRF-1. Abbreviations **C/EBPβ** (CCAAT Enhancer Binding Protein β), **HIF1α** (Hypoxia Inducible Factor 1α), **CBP** (CREB Binding Protein), **PCAF** (p300/CBP Associated Factor), **hGCN5** (General Control Amino Acid Synthesis 5), **HDAC-1** (Histone De acetylase-1) **TFIIB** (Transcription Factor 2b), **RNA Pol II** (RNA Polymerase 2), **HMG1** (High Mobility Group Box 1), **NPM** (Nucleophosmin), **CK2** (Casein Kinase 2), **PKCα** (Protein Kinase Cα), **ULK2** (Unc51 Like Kinase 2) **PIASγ** (Protein Inhibitor of Activated STAT γ), **Ubc9** (Ubiquitin Conjugating Enzyme 9), **MyD88** (Myeloid Differentiation Gene 88), **VEGFR2** (Vascular Epithelial Growth Factor Receptor 2), **KNPA2** (Karyopherin A2), **GAGE** (G Antigen 1), **Hsp70/90** (Heat Shock Protein 70/90).

1.3.7. Phosphorylation

IRF-1 has been referred to as a phospho-protein in several reports. During the original cloning of human IRF-1 (then designated ISGF2) isoelectric focusing produced three distinct species with a pI range between 5.3 and 4.7. Treatment of extracts with potato acid phosphatase eliminated two of these bands, only leaving the most basic. This also reduced the DNA binding ability of IRF-1 by EMSA analysis. Addition of phosphatase inhibitors rescued this loss (Pine and Darnell 1989). The serine/threonine kinase inhibitor staurosporine has been shown to prevent Newcastle Disease Virus (NDV) dependent transactivation of IRF-1 on an IFNβ promoter reporter, suggesting that NDV activates IRF-1 by phosphorylation (Watanabe *et al.* 1991).

PKCα phosphorylates IRF-1, and can physically interacting with it (table 1.5). This phosphorylation is required for IRF-1 to transactivate the CTIIA (MHC Class II Transactivator) promoter (Giroux *et al.* 2003). Phorbol ester treatment of the mouse macrophage cell lines RAW264.7 increases iNOS expression and IRF-1 activity, while the PKC inhibitor Ro 31-8220 decreases IRF-1 dependent transcriptional activity on the iNOS promoter suggesting that PKC may be required for IRF-1 activity (Momose *et al.* 2000).

IRF-1 has been shown to interact with CK2, and these interactions result in phosphorylation *in vitro*. Mapping and *in vitro* kinase assays of IRF-1 showed that phosphorylation occurs at Ser^{219}, Ser^{221}, Thr^{224} or Thr^{225}. Substitution of these residues with alanine resulted in decreased reporter activity (Lin and Hiscott 1999).

IRF-1 is phosphorylated on tyrosine residues during IFNγ induced differentiation of U937 cells. Substitution mutants showed that Y^{109} was the sole phospho-tyrosine residue. This modification is needed for interaction with IRF-8 and transactivation of promoters (Kautz *et al.* 2001 and la Sala *et al.* 2009).

1.3.8. SUMOylation

Yeast two hybrid screens with IRF-1 pulled out PIAS3 and Ubc9 as IRF-1 interacting proteins. This led to the finding that IRF-1 is SUMOylated by PIAS3. SUMO-1 is an ubiquitin like protein that is conjugated to lysine residues using a similar enzymatic cascade to ubiquitination (see section 1.1.6). Assays using a ISRE-Luc reporter showed that SUMOylation of IRF-1 repressed reporter activity, as co-transfection of wild type, but not mutant PIAS3 reduced reporter activity (Nakagawa and Yokosawa 2002). The SUMO-1 binding sites were then identified to be Lys^{275} and Lys^{299}; this was reported using K-R mutants with *in vitro* SUMO assays and immunoprecipitations with SUMO-1 and IRF-1. The SUMO isopeptidsase SENP1 (Sentrin specific protease 1) de-SUMOylates IRF-1. This study also showed that SUMOylated IRF-1 is commonly found in ovarian cancer samples. Functionally SUMOylated IRF-1 does not induce p21 dependent reporter activity, as SUMO-1 conjugation mutants K275R and K299R have higher reporter activity than wild type. These SUMO-1 conjugation mutants also showed enhanced apoptotic activity compared to wild type (Park *et al.* 2007).

The interaction between IRF-1 and SUMO-1 was mapped to amino acids 233-255 in a separate study, this region resides within the TAD of IRF-1. Therefore IRF-1 is able to interact with SUMO-1 as well as become SUMO-1ylated. This group was also able to demonstrate *in vivo* and *in vitro* SUMO-1ylation of IRF-1 and confirmed that IRF-1 interacts with Ubc9 through its DBD (Kim *et al.* 2008).

1.3.9. Ubiquitination

Following treatment with the proteasome inhibitor MG132 multi-ubiquitin conjugated IRF-1 can be detected (Nakagawa and Yokosawa 2000). Splice variants lacking exon nine or seven and eight were found to be more stable than wild type IRF-1. This suggests that the degradation signal or ubiquitination sites may reside in protein corresponding to these exons (Lee *et al.* 2006). The majority of IRF-1 is ubiquitinated by K^{48} linked ubiquitin. This form of branching is predominantly involved in proteasomal degradation (Pion *et al.* 2009). SUMO-1ylation of IRF-1 at Lys^{275} and Lys^{299} prevents ubiquitination and increases protein stability. It is likely that SUMO-1 and ubiquitin compete for Lys residues on the IRF-1 protein (Park *et al.* 2007).

1.3.10. Acetylation

IRF-1 may be acetylated by the KAT (lysine acetyltransferases) proteins with which it interacts including PCAF, GCN5, p300, SRC-2 or CBP (Masumi et al. 1999, Deng and Wu 2003, Bhandare *et al.* 2009 and Dornan *et al.* 2004). Co-transfection of PCAF with IRF-1 increased reporter activity on an ISRE driven promoter suggesting this interaction, and possibly acetylation increases activity of IRF-1 (Masumi *et al.* 1999).

1.3.11 IRF-1 transgenic mice.

IRF-1 and IRF-2 mice were first generated by Matsuyama *et al.* 1993. The IRF-1^{tm1Mak} mice strain has a neomycin cassette inserted into the IRF-1 gene which leads to removal of amino acids 63-223. Early studies on this mouse strain identified a role for IRF-1 in T cell development (see section 1.5.8) (Matsuyama *et al.* 1993).

A separate strain of IRF-$1^{-/-}$ mice was generated by Reis and co-workers in 1994. IRF-1^{tm1cew} mice were generated by adding a disrupting neomycin cassette into the IRF-1 gene between exon four and six. This region was chosen because it was thought to contain part of the DBD. This mutation removes amino acids 63-182 from the protein. EMSA studies show that this disrupted species does not bind DNA. Many of the original phenotypic characteristics of this knockout are similar to the strain produced by Matsuyama *et al.* These similarities include a reduction in iNOS expression following IFNγ or LPS treatment in macrophages, a reduction in the amount of $CD8^+$ T cells and a decrease in MHC I expression in thymocytes and splenocytes (Reis *et al.* 1994).

1.4.1. IRF-1 expression

IRF-1 is ubiquitously expressed. IRF-1 levels are particularly high in cells of the immune system (Harada *et al.* 1990). It is not yet known what roles basal (not induced by exogenous agents) IRF-1 plays in cells. Levels of IRF-1 protein and mRNA change during the cell cycle, suggesting that IRF-1 expression is cell cycle regulated. It was found that the first wave of expression occurred in the G1 stage between fithteen minutes and two hours and was highly transient. The second wave of expression in the G1/S phase was broader, occurring at eight hours. Both phases of expression required *de novo* synthesis of IRF-1 protein and the two pools of IRF-1 exhibited distinct half lives, with the first having a half-life of twenty minutes and the second, a half-life of sixty minutes (Stevens and Yu-Lee 1992).

1.4.2. Regulation by STAT family members

Several members of the STAT family of transcription factors have been found to occupy the GAS element in the IRF-1 promoter (see figure 1.11). IFNα causes IRF-1 induction in cells via STAT-1 / STAT-2 complexes (Li *et al.* 1996). IFNα treatment also promotes the binding of STAT-3 and STAT-4 to the GAS element (Matikainen *et al.* 1999). IRF-1 is inducible by IFNβ (Fujita *et al.* 1989). Tyrosine phosphorylated STAT-1 binds the GAS element on the IRF-1 promoter. Several interleukins and growth factors that signal to the STAT family of transcription factors modulate IRF-1 expression including IL-12 (STAT-3), IL-4 (STAT-6) Epidermal Growth Factor (STAT-1/3) Prolactin (STAT-1) and Growth Hormone (STAT-1/3) (Galon *et al.* 1999, Goenka *et al.* 1999, Book McAlexander and Yu-Lee 2001a, Book McAlexander and Yu-Lee 2001b, Andersen *et al.* 2008 and Le Stunff and Rotwein 1998). STAT-1 binding has been identified on the IRF-1 promoter by ChIP on Chip profiling of tiling arrays within the ENCODE regions. Three STAT-1 binding sites were found at -160, -4786 and -5997. RNA Pol II binding closely matched STAT-1 binding confirming earlier findings that IRF-1 transcription is regulated by STAT transcription factors (Wormald *et al.* 2006).

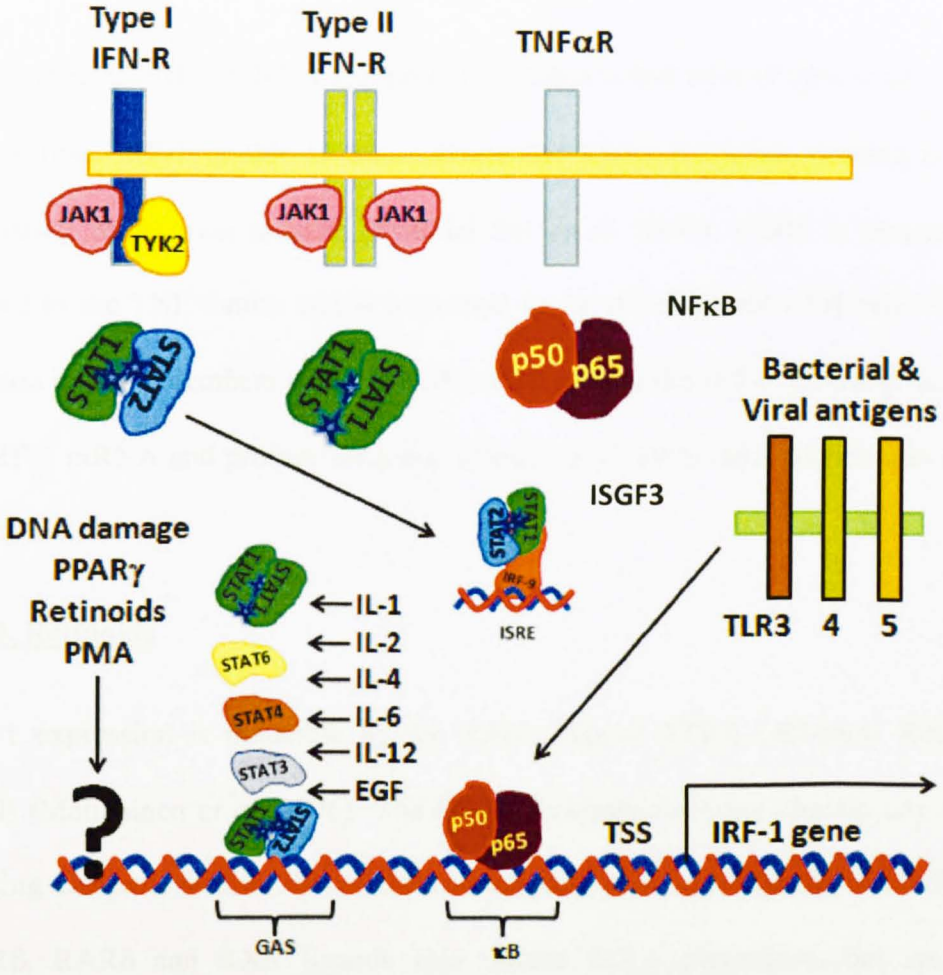

Figure 1.11 The IRF-1 promoter and agents that regulate its expression. Cartoon illustrating the major pathways that regulate IRF-1 expression. Type I IFN receptors (IFNα, IFNβ etc) when bound promote phosphorylation of STAT-1 and STAT-2 by the tyrosine kinases TYK2 (Tyrosine Kinase 2) and JAK1 (Janus Activated Kinase 1). This promotes heterodimerisation and binding to GAS elements in ISGs. The STAT-1/2 heterodimers can also interact with IRF-9 to promote the formation of ISGF3 (Interferon Stimulated Gene Factor 3) complexes, which interact with ISRE sequences through the DBD of IRF-9. Type II IFN receptors are bound by IFNγ, which promotes phosphorylation of STAT-1 homodimers, which can also bind the GAS elements. Several other cytokines are able to promote STAT binding to the GAS element in the IRF-1 promoter including Interleukins and EGF (Epidermal Growth Factor). The κB element is activated by NFκB p50-p65 heterodimers which can be activated by TNFα signalling, but also through the CD40 and TLR pathways. A number of other agents also regulate IRF-1 expression through unknown mechanism including PPARγ (Peroxisome Proliferator Activated Receptor γ) agonists, and PMA (Phorbol-12-myristate-13 acetate).

1.4.3. Tumour necrosis factor (TNFα)

TNFα induces IRF-1 mRNA and protein in humans and mice (Fujita *et al.* 1989). In addition, IRF-1 is able to transactivate the TNFα promoter, causing an up-regulation of its own inducer (Vila-del Sol *et al.* 2008). CD40 is structurally related to the TNF family and is important in the development of B cells. CD40 ligation induces members of the NFκB family to bind the IRF-1 promoter leading to IRF-1 mRNA and protein induction (Gupta *et al.* 1998 and Moschonas *et al.* 2008).

1.4.4. Retinoids

IRF-1 expression is inducible by the RARα ligand ATRA (*All-trans* Retinoic Acid) (Matikainen *et al.* 1996). The IRF-1 promoter does not contain any RAR binding elements within 3kb of the transcription start site (Clarke *et al.* 2004). RARβ, RARδ and RXR ligands also induce IRF-1 expression, but are less effective than RARα (Luo and Ross 2006). It has been suggested that some of the cellular activities of retinoids (cell cycle arrest, apoptosis and differentiation) may be achieved (at least partially) through the activation of IRF-1. Several important IRF-1 target genes have been identified to be strongly induced by synergistic action of retinoids and IFNγ, including TRAIL (TNF Related Apoptosis Inducing Ligand), OAS 2 (2'-5' Oligoadenylate Synthase 2), p21, CIITA and XAF 1 (XIAP Associated Factor 1) (Clarke *et al.* 2004, Arany *et al.* 2003b, Sanda *et al.* 2007 and Wang *et al.* 2006).

1.4.5. Bacterial and viral induction

IRF-1 mRNA and protein is inducible by a number of ligands for the Toll Like Receptors (TLR). These ligands are components of bacteria or viruses which activate transcription via signalling to NFκB family members. Each TLR responds to a different bacterial or viral ligand, conferring a high degree of specificity to the transcriptional response. TLR ligands which activate IRF-1 expression include messenger RNA (TLR3), oligodeoxyribonucleotides (TLR9) and LPS (TLR4) (Fujita *et al.* 1989, Kariko *et al.* 2004, Uchijima *et al.* 2001 and Schmitz *et al.* 2007).

1.4.6. Genotoxic stress

Ionising radiation (IR) and etoposide cause an induction of IRF-1 protein (Tanaka *et al.* 1996 and Pamment *et al.* 2002). Genotoxic induction of IRF-1 occurs at the transcriptional rather than post translational level (in contrast to p53). IR and etoposide also caused an increase in IRF-1 t½ (half life) from thirty minutes to two hours, suggesting genotoxic stress effects the degradation of IRF-1. The induction of IRF-1 by genotoxins is dependent on the ATM (Ataxia telangiectasia mutated) pathway, although it is not thought that ATM directly phosphorylates IRF-1, as it does not contain any ATM consensus phosphorylation sites (Pamment *et al.* 2002). The DNA damaging agent MNU (N-methyl-N-nitrosourea) promotes an increased expression of IRF-1 mRNA in mice (Liu *et al.* 2004).

1.5.1. IRF-1 and transcription

Like most TFs, IRF-1 co-operates with a number of other transcription factors including STAT-1, NFκB, p53 and GRα (see table 1.5). IRF-1 also co-operates with other members of the IRF family including IRF-2 and IRF-8 (Meraro *et al.* 1999). Additionally, anti-cooperative interactions with IRF family members have also been reported (Brass *et al.* 1999) with IRF-4 preventing the IRF-1 dependent activation on the TRAIL promoter (Yoshida *et al.* 2005). The mechanism by which IRF-1 brings about transcriptional activation includes recruitment of other TFs and coactivator proteins. IRF-1 has been shown to interact with the coactivators CBP, p300, PCAF and TIF2 in addition to making direct contacts with RNA Pol II (see table 1.5). Detailed studies on the GBP promoter in mice shows that following IFN treatment STAT-1 is recruited to the promoter along with CBP, with IRF-1 binding occurring much later. IRF-1 recruitment was closely matched by Pol II recruitment, STAT-1-Pol II protein interaction could not be detected, while an IRF-1-Pol II interaction was detected. Consequently IRF-1 serves to initiate transcription of GBP mRNA on a promoter that has been made available by previous STAT and CBP binding (Ramsauer *et al.* 2007). The ability of IRF-1 to bring about transcription is likely regulated by the agents that induce IRF-1 expression. Low levels of IRF-1 are present in most cells, but may not be high enough to promote transcription of some target genes. The quick increase in IRF-1 expression is usually driven by external stimuli such as IFNs, retinoids, LPS or TNFα. Some examples of differential regulation of IRF-1 by external induction have been reported, for example, IRF-1 regulates the expression of IL-10 following IFNα treatment, but not LPS. Activation of other

TFs that interact with IRF-1 or PTMs initiated by external agents may explain the differences in response (Ziegler-Heitbrock *et al.* 2003).

IRF-1 has been shown to up-regulate the expression of numerous genes in several reported cDNA microarray experiments (Erickson *et al.* 2004, Liu *et al.* 2004 Kroger *et al.* 2007, Dror *et al.* 2007, Schmitz *et al.* 2007 and Aly *et al.* 2008). Many of these genes are involved in immune regulation, although genes involved in metabolism, cell cycle and apoptosis are also regulated by IRF-1 confirming its role in diverse processes. ChIP-chip analysis of IFNγ treated breast cancer cells also suggests that IRF-1 regulates genes involved in numerous processes, with DNA damage and repair being a major functional group of regulated genes. IRF-1 protein was also chromatin immunoprecipitated at a number of promoters of other TFs suggesting IRF-1 may regulate transcriptional cascades (Frontini *et al.* 2009).

Traditionally thought of as a transcriptional activator, IRF-1 has been shown to repress the expression of a number of genes including IL-4, Survivin, CDK2 (Cyclin Dependent Kinase 2), Cyclin D1, and Foxp3 (Forkhead Box P3) (Elser *et al.* 2002, Pizzoferrato *et al.* 2004, Xie *et al.* 2003, Kroger *et al.* 2007 and Fragale *et al.* 2008). Micro-array analysis in IRF-$1^{+/+}$ and IRF-$1^{-/-}$ mice found 55 genes down-regulated and 17 up-regulated genes in mice with experimentally induced colitis (Mannick *et al.* 2005). Similarly IRF-1 was shown to both up-regulate and down-regulate gene expression in other micro-array studied (Liu *et al.* 2004a, Kroger *et al.* 2007, Schmitz *et al.* 2007 and Aly *et al.* 2008). Mechanistically, little is known about how IRF-1 brings about transcriptional repression, although one study showed that IRF-1 was able to form a complex with HDAC1 (Histone de-acetylase 1) and NFκB-p65 on the PDGF-D (Platelet

Derived Growth Factor-D) promoter (Liu and Khachigian 2009). The LxxLL motif of IRF-1 is needed for transcriptional repression of the CDK2 promoter (Eckert *et al.* 2006).

The oncoviral E7 protein interacts with IRF-1 and promotes a switch from activator to repressor on the IFNβ promoter. It is possible that the ability of E7 to recruit the NuRD (Nuclear Remodelling and De-acetylation complex) repressor complex is responsible for this switch (Park *et al.* 2000).

IRF-1 may be able to regulate transcription without direct DNA binding. The cell cycle inhibitor p21 was one of the earliest IRF-1 target genes identified, although the p21 promoter does not contain any functional IRF-1 binding sites (Tanaka *et al.* 1996). Rather than directly binding the p21 promoter, IRF-1 interacts with p53 and stimulates its transcriptional activity (Dornan *et al.* 2004). It is not yet known if IRF-1 has any roles not directly related to transcription, although IRF-1 has been shown to interact with VEGFR2 (Vascular Epidermal Growth Factor Receptor 2), this interaction may be important for the anti-angiogenic activity of IRF-1 (Lee *et al.* 2008).

1.5.2. Apoptosis

IRF-1 regulates apoptosis at several levels, including transcriptional up-regulation of death ligands and death receptors, caspases and pro-apoptotic factors. Additionally IRF-1 can down regulate the expression of anti-apoptotic factors. IRF-1 is capable of promoting both extrinsic death receptor mediated apoptosis and intrinsic mitochondrial apoptosis (Clarke *et al.* 2004 and Gao *et al.* 2009).

IRF-1 regulates the expression of CD95 (FasL) in a number of cell types including, monocytes, esophageal cancer cells, breast cancer cells and renal cancer cells (Conte *et al.* 2003, Porta *et al.* 2005, Watson *et al.* 2006 and Tomita *et al.* 2003). Additionally, the ligand for CD95, has been shown to be transcriptionally up-regulated by IRF-1 (Chow *et al.* 2000 and Kirchhoff *et al.* 2002).

TRAIL, (TNFα Related Apoptosis Inducing Ligand) is a member of the TNFα super family, but unlike TNFα and Fas, its receptors are more widely expressed, suggesting that TRAIL can act on many cell types. TRAIL brings about apoptosis via two receptors DR4 and DR5 (Death Receptor 4/5) which signals via caspases to bring about apoptosis. TRAIL is induced in APL and breast cancer cell lines by co-treatment with IFNγ and retinoids. Recruitment of IRF-1 to the TRAIL promoter was identified by EMSA (Electrophoretic Mobility Shift Assays) and ChIP (Chromatin Immunoprecipitation). In co-culture experiments using the breast cancer cell line SK-BR3 and the T cell line Jurkat, treatment with IFNγ and RA (retinoic acid) caused TRAIL dependent cell death in both cell lines. Using normal T cells in place of Jurkat cells caused a marked decrease in apoptosis in these cells, suggesting that TRAIL is selective for cancer

cells (Clarke *et al.* 2004). IRF-1 also up-regulates TRAIL expression in A549, H1299 and UM-UC-12 cells (Park *et al.* 2004, Eckert *et al.* 2006 and Papageorgiou *et al.* 2007).

Many groups have reported caspase 1 dependent apoptosis following IRF-1 induction. caspase 1 levels are up-regulated by IRF-1 and down-regulated by IRF-2 in vascular smooth muscle cells, rat and mouse islet cells, ovarian cancer cell lines, monocytic cells, pancreatic cancer cell lines, gastrointestinal neuroendocrine tumours and the Daudi cell line (Tamura *et al.* 1996b, Horiuchi *et al.* 1999, Karlsen *et al.* 2000, Detjen *et al.* 2001, Kim *et al.* 2002 and Iwase *et al.* 1999). Caspase 8 is an important initiator caspase which is involved in signalling via the TNFα, Fas and TRAIL death receptors. IRF-1 transcriptionally increases caspase 8 in neuroblastoma cells, and breast cancer cells (Casciano *et al.* 2004, Ruiz-Ruiz *et al.* 2004, De Ambrosis *et al.* 2007). A number of other caspases have been suggested to be regulated by IRF-1 including caspase 7 (Kim *et al.* 2004, Sanceau *et al.* 2000 and Bouker *et al.* 2005) and caspase 3 (Sun *et al.* 2006).

Several other pro-apoptotic factors including GADD153 (Growth Arrest and DNA damage inducible 153), BclG, (B Cell Lymphoma G) NOXA (Latin for *damage*) and XAF1 are regulated by IRF-1 (Watanabe *et al.* 2003, Zhang *et al.* 2006, Lallemand *et al.* 2007 and Wang *et al.* 2006). IRF-1 promotes mitochondrial intrinsic apoptosis in gastric cancer cell lines. IRF-1 transcriptionally up-regulates the apoptotic protein PUMA (p53 Up-regulated Modulator of Apoptosis) although it does not effect the expression of other BH3 proteins such as Bid, Bad or Bim. IRF-1 is capable of up-regulating PUMA independently of p53 (Gao *et al.* 2009).

In addition to inducing expression of pro-apoptotic factors IRF-1 also down regulates anti-apoptotic factors. Microarray analysis of breast cancer cell lines (MDA-MB-468 and SK-BR3) that over express Ad-IRF-1 (adenovirally transduced IRF-1) show a 15 fold down regulation of survivin. This down-regulation was confirmed, and shown to be independent of p53. The authors noted that cells that express Ad-IRF-1 show increased rates of apoptosis. Xenograph models of breast cancer in which Ad-IRF-1 was injected into tumours show that IRF-1 was able to cause growth inhibition *in vivo,* cancer cells removed from these tumours show high expression of IRF-1 and no expression of survivin (Pizzoferrato *et al.* 2004). Survivin levels were also decreased in esophageal cell lines that have been transfected with IRF-1 (Watson *et al.* 2006).

1.5.3. IRF-1 and cell cycle

In normal cells, genotoxic stress such as IR or adriamycin causes cell growth arrest. Embryonic fibroblasts from IRF-$1^{-/-}$ mice do not undergo cell cycle arrest - in a similar fashion to $p53^{-/-}$ embryonic fibroblasts (EFs). In wild type EFs a 90% decrease in S phase cells occurs following γ irradiation, however in IRF-$1^{-/-}$ EF only a 10% decrease occurs. This is a similar level to $p53^{-/-}$ EFs (Tanaka *et al.* 1996). Since CDK2 and CDK4 are involved in this process, they were assayed for their phosphorylation by *in vitro* kinase assays. In IRF-$1^{+/+}$ cells a strong decrease in phosphorylation was seen in both CDK2 and CDK4 following γ irradiation, this did not occur in IRF-$1^{-/-}$ cells. This suggested a defect in CDK inhibitors (CKI). The levels of these proteins were tested in IRF-$1^{-/-}$ cells. Of the CKIs tested only p21 was found to be down regulated in IRF-$1^{-/-}$ cells, while p27, p15, p16, p18 and p19 were unchanged (Tanaka *et al.* 1996).

The G1/S related cyclin dependent kinase 2 (CDK2) is repressed by IRF-1, but not by IRF-2, IRF-3 or IRF-7. This repression is independent of p53 and CDP/Cut/Cux1 homeodomain protein, which all repress CDK2 by acting on different regions of the promoter. The promoter region found to be responsive to IRF-1 was found not to contain any binding elements for IRF-1, suggesting that IRF-1 does not directly bind this region. Rather a Sp1 site is located in this area. It was found that Sp1 positively regulates this portion of the promoter, while transfection of IRF-1 causes repression. Biochemical analysis suggests that IRF-1 indirectly represses CDK2 by interfering with Sp1 expression (Xie *et al.* 2003).

IRF-1 has been shown to revert an oncogenic gene signature in NIH3T3 cells that express ectopic c-Myc and c-Ha-Ras. Microarray analysis identified 1,347 genes that were de-regulated by the expression of these oncogenes. Activation (by addition of extradiol) of the hER-IRF-1 chimeric protein caused 60% of these genes to revert back to untransformed levels (cells not expressing c-Myc and c-Ha-Ras). Cyclin D1 was among the transcripts regulated by IRF-1. The cyclin D1 protein is involved in the G1/S phase of the cell cycle. In untransformed cells IRF-1 had little effect on cyclin D1 expression, with transformation being required for IRF-1 dependent cyclin D1 repression. The DBD of IRF-1 was required for IRF-1 to repress cyclin D1 expression, although no IRF binding sites could be found up to 3kb from the TSS (transcription start site). The repression of cyclin D1 also occurred twenty four to forty eight hours after IRF-1 activation. It is possible that IRF-1 has an indirect activity towards cyclin D1. Experiments in mice show that cyclin D1 repression decreases tumour formation, as such this may be one mechanism by which IRF-1 acts as a tumour suppressor (see section 2.1.5) (Kroger *et al.* 2007). Mouse breast cancer cell lines undergo cell cycle

arrest when infected with Ad-IRF-1, however when two non-malignant breast cancer cell lines (C127I and NMuMG) were infected the cell cycle profile remained unchanged (Kim *et al.* 2004).

1.5.4. DNA damage and repair

Splenocytes from IRF-$1^{-/-}$ mice are not able to undergo apoptosis following γ irradiation, Adriamycin or Etoposide treatment unlike splenocytes from wild type mice (Tamura *et al.* 1995). In addition, MEFs from IRF-$1^{-/-}$ mice do not undergo cell cycle arrest when treated with γ radiation or adriamycin (Tanaka *et al.* 1996). Consequently IRF-1 is needed for cells to respond appropriately to DNA damage. IRF-$1^{-/-}$ hepatocytes are significantly less able to repair a UVC damage reporter construct that hepatocytes from IRF-$1^{+/+}$ mice (Prost *et al.* 1998). IFNγ treatment in the breast cancer cell line H3396 promotes IRF-1 recruitment to a number of genes that are involved in DNA damage and repair responses. Some of these genes include BARD1 (BRCA Associated RING Domain 1), BRIP1 (BRCA Interacting Partner 1), PMS2L4 (Post Meiotic Segregation Increased 2 Like 4), LIG4 (DNA Ligase 4), UNG (Uracil DNA Glycosylase) and PCNA (Proliferating Cell Nuclear Antigen). IFNγ treatments and IRF-1 over-expression also leads to an increase in mRNA level for these genes. BRIP1 (a member of the Fanconi Anaemia family of proteins) is involved in repair of intra-strand crosslinks (ICL). BRIP1 does not localise to ICL foci following melphalan (an ICL inducing agent) treatment in IRF-1 depleted cells. In addition, the characteristic G2/M accumulation that occurs in patients deficient in BRIP-1 is evident when IRF-1

protein is depleted. This suggests that IRF-1, via its transcriptional regulation of BRIP1 is involved in ICL repair (Frontini *et al.* 2009).

1.5.5. IRF-1 and cancer

Strong evidence suggests that IRF-1 has tumour suppressor activities. IRF-1 can act as a tumour suppressor intrinsically via its ability to regulate the expression of genes involved in cell cycle regulation, apoptosis and DNA damage/repair. IRF-1 also has an extrinsic activity in tumour suppression, as it is required for antigen presentation and the proper differentiation of immune cells required for immune surveillance and thus destruction of damaged cells. Four main arguments can be made in support of IRF-1s role in tumour suppression.

1. IRF-1 levels (mRNA and protein) are decreased in several cancers. There is often an inverse relationship between IRF-1 expression and patient survival (see table 1.6).
2. IRF-1 is able to antagonise the transforming abilities of oncogenes.
3. Animals models of tumour growth support cell culture data suggesting IRF-1 is involved in apoptosis and cell growth/proliferation.
4. IRF-$1^{-/-}$ mice have increased susceptibility to spontaneous tumour development when crossed with $p53^{-/-}$ mice.

Reduced expression	Cytosolic localisation	Exon Skipping	Point Mutations	PTM defects	Increased expression
Bladder[1]	Breast[2]	Cervical[3]	Lung[9]	Ovarian[10]	Liver[15]
Brain[2]	Colorectal[4]	Leukaemia[7]	Stomach[16]		
Breast[3]	Endometrial[5]	Liver[8]			
Cervical[4]	Esophageal[7]				
Colorectal[5]	Skin[13]				
Endometrial[6]					
Esophageal[7]					
Leukaemia[8]					
Liver[9]					
Lung[10]					
Neuroendrocrine[11]					
Ovarian[12]					
Skin[13]					
Stomach[14]					

Table 1.6 Abnormal expression of IRF-1 in human cancers. As discussed in section 1.2.2, 1.2.3 and 1.2.4 the IRF-1 gene is prone to exon skipping, deletions and LOH. Immunohistochemical analysis has identified a correlation between IRF-1 expression and clinical outcome for a number of malignancies including breast, skin and colorectal cancers. In addition excess SUMO-ylation and nuclear exclusion have also been noted in some cancer biopsies. Above is a summary of the types of deregulation that occur on the IRF-1 protein, and the cancers in which they occur. The reduced expression is either due to the 5q abnormality or an unknown loss of IRF-1 expression. So far the only PTM defect of IRF-1 was enhanced SUMO-1ylation. Leukaemia includes MDS, AML and CML. References: **1)** Kram *et al.* 2001 **2)** Yoshino *et al.* 2005. **3)** Doherty *et al.* 2001 Connett *et al.* 2005 Cavalli *et al.* 2009 **4)** Lee *et al.* 2006 **5).** Camus *et al.* 2009, Coppola *et al.* 2009. **6)** Kuroboshi *et al.* 2003 Giatromanolaki *et al.* 2004 **7)** Watson *et al.* 2006 Wang *et al.* 2007, Ogasawara *et al.* 1996 and Peralta *et al.* 1998 **8).** Tzoanopoulos *et al.* 2002, Maratheftis *et al.* 2006 Harada *et al.* 1993, Green *et al.* 1999 Hochhaus *et al.* 1997 and Mild *et al.* 1999 Preisler *et al.* 2001 **9).** Moriyama *et al.* 2001 and Tnani and Bayard 1999 . **10).** Mendes-da-Silva *et al.* 2000 and (Eason *et al.* 2003) **11).** Zhou *et al.* 2000 **12). 13).** Lowney *et al.* 1999. **14).** Nozawa *et al.* 1998 , **15).** Shen *et al.* 2009 . **16).** Nozawa *et al.* 1998 .

Several studies have shown that IRF-1 can antagonise the activities of a number of oncogenes. The first study to show that IRF-1 is involved in cancer used the oncogene c-Ha-Ras (Rous sarcoma oncogene). Normally, when transfected in MEFs ras can only induce transformation when another oncogene such as c-Myc is introduced. IRF-$1^{-/-}$ MEFs infected with c-Ha-ras undergo transformation, suggesting that loss of IRF-1 has a similar effect as gain of an oncogene.

The IRF-$1^{-/-}$ c-Ha-Ras expressing MEFs show increased rates of growth in soft agar assays. Introduction of either mouse or human IRF-1 into the IRF-$1^{-/-}$ ras expressing MEFs prevented transformation (Tanaka *et al.* 1994). To determine if loss of IRF-1 or the dominance of IRF-2 was the cause of this transformation, double IRF-1 / IRF-2 knockouts were generated. The transformed phenotype was the same as the IRF-$1^{-/-}$ singe knockout. As such it is the loss of IRF-1 rather than the predominance of IRF-2 activity that allows ras transformation. Apoptosis was promoted by ras transformation in wild type MEFs, but not in $p53^{-/-}$ or IRF-$1^{-/-}$ mice when treated with the DNA damaging agents adriamycin, 5-flouro-uracil or ionising radiation. Therefore IRF-1 is important in c-Ha-Ras dependent apoptosis (Tanaka *et al.* 1994). IRF-1 can also revert the transformed phenotype of cells expressing the oncogenes c-Myc, c-Fos, E1a/b and HER-1 (Tanaka *et al.* 1994, Kirchhoff and Hauser 1999 and Kroger *et al.* 2003).

NIH 3T3 cells stably expressing the estradiol activatable hER-IRF-1 (estrogen receptor ligand binding domain fused to IRF-1 protein) chimera with a bi-directional c-Myc/ c-Ha-Ras Tet off system were used to further probe the role of IRF-1 following oncogene transformation. Expression of tetracycline inducible c-Myc/Ras (by addition of doxycycline) causes an increase in S phase and a decrease in G1 phase of the cell cycle – consistent with the transforming properties of these oncogenes. Activation of IRF-1 reverses this pattern back to non transformed levels (Kroger *et al.* 2003).

The hER-IRF-1 c-Myc/ c-Ha-Ras cells were implanted in nude mice (without B and T cells). Transformation (by dox treatment) of these cells led to tumour formation in all mice within three weeks with a mean tumour size of 2 cm^3. In the non transformed (untreated) cells no mice developed tumours. Cells that were transformed by c-Myc/ c-Ha-Ras induction, but had activated IRF-1 (estradiol treatment) delayed tumour formation by three weeks; the mean tumour volume was 1.5cm^3 and 40% of the mice did not develop tumours at all. This suggests that IRF-1 is able to bring about repression of transformation independently of IFNs and lymphocytes. To address the delay in the tumour formation, tumours were removed from the mice. It was found that in the delayed tumours only 10% of the IRF-1 –hER remained. This suggests that the delay in tumour formation is caused by clearance of the IRF-1 expressing cells, rather than an inability of IRF-1 to revert the transformation (Kroger *et al.* 2003).

Hepa 1-6 cells which stably express hER-IRF-1chimera demonstrate a decrease in anchorage dependent cell growth via soft agar colony forming assays. Implantation of control Hepa 1-6 cells into mice resulted in a high incidence of

tumour formation. Treatment of the mice with estradiol (and therefore activation of IRF-1) caused complete protection of the mice on six out of eight cases, with the other two mice having small, slow growing tumours. Re-challenge experiments suggest that T memory cell immunity occurs following IRF-1 activation, an increase in cytotoxic T lymphocyte immunity and recognition of tumour specific antigens was also found. Mice injected with Hepa 1-6 hER-IRF-1 which had undergone $CD4^+$ or $CD8^+$ T cell depletion did form tumours, but the growth rate was delayed, suggesting that the host immune system is not entirely responsible for the reduction in tumour formation. Estradiol treatment of mice infected with Hepa 1-6 hER-IRF-1 cells 19 days later (when the tumours have grown to around 200 mm^3) caused a permanent growth arrest in these tumours 4 days later (Kroger *et al.* 2001).

The MCA-101 cell line is a highly aggressive methylcholanthrene induced sarcoma which expresses little or no MHC I molecules on its surface. Injection of these cells into mice caused rapid tumour formation and death. Stable transfection of murine IRF-1 under the control of the CMV promoter into these cells leads to an induction of MHC I molecules. Additionally cell growth was decreased and anchorage independent cell growth in soft agar assays was reduced. Transplanting these cells into mice increased the tumour latency and slowed tumour growth, while MCA-101 cells carrying empty vector displayed their characteristic oncogenicity. Mice infected with IRF-1 expressing MCA-101 cells were immune to subsequent re-challenge with these cells, suggesting immunity is developed. Gamma irradiation of mice infected with the IRF-1 expressing sarcoma cells caused a shorter tumour latency and faster tumour growth. This suggests that an

intrinsic reversion of phenotype and an immune recognition play a role in IRF-1's ability to regulate oncogenesis (Yim *et al.* 1997).

Although there is considerable evidence for IRF-1's role in cancer, IRF-1 null mice develop a surprisingly low incidence of spontaneous tumours. Up to two hundred days after birth only 2 % (6 / 315) of IRF-$1^{-/-}$ mice developed tumours (a malignant fibrous histiocytoma like sarcoma). No wild type mice (0/625) developed spontaneous tumours. However the incidence of spontaneous tumour formation in the IRF-$1^{-/-}$ mice was not considered statistically significant.

A possible explanation for this low incidence of tumour formation is that IRF-1 co-operates down stream of another tumour suppressor. IRF-1 has been shown to co-operate with the prototypical tumour suppressor p53 (Tanaka *et al.* 1996). Experiments were conducted in which IRF-$1^{-/-}$ mice were crossed with $p53^{-/-}$ mice. If IRF-1 was a downstream mediator of the p53 pathway the incidence and spectrum of tumour incidence in the double knockout mice would be expected to remain the same (Nozawa *et al.* 1999).

Within two hundred days, 56% (137 / 254) of $p53^{-/-}$ developed tumours, while 96% (322 / 355) of the p53/IRF-$1^{-/-}$ developed tumours, with a seven fold increase in the number of mice carrying multiple tumours compared to the $p53^{-/-}$ single mutants. In addition, the spectrum of tumour incidence was drastically different, with some types of tumour only occurring in the double knockout mice (ganglioneuroblastomas and medulloblastomas). Therefore IRF-1 is not hypostatic to p53 in tumour predisposition. One possibility for the massive increase in tumour incidence in the double knockout mice was suggested to be caused by a

fault in tumour immune-surveillance, as IRF-1 is important in the functioning of the immune system.

To determine if this was the case, chimeric mice were generated to the point at which the immunological defects associated with loss of IRF-1 were not detectable. In these mice, 9/12 tumours originated from the double$^{-/-}$ cells while three originated from the p53 $^{-/-}$ cells. This suggests that there is an intrinsic increased susceptibility to tumorigenesis in cells that have lost both p53 and IRF-1. In support of their increased tumour formation, cells from the double $^{-/-}$ mice were less able to undergo apoptosis in response to DNA damage and showed impaired growth characteristics (Nozawa *et al.* 1999).

IRF-1$^{-/-}$ mice were also crossed with mice that contain five to six copies of the oncogenic c-Ha-Ras oncogene (RasH2 mice). Six months after birth, the mice were sacrificed. 7% (2/30) of RasH2 heterozygous IRF-1$^{-/+}$ developed tumours, while 44% of IRF-1$^{-/-}$ RasH2 mice developed tumours - mostly angiosarcomas (Nozawa *et al.* 1999). This suggests that loss of IRF-1 and gain of an oncogene increases the incidence of tumours.

A contrasting study by Eason *et al.* showed that IRF-1$^{-/-}$ mice are prone to developing an anaplastic large cell lymphoma like condition. The Nowaza study showed that IRF-1$^{-/-}$ mice are not significantly prone to developing spontaneous neoplasia. The key difference between these studies was the age of mice used. The Nowaza study used two hundred days mice and the Eason study used three hundred days old mice. To address the discrepancy the latter group tested two hundred daya IRF-1$^{-/-}$ mice for lymphoma and found no abnormalities in the

lymph nodes. This suggests that IRF-1 alone may be important in the development of neoplasia, but the development is delayed compared to other tumour suppressors such as p53 (Eason *et al.* 2003).

IRF-1 may also be involved in the development of lymphomas following HCV (Hepatitis C virus) infection. IRF-1 null mice which express HCV core proteins are significantly more prone to T and B cell lymphomas, lymph node and thymic hyperplasia, splenomegaly and abdominal adenocarcinomas (Machida *et al.* 2009). The number and onset of tumour formation is higher in IRF-$1^{-/-}$ HCV mice than the HCV IRF-$1^{+/+}$ mice 500 days post infection. The type of tumour developed was not different between IRF-$1^{-/-}$ and IRF-$1^{+/+}$ HCV expressing mice. In agreement with previous studies IRF-$1^{-/-}$ mice were not susceptible to spontaneous tumour development when compared to their wild type littermates within 500 days of observation. Slightly higher levels of spleen, liver and thymic hyperplasia was noted in the IRF-$1^{-/-}$ mice suggesting that with time, malignancies may develop in these mice (Machida *et al.* 2009).

In addition to oncogenes and HCV infection, IRF-$1^{-/-}$ mice are susceptible to tumour development when treated with the alkylating agent MNU. Two out of twenty five IRF-$1^{+/+}$ mice developed thymic lymphomas, but 24/25 IRF-$1^{-/-}$ developed thymic lymphomas following MNU treatment. They displayed enlarged spleens, lymph nodes and thymus. The splenic T lymphocytes had a malignant phenotype with giant multinucleated mitotic figures. MNU treated IRF-$1^{-/-}$ mice showed decreased expression of LTα , LTβ (Lymphotoxin), IFNγ, IL12-p35 and IL12-p40, all of which have been shown to be important in immune surveillance. In another experiment 80% of IRF-$1^{+/+}$ mice survived MNU

treatment for 18 weeks, while only 10% of IRF-$1^{-/-}$ survived. Treatment of mice with IL-12 partially rescued the IRF-1 deficiency, as 60% of the IL-12 treated IRF-$1^{-/-}$ mice survived. This study shows that IL-12 (an IRF-1 target gene), is required for the prevention of thymic lymphoma formation, and thus tumour immunosurveilance is important for IRF-1 tumour suppressor activity (Liu et al. 2004).

From the studies conducted to date it can be concluded that IRF-1 does not strongly promote tumour initiation, - since loss of both IRF-1 allele's does not initiate a significant development of tumours. However IRF-1 is more likely involved in tumour development, as IRF-1 loss synergises with either the loss of tumour suppressors (p53) or treatments with tumour inducing agents in promoting tumour development.

1.5.6. IRF-1 and Immunity

IRF-1 is a key player in the immune system and is essential for the proper functioning of the innate and acquired immune responses. Evidence for the role of IRF-1 in immunity includes;

1. IRF-1 is needed for the development of diverse types of immune cell.
2. IRF-$1^{-/-}$ mice are less able to combat a number of pathological infections.
3. Co-operation between the pathogen sensing TLR pathway and IRF-1.
4. IRF-1 is required for proper antigen presentation.
5. IRF-1 transcriptionally regulates a large number of cytokines.
6. IRF-1 is important for anti-viral defence.

1.5.7. Role of IRF-1 in development of immune cells.

A large body of research suggests that the transcriptional programme initiated by IRF-1 is required for the proper differentiation of immune cells. IRF-$1^{-/-}$ mice display a prevalence of immature granulocytes and lack mature functional granulocyte cells. Ectopic expression of IRF-1 in myeloblast cells promotes differentiation into the neutrophil lineage, confirming IRF-1 plays a role in granulopoesis (Manzella *et al.* 1999, Coccia *et al.* 2001 and Testa *et al.* 2004).

Dendritic cells are an important group of antigen presenting cells that process and expose antigens to immune cells enhancing immunological responses. Several subtypes of dendritic cells exist, and IRF-$1^{-/-}$ mice were equipped with an abnormal proportion of some subtypes while others are completely absent or immature. Dendritic cells from IRF-$1^{-/-}$ mice also have decreased cytolytic activity compared to cells from IRF-$1^{+/+}$ mice (Gabriele *et al.* 2006, Remoli *et al.* 2007 and De Creus *et al.* 2002).

IRF-1 deficient mice carry normal numbers of natural killer (NK) T cells, but functionally, these cells are far less cytotoxic. NK cells from IRF-$1^{-/-}$ mice were found to be less able to clear tumour cells from mice (Duncan *et al.* 1996). It has been suggested that the lack of IL-15 (an IRF-1 target gene) is responsible for the lack of mature functional NK cells in IRF-$1^{-/-}$ mice (Ogasawara *et al.* 1998). IRF-1 is also needed for the functioning and development of cytotoxic T cells (White *et al.* 1996 and Penninger *et al.* 1997). T regulatory cells (T_{reg}) can dampen immune responses and are thought to be involved in inflammation. IRF-$1^{-/-}$ mice had high levels of T_{reg} cells. IRF-1 can repress the expression of FOXP3, which is

needed for T_{reg} development. Consequently IRF-$1^{-/-}$ cells express higher levels of FOXP3 which promotes the development of T_{reg} cells (Fragale *et al.* 2008).

The ability of IRF-1 to promote differentiation of T helper cells has been intensely studied. There are two major subtypes of T helper cells (Type I and II), Type I aid immune responses to cellular threats by macrophages, while type II helper cells are involved in humoral responses through B cells. IRF-1 regulates the balance of these two subsets, as IRF-$1^{-/-}$ mice express high levels of type II, with very little type I cells being present. An explanation for this may involve IRF-1 dependent regulation of cytokines which regulate T helper differentiation. IRF-1 up-regulates the expression of IL-12 and the IL-12 receptor. IL-12 excretion promotes differentiation of naïve cells into T helper type I cells. IL-4 is repressed by IRF-1; IL-4 promotes the differentiation into type II helper cells. Consequently the altered balance of cytokines found in IRF-$1^{-/-}$ cells promotes and abnormal eschewing of T helper cells (McElligott *et al.* 1997, Elser *et al.* 2002 and Kano *et al.* 2008).

1.5.8 IRF-1 and immune defence against pathogens.

IRF-1 is involved in combating infection from a variety of pathogens. In numerous studies IRF-$1^{-/-}$ mice succumb to infection while their wild type littermates survive. Some of the pathogens IRF-$1^{-/-}$ mice are less able to combat include; *Mycobacterium bovis, Brucella abortus, Toxoplasma gondii*, and *Anaplasma phagocytophilum* (Ko *et al.* 2002, Lang *et al.* 2006 and Thomas *et al.* 2005).

1.5.9 Co-operation between IRF-1 and the Toll Like Receptor (TLR) pathway

The activities of IRF family members are closely entwined with the TLR (Toll Like Receptor) signalling pathway (Honda and Taniguchi 2006a). IRF-1 transcriptionally regulates a number of TLR genes including TLR3, TLR4, TLR5 and TLR9 (Heinz *et al.* 2003, Nhu *et al.* 2006 and Guo *et al.* 2005). IRF-1 interacts with the TLR adapter protein MyD88 (see table 1.5). This interaction increases the shuttling of IRF-1 into the nucleus and causes a shift in the IRF-1 pI (isoelectric charge), possibly via phosphorylation. The interaction with MyD88 may be important in the synergy with NFκB, which is an essential requirement for the IRF-1 dependent immune response (Negishi *et al.* 2006 and Schmitz *et al.* 2007). The stimulation of TLR9 causes activation and nuclear translocation of both IRF-1 and NFκB through different pathways involving MyD88. This allows both IRF-1 and NFκB to be available in the nucleus at the same time, allowing them to co-operate with each other on a number of promoters involved in the immune response (Colonna 2007).

1.5.10. IRF-1 involvement in antigen presentation.

MHC I and MHC II molecules (major histocompatability class I / II) are involved in the presentation of cell surface antigens used to define self and non self to the immune system. MHC I molecules are involved in the presentation of antigens to cytotoxic T cells. MHC II molecules modulate peptide loading on the lysosomal membrane. MHC refers to the gene dense region which also contains molecules involved in the antigen processing including TAP (Transporter Associated with Antigen Processing) and Tapasin while HLA (Human Leukocyte Antigen) refers

to the antigen binding molecules. IRF-1 is important in the expression of MHC I and MHC II in several cell types (Hobart *et al.* 1997). IRF-1 induces MHC I expression in synergy with NFκB when induced with Newcastle Disease Virus (Ten *et al.* 1993).

The IFNγ dependent induction of both MHC I and II are reduced in the IRF-$1^{-/-}$ mice. Lower levels of CTIIA in the IFNγ treated IRF-$1^{-/-}$ mice may be involved in the lower levels of MHC II (Hobart *et al.* 1997 and Jarosinski and Massa 2002). CTIIA is a master regulator of MHC II transcriptional activation. Promoter analysis has shown that the IFN inducible promoter IV is the site in which IRF-1 binds to help bring about transactivation (Nikcevich *et al.* 1999, Rahat *et al.* 2001 and Morris *et al.* 2002).

IRF-$1^{-/-}$ fibroblasts do not express Tapasin following IFNγ/TNFα stimulation, suggesting a role of IRF-1. Tapasin is involved in peptide loading for MHC I (Abarca-Heidemann *et al.* 2002). The chaperone β2 microglobulin, which is involved in MHC I antigen presentation, IgG transport and iron metabolism is transcriptionally regulated by IRFs (IRF-1, IRF-2, IRF-4 and IRF-8) and the NFkB family members p50 and p65 (Gobin *et al.* 2003).

The HLA genes are involved in presenting antigens to cytotoxic lymphocytes, and are critical for immune response. Many HLA antigens are regulated by IRF-1 and IRF-2 including HLA-A, HLA-B, HLA-C, HLA-F, HLA-I and HLA-G (Girdlestone *et al.* 1993, Gobin *et al.* 1999, Lefebvre *et al.* 2002 and Frontini *et al.* 2009).

Several components of the immunoproteosome complex are regulated by IRF-1 including LMP-7 (Low Molecular Weight Protein 7), LMP-2 , TAP and MECL-1 (Multicatalytic endopeptidase complex 1) (Namiki *et al.* 2005, Foss and Prydz 1999, Brucet *et al.* 2004, Chatterjee-Kishore *et al.* 1998, Chatterjee-Kishore *et al.* 2000, White *et al.* 1996 and Moschonas *et al.* 2008). Following IFNγ treatment, these three components replace constitutive components of the proteasome causing a shift to the formation of antigenic peptides. The HIV (Human Immunodeficiency Virus) protein Tat is a transcriptional activator which is able to cause LMP-7 and MECL-1 to be induced, but down regulates the expression of LMP-2. This causes the immunoproteosome to form sub-dominant and cryptic epitopes. Tat competes for STAT-1 binding on the STAT-1 / IRF-1 binding site. It prevents the interaction between IRF-1 and STAT-1 by sequestering IRF-1 away (Remoli *et al.* 2006).

1.5.11 Transcriptional regulation of cytokines.

IRF-1 transcriptionally regulates the expression of numerous cytokines, which are essential for the proper functioning of the immune system. IRF-1 was originally identified for its ability to activate the IFNα and IFNβ promoters (Miyamoto *et al.* 1988). In addition to IRF-1, IRF-5, IRF-3 and IRF-7 have been shown to be involved in induction of type I interferons. Knockouts of IRF-1 and IRF 5 have normal levels of type I IFN following infection with Newcastle Disease Virus suggesting that these factors are redundant in type me signalling. It was found that IRF-3 and IRF-7 are required for this signalling (Honda and Taniguchi 2006b). IRF-1 is also involved in type III IFN signalling, which has similarities to type I IFNs (Osterlund *et al.* 2007).

IRF-1 regulation of Interleukin 12 (IL-12) has been extensively studied, and is believed to be key to the role of IRF-1 in regulating T helper cell differentiation (Kano *et al.* 2008). IRF-1 up-regulates the expression of both IL-12 subunits p35 and p40 (Liu *et al.* 2004a and Maruyama *et al.* 2003). IRF-1 has also been implicated in regulating the expression of the IL-12 receptor sub-units IL-12Rβ1 and IL-12Rβ (Kano *et al.* 2008). IRF-1 also transcriptionally up-regulates IL-1β, IL-6, IL-8, IL-27, IL-15 and IL-7 (Marecki *et al.* 2001, Sanceau et al. 1995, Yamaoka *et al.* 2004, Pirhonen *et al.* 2007, Liu *et al.* 2007, Ogasawara *et al.* 1998 and Oshima *et al.* 2004). IRF-1 represses the expression of IL-4 which is involved in T helper cell differentiation (Elser *et al.* 2002). IRF-1 increases the expression of IL18BP (Interleukin 18 Binding Protein). This protein interacts with and reduces the activity of IL-18 (Hurgin *et al.* 2002).

1.5.12 IRF-1 and viral immunity.

Several viruses have been reported to utilise IRF-1 to regulate the expression of viral gene products, including Human Papillomavirus 16, Hepatitis B virus and HIV-1 (Alcantara *et al.* 2002, Arany *et al.* 2003a and Sgarbanti *et al.* 2002). The role of IRF-1 in HIV infection has been studied further, with IRF-1 dependent recruitment of CBP/p300 to the HIV LTR promoter and synergy with the NFκB family member p65 being proposed as molecular mechanisms by which IRF-1 acts on the LTR promoter (Marsili *et al.* 2004 and Sgarbanti *et al.* 2008).

Viruses are also able to interfere with IRF-1 expression and transcriptional activity. HCV infections can be treated with type I IFN, although approximately 50% of patients are unresponsive to IFN therapy. A large body of evidence suggests that IRF-1 is a critical mediator of IFN in HCV therapy. The hepatitis C protein NS5A reduces IRF-1 expression and DNA binding activity (Jung *et al.* 2007). Other gene products of the hepatitis C virus also disrupt IRF-1 action, the core protein, when over-expressed in HuH7 cells is able to severely reduce IRF-1 expression, possibly by blocking the activity of the IRF-1 promoter (Pflugheber *et al.* 2002, Kanazawa *et al.* 2004 and Ciccaglione *et al.* 2007). Human herpes virus 8 (HHV-8) is the causative agent of Kaposi sarcoma and encodes a viral relative of IRF-1. vIRF is able to block type I and II IFN signalling, and IRF-1 mediated transcription. This does not occur via competition for DNA binding, or involve the DNA binding domain, but may involve another region of IRF-1 important in its transcriptional activity (Zimring *et al.* 1998 and Burysek *et al.* 1999).

1.5.13 Inflammation

Studies in IRF-1$^{-/-}$ mice suggest that IRF-1 is involved in a number of pathologies that are associated with inflammation. A summary of the role of IRF-1 in these pathologies is given in table 1.7. Some of the key genes which are thought to be involved in these diseases are IRF-1 targets. The inducible form of the enzyme cyclooxygenase (COX-2) is involved in the generation of prostanoids from arachidonic acid. These signalling compounds are well known to regulate inflammation. COX-2 mRNA expression is regulated by IRF-1 and IRF-2 (Blanco *et al.* 2000 and Zhang *et al.* 2002).

Significant study has been directed towards controlling NO (nitric oxide) production via iNOS (Inducible Nitric Oxide Synthase) since the formation of this free radical is highly deleterious and is associated with several diseases such as enodotoxemia, heart disease and multiple sclerosis (Flodstrom and Eizirik 1997). IRF-1's ability to regulate iNOS expression (and consequently NO release) has been thoroughly studied with particular emphasis on identifying agents that prevent IRF-1 transactivating the iNOS promoter. Some agents which are able to do this include anti-oxidants, IL-13 and the DNA binding agent distamycin A (Cho *et al.* 2008 and Baron *et al.* 2004). Chemokines regulate immune cell activity, and play an important role in inflammation. Several chemokines are transcriptionally regulated by IRF-1 including, RANTES (**R**egulates on **a**ctivation, **n**ormal **T** cell **e**xpressed and **s**ecreted), CXCL10 and CXCL11 (Lee *et al.* 2000, Baker *et al.* 2003, Liu and Ma 2006, Kanda *et al.* 2007 and Yang *et al.* 2007). The ability of leukocytes to adhere and infiltrate blood vessels is linked to inflammation. The VCAM (Vascular Cell Adhesion Molecule) protein is a well

studied IRF-1 target gene that is involved in this process (Neish *et al.* 1995 and Lechleitner *et al.* 1998). IRF-1 has also been shown to regulate the expression of genes whose products are involved in degradation of cell-cell contacts. Some of these genes include; ADAM8 (a disintegrin and metalloprotease 8) and the matrix metalloprotease enzymes MMP8 and MMP9 - both of which are linked with tumour invasion and are repressed by IRF-1 (Schlomann *et al.* 2000) (Sanceau *et al.* 2002 and Nguyen *et al.* 2005). MMP-10 transcripts were found to be significantly lower in IRF-$1^{-/-}$ mice infected with *Mycobacterium avium.* Several other genes involved in tissue re-modelling were also identified and may be linked to IRF-1 function in developing granulomas during tuberculosis (Aly *et al.* 2008).

Pathology	Role of IRF-1	Reference(s)
Hepatitis	IRF-$1^{-/-}$ mice do not develop hepatitis when treated with concavalin A. Several gene products known to be involved in leukocyte infiltration of the liver are regulated by IRF-1.	(Streetz *et al.* 2001), (Jaruga *et al.* 2004)
Psoriasis	IRF-1 levels are low in epidermal cells from patients with psoriasis. IRF-1 may be involved in the proliferation of T cells	(Jackson *et al.* 1999)
Colitis	Dextran sulphate (an inducer of intestinal inflammation) treated IRF-$1^{-/-}$ mice display increased disturbance of crypt architecture and colonic dysplasia. Levels of lethality and severity of colitis are higher in IRF-$1^{-/-}$ mice treated with dextran sulphate sodium or trinitrobenzene sulfonic acid compared to wild type mice.	(Mannick *et al.* 2005)., (Siegmund *et al.* 2004).
Ischemia	Levels of IRF-1 mRNA are increased in neurons from ischemia biopsies. IRF-1 immunoreactivity has been found in intravascular neutrophils and, later in the clinical course, in neutrophils infiltrating ischemic tissues and neurones. IRF-$1^{-/-}$ mice have lower infarct volume following induced ischemia then their wild type or $^{-/+}$ littermates, they also show lower neurological defects. IRF-$1^{-/-}$ hepatocytes are protected from ischemia / reperfusion injury. Transduction with Ad-IRF-1 promoted liver damage, as did liver transplant from mice with Ad-IRF-1 infected livers	(Paschen *et al.* 1998) (Alexander *et al.* 2003) (Iadecola *et al.* 1999) (Tsung *et al.* 2006)
Diabetes	IRF-$1^{-/-}$ mice crossed with diabetes prone mice do not develop diabetes, while their $^{-/+}$ and $^{+/+}$ littermates developed spontaneous diabetes. Analysis of immune markers involved in the diabetes suggest that the T_H2 response is protective in the development of diabetes, since IRF-$1^{-/-}$ T cell development is eschewed towards T_H2 over T_H1, this may explain the lack of diabetes in IRF-$1^{-/-}$ mice	(Gysemans *et al.* 2009) (Nakazawa *et al.* 2001)
Lupus	IRF-$1^{-/-}$ mice crossbred with a strain that develops lupus were found to be more resistant to the pathological effects of lupus in the kidney. Additionally the IRF-$1^{-/-}$ mice survived longer than the IRF-$1^{+/+}$ mice.	(Reilly *et al.* 2006)
Graft Rejection	IRF-1 is required for prevention of necrosis in kidney transplant mouse models. Wild type mice developed arteritis and tuberitis but were otherwise viable twenty one days after transplant, the IRF-$1^{-/-}$ mice however showed massive necrosis	(Afrouzian *et al.* 2002)
Endotoxic Shock	IRF-$1^{-/-}$ mice are resistant to LPS poisoning, and express much lower levels of TNFα and IFNγ following LPS treatment.	(Senaldi *et al.* 1999)

Table 1.7 Inflammatory pathologies associated with IRF-1. Summary table to some of the inflammatory diseases which are thought to involve IRF-1.

phosphorylating β -Catenin which in turn allows it to promote transcription of its target genes (Yost *et al.* 1996).

In addition to control of the GSK3 protein, substrates of GSK3 may also require prior phosphorylation. This unique mechanism of "priming" greatly enhances the interaction between GSK3 and its substrates, thus allowing further fine tuning of GSK3 dependent phosphorylation (Frame and Cohen 2001). A third level of control of GSK3 is alterations in its subcellular distribution. GSK3 is predominantly located in the cytosol, but can also be found in the nucleus and mitochondria (Bijur and Jope 2003). The levels of GSK3 in the nucleus are regulated throughout the cell cycle, and are increased during apoptosis (Diehl *et al.* 1998 and Bijur and Jope 2001). This is important when considering that GSK3 regulates the activity of a number of transcription factors.

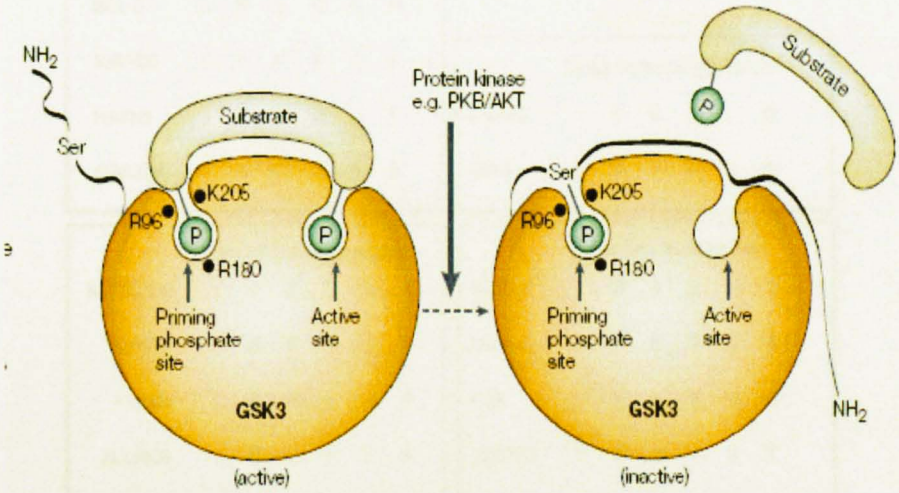

Figure 1.12 Schematic of GSK3. A substrate is shown interacting with GSK3, with its + 4 priming residue interacting with the priming site and its target residue interacting with the active site. Inactive GSK3 is illustrated with its phosphorylated N terminal Ser residue, which is blocking the substrate from being phosphorylated. Adapted from Frame & Cohen 2001.

1.6.2. GSK-3 substrates

The GSK3 consensus motif has been identified as T/S-X-X-X-pT/S, where X represents any amino acid, and p indicates phosphorylated Thr or Ser residues (see figure 1.13). This priming effect enhances the interaction between GSK3 and its substrate significantly. Occasionally the + 4 residue is an acidic aspartic or glutamic acid amino acid. These substrates can be considered to be constitutively primed. Some substrates do not require the + 4 priming site, while others posses +5 priming sites. Phosphorylation of Ser/Thr residues may promote the formation of a new primed site for additional residues in substrate. Consequently GSK3 may phosphorylate a series of residues (Doble and Woodgett 2003). Examples of GSK3 substrates are given in Figure 1.14.

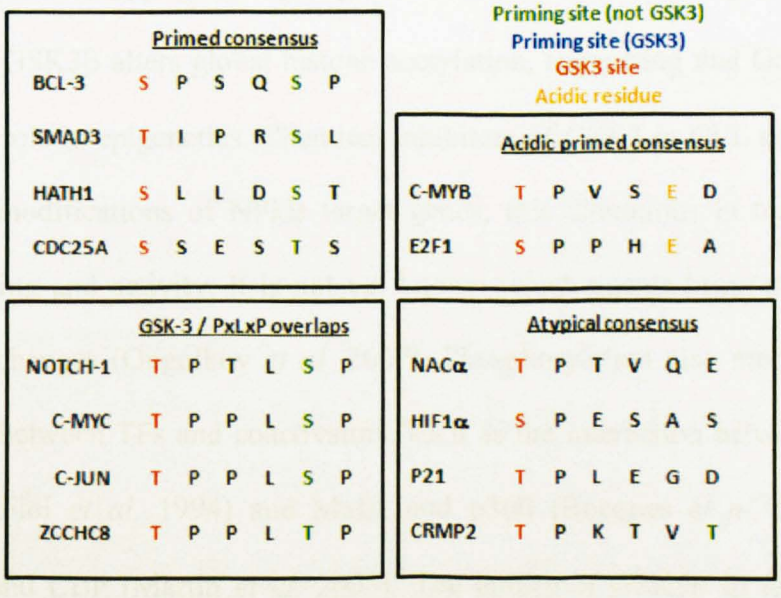

Figure 1.13 GSK3 β substrates. A selection of GSK3 β substrates are illustrated here, some of these proteins can also be phosphorylated by GSK3α. The substrates are subdivided into groups depending on the amino acids within the consensus. Abbreviations **SMAD3** (MAD protein 3), **HATH1** (Human Homolog of MATH), **ZCCHC8** (Zinc finger CCHC Domain containing 8), **NAC** (Nacent Polypeptide Chain Associated), **CRMP2** (Collapsin Response Mediator Protein 2)

1.6.3. GSK-3 and transcription

Proteins involved in transcription constitute the largest functional group of GSK3 substrates. A number of transcriptional coactivators and co-repressors are phosphorylated by GSK3β, including Bcl3 (B Cell Lymphoma 3), SRC-3 (Steroid Receptor Coactivator 3), CIITA, PGC1α, MAML (Mastermind Like 1), αNAC (Viatour *et al.* 2004, Wu *et al.* 2007, Olson *et al.* 2008, Xu *et al.* 2008 and Quelo *et al.* 2004). For some of these proteins phosphorylation results in degradation and reduction in activity (Bcl3 and αNAC), while other coactivators require GSK3β dependent phosphorylation for their activity (SRC-3 and CIITA). Phosphorylation of CIITA promotes protein-protein interactions with the transcriptional repressor protein Sin3B and HDAC2, and is required to bring about repression of type 1 collagen genes (Xu *et al.* 2008). Phosphorylation of MAML by GSK3β alters global histone acetylation, suggesting that GSK3β may also play a role in epigenetics. Chemical inhibitors of GSK3 in CLL cells induce epigenetic modifications of NFkB target genes, this alterations in turn prevent NFkB binding and activity. It is not yet known which agents bring about these epigenetic changes (Ougolkov *et al.* 2007). Phosphorylation also modulates the interaction between TFs and coactivators, such as the interaction between CREB and CBP (Fiol *et al.* 1994) and MafA and p300 (Rocques *et al.* 2007) and NFkBp65 and CBP (Martin *et al.* 2005). The ability of GSK3β to regulate the degradation of a number of TFs has been discussed in section 1.5. Phosphorylation of NFATc by GSK3β promotes nuclear export, preventing NFATc from accessing DNA and promoting transcription (Benedito *et al.* 2005). The TF C/EBPβ requires phosphorylation by MAPK and GSK3β to acquire DNA

binding activity. Phosphorylation of C/EBPβ promotes the formation of disulphide bridges needed for DNA binding (Kim *et al.* 2007).

1.6.4. GSK-3 is disease and development.

GSK3β is important for the development of the nervous system, with a role in neurite extension and retraction (Etienne-Manneville and Hall 2003). Proteins that regulate the cytoskeleton including kinesin and microtubule associated proteins are also regulated by GSK3, suggesting a role for GSK in cell architecture (Wakefield *et al.* 2003). GSK3 proteins are involved in the development of body plans in a number of organisms including *Drosophila, C. elegans, Xenopus* and *Dictyostelium.* GSK3β may not be involved in patterning in mammals, however as GSK3β$^{-/-}$ mice do not suffer from development defects (Kim and Kimmel 2000). Up-regulation of GSK3 expression promotes apoptosis and GSK3 has been shown to be an important mediator of apoptosis following DNA damage, hypoxia, ER stress and Anoikis (Jope and Johnson 2004).

GSK3β also regulates cell survival, mice that are devoid of GSK3β die *in utero* at day 14. A contributing factor to GSK3β$^{-/-}$ mice lack of viability is the massive TNFα induced hepatic apoptosis. It has been suggested that proper control of NFκB family members by GSK3β is needed to restrain this inappropriate apoptosis (Hoeflich *et al.* 2000). GSK3β has been linked to a plethora of human diseases, including diabetes, Alzheimers, Bi-polar disorder, cancer and Schizophrenia (Jope and Johnson 2004).

1.6.5. GSK3 inhibitors

Unsurprisingly, given the number of human pathologies to which GSK3 has been implicated, considerable interest has been directed at the study of GSK inhibitors. For over 50 years Lithium salts have been used in the treatment of mania, although it has only recently been shown to act through GSK3. Most GSK3 inhibitors act on the ATP binding pocket, however this region is similar to CDK enzymes, producing off target effects. The ATP binding pockets of GSK3α and GSK3β are almost identical, making most GSK3 inhibitors non selective for each isoform. Alternative approaches to the use of chemical inhibitors, is the use of peptides based on proteins that interact with and inhibit GSK3. Most commonly these include FRAT and GID peptides derived from the axin-GSK3 interaction. Other sites of GSK3 are also being investigated for their drugability including the activator tyrosine phosphorylation site (Meijer *et al.* 2004).

PhD objectives

Although a small number of IRF-1 PTMs have been described, very little is known about how these modifications regulate the transcriptional activity of IRF-1. In addition there is a distinct lack of understanding concerning the mechanisms by which IRF-1 brings about transcription, as such this project sought to answer some of the questions regarding the fundamental control and activity of the IRF-1 protein. By identifying kinases that modulate IRF-1 activity, it is hoped that novel therapeutic agents could later be developed to regulate the IRF-1 transcriptional programme.

The specific goals of this project are given below.

1. Identify novel kinase(s) that phosphorylate IRF-1 and locate the residues phosphorylated *in vivo*.

2. Determine the role of the kinase and the specific modified residues on the transcriptional activity of IRF-1 using the TRAIL promoter as a model system.

3. Delineate the mechanism by which the newly identified phosphorylation event regulates IRF-1 activity, for example through changes in subcellular localisation, DNA-protein interactions, protein-protein interactions or through PTM crosstalk.

Chapter 2. Methods

2.1.1 Polymerase Chain Amplification (PCR)

All PCR reactions were carried out on a Thermal Cycler 2720 (Applied Biosystems). The total reaction volume used was 50 µL with the volume being bought up with ddH_2O. All primer sequences are given on table 2.1. A 50 µL reaction mix contained 5 µl of reaction buffer (10X), 1 µL of 10mM dNTPs, 1.5 µL of 50 mM magnesium chloride, 5 µL of 5µM primers (Fwd and Rev) 50ng of template DNA and 0.25 µL of Taq Polymerase (1.25U) (Invitrogen). The cycling conditions were 30 rounds of; 94°C (180 seconds), 94°C (45 seconds), 55° C (30 seconds), and 72 ° C (90 seconds) with a final extension of 72 ° C for 7 minutes.

2.1.2 Colony PCR

Colony PCR was used when a background (ligation controls) level of higher than 10% occurred (see section 2.1.7), or when a single restriction site was used for cloning and the orientation of the insert had to be tested. From the LB-AMP plate, single isolated bacteria clones were lifted with a pipette tip and placed in cultures containing 50 µL of LB-AMP. These cultures were then incubated for two hours at 37°C. The PCR reaction was carried out according to section 2.1.1 with the exception that 5 µL of the LB-AMP bacteria was added to the PCR mix. To determine if the insert was ligated into the vector, the primers used for the cloning were employed. A negative control of ddH_2O in place of bacteria, and a positive control of expression plasmid (5 ng) were used to check the identity of the PCR product.

Oligo name	Template	Sequence (5'--> 3')
mIRF1 K233R	FLAG-mIRF1 WT	Fwd: GGATGAGGAAGGGAGGATAGCCGAAGACC Rev: GGTCTTCGGCTATCCTCCCTTCCTCATCC
mIRF1 K276R	FLAG-mIRF1 WT	Fwd:GGAGACTTCAGCTGCAGAGAGGAACCAGAGATTG Rev:CAATCTCTGGTTCCTCTCTGCAGCTGAAGTCTCC
mIRF1 K300R	FLAG-mIRF1 WT	Fwd:CATGTCTTCACGGAGATGAGGAATATGGACTCCATCATG Rev:CATGATGGAGTCCATATTCCTCATCTCCGTGAAGACATG
mIRF1 K255R	FLAG-mIRF1 WT	Fwd: GACACACATCGATGGCAGGGGATACTTGCTCAATG Rev: CATTGAGCAAGTATCCCCTGCCATCGATGTGTGTC
mIRF1 K240R	FLAG-mIRF1 WT	Fwd: GATAGCCGAAGACCTTATGAAGGCTCTTTGAACAGTCTGAG Rev: CTCAGACTGTTCAAAGAGCCTCATAAGGTCTTCGGCTATC
mIRF1 T180D	pcDNA3.mIRF1 WT	Fwd: GGACTTGGATATGGAAAGGGACATAGATCCAGCACTGTCA Rev TGACAGTGCTGGATCTATGTCCCTTTCCATATCCAAGTCC
mIRF1 S184E	pcDNA3.mIRF1 WT	Fwd: AGGGACATAACTCCAGCACTGGAGCCGTGTGTCGTCAGCAGCAGT Rev: TCCCTGTATTGAGGTCGTGACCTCGGCACACAGCAGTCGTCGTCA
mIRF1 T180A	pcDNA3.mIRF1 WT	Fwd: ATGGAAAGGGACATAGCTCCAGCACTGTCACCG Rev: CGGTGACAGTGCTGGAGCTATGTCCCTTTCCAT
mIRF1 S184A	pcDNA3.mIRF1 WT	Fwd: CATAACTCCAGCACTGACACCGTGTGTCGTCAG Rev: CTGACGACACACGGTGTCAGTGCTGGAGTTATG
mIRF1 T180A/S184A	pcDNA3.mIRF1 S184A	Fwd: GGAAAGGGACATAGCTCCAGCACTGGC Rev: GCCAGTGCTGGAGCTATGTCCCTTTCC
mIRF1 YFP	pcDNA3.mIRF1 WT	Fwd: ATAATAAGATCTATGCCAATCACTCGAATG Rev; ATAATATCTAGACTATGGACAAGGAAT
mIRF1 FLAG	pcDNA3.mIRF1 WT	Fwd; ATAATAAAGCTTATGCCAATCACTCGAATG Rev; ATAATATCTAGACTATGGACAAGGAAT
HA-Fbxw7α FL	pDEST27 -Fbxw7α	Fwd: ATAATAGAATTCATGAATCAGGAACTGCTCTCTGTG Rev: TATTATTCTAGATCACTTCATGTCCACATCAAAGTC
HA-Fbxw7β FL	pDEST27 -Fbxw7β	Fwd: ATAATAGAATTCATGTGTGTCCCGAGAAGCGGTTTG Rev: TATTATTCTAGATCACTTCATGTCCACATCAAAGTC
HA-Fbxw7α N terminus deletion	pDEST27 -Fbxw7α	Fwd: ATAATAGAATTCATGAATCAGGAACTGCTCTCTGTG Rev: TATTATTCTAGATCAAGATTTGAGTTCTCCTCGCCT
HA-Fbxw7β N terminus deletion	pDEST27 -Fbxw7β	Fwd: ATAATAGAATTCATGTGTGTCCCGAGAAGCGGTTTG Rev: TATTATTCTAGATCAAGATTTGAGTTCTCCTCGCCT
HA-Fbxw7 C terminus deletion	pDEST27 -Fbxw7β	Fwd: ATAATAGAACCTAAGGTGCTGAAAGGACATGAT Rev: TATTATTCTAGATCACTTCATGTCCACATCAAAGTC
T7-Fbxw7α FL	pDEST27 -Fbxw7α	Fwd: TAATACGACTCACTATAGGGAGACCACCATGGATGAATCAGGAACTGCT Rev: TATTATTCTAGATCACTTCATGTCCACATCAAAGTC
murine IRF-1	Sequencing	Fwd: AGCTGGGCCATTCACACAG Rev: GTTCATGGCACAACGGAAGT
Hs_GSK3B_8_HP	siRNA	Fwd r(GCA UUU AUC GUU AAC CUA A)dTdT Rev: r(UUA GGU UAA CGA UAA AUG C)dAdG

Table 2.1 Oligonucleotides used in this study. The Oligonucleotides used in this study for cloning, mutagenesis, sequencing and siRNA knockdown. All oligos were from Sigma Genosys, except the siRNA oligos which were purchased from QIAGEN.

2.1.3 Site directed mutagenesis

Primers for site directed mutagenesis were designed using PrimerX software (http://www.bioinformatics.org/primerx/). All primers were synthesised by Sigma Genosys UK. Site directed mutagenesis was performed using the Stratagene Quikchange XL kit (Stratagene). All reactions were carried out according to the manufacturer's instructions, using 25 ng of template DNA and 2.5 U per reaction of Pfu ultra polymerase. The PCR conditions were (denaturing) 95°C for 110 s, (annealing) 62°C for 50 s followed by (extension) 68°C for 7 minutes. This was repeated 18 times with an additional cycle at 68°C for 7 minutes. Transformations were carried out using the supplied Ultra-competent bacteria provided. Following transformation of the DpnI digested DNA product, bacteria were plated on AMP-Agar plates (50 μg/mL) and incubated for 24 hours at 37°C. At least four colonies were picked and grown in 5mL of LB AMP (50 μg/mL) overnight with mild shaking at 37°C. 2mL of the culture was then used for mini-preps. The eluted DNA was then subjected to restriction digests with EcoR1, or XbaI / HindIII for the pcDNA3.1 or 3X Flag vectors respectively.

2.1.4 DNA purification

DNA purifications following gel extraction or PCR / restriction digestion was carried out using the YORBIO PCR / gel extraction cleanup kit (YORBIO). When purifying DNA from agarose gel, the relevant fragment was excised from the gel after visualising on a UV light box. The gel slice was weighed and mixed at a 1:1 ratio with binding buffer. The gel slice was incubated at 65°C for 10 minutes, with vortexing every two minutes. For purification from PCR or restriction digest, the

DNA was mixed 1:1 with binding buffer, vortexed, and allowed to incubate at room temperature for two minutes. The DNA / binding buffer mix was then added to a spin column and left to stand at room temperature for a further 5 minutes. The spin columns were then centrifuged at 12,000 rpm for 1 minute. The flow through was discarded, and the column washed twice with 500 μL of wash buffer. A final spin at 12,000 rpm for 1 minute was used to dry the membrane. The column was transferred to a clean collection tube, and 50 μL of elution buffer was added to the membrane. The elution buffer was incubated on the membrane at 37°C for 10 minutes. The columns were then centrifuged at 12,000 rpm for 1 minute. The flow-through was collected in a labelled fresh tube and stored at -20°C.

2.1.5 Restriction endonuclease digestion

Restriction endonuclease digestions were carried out in 30 μL total volume at 37°C unless otherwise stated. All restriction enzymes were purchased from Roche. Typically 10 units of restriction enzyme were used to cut 1 μg of DNA for 1 hour in a water bath. When two restriction enzymes were used, 10 U of each enzyme was used and appropriate buffer was selected to enable both enzymes to work at 100% efficiency.

2.1.6 DNA dephosphorylation

Phosphatase treatment of restriction digested vector was carried out on all vectors regardless of use of two different restriction sites. De-phosphorylation was carried

out using TSAP (Promega) according to manufacturer's instructions using 1 U of TSAP per reaction.

2.1.7 Ligation

Ligations were carried out in a total volume of 10 μL. The vector: insert ratios used in the ligations varied from 1:2 to 1:4 depending on the size of the insert (1=10 ng of DNA). Typically a range of ratios was used to ensure positive ligations. Vector and insert DNA were mixed with ddH_2O to a total volume of 8 μL in PCR tubes. The DNA was heated at 65°C for 5 minutes followed by rapid cooling in ice. One μL of 10X ligation buffer and 1 μL (1 U) of T4 Ligase (Roche) was added to the DNA. Ligations were carried out at 12°C overnight. Controls in which no T4 was added, or in which there was no insert were always included to check for vector re-ligation.

2.1.8 Preparation of chemically competent DH5α

A single colony of freshly grown *E.coli* DH5α bacteria was picked into 10 mL of LB broth and grown overnight at 37°C with shaking at 200-250 rpm. One mL of this culture was then added to 100 mL of LB and grown until it reached an OD595 of 0.3. The contents of the flask were then transferred to two 50 mL tubes and centrifuged for 5 minutes at 3500 rpm at 4°C. Supernatant was then discarded and the bacteria pellet re-suspended in 20 mL ice cold 100 mM $MgCl_2$. The cells were then pelleted again as before and re-suspended in 10 mL of 100 mM $CaCl_2$. The cells were then left on ice for 30 minutes in $CaCl_2$. The bacteria were then mixed with glycerol to produce a 30% glycerol mix, aliquoted and frozen at -80°C.

2.1.9. Transformations

For transformation of plasmid DNA the *E.coli* DH5α strain was used. For transformations from ligation reactions 3 μL of the ligation mix was added to 50 μL of chemically competent DH5α which had been thawed on ice. The DNA was incubated with the bacteria for 45 minutes on ice. Bacteria were heat shocked at 42°C for 2 minutes, and cooled on ice. The transformed bacteria were grown in 450 μL of LB-AMP without antibiotics at 37°C with shaking for 1 hour. The bacteria were pelleted and re-suspended in 50 μL of LB-AMP. The pellet was re-suspended in the LB-AMP and the entire pellet plated on a 10 cm plate containing LB-AMP Agar supplemented with 50 μg/mL Ampicilin. For eYFP plasmids; 25 μg/mL of Kanamycin was used. The plates were incubated overnight at 37°C to allow colonies to grow. When known amounts of DNA were being transformed, 100 ng of DNA was transformed as above; with the exception that 50 μL of the bacterial culture was plated. Transformations from site directed mutagenesis were carried out using the Ultra competent bacteria provided with the Quikchange II site directed mutagenesis kit (Stratagene). Transformations were carried out according to manufacturer's instructions.

2.1.10. Small scale purification of plasmid DNA

Small scale purification of plasmid DNA was performed using the YORBIO Plasmid purification kit (YORBIO). Three mL of an overnight culture of transformed DH5α cells were pelleted in 1.5 mL microfuge tubes. To the pellet, 150 μL of solution I was added and vortexed to homogenise the pellet. Cells were lysed with 150 μL of solution II, the microfuge tube was inverted eight times to

aid lysis of cells. Lysis was allowed to occur for 5 minutes. 300 μL of solution III was then added to stop the lysis and precipitate genomic DNA and protein. The contents were gently mixed and allowed to stand at room temperature for two minutes. The precipitate was pelleted by centrifugation at 12,000 rpm for 10 minutes at room temperature. The supernatant was transferred to spin columns, centrifuged at 12,000 rpm for 1 minutes followed by two washes with wash buffer for 30 seconds. A final spin to remove any remaining wash buffer was performed before elution buffer was added to the column (50 μL) for 5 minutes at room temperature. The column was transferred to a clean collection tube and centrifuged at 12,000 rpm for 1 minute. The eluted DNA was transferred to a clean capped tube and stored at -20°C until needed.

2.1.11. Large scale purification of plasmid DNA

For large scale preparation of plasmid DNA, Nucleobond Maxi (Machery Nagel) columns were used. Extraction of DNA was performed according to manufacturer's instructions from a culture of 200 mL.

2.1.12. DNA Quantification

All DNA was quantified using the Nanodrop Spectroanalyser 2000.

2.1.13. Glycerol stocks

To produce bacterial glycerol stocks, 700 µL of growing bacterial culture transformed with desired plasmid was mixed with 300 µl of 50% glycerol (sterile filtered). The glycerol stocks were stored at -80°C. To inoculate cultures from glycerol stocks, the frozen culture was stabbed with a pipette tip and transferred to 5 mL of LB containing the relevant antibiotic. This starter culture was then grown at 37°C for 5 hours with shaking before being transferred to a 200 mL culture which was left to grow overnight at 37°C.

2.1.14. Agarose gel electrophoresis

All DNA was run on agarose at a concentration of 0.8-1.0% made up in 1X TBE buffer (40 mM Tris pH 8.3, 40 mM Boric acid, 0.037% SDS). DNA was diluted to 1X in gel loading buffer (0.25% Bromophenol Blue (w/v) 30% glycerol). The final concentration of Ethidium Bromide used was 0.05 µg/mL. The gels were electrophoresed using the Biorad system (BIORAD). The gels were visualised using a Gel Doc 2000 (BIORAD).

2.1.15. DNA sequencing

Sequencing of cloned DNA was performed to confirm the identity of cDNA donated from external sources, mutagenesis and cloning. DNA was sequenced in both the forward and reverse orientation to ensure full coverage of the cDNA insert. Longer cDNA inserts (such as for Fbxw7) were sequenced with internal primers to ensure full coverage. Sequencing was performed by GATC (Konstanz, Germany).

2.1.16. 3XFLAG N terminal tagged IRF-1

N terminal 3x FLAG (Sigma Aldrich) tagged murine IRF-1 constructs were made by PCR amplifying IRF-1 from the original pcDNA3.1 expression plasmid using primers that add XbaI and HindIII sites. These primers and the PCR conditions are detailed in table 2.3. After PCR amplification, DNA was purified, cut with XbaI and HindIII, and re-purified according to sections 2.1.4. The 3xFLAG vector plasmid was restriction digested with XbaI *and* HindIII, then purified. Insert and vector were ligated together (see 2.1.7). DNA was transformed; positive clones were selected and grown in 5 mL of LB-AMP over night. DNA from 5 clones of each construct was then purified (2.1.10) and subjected to restriction digest with XbaI and HindIII to confirm presence of the IRF-1 insert. DNA was sequenced (2.1.15) and maxipreped (2.1.11). To confirm the constructs produce viable, in-frame proteins, transfection of 5 μg of DNA was carried out in HEK293 cells, followed by immunoblot for both murine IRF-1 and FLAG.

2.1.17. eYFP – IRF-1

N terminal enhanced YFP (eYFP C1 Clontech) fused murine IRF-1 constructs were made my PCR amplifying IRF-1 from the original pcDNA3.1 expression plasmid using primers that add XbaI and BglII sites. These primers and the PCR conditions are detailed in table 2.1. After PCR amplification, DNA was purified, cut with XbaI and BglII, and re-purified. The eYFP vector was restriction digested with XbaI and BglII, then purified. Insert and vector were ligated together (2.1.7). DNA was transformed; positive clones were selected and grown in 5 mL of LB-AMP over night. DNA from five clones of each construct was then purified (2.1.4) and subjected to restriction digest with XbaI and BglII to confirm presence

of the IRF-1 insert. DNA was sequenced (2.1.15) and maxipreped (2.1.11). To confirm the constructs produce viable, in-frame proteins, transfection of 5 μg of DNA was carried out in HEK293 cells, followed by immunoblot for both murine IRF-1 and GFP.

2.1.18. GST – IRF-1

N terminal GST (glutathione-s-transferase) fused murine IRF-1 constructs were made by restriction digest of the entire murine IRF-1 cDNA from the original pcDNA3.1 plasmid with EcoR1. The digested DNA was run on a 0.8% agarose gel containing 0.05 μg/mL Ethidium Bromide. The smaller fragment (2.2kb) was excised from the gel, purified (2.1.4) and ligated with EcoR1 digested pGEX-4T1 (GE Healthcare) plasmid. DNA was transformed; positive clones were selected and grown in 5 mL of LB-AMP over night. DNA from five clones of each construct was then purified and subjected to restriction digest with XhoI to determine if the insert was orientated in the correct orientation. To confirm the presence of the IRF-1 insert. DNA was sequenced and maxipreped.

2.1.19. pcDNA4-TO-IRF-1

The entire murine IRF-1 cDNA was transferred into the pcDNA4-Tet Off vector (Invitrogen) from the pcDNA3.1 by restriction digest using EcoR1. The cloning strategy used was identical to that used for cloning GST-IRF-1 with the exception that ApaI was used to determine if the IRF-1 insert was in the correct orientation.

2.1.20. HA-Fbxw7

Fbox WD40 repeat containing seven cDNA was transferred from the pDEST27 GST vector to the CMV-HA vector using primers that introduced restriction digest sites specific to the CMV-HA multiple cloning site. Forward primers were generated that added an *EcoR1* site on the 5' end of the Fbxw7α and Fbxw7β cDNA. Reverse primers were designed to add an XbaI restriction digest site. To generate truncation mutants in which the entire N terminus (encoding the Fbox) was truncated, forward primers were generated that annealed to beginning of the WD40 repeats. This primer contained an EcoR1 restriction site. To generate truncation mutants of Fbxw7α/ β which do not contain WD40 repeats (only N terminus and Fbox) reverse primers were made that annealed before the DNA that encodes the WD40 repeats. These reverse primers contained a stop codon and an XbaI site. PCR was performed using primer pairs detailed in table 2.1 to generate DNA inserts. The PCR amplified inserts was then purified and restriction digested with EcoR1 and XbaI to generate compatible ends. This digested DNA was then purified. Two μg of the pCMV5 plasmid (containing the HA tag) was restriction digested with EcoR1 and XbaI, followed by purifications. The DNA inserts were then ligated together according to section 2.1.7. Five positive clones were selected for each construct and subjected to colony PCR (2.1.2) with pCMV5 being used as a negative control and pDEST27-Fbxw7α and pDEST27-Fbxw7β being used as positive controls. Clones that contained the Fbxw7 inserts were grown in 10 mL LB AMP overnight. Mini-preps of the cultures were carried out, with the DNA being sent for sequencing to check the identity of the clones.

Vector	Name	Originator
pcDNA3.1+	pcDNA3	Invitrogen
pcDNA3.1+ Mouse IRF-1 WT	IRF-1 WT	Keiko Ozato, USA
pcDNA3.1+ Mouse IRF-1 T180A	IRF-1 T180A	This study
pcDNA3.1+ Mouse IRF-1 S184A	IRF-1 S184A	This study
pcDNA3.1+ Mouse IRF-1 T180A/S184A	IRF-1 TS-A	This study
pcDNA3.1+ Mouse IRF-1 T180D	IRF-1 T180D	This study
pcDNA3.1+ Mouse IRF-1 S184E	IRF-1 S184E	This study
pCMV-3XFLAG	FLAG	Sigma Aldrich
pCMV-3XFLAG Mouse IRF-1 WT	FLAG - IRF-1 WT	This study
pCMV-3XFLAG Mouse IRF-1 T180A	FLAG - IRF-1 T180A	This study
pCMV-3XFLAG Mouse IRF-1 S184A	FLAG - IRF-1 S184A	This study
pCMV-3XFLAG Mouse IRF-1 T180A/S184A	FLAG - IRF-1 TS-A	This study
pCMV-3XFLAG Mouse IRF-1 T180D	FLAG - IRF-1 T180D	This study
pCMV-3XFLAG Mouse IRF-1 S184E	FLAG - IRF-1 S184E	This study
pCMV-3XFLAG Mouse IRF-1 K233R	FLAG - IRF-1 K233R	This study
pCMV-3XFLAG Mouse IRF-1 K240R	FLAG - IRF-1 K240R	This study
pCMV-3XFLAG Mouse IRF-1 K255R	FLAG - IRF-1 K255R	This study
pCMV-3XFLAG Mouse IRF-1 K276R	FLAG - IRF-1 K276R	This study
pCMV-3XFLAG Mouse IRF-1 K300R	FLAG - IRF-1 K300R	This study
pCMV-3XFLAG Mouse IRF-1 K276R/K300R	FLAG - IRF-1 K276/300R	This study
pCMV-3XFLAG Mouse IRF-1 K240R/K255R	FLAG - IRF-1 K240/255R	This study
pCMV-3XFLAG Mouse IRF-1 K255R/K276R/K300R	FLAG - IRF-1 3KR	This study
pCMV-3XFLAG Mouse IRF-1 K240R/K255R/K276R/K300R	FLAG - IRF-1 4KR	This study
pCMV-3XFLAG-HA	FHA	J. Xicluna
pCMV-3XFLAG-HA Mouse IRF-1 WT	FHA-IRF-1	J. Xicluna
peYFP-C1	eYFP	Clontech
peYFP-C1 Mouse IRF-1 WT	eYFP IRF-1 WT	This study
peYFP-C1 Mouse IRF-1 T180A	eYFP IRF-1 T180A	This study
peYFP-C1 Mouse IRF-1 S184A	eYFP IRF-1 S184A	This study
peYFP-C1 Mouse IRF-1 T180A/S184A	eYFP IRF-1 TS-A	This study
peYFP-C1 Mouse IRF-1 T180D	eYFP IRF-1 T180D	This study
peYFP-C1 Mouse IRF-1 S184E	eYFP IRF-1 S184E	This study
pcDNA6-TetR	TetR	Invitrogen
pcDNA4-TO	pcDNA4-TO	Invitrogen
pcDNA4-TO Mouse IRF-1 WT	pcDNA4- IRF-1 WT	This study
pcDNA4-TO Mouse IRF-1 T180A	pcDNA4- IRF1 T180A	This study
pcDNA4-TO Mouse IRF-1 T180A/S184A	pcDNA4- IRF1 TS-A	This study
pGEX4T1	GST	GE Healthcare
pGEX4T1 Mouse IRF-1 WT	GST-IRF-1 WT	This study
pDEST27 GST	GST	Invitrogen
pDEST27 GST-Fbxw7α	GST-Fbxw7α	J Wade Harper, USA
pDEST27 GST-Fbxw7β	GST-Fbxw7β	J Wade Harper, USA
pDEST27 GST-Fbxw7γ	GST-Fbxw7γ	J Wade Harper, USA
pCMV5-HA	HA	GS. Winkler
pCMV-HA Fbxw7α	HA-Fbxw7α	This study
pCMV-HA Fbxw7β	HA-Fbxw7β	This study
pCMV-HA ΔWD40-Fbxw7α	HA-ΔWD40-Fbxw7α	This study
pCMV-HA ΔWD40-Fbxw7β	HA-ΔWD40-Fbxw7β	This study

Vector	Name	Originator
pCMV-HA-ubiquitin	HA-ubiquitin	Carol Prives, USA
pCMV-FLAG-ubiquitin	FLAG-ubiquitin	Carol Prives, USA
pcDNA-GSK3β-HA WT	GSK3β-HA WT	Jim Woodgett, Canada
pcDNA-GSK3β-HA K85A	GSK3β-HA K85A	Jim Woodgett,Canada
pcDNA-GSK3β-HA S9A	GSK3β-HA WT S9A	Jim Woodgett,Canada
pcDNA-GSK3β-HA R96A	GSK3β-HA WT R96A	Gail Johnson, USA
p220-TRAIL-Luc	TRAIL Luc	Nicole Clarke
p4XIRF1/H4 site II -Luc	4XISRE-Luc	Gary Stein, USA
pcDNA4-TO-LUC	TET-OFF Luc	Invitrogen
pCH110	CMV- βGAL	Pharmacia

Table 2.2. Plasmid used in this study. Both the full names and abbreviated names used in this study are indicated.

2.2.1. HEK293 cells

Human Embryonic Kidney 293 (HEK293) cell lines are human embryonic kidney cells that were transformed with adenovirus 5 DNA. HEK293 cells were maintained in DMEM (Dulbecco's Modified Eagles Media) containing 10% FBS, 50 U/mL Penicillin-Streptomycin and 2 mM L-Glutamine. HEK293 cells were sub-cultured every 4 days to prevent their confluence from exceeding 80%. For sub-culture, cells were gently agitated by pipetting to remove from the plate and produce a single cell suspension. The cells were re-suspended in new media at a 1:10 ratio and maintained at 37°C, 5% CO2 with humidity.

2.2.2. COS-7 cells

African Green Monkey kidney cells (COS-7) cells are monkey kidney fibroblast cells transformed with the SV40 virus. COS-7 cells were maintained in the same conditions as HEK293 cells with the exception that they required trypsinisation.

This was carried out by removing the media, followed by 2x washes with pre-warmed 1X PBS. For 10 cm plates 1 mL of 0.25% trypsin EDTA (Invitrogen) was added to the plate. The plate was then gently rocked to ensure full coverage of trypsin before being placed at 37°C for 3 minutes. The trypsinisation was stopped by the addition of 9 mL of DMEM media. The media/cell mix was gently pipetted to break up any clumps of cells. COS-7 cells were diluted 1:10. Sub-culture of COS-7 was required every 4 days.

2.2.3. MRC-5 cells

MRC-5 cells are human foetal lung fibroblast cells. They have not been transformed so undergo limited population doublings before succumbing to senescence. Typically MRC-5 cells were only used for 15 passages before being replaced with new cells. MRC-5 cells were maintained in α-MEM (alpha Modified Essential Medium). The media was supplemented with 50 U/mL Penicillin-Streptomycin, 2 mM L-glutamine and 10% FBS (specially selected for primary fibroblasts –PAA). MRC-5 cells were sub cultured every 3 days using trypsinisation as for HEK293 and COS-7 cells. MRC-5 cells were diluted at a dilution of 1:5.

2.2.4. H3396 cells

The H3396 cell line is a human breast carcinoma cell line established by Bristol-Myers Squibb (Seattle USA). The H3396 cell line is not commercially available and was used under a Material Transfer Agreement issued to Dr Nicole Clarke.

The H3396 cell line expresses endogenous IRF-1 which is inducible by a number of stimuli, including retinoids and interferons. The H3396 cell line has previously been used as a model for IRF-1 dependent cell death (Clarke *et al.* 2004) and (Frontini *et al.* 2009). H3396 cells were maintained in RPMI 1640 (Roswell Park Memorial Institute) media supplemented with 10% FBS, 2 mM L-glutamine and 50 U/mL penicillin-streptomycin. Sub-culture of H3396 cells was carried out as for MRC-5 cells.

2.2.5. Cell counting.

Counting was carried out on cells diluted 1:1 in trypan blue stain (Autogen Bioclear). 20 µL of stained cells were counted on a Neubauer improved haemocytometer. Cell count in a single central square (0.1 mm^2) was multiplied by two (to account for 1:1 dilution in trypan blue), then 10,000 to obtain a measure of cells per mL^3.

2.2.6. Cryo preservation of cell lines

Cells are trpsinised as for sub-culture, with the exception, that after 1 minute the trypsin was removed and the plate was returned to the incubator. The cells were then re-suspended in the appropriate media – 2 mL for a 10 cm dish, counted (see section 2.2.5) and diluted to the appropriate concentration. 900 µL of cell suspension was transferred to labelled cryovials containing 100 µL of DMSO. The DMSO cell suspension was then gently pipetted to ensure an even mixing of DMSO and media. The vials were then transferred to a -20°C freezer until the

vials were frozen solid. The cryovials are then placed at -80°C overnight, after which the vials are stored in liquid nitrogen.

2.2.7. Culturing cells from frozen stocks

Prior to recovery of cryovials from liquid nitrogen, 10 mL of the appropriate media was added to a 10 cm cell culture plate (TPP) and returned to the incubator to warm the media. Cryovials containing frozen cells were thawed at 37°C for approximately 1 minute. The cells were transferred to the pre-warmed media and returned to the incubator. Six hours after the cells were plated; the media was replaced with fresh media. This is to remove dead and un-attached cells and the small volume of DMSO from the frozen cells. The media was then changed again 24 hours after the cells were plated to remove dead cells. Cells were left for at least 7 days prior to be used for any experiments. For Cos7 reporters, cells were left for 14 days prior to use.

2.2.8. Generation of stable cell lines.

The breast cancer cell line H3396 was chosen as a model system for over-expression of IRF-1 and IRF-1 phosphorylation mutants. This H3396 cell line offers the benefit that it has been previously described to be sensitive to IRF-1 dependent apoptosis (Clarke *et al.* 2004). Transient transfections are problematic in this cell line however, as they are prone to undergo cell death after transfection. This poses potential problems in studying the ability of IRF-1 to promote apoptosis. An alternative to transient transfections was pursued in which the murine IRF-1 gene and its phosphorylation mutants were stably integrated into the

H3396 genome. Constitutive over-expression of IRF-1 in cell lines is difficult given IRF-1's pro-apoptotic activity, as such an inducible system was used, in which IRF-1 expression could be "switched on" by the addition of doxycline (dox). Prior to integration of the IRF-1 gene, the gene for the tetracycline Repressor (TetR) was integrated. The TetR protein (which is produced from a constitutive viral promoter) binds TetR binding sites in DNA and silences expression of adjacent genes (Invitrogen). The IRF-1 gene inserted into the H3396 cells is under the control of a promoter containing these binding sites. As such the high levels of TetR in the cells are able to repress the expression of IRF-1. Addition of dox causes a conformational change in the TetR protein, which prevents it from repressing the target gene (in this case IRF-1) which in turn leads to large levels of IRF-1 protein expression. The individual steps for generating the stable cell lines are explained below.

2.2.9. Blasticidin response curve

H3396 cells were plated on six well dishes in RPMI containing blasticidin (Melford UK) between 3 and 15 μg/mL. Media was changed after 48 hours. 96 hours post treatment cells were trypsined and counted by trypan blue staining (2.2.5). The optimum concentration as which blasticidin prevented any cell growth was 8 μg/mL.

2.2.10. Transfection of TetR into H3396 cells.

Low passage H3396 cells were plated at 5% confluency on two 10 cm cell culture dishes in RPMI medium. One day later the cells were transfected with 2.5 μg of pcDNA6-TetR (Invitrogen, Paisley UK). The transfection procedure was the same as used in section 2.3.1. Forty eight hours post transfection, the H3396 cells were split 1:5 onto new 10 cm plates. The RPMI media was supplemented with 8μg/mL blasticidin to begin selection of positive clones. Due to the ability of H3396 cells to grow in extremely tight islands it was important to keep them at low density during the initial stages of transfection. Media was changed every 48 hours to maintain high levels of blasticidin and remove dead or dying cells. Significant cell death occurred approximately 5 days post addition of blasticidin.

2.2.11. Selection and testing of TetR expressing cells.

Two weeks post selection individual colonies of cells were large enough for transfer into 96 well plates. Clones were scraped from the original 10 cm plate and pipetted vigorously into wells (96 well plate) containing 100 μL of blasticidin containing RPMI. The disaggregation of the clones was essential as intact clumps of cells do not survive the transfer procedure. In total sixty two clones were isolated. Approximately 50% of the clones survived the transfer to the 96 well plates. Typically the clones required 5-7 days of growth before they could be transferred to twelve well plates. Rather than physically removing the cells, each clone was transferred by trypsin disaggregation. A total of twenty four clones were transferred onto twelve well plates, with each well containing 1 mL of 8 μg/mL blasticidin supplemented RPMI. The cells were grown in twelve well plates for 1 week. Each clone was then split into two wells of a 6 cm dish. Upon

reaching 80% confluence, cells were scraped from one of the two wells and protein extracts were made using Whole cell extraction buffer (50 mM Tris-HCl (pH 8.0), 420 mM NaCl, 1 mM EDTA, 0.2% NP40. Supplemented with 1 mM DTT, 10 mM NaF, 1x complete protease inhibitor 1 mM PMSF, 1 mM Na_3VO_3 and 10 mM βGP – see section 2.4.1. Immunoblot were carried out on the clone lysates against the TetR antibody and β-actin as a loading control. Of the eleven clones tested all expressed the TetR protein, although there was wide variation in the levels of expression The remaining cells in the six well plate were transferred onto 10 cm plates and allowed to grow for an additional 5 days. The clones that expressed lower levels of TetR were frozen once they had reached 80% confluence on the 10 cm plates (E11, C08, and G02). The remaining clones were further expanded by transferring onto 5x 10cm plates of each.

To confirm the activity of the TetR, four clones (C06, D04, E04 and E08) were each seeded on twelve well plates (six wells per clone). Twenty Four hours post seeding cells were transfected with 50 μg or 100 μg per well of pcDNA4-TO-Luc (Invitrogen, Paisley UK), and 10 ng/well of a β-GAL expression vector (to serve as a transfection control). The transfection was carried out for 24 hours, after which media was replaced with either RPMI (+ blasticidin) or RPMI with 1 μg/mL dox (+ blasticidin). Luciferase reporter assays were carried out 24 hours later (see section 2.3.3.). The pcDNA4-TO-Luc plasmid contains the Luciferase gene under transcriptional control of the CMV promoter and TetR binding sites. Presence of the TetR protein in the cells causes a repression of Luciferase expression, which can then in be relieved by addition of dox. The clone exhibiting the highest level of de-repression was chosen as the background for the inducible cell lines. Clone E04 was expanded and frozen for future use.

2.2.12. Zeocin response Curve.

As for the blasticidin, a kill curve of zeocin (the selection marker for pcDNA4-TO-IRF-1 expression) was employed to determine the optimum concentration required for selection of positive clones. A concentration range between 50 and 400 μg/mL was used. The cells were counted as in section 2.2.5. Zeocin was purchased from Invivogen.

2.2.13. Transfection of pcDNA4-IRF-1 into TetR expressing cells.

H3396-E08 cells were plated at 5% on 10 cm plates in RPMI media supplemented with Tet-free FBS (PAA) and blasticidin for 24 hours. The H3396-E08 cells were then transfected with 2.5 μg of empty vector, pcDNA4-TO wild type, T180A or TS-A IRF-1 for 48 hours. Each plate was then sub-cultured onto 3x10 cm plates in media containing 200 μg/mL zeocin. Two days later the media was changed to remove dead cells. Large levels of cell death occurred within 5 days of zeocin treatment.

2.2.14. Selection and testing of inducible cell lines.

Seven days after zeocin selection individual clones were large enough for selection onto 96 well plates. Scraping cells was carried out exactly as for the TetR cell lines. Between 70 and 90 clones of each cell line (vector, wild type, T180A, TS-A) were expanded on the 96 well plates. The most vigorous clones were then transferred onto twelve well plates as before. Another week of selection

was then required prior to clones being divided evenly onto three wells of twelve well plates. Upon reaching 75% confluence 1 well from each clone was treated with 2 μg/mL of dox for 24 hours, while another well was treated with blank media for the same time period. Lysates were then made and immunoblotted with IRF-1 (M-20) Ab and β-actin as a loading control (see section 2.4.1). For the most promising clones, the remaining cells in the twelve well plates were re-seeded on 6cm dishes for approximately 5 days, and then transferred to 10 cm plates. Once the cells reached 80% confluence half of the cells were frozen, while the remaining cells were split onto a 10 cm plate and two wells on a twelve well plate. To check that the selected clones were re-producible in their expression of IRF-1 the cells were induced as before and protein lysates made and immunoblotted. 13 clones were re-tested, the majority of which produced a reproducible induction of IRF-1. Each of these clones was then expanded on 15 cm plates, grown for an additional week, and frozen to provide a large number of aliquots of cells at the same passage.

2.3.1. Transient transfections

Transient transfections were carried out using 1 mg/mL PEI (Polyethylene Imine). 4 μL of PEI was used per μg of DNA transfected. Typically for a 10 cm plate no more than 10 μg of DNA was used for transfection. DNA was diluted in a total of 500 μL of media (without FBS) followed by addition of the PEI. The samples were then briefly vortexed and allowed to stand at room temperature for 20 minutes in order for DNA:PEI complexes to form. The DNA: PEI mixture was

then added directly to the cells. The low toxicity of PEI does not necessitate the changing of media after transfection.

2.3.2. Small interfering RNA transfections

GSK3β mRNA was depleted using small interfering RNA duplexes from QIAGEN (Hs_GSK3B_8_HP Validates siRNA). A control siRNA which does not target any human mRNA was used as a negative control (AllStars Negative Control siRNA QIAGEN). Prior to use in reporter assays the knockdown efficiency was optimized so at least 60% of GSK3β protein was depleted. A titration of siRNA duplexes between 5 and 20 nM was used, in addition to a number of concentrations of the INTERferin transfection reagent. Additionally length of transfection and cell density required optimization. Knockdown was carried out in MRC-5 cells seeded on twelve well plates for 24 hours. siRNA duplexes were diluted in re-suspension buffer (QIAGEN) then further diluted in FBS free αMEM media with 1.5 μL per well INTERferin transfection reagent (Polyplus). The solution was then vortexed for 10 seconds, followed by incubation for 10 minutes at room temperature. 100 μL of media containing siRNA's was added per well, with each well containing 900 μl of fresh media (containing FBS). The final concentration of siRNA in each well was 5 nM. 16 hours post transfection the media was removed and replaced with fresh media. Six hours later the cells were transfected for reporter assays. Each well was transfected with 125 ng of TRAIL promoter reporter, 20 ng βGAL internal control plasmid and 100 ng of pcDNA3.1 IRF-1 or pcDNA3.1. Transfections were carried out for 24 hours. Cells were lysed and assayed according to (2.3.3).

2.3.3. Luciferase reporter assays

Unless stated otherwise all reporter assays were carried out in COS-7 cells. Cells were seeded at 0.03 $x10^6$ in DMEM media for 24 hours in 24 well plates. Transfections were carried out using PEI (see section 2.3.1). Per well, cells were transfected with 50 ng of IRF-1 expression plasmid, 75 ng of reporter plasmid (either TRAIL promoter or 4X ISRE reporter) and 5 ng of βGAL internal control plasmid. The total amount of DNA per well was bought up to 250 ng with the addition of sheared salmon sperm DNA. DNA was diluted in DMEM media without FBS (but containing penicillin-streptomycin and L-glutamine) prior to the addition of PEI. The samples were briefly vortexed followed by incubation for 20 minutes prior to being added to well containing cells (in 1mL DMEM). Per well 50 μL of DNA/media was added. Media was changed 16 hours post transfection. The cells were lysed 48 hours post transfection. Lysis was carried out essentially according to manufacturer's instructions (Applied Biosystems). Media was removed from the wells followed by two washes with 1X PBS at 0.5 mL per well. For twenty four well plates, 50 μL of lysis buffer was added per well, while 100 μL was used for twelve well plates. The plates were placed at -80°C to snap freeze the lysates. Plates could be stored at this point until ready for the reporter assay. The plates were de-frozen at 4°C, using a pipette tip; the remaining cells attached to the plate were scraped into the lysis solution, and transferred to microfuge tubes. The tubes were centrifuged at 6,000 rpm for 10 minutes to pellet any cell debris. The reporter assays were carried out in white walled 96 well plates (Nunc). Per well 10 μL of buffer A was added, followed by 5 μL of protein lysates. The assay was carried out according to manufacturer's instruction from here on. Luminescence was detected on a Berthold Orion micro-plate

Luminometer. For analysis, each Luciferase value was corrected to the βGAL value. The βGAL dependent luminescence served as both a transfection control and a loading control for the assay. These values were expressed as RLU (Relative Luciferase Units). IRF-1 dependent transactivation of the reporter constructs was expressed as a fold change between cells expressing IRF-1 and those transfected with the appropriate empty vector. This was required as some cellular factors were able to produce a basal activity on the Luciferase reporters.

For GSK3 inhibitor treatments, the inhibitors were added to the wells containing fresh media, following the 16 hours media change. Inhibitors which required dilution in DMSO were diluted so that the final concentration of DMSO was consistent (0.01%) rather than serial dilution in media. Inhibitors were added to wells transfected with either IRF-1 or vector, and for each treatment the fold was determined between these two. This allowed for compensation for any effects the inhibitors may have on background Luciferase expression. For determining the knockdown efficiency of GSK3β, 20 μg/lane of reporter extracts were immunoblotted. However, as IRF-1 is a highly unstable protein and low concentrations were used in the reporter assays, detection by immunoblot was problematic and high concentrations of protein extracts were required for detection. An alternative method of cell lysis was used in which parallel wells were lysed directly with 4 X Lamelli buffer (500 mM Tris-HCl (pH 6.8), 10% SDS, 0.5% Bromophenol blue, 50% glycerol and 100 mM DTT) that had been pre-heated at 100°C for 5 minutes. The resulting lysates were scraped from the wells and centrifuged at 12,000 rpm for 10 minutes to remove insoluble debris. The entire extract for each well was then added per lane for immunoblot.

2.4.1. Preparation of whole cell extracts.

Media was removed from the plate, followed by a single wash in 1x PBS to remove any remaining media. For a 10 cm plate 1mL of 1x PBS was used to re-suspend the cell pellet. HEK293 cells required gentle pipetting to remove them from the surface of the plate, while more adherent cells (Cos7, H3396 and MRC-5) required scraping with cell scrapers. The cell suspension was collected in a microfuge tube. The cells were pelleted by centrifugation at 1000 rpm at 4°C for 5 minutes. The 1x PBS was removed from the pellet. Typically for a 10 cm plate of 90% confluent cells 1mL of WCE buffer was used to make cell extracts between 2-4 μg/mL, although when more concentrated extracts were required half this volume could be used. The cell pellets were then gently re-suspended in the WCE buffer (50 mM Tris-HCl (pH 8.0), 42 0mM NaCl, 1 mM EDTA, 0.2% NP40. Supplemented with 1 mM DTT, 10 mM NaF, 1x complete protease inhibitor, 1 mM PMSF, 1 mM Na_3VO_3 and 10 mM βGP) until a homogenous mixture was produced. When volumes of 500 μL or higher were used the cells were snap frozen in liquid nitrogen, then thawed in slushy ice water. This freeze fracturing was repeated 3x. Where sample volume was smaller (such as CHX chases or the testing of stable cell lines) the samples were placed in a -80°C freezer to snap freeze them. Once the extracts were completely thawed (on ice) they were centrifuged at 12,000 rpm for 20 minutes at 4°C. The clarified extracts were transferred to fresh tubes and frozen at -80°C.

2.4.2. Preparation of RIPA extracts.

Protein extracts that were used for immunoprecipitations were made using RIPA (Radioimmunoprecipitation Assay) buffer rather than WCE buffer. Plates were prepared in the same manner as for WCE extracts except 1mL (for 10cm plates) of RIPA buffer (50 mM Tris-HCl (pH 7.5), 150 mM NaCl, 1% NP40, 0.1% SDS, 0.5% sodium deoxycholate and 1 mM EDTA. Supplemented with 1 mM DTT, 10 mM NaF, 1x complete protease inhibitor, 1 mM PMSF, 100 mM NEM, 1 mM Na_3VO_3 and 10 mM βGP) was left on the plate for 5 minutes at 4°C. The resulting cell / RIPA mix was then scraped into 1.5 mL centrifuge tubes and left on ice for 20 minutes. The cell / RIPA mix was then vigorously pipetted 10 times before the cells were centrifuged at 12,000 rpm for 20 minutes at 4°C. The extracts were then transferred to clean tubes and frozen at -80°C.

2.4.3. Preparation of NP40 extracts

For GST-Fbox co-immunoprecipitations extracts were made in NP40 lysis buffer (50 mM Tris pH 7.5, 150 mM NaCl, 0.5% NP40 and phosphatase/protease inhibitors). The extracts were made essentially as for WCE extracts, but with NP40 buffer being used instead.

2.4.4. Preparation of *in vivo* ubiquitination assay extracts

HEK293 cells were transfected with expression plasmids for HA-ubiquitin (human) at 2.5 μg and FLAG IRF-1 (mouse) at 2.5 μg on a 10cm plate (see 2.3.1). Cells were incubated for 40 hours before addition of MG132 at 10 μM for 5

hours. Duplicate transfected plates were treated with DMSO as vehicle control. The total amount of DMSO in medium was 0.01%. Extracts were made by scraping the HEK293 cells in 1 mL of 1X PBS. Samples were collected in microfuge tubes and centrifuged at 1300 rpm for 5 minutes at room temperature. The PBS was aspirated from the cell pellets. The cell pellets were snap frozen at -80°C. Samples were then thawed, for each pellet 1 mL of ubiquitination assay buffer (10 mM Tris-HCl (pH 7.8), 150 mM NaCl, 1% SDS and 1 mM EDTA. Supplemented with 1 mM DTT, 10 mM NaF, 1x complete protease inhibitor 1 mM PMSF, 100 mM NEM, 1 mM Na_3VO_3 and 10 mM βGP) was added, followed by quick disaggregation of the cell pellet. Extracts were boiled at 100°C for 10 minutes. The denatured extracts were clarified by centrifugation at 13000 rpm for 30 minutes at 4°C. Extracts were transferred to clean tubes and stored at -80°C. For determination of protein content, extracts were diluted 10x in 10mM Tris pH 8 due to the high levels of SDS interfering with the Bradford assay.

2.4.5. Protein assay

Protein assays were carried out according to the manufacturer's instructions using the BIORAD Bradford protein assay (BIORAD). A standard curve of BSA protein ranging from 2 to 10 μg/mL was used for calibration. Absorbance was detected using an Eppendorf spectrophotometer (Eppendorf).

2.4.6 *In vitro* transcription and translation.

In vitro transcription and translation was carried out using the TnT Rabbit Reticulocyte lysates kit (Promega). Fbxw7α was in vitro transcribed and translated from a PCR product rather than the plasmid, as pCMV-HA does not contain the required T7 promoter. The PCR product contained a T7 binding site and a Kozak sequence and was designed using the recommended parameters set out by Promega. The primer sequence and PCR conditions can be found in table 2.1. For a 50 μL reaction mix, the following was used, 1 μg PCR template, 2 μL TnT reaction mix (10X), 1 μL amino acid mix (without methionine), 1 μL RNasin ribonuclease inhibitor (Invitrogen), 1 μL T7 Polymerase, 25 μL of Rabbit reticulocyte lysate and 1 μL [^{35}S] methionine (1 mM) at 1000 Ci/μmol (GE Healthcare). The reaction was incubated at 30°C for 90 minutes. A 1 μL aliquot was run on a SDS PAGE gel for quantification.

2.4.7. Separation of proteins on SDS PAGE gels

Proteins were separated on SDS-PAGE gels using the Tetra System (Biorad). Typically PAGE gels using 8% acrylamide were used as these allow good separation of IRF-1 (50 kDa) and β-actin (37 kDa). 1 mm gels with 15 wells were cast according to manufacturer's instructions. Protein extracts were prepared in Lamelli buffer supplemented with 100 mM DTT (500 mM Tris-HCl (pH 6.8), 10% SDS, 0.5% Bromophenol blue, 50% glycerol) to a final concentration of 1x. Typical protein concentrations used were between 10 and 25 μg. higher concentrations of protein extract result in the β-actin being over-loaded making

densitometry problematic. Protein extracts were boiled for 5 minutes, followed by centrifugation at 12,000 rpm for 30 seconds. A protein pre-stained 250-10 kDa ladder (BIORAD) was used to determine the progress of the electrophoresis as well as act as a molecular weight marker and indicator of transfer. For 15 well gels 5 μL was used per lane, while 8 μL was used for 10 well gels. SDS-PAGE gels were subjected to electrophoresis at 100 V in 1X TGS (25 mM Tris, 200 mM Glycine, 3.5 mM SDS) typically for 90 minutes.

2.4.8. Coomassie brilliant blue staining

To determine induction of GST-IRF-1 proteins coomassie staining was employed. Gels were stained in coomassie stain (10% acetic acid, 40% methanol and 0.25% coomassie blue R250) for 20 minutes with gently rocking followed by de-staining overnight with de-stain solution (10% acetic acid and 40% methanol.).

2.4.9. Transfer to nitrocellulose membrane.

After electrophoresis gels were removed from the plates by cutting away the stacking gel and gently lifting using a piece of blotting paper. Transfer was performed using the Tetra system (BIORAD). Protein was transferred onto 0.45 μm nitrocellulose (BIORAD) using Transfer buffer (39 mM glycine, 48 mM Tris 0.037% SDS 20% methanol (v/v) pH 8.3). Typically the transfer was carried out at 300 mAmps for 60 minutes at 4°C. To ascertain if transfer has been successful the membrane is stained with Ponceu S stain (Sigma Aldrich) for 2 minutes at

room temperature with gentle rocking. Excess stain was then removed using ddH_2O until clear pink bands can be visualised.

2.4.10. Blocking

After confirmation of successful transfer, nitrocellulose membranes were blocked with a solution containing 5% milk in 1X PBS. Blocking was carried out at room temperature for 30 minutes with gentle rocking. When the c-Myc phospho Thr^{62}/Ser^{60} antibody was used, blocking was carried out with BlottoB (1% milk, 1% BSA, 0.05% Tween-20, 1 mM NaF, and 1 mM βGP and 0.1 μL/mL phosphatase inhibitor cocktail in TBS) rather than 5% milk. This blocking was carried out in the same manner as for the 5% milk but was left for 90 minutes.

2.4.11. Immunoblot

Immunoblots were carried out in 50 mL tubes containing 5 mL of indicated antibody with gentle mixing. The conditions for each antibody are detailed in table 2.2. Following incubation with primary antibody, the blots were washed with 1X TBST (10 mM Tris-HCl (pH 7.5), 150 mM NaCl and 0.05% Tween-20) for 10 minutes three times. The secondary antibody was then incubated in 50 mL tubes as for the primary antibody. Blots were incubated with secondary antibody for 1 hour at room temperature. The blots were then washed 3x in 1X TBST - the final wash being carried out with TBS (no TWEEN-20). The chemilumiscence reaction was carried out by preparing ECL reagent (see table) without Hydrogen Peroxide. The blots were gentle tapped on paper towel to remove any remaining

TBS, then placed flat on saran wrap. Hydrogen Peroxide was then added to the ECL reagent, which was then placed on the blot for 2 minutes (ECL reagent 0.2 mM p-coumaric acid 1.25 mM luminol in 0.1 M Tris pH 8.5, 0.009% hydrogen peroxide). For a 6x4 inch blot 5 mL of ECL reagent was used. After 2 minutes of incubation at room temperature, the ECL reagent was gentle tapped from the blot, which was the wrapped in a single layer of saran wrap. Chemilumiscence was detected using a Fujifilm LAS-4000. If further antibodies were to be incubated on the blot, washing for 10 minutes with 1X TBST was carried out prior to the addition of new primary antibody.

Primary Antibodies

Antibody	Type	Species	Dilution	Incubation conditions	Manufacturer
IRF-1 M20	Poly	Rabbit IgG	1:1000 (WB) 1ug/mL (IP)	5% milk	Santa Cruz
IRF-1 C20	Poly	Rabbit IgG	1:1000 (WB) 1ug/mL (IP)	5% milk	Santa Cruz
Phospho-c-Myc	Poly	Rabbit IgG	1:1000 (WB) 1ug/mL (IP)	BlottoB	Santa Cruz
FLAG M2	Mono	Mouse	1:2000 (WB) 0.2ug/mL (IP)	5% milk	Sigma-Aldrich
HA 12CA5	Mono	Mouse	1:1000 (WB) 0.5ug/mL (IP)	5% milk	In house
β-actin	Mono	Mouse	1:2000 (WB)	5% milk	Sigma-Aldrich
GSK3β	Poly	Rabbit	1:2000 (WB)	5% milk	CST
GST	Poly	Rabbit	1:2000 (WB)	5% milk	Sigma-Aldrich
pT-P	Mono	Mouse	1:500 (WB) 5mL/ mg extract (IP)	5% BSA	CST

Secondary Antibodies

Antibody	Dilution	Incubation conditions	Manufacturer
Goat anti Mouse IgG - HRP	1:5000	5% milk	Santa Cruz
Goat anti Mouse IgM - HRP	1:5000	5% BSA	Santa Cruz
Goat and Rabbit IgG - HRP	1:5000	5% milk	Santa Cruz
Mouse anti Rabbit Kappa light chain specific - HRP	1:5000	BlottoB	Chemicon

Table 2.2. Antibodies used in this study. Antibody concentration was 200μg/mL for all Santa-Cruz antibodies.

2.4.12. Stripping blots

To remove primary antibody (for example when two similar sized proteins which the same secondary need to be immunoblotted) blots were stripped with a mercaptoethanol based stripping buffer (100 mM β-mercaptoethanol 2% (w/v) SDS 62.5 mM Tris pH 6.7). The blots were placed in a sealable container and covered with enough stripping buffer to cover the blot with approximately half a mL. The container was then sealed tightly and placed in a rocking incubator at 65°C. After 30 minutes of incubation the stripping buffer was gently tipped away

in a fume hood. The blots were then washed with large amounts of ddH_2O to remove any remaining stripping buffer. Blots were then re-probed with 5% milk. To determine if any secondary antibody remains on the blot, ECL detection was carried out on the blot. If any signal remains, the stripping was repeated. Otherwise primary antibody was added as per section 2.4.11.

2.4.13. Densitometry

Densitometry was performed using the Scion software package.

2.5.1. Immunoprecipitations

The conditions of the various immunoprecipitations carried out are given in the table below.

IP protein	IP Ab	Protein being detected	Beads	Washes
eYFP-IRF-1 (500μg)	IRF-1 M20 (Rabbit)	p-T/S (Rabbit)	Protein A agarose	3x low salt RIPA buffer
Phospho-IRF-1 (p-T/S) (500μg)	p-T/S (Rabbit)	IRF-1 M20 (Rabbit)	Protein A agarose	2x low salt RIPA, 3x high salt RIPA buffer
FLAG-IRF-1 (500μg)	FLAG M2 (Mouse)	p-T/S (Rabbit)	Protein G agarose	3x low salt RIPA buffer
Phospho-IRF-1 (p-T/S) (500μg)	p-T/S (Rabbit)	IRF-1 M20 (Rabbit)	Protein G agarose	2x low salt RIPA, 3x high salt RIPA buffer
Phospho-IRF-1 (p-TP) (1mg)	p-TP (Mouse)	IRF-1 M20 (Rabbit)	Mouse IgM agarose	3x low salt RIPA buffer
FLAG-IRF-1 (1mg)	FLAG M2 (Mouse)	HA (GSK3β-HA)	Protein G agarose	3x low salt RIPA buffer
FLAG-IRF-1 (1mg)	FLAG M2 (Mouse)	HA (HA-Fbxw7)	Protein G agarose	3x TNE buffer
GSK3β (1mg)	HA 12CA5 (Mouse)	FLAG M2 (IRF-1)	Protein G agarose	3x low salt RIPA buffer
HA-Fbxw7 (1mg)	HA 12CA5 (Mouse)	FLAG M2 (IRF-1)	Protein G agarose	3x TNE buffer
Endogenous human Phospho-IRF-1 (p-T/S) (500μg)	p-T/S (Rabbit)	IRF-1 C20 (Rabbit)	Rabbit IgG agarose	3x low salt RIPA buffer
Endogenous human IRF-(500μg)	IRF-1 C20 (Rabbit)	p-T/S (Rabbit)	Rabbit IgG agarose	3x low salt RIPA buffer

Table 2.3. IP Conditions. Protein A Agarose was from Santa Cruz, Protein G Agarose from Millipore and Rabbit IgG Agarose from eBiosciences.

To IP 500 μg of protein, lysates were diluted in a total volume of 500 μL of low salt RIPA buffer supplemented with inhibitors. Or, for co-IP with HA-Fbxw7 NETN buffer supplemented with inhibitors. Lysates were pre-cleared against proteins that non specifically interact with the IP beads. Pre-clearing was carried out by incubating 5 μL packed volume of beads at 4°C with gently rocking for 30 minutes. After pre-clearing the lysates were centrifuged to pellet the beads and removed to a new tube. Overnight at 4°C the lysates were incubated with the appropriate antibody, for antibody concentrations see table 2.2. The samples were then incubated for 3 hours with the appropriate BSA blocked beads at 4°C with gentle rocking. The samples were centrifuged at 3,000 rpm for 30 seconds, the protein lysates removed and the beads washed 3x with low salt RIPA buffer. The residual volume of buffer was removed using insulin syringes U-100 (Beckton Dickinson) to leave a completely dry pellet, which was re-suspended in 20-30 μL of 5X Lamelli buffer supplemented with 100 nM DTT. The samples were boiled for 5 minutes at 100°C and briefly centrifuged to settle the beads. The eluates were removed from the beads using U-100 insulin syringes and placed in fresh tubes. The eluates were centrifuged at high speed for 30 seconds to remove any bubbles. The samples were subjected to western blot with the indicated antibodies. When phosphorylation was being detected, BlottoB solution was used for blocking an addition of antibodies. Additionally wash steps were performed in the presence of phosphatase inhibitors.

2.5.2. Co-immunoprecipitations

Co-immunoprecipitations were carried out essentially as for section 2.2.1 protein extracts for co-immunoprecipitations were made using low salt RIPA. For co-immunoprecipitation between FLAG-IRF-1 and HA-GSK3β, washes were carried out using low salt RIPA buffer, while co-immunoprecipitations between FLAG-IRF-1 and HA-Fbxw7 used TNE buffer (10 mM Tris (pH 7.4), 1 mM EDTA and 200 mM NaCl. The buffer was supplemented with 1 mM DTT, 10 μM NaF, 1x complete protease inhibitor (Roche), 1 mM PMSF, 100 mM NEM, 1 mM Na_3VO_3 and 10 mM βGP). For all co-immunoprecipitations 1 mg of extract was used.

2.5.3. *In vivo* ubiquitination assays

500 μg of protein extract were diluted in 750 μl of TNE buffer (10 mM Tris (pH 7.4), 1 mM EDTA and 200 mM NaCl. Supplemented with 1 mM DTT, 10 μM NaF, 1x complete protease inhibitor, 1 mM PMSF, 100 mM NEM, 1 mM Na_3VO_3 and 10 mM βGP) and pre-cleared with 5 μl (packed bead volume) of protein G agarose beads (Santa Cruz). Pre-clearing was carried out for 30 minutes at 4°C with gentle rocking. The protein extracts were centrifuged at 3,000 rpm for 1 minute to pellet the protein G beads. The extracts were transferred to new microfuge tubes with 0.4 μg FLAG M2 antibody overnight at 4°C with gentle mixing. BSA blocked protein G beads were added to the extracts (5 μl packed volume) for 3 hrs at 4°C with gentle mixing. Extracts were centrifuged at 3,000, 4°C for 1 minute to pull down the protein G beads. The beads were washed 3 times with TNE buffer supplemented with 1X protease inhibitor cocktail (Roche).

Protein was eluted from the beads using 5x Lamelli buffer supplemented with 100 mM DTT Beads were boiled with the Lamelli buffer for 6 minutes at 100°C. Lamelli buffer containing eluted protein was drawn off the beads using U-100 0.5mL insulin needles (Becton-Dickinson). Extracts were run on 8% SDS polyacrylamide gels, transferred to nitrocellulose, blocked for 30 minutes in 5% milk and blotted with anti HA antibody. Following immunoblot with HA antibody, FLAG antibody was used to determine immunoprecipitation of FLAG-IRF-1.

2.5.4. *In vivo* GST pull-downs

500 μg of extracts containing transfected GST-Fbxw7 and FLAG-IRF-1 were incubated with gentle rocking at 4°C in a total reaction mix of 500 μL with 10 μL (packed bead volume) of glutathione – sepharose beads (GSH beads) (GE Healthcare). The protein extracts were diluted in low salt NP40 buffer (50 mM Tris pH 7.5, 150 mM NaCl, 0.5% NP40 and phosphatase/protease inhibitors). The beads were incubated with the protein extract for 3 hours, after which the samples were centrifuged at 3,000 rpm for 30 seconds and washed with 500 μl of low salt NP-40 buffer, followed by two washes with medium salt NP40 buffer and a further wash with low salt NP40 buffer. The samples were centrifuged and NP40 buffer removed using a U-100 insulin needle (BD) The beads were incubated at 100°C for 6 minutes with 20 μL of 5x Lamelli buffer supplemented with 100 nM DTT. The protein eluates were then removed from the beads using a U-100 and transferred to fresh tubes. The samples were centrifuged briefly and subjected to PAGE and western blot against FLAG and GST antibodies.

2.5.5. *In vitro* GST pulldown assays.

For *in vitro* GST pulldown assays between GST-IRF-1 and [^{35}S] Met labelled GSK3β or Fbxw7α approximately 1 μg of each protein was used. The GST-IRF-1 conjugated GSH beads were diluted in 1mL NETN buffer (20 mM Tris pH 8, 100 mM NaCl, 1 mM EDTA, 0.5% NP40 and 1x complete protease inhibitor cocktail). The IVT product was mixed with the beads overnight at 4°C on a rotating wheel. The beads were washed 3 times with NETN buffer before being dried in a speed-vac vacuum. The dried beads were re-suspended in 2x Lamelli buffer supplemented with 100 mM DTT. The eluates were then separated by SDS-PAGE for 45 minutes at 200 V. The gel was fixed in fixing solution (10% acetic acid 10% methanol) for 30 minutes before being treated with amplifier solution (Amersham) for 30 minutes with gentle rocking. The gels were then dried and exposed to film at -80°C.

2.5.6. Cycloheximide time courses

HEK293 cells were seeded on six well plates at $0.3x10^6$ in DMEM media and allowed to attach for 24 hours. The cells were then transfected with 2.5 μg/well of IRF-1 plasmid. For transfections with more than one plasmid, GSK3β–HA was also transfected at 2.5 μg/well or empty plasmid. Transfections were carried out as in section 2.3.1. Twenty four hours post transfection cells were treated with Cycloheximide at 25 μg/mL for the indicated time period. MRC-5 cells were seeded on 6cm dishes for the same period of time as for HEK293 cells. 4 μg of IRF-1 plasmid was transfected in MRC-5 cells according to section 2.3.1. Cells were lysed according to section 2.4.1. Extracts were separated on 8% SDS

polyacrylamide gels at 15 μg/lane, transferred to nitrocellulose, blocked with 5% milk for 30 minutes and immunoblotted with the indicated antibodies.

2.6.1. Small scale preparation of GST proteins

To identify a bacterial clone that expressed high levels of the GST fused IRF-1 protein, mini inductions were carried out as a screen. The GST constructs (1μg) were transformed in chemically competent BL21 cells using the same protocol as for DH5α cells (see section). Five colonies of each construct were picked and grown in 2.5 mL of LB AMP for 2 hours with shaking. The cultures were then split into two 1mL aliquots in microfuge tubes, with the remaining 500 μl being kept back to inoculate further cultures. To one of each clone, 25 μl of 20mM IPTG was added, while the same volume of water was added to the other half of the culture as a control. The BL21 cells were then grown for a further 2 hours at 37°C with shaking. Bacteria were then centrifuged at 12,000 rpm for 60 seconds to form a pellet. The LB-AMP was aspirated, and the pellets were re-suspended in 50 μl of 4X Lamelli loading dye. The pellets were then boiled for 5 minutes to denature the protein. 20 μl of the sample was loaded onto SDS polyacrylamide gels (8%) and separated by electrophoresis. The gels were then stained with Coomassie Brilliant Blue to determine GST protein induction. Clones that produced a high amount of GST fused IRF-1 were then grown overnight in 5 mL of LB AMP.

2.6.2. Medium scale preparation of GST proteins

The 5 mL overnight culture was first inoculated into a 50 mL volume of LB AMP and grown for 1 hour at 37°C. IPTG was then added to the culture at a final concentration of 0.5 mM. The cultures were incubated for an additiona l 3 hours at 37°C. The bacteria were then pelleted by centrifugation at 4,000 rpm for 5 minutes, media was aspirated and the pellet was re-suspended in 5mL of NETN buffer (20 mM Tris pH 8, 100 mM NaCl, 1 mM EDTA, 0.5% NP40 and 1x Roche complete protease inhibitor cocktail). The lysates was sonicated for 30 seconds and 20 seconds off three times at medium power with a Diagenode Bioruptor. The debris was centrifuged at 4,000 rpm at 4°C for 10 minutes. Glutathione sepharose beads (Amersham) were mixed at a 1:1 ratio with NETN buffer and 0.5% milk. The slurry was centrifuged at 2,000 rpm for 2 minutes; supernatant was removed leaving a small volume on top of the packed beads. An equal amount of the NETN/milk solution was then added to the beads, and the washing was repeated twice more. On the last step the supernatant was not removed, but was used to make a 1:1 slurry mixture which was added to the cleared bacterial lysates. In a 15 ml tube 150 µl of glutathione sepharose beads was mixed with the lysates and incubated on a rotating wheel at 4°C for 1 hour. Beads were span down at 2,000 rpm, 4°C for 2 minutes, supernatant was removed and replaced with 5 mL of NETN buffer without milk. This wash step was repeated three times. GST fusion proteins were eluted from the beads using a glutathione elution buffer (20 mM Glutathione, 100 mM Tris-HCl pH 8 and 120 mM NaCl) which was added to the bead pellet (1 mL of elution buffer per 0.25 mL of beads). The samples were then rotated at 4°C for 1 hour. Beads were then centrifuged at 13,000 rpm for 5 minutes, the supernatant was transferred to a fresh tube and stored ready for

protein determination using the Nanodrop according to manufacturer's instructions. Protein was then aliquoted into small volumes and stored at -80°C until ready to use.

2.6.3. *In vitro* kinase assays

Recombinant GSK3β (New England Biolabs) was diluted to 20 ng/μL in the supplied kinase buffer and incubated with 4 μg of GST-IRF-1. The final concentration of ATP was 250 μM, which was supplemented with 0.16 μCi of [γP^{32}]-ATP (Becton Coulter) per reaction. The final reaction volume was 25 μL in 1x kinase buffer. The reaction was carried out at 37°C for 30 minutes, and was terminated by the addition of 6 μL of 5X Lamelli buffer (with 100 mM DTT). Samples were subjected to gel electrophoresis on a 8% acrylamide gel. The acrylamide gel contained a 14% skirt at the bottom of the gel to help contain free [γP^{32}]-ATP. This skirt was removed, and the gel dried before being subjected to autoradiography. For cold kinase assays, conditions were identical, but with non radioactive ATP and 60 minute incubation.

2.6.4. Direct immunofluorescence microscopy

HEK293 and COS-7 cells were seeded on six well dishes at $2x10^5$ cells per well on sterile 10x10 mm coverslips. The cells were transfected with eYFP-IRF-1 constructs according to section 2.3.1. Twenty four hours post transfection media was removed from the wells, followed by 4x washes with 1X PBS. Cells were fixed for 10 minutes with fixative solution (4% Paraformaldehyde in 1x PBS 5

mM NaOH). Fixative solution was then removed and the wells washed 5x with 1X PBS. The cells were then incubated with 0.5 μg/mL Hoechst 33258 for 5 minutes in PBS. The hoechst 33258 was then removed and the cells were washed a further 5x with 1X PBS. The coverslips were removed from the wells, inverted and placed on microscope slides with 10 μL of mounting media (49% PBS 49% Glycerol 2% (w/v) n-propyl gallate), dried and sealed using nail polish. A Zeiss LSM 510 META Confocal microscope was used to image the eYFP-IRF-1 transfected cells. Fluorescence from the eYFP was detected using 488 nm laser excitation at 2% power and the Long Pass 505 filter for emission. The hoechst counter stain for DNA was measured using a mercury bulb. The lens used was a 63x/1.4 oil lens (Zeiss).

Chapter 3.

IRF-1 is phosphorylated at Thr^{180} by GSK3β

3.1. Introduction

IRF-1 was described as a phospho-protein over two decades ago, to date; only two IRF-1 kinases have been identified. There is no evidence that either of these kinases phosphorylate IRF-1 *in vivo*, and almost nothing is known about the molecular outcomes of IRF-1 phosphorylation. In this chapter, I set out to identify potential IRF-1 kinases by *in silico* prediction. A conserved Thr/Ser pair situated just outside the mapped TAD of IRF-1 was chosen for this study. GSK3β was predicted to phosphorylate Thr^{180}, with Ser^{184} being phosphorylated first and acting as "priming" site for GSK3β. Direct phosphorylation of IRF-1 by GSK3β was demonstrated by an *in vitro* kinase assay, this was followed by *in vivo* experiments in which over-expressed GSK3β was shown to phosphorylate IRF-1 in HEK293 cells at threonine 180. Phosphorylation of IRF-1 in the human breast cancer cell line H3396 and the primary fibroblast cell line MRC-5 was also demonstrated suggesting that this phosphorylation occurs with endogenous GSK3β. Direct interaction between IRF-1 and GSK3β was demonstrated by GST pulldown assays, while co-immunoprecipitations in HEK293 cells demonstrated an *in vivo* interaction. This interaction was independent of phosphorylation, as kinase inactive GSK3β interacts with IRF-1, while wild type GSK3β was also capable of interacting with mutants of IRF-1. Collectively I have identified a novel interacting partner of IRF-1 in GSK3β, while also pin-pointing a specific target residue in Thr^{180}.

3.2. Prediction of potential phosphorylation sites on mouse IRF-1.

To predict potentially phosphorylated residues, and the kinases which phosphorylate them, the amino acid sequences of human and mouse IRF-1 were submitted to ten online prediction programmes (figure 3.1A). Human IRF-1 contains thirty four serine residues, eighteen threonine residues and seven tyrosine residues, most of these residues are conserved between human and mouse (figure 3.1B).

A.

>gi|49456387|emb|CAG46514.1| IRF1 [Homo sapiens]
MPITRMRMRPWLEMQINSNQIPGLIWINKEEMIFQIPWKHAAKHGWDINKDAC
LFRSWAIHTGRYKAGEKEPDPKTWKANFRCAMNSLPDIEEVKDQSRNKGSSAVRV
YRMLPPLTKNQRKERKSKSSRDAKSKAKRKSCGDSSPDTFSDGLSSSTLPDDHSSYT
VPGYMQDLEVEQALTPALSPCAVSSTLPDWHIPVEVVPDSTSDLYNFQVSPMPSTS
EATTDEDEEGKLPEDIMKLLEQSEWQPTNVDGKGYLLNEPGVQPTSVYGDFSCKEE
PEIDSPGGDIGLSLQRVFTDLKNMDATWLDSLLTPVRLPSIQAIPCAP

>gi|71059797|emb|CAJ18442.1| Irf1 [Mus musculus]
MPITRMRMRPWLEMQINSNQIPGLIWINKEEMIFQIPWKHAAKHGWDINKDAC
LFRSWAIHTGRYKAGEKEPDPKTWKANFRCAMNSLPDIEEVKDQSRNKGSSAVRV
YRMLPPLTRNQRKERKSKSSRDTKSKTKRKLCGDVSPDTFSDGLSSSTLPDDHSSYTT
QGYLGQDLDMERDITPALSPCVVSSSLSEWHMQMDIIPDSTTDLYNLQVSPMPST
SEAAKDEDEEGKIAEDLMKLFEQSEWQPTHIDGKGYLLNEPGTQLSSVYGDFSCKEE
PEIDSPRGDIGIGIQHVFTEMKNMDSIMWMDSLLGNSVRLPPSIQAIPCAP

B.

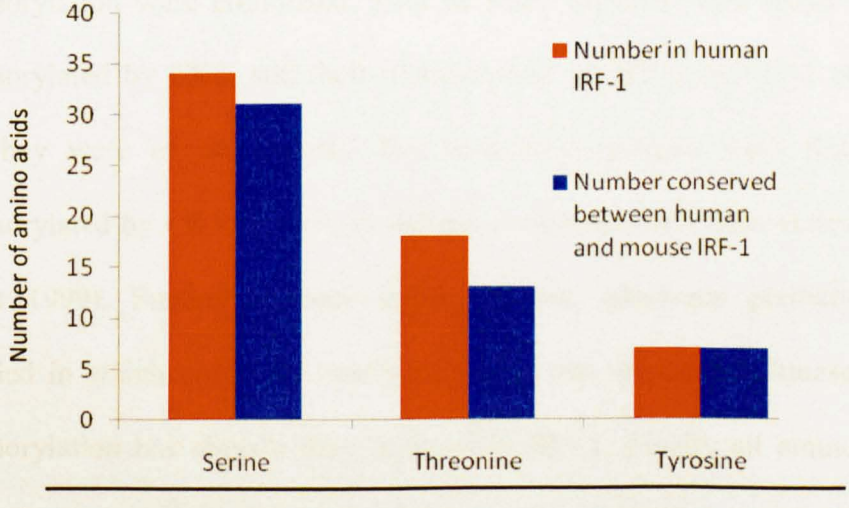

Figure 3.1. Human and Mouse IRF-1 amino acid sequences. A) The human and mouse IRF-1 amino acid sequences used throughout this study. **B)** The number of serine, threonine and tyrosine residues in human IRF-1 (red) and the number of residues conserved with mouse (blue).

Of the 59 potentially phosphorylated Ser / Thr / Tyr residues, 49 amino acids were predicted as potential phosphorylation sites by at least one of the programmes. To filter out the predictions, several steps were employed (figure 3.2). First, all of the non conserved residues were removed, as mouse IRF-1 was to be used in this study, and residues that were not conserved at least between human and mouse IRF-1 were not of interest. Next, tyrosine residues were removed. Studies by Kautz et al, have established that IRF-1 is phosphorylated at $Tyr^{109,}$ but this is the sole Tyr phosphorylated (Kautz *et al.* 2001 and la Sala *et al.* 2009). The kinase(s) responsible remains to be identified. Four of the seven Tyr were predicted to be phosphorylated by multiple prediction programmes; however no single kinase was consistently selected for any of these Tyr residues making identification problematic (there are over one hundred Tyr kinases in the human genome). Consequently Tyr phosphorylation of IRF-1 was not pursued. Next, eihgt residues which have previously been mutated in the study of CK2 phosphorylation were eliminated. Four of these residues were found not to be phosphorylated by CK2, and their mutation had no effect on IRF-1 activity, as such they were of no interest. The remaining residues were found to be phosphorylated by CK2 *in vitro*, so did not constitute novel discoveries (Lin and Hiscott 1999). Further to these eight residues, additional predictions were discarded in which only CK2 was predicted as the responsible kinase, as CK2 phosphorylation has already been mapped in IRF-1. Finally all amino acids in which there was little agreement between the prediction programmes were discarded. This resulted in a short list of seven amino acids (figure 3.3)

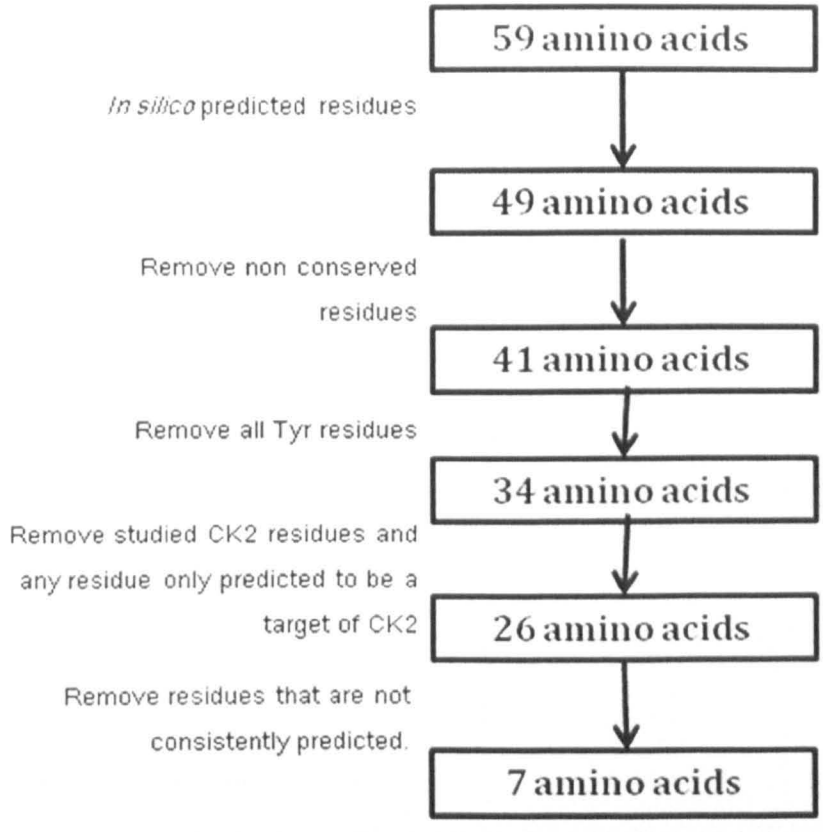

Figure 3.2 Work flow of phosphorylation prediction. Flowchart of rationale used to produce a shortlist of potentially phosphorylated residues in IRF-1.

Residue	Kinase	Phosida	GPS 2.1	HPRD	PredPhospho	NetPhosK	PPSearch	PPSP	KinasePhos	ELM	Motif Scan	Number of predictions
S125	CK1	•	•	•					•	•		5
	CK2								•			1
	PKA		•	•		•				•		4
	PKC		•	•					•			3
	DAPK3		•									1
	PAKA		•									1
	PKG1		•						•			2
	RSK		•									1
	CAMK		•									1
	Aurora Kinase		•									1
S127	PKA			•					•			2
	PKC		•	•		•			•			4
	PKG								•			1
	AKT								•			1
	PDK			•								1
	GPRK1			•								1
	Chk 1		•				•		•		•	4
	DAPK		•									1
	ROCK1		•									1
S128	CK1			•								1
	CK2			•	•							2
	PKA			•								1
	PKC			•	•	•			•			4
	PKR		•									1
	DMPK		•									1
	PKG1		•									1
	CAMK								•			1
	CDK7		•									1
	DAPK		•									1

Residue	Kinase	Phosida	GPS 2.1	HPRD	PredPhospho	NetPhosK	PPSearch	PPSP	KinasePhos	ELM	Motif Scan	Number of predictions
S162	CK1			•		•			•	•		4
	CK2			•								1
T180	GSK3		•	•		•				•	•	5
	ERK1/2		•	•					•	•		4
	CDK5		•	•					•	•		4
	RAF1			•								1
	p38		•			•			•	•		4
S184	GSK3			•		•						2
	ERK1/2		•	•					•	•		4
	p38		•						•	•		3
	CDK5, 4, 6		•	•					•	•		4
	NIMA							•				1
S215	GSK3	•	•	•	•			•		•		6
	ERK1/2		•	•						•		3
	CDK4, CDK5		•	•					•	•		4
	GPKR1			•								1
	KIS		•									1
	FRAP		•									1

Figure 3.3 Shortlist of predicted phosphorylation events in IRF-1. Table of the seven shortlisted amino acids, and the potential kinases. Kinases highlighted in red were predicted four or more times. Abbreviations **CK1** (Casein Kinase I), **CK2** (Casein Kinase II), **PKA** (Protein Kinase A), **PKC** (Protein Kinase C), **DAPK3** (Death Associated Protein Kinase 3), **PAKA** (p21 Activated Kinase 1), **PKG1** (Protein Kinase G), **RSK** (Ribosomal Protein S6 Kinase), **CAMK** (Calmodulin Dependent Kinase), **Akt** (Protein Kinase B), **PDK** (Pyruvate Dehydrogenase Kinase), **GPRK1** (G Protein Receptor Kinase 1), **Chk1** (Checkpoint Kinase 1), **ROCK1** (Rho- Associated coiled coil containing Protein Kinase), **CDK** (Cyclin Dependent Kinase), **GSK-3** (Glycogen Synthase Kinase – 3), **ERK** (Extra-cellular Regulated Kinase), **FRAP** (Mammalian Target of Rapamycin)

Three residues, Ser^{125}, Ser^{127} and Ser^{128} are all in close proximity. All three were matched to multiple kinases, including CK1, PKA and Chk1. Additionally; all were predicted to be substrates of PKC. Previous studies have shown that IRF-1 interacts with and is phosphorylated by PKCα (Giroux *et al.* 2003), although the residues targeted were not identified. PKC has been suggested to regulate IRF-1 localisation, so it was interesting to note that the three predicted residues were all located close to the IRF-1 NLS. As this study was an attempt to identify entirely novel phosphorylation events in IRF-1, it was decided not to investigate PKC phosphorylation of IRF-1. Ser^{162} was only predicted to be phosphorylated by CK1 (not including CK2 which had been previously discounted). It was preferable to study amino acids that could be targeted by more than one kinase, in order to increase the probability that a kinase would be identified. For this reason Ser^{162} was not studied further. The three remaining amino acids were each predicted by numerous kinases. All three were predicted to be phosphorylated by GSK3 (Glycogen Synthase Kinase 3). An unusually feature of GSK-3 phosphorylation is its preference for "priming" of a +4 Ser / Thr residue by phosphorylation, often by another kinase. As such when studying GSK-3 substrates the +4 residue is of equal interest. For Thr^{180} the +4 residue would be Ser^{184}, which was itself predicted to be phosphorylated by numerous kinases, including many proline directed kinases. The +4 priming site for Ser^{215} would be Ser^{219}. This amino acid was discarded, because only a single prediction was made for its phosphorylation.

Looking further at the amino acid sequence of IRF-1 an adjacent potential GSK-3 site was also identified (see figure 3.5). The spacing of the residues is not optimal for a four amino acid phosphorylation cascade (such as those noted for other GSK-3 substrates such as β-Catenin and MafA (Yost *et al.* 1996 and Rocques *et al.* 2007). The amino acids surrounding this region were then aligned against IRF-1 from seven different species. Conservation was high among amino acids 213-229 among mammals, but less conserved with chicken IRF-1 (see figure 3.4). The amino acids surrounding Thr^{180} and Ser^{184} were then aligned in the same fashion (see figure 3.5). Again these residues were well conserved throughout evolution, but unlike Ser^{215} and Ser^{219}, potential phosphorylation by GSK-3 was maintained in chicken IRF-1.

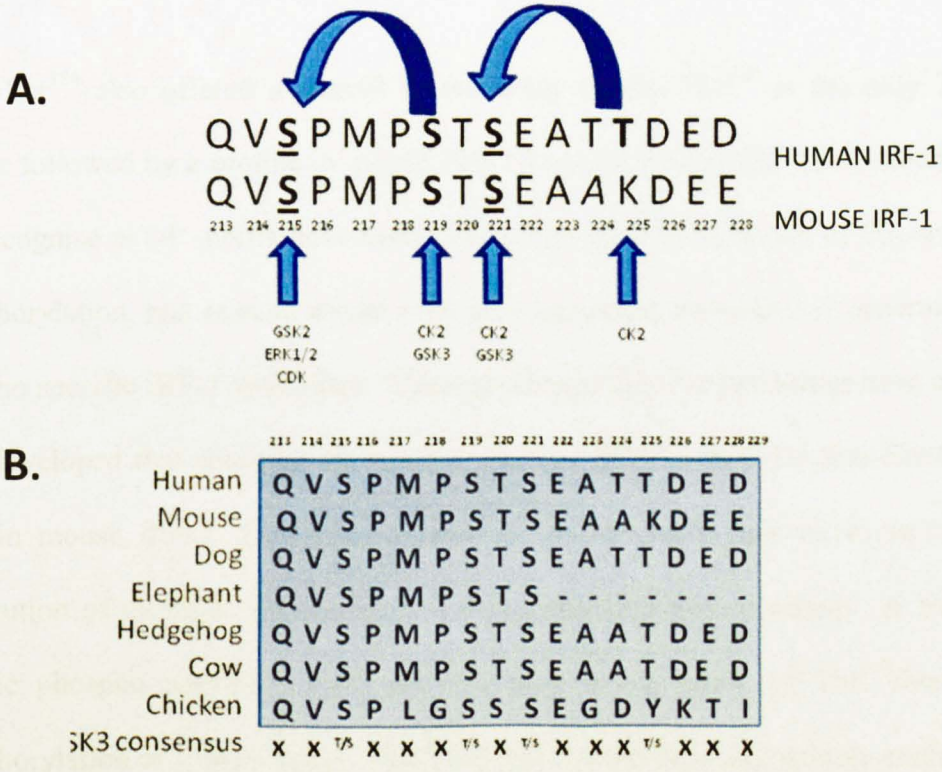

Figure 3.4 Conservation of Ser^{215}. **A)** The top curved arrows represent the "priming" events (see text). Bottom arrows indicate kinases that are predicted to phosphorylate the surrounding residues') **B)** Top numbers indicate amino acid number relative to human IRF-1. Bottom is the GSK3 consensus, where x is any amino acid and T/S is threonine / serine,

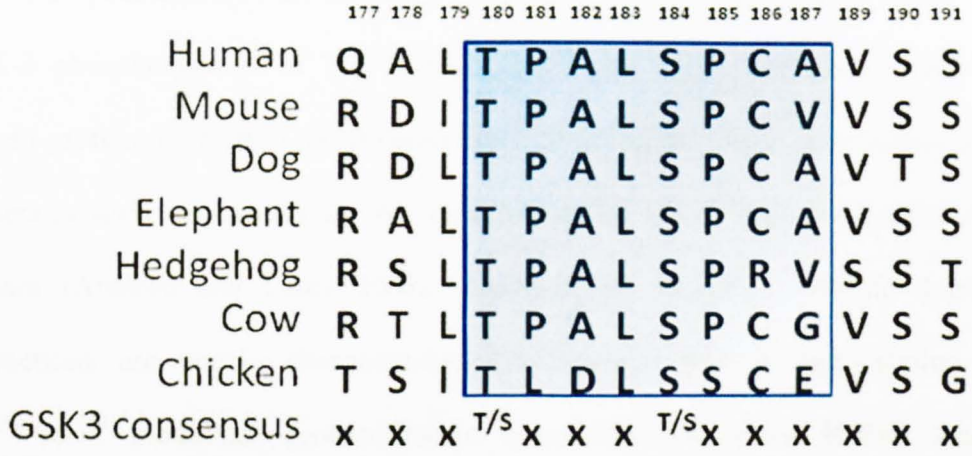

Figure 3.5 Conservation Thr[180] and Ser[184] among seven different species of IRF-1. Top numbers indicate the amino acid number relative to human IRF-1. Bottom is the GSK3 consensus, where x is any amino acid and T/S is threonine / serine.

Thr[180]/Ser[184] also offered a benefit to the study in that Thr[180] is the only Thr residue followed by a proline in mouse IRF-1 (but not human IRF-1). Antibodies that recognise p-T-P motifs have been extensively used in the study of threonine phosphorylation, and as such would offer an economical alternative to generating phospho specific IRF-1 antibodies. Although phospo-Ser-Pro antibodies have also been developed that could be used in the study of IRF-1, there are four Ser-Pro pairs in mouse IRF-1. Consequently use of this antibody may have required substitution of multiple Ser residues to determine antibody specificity. A more specific phospho antibody could also be used in the study of Thr[180]/Ser[184]. Phosphorylation of c-Myc at Thr[58]/Ser[62] by GSK3β has been extensively studied, and an antibody that detects dual phosphorylation is available. Crucially, this antibody has been shown to be non specific towards other proteins that carry similar phosphorylation motifs, and has been used to identify novel GSK-3

substrates (Gustafson *et al.* 2005). Finally, in addition to the high potential for GSK-3 phosphorylation of Thr^{180}, both Thr^{180} and Ser^{184} are nested within a protein-protein interaction motif named the PxLxP motif. These short amino acid sequences serve as ligands for the zinc finger MYND (MTG8-Nervy-DEAF1) domain (Ansieau and Leutz 2002). Although the PxLxP – MYND domain interactions are poorly characterised, the potential that phosphorylation of Thr^{180}/Ser^{184} modulates protein-protein interactions warranted further study. Figure 3.6 shows the IRF-1 PxLxP aligned against other known PxLxP motifs.

PxLxP protein							MYND domain protein
IRF-1	T	P	A	L	S	P	Unknown
skNAC	L	P	P	L	I	P	SMYD2[1]
E1A	M	P	N	L	V	P	BS69[2]
EBNA2	M	P	E	L	S	P	BS69[2]
MGA	M	P	K	L	T	P	BS69[2]
EMSY	M	P	R	L	V	P	BS69[3]
ZHX1	P	P	V	L	I	P	BS69[4]
PRKDC	M	P	K	L	K	P	SMYD2[5]
AHI1	S	P	P	L	S	P	SMYD2[5]
CLASP2	V	P	R	L	S	P	SMYD2[5]
NCoR	P	P	P	L	P	P	ETO[6]
NCoR	P	P	P	L	I	P	ETO[6]

Figure 3.6. The IRF-1 PxLxP motif. Alignment of known PxLxP motifs, and the MYND domain proteins in which they interact. References 1:(Sims *et al.* 2002) 2: (Ansieau and Leutz 2002) 3: (Hughes-Davies *et al.* 2003) 4: (Ogata-Kawata *et al.* 2007) 5:(Abu-Farha *et al.* 2008) 6: (Liu *et al.* 2007). Abbreviations **E1A** (Adenoviral E1A protein), **EBNA2** (Epstein Barr Nuclear Antigen), **MGA** (Myc related cellular factor), **ZHX1** (Zinc finger and Homeobox 1), **PRKDC** (Protein Kinase DNA activated), **BS69** (Adenovirus 5 E1A binding), **AHI1** (Abelson Helper Integration Site1), **CLASP2** (CLIP Associated Protein 2), **NCoR** (Nuclear Receptor Co-Repressor), **SMYD2** (SET and MYND domain Protein 2), **ETO** (Eight-Twenty-One) and **skNAC** (Skeletal Nascent Polypeptide Associated Complex).

3.3. IRF-1 is phosphorylated *in vitro* by GSK3β

To determine if IRF-1 is phosphorylated directly by GSK3β, an *in vitro* kinase assay was performed using recombinant GSK3β (Cell Signalling Technology) which was incubated with GST-IRF-1 wild type and T180A. The reaction was carried out in the presence of [γP^{32}]-ATP which enabled detection of phosphate transfer by GSK3β to IRF-1. GST-IRF-1 incubated with GSK3 but in the absence of "hot" ATP did not result in detection of IRF-1. No phosphorylated IRF-1 was detected without the addition of GSK3β, but [γP^{32}]-ATP labelled IRF-1 was detected when incubated with GSK3β. Both wild type and T180A IRF-1 were phosphorylated by GSK3β.

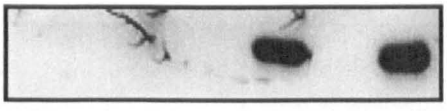

ATP	+	+	+	+	+	+
γP^{32}ATP	-	-	+	+	+	+
GST-IRF-1 WT	+	-	+	+	-	-
GST-IRF-1 T180A	-	+	-	-	+	+
GSK3β	+	+	-	+	-	+

Figure 3.7 GST-IRF-1 is phosphorylated *vitro* by GSK3β. 4 μg of GST-IRF-1 was incubated with 250 μM ATP, 0.8 μCi [γP^{32}]-ATP and GSK3β for 30 minutes at 37°C. Phosphorylation was detected by autoradiography.

Although IRF-1 was determined to be a substrate of GSK3β *in vitro*, the T180A mutant was found to be equally phosphorylated in comparison to the wild type IRF-1. This suggested that other residues are potentially phosphorylated by GSK3β *in vitro*. An antibody that detects phosphorylated threonine-proline was used to determine if Thr^{180} was phosphorylated by GSK3β. Thr^{180} is the only Thr residue followed by a proline in mouse IRF-1 (although human IRF-1 contains two). An *in vitro* phosphorylation was carried out without [γP^{32}]-ATP. The products of the reaction were subjected to SDS-PAGE and immunoblotted with the pT-P Ab (Antibody). In the absence of GSK3β, GST-IRF-1 was not phosphorylated at Thr^{180}; however addition of GSK3β resulted in a detectable shift in IRF-1 migration. The slower migrating form of IRF-1 was detected by the pT-P Ab suggesting that Thr^{180} is one of the phosphorylated residues.

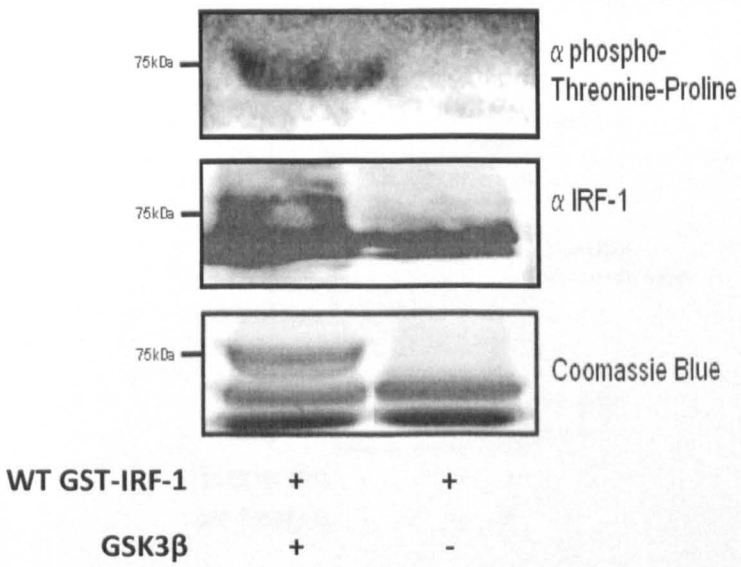

Figure 3.8 Thr^{180} is phosphorylated by GSK3β *in vitro*. 1 μg of wild type GST-IRF-1 was incubated with and without GSK3β in the presence of 250 μM ATP. The samples were separated by SDS-PAGE. The gel was stained with Coomassie Blue to highlight the decreased migration following phosphorylation. Immunoblot was carried out to detect p-T-P and total IRF-1.

3.4. IRF-1 is phosphorylated at Thr^{180} *in vivo*

To determine if IRF-1 is phosphorylated in response to GSK3β, HEK293 cells were co-transfected with FLAG-HA-IRF-1 and GSK3β HA. The phospho-Thr-Pro Ab was used to determine if IRF-1 was phosphorylated at Thr^{180}. Protein extracts were immunoprecipitated using the p-T-P Ab and immunoblotted with IRF-1 Ab (figure 3.9). FHA-IRF-1 (3x-FLAG-HA) was immunoprecipitated by the p-T-P Ab in the absence of GSK3β, suggesting that when expressed in HEK293 cells FHA-IRF-1 is phosphorylated at Thr^{180}. Increasing the expression of GSK3β by transfection increased the proportion of IRF-1 that was phosphorylated at Thr^{180}, without increasing the amount of FHA-IRF-1 in the protein lysates. The blots were re-probed with the p-T-P Ab to determine the amount of total protein immunoprecipitated by the p-T-P Ab. The amounts of phosphorylated proteins were similar between different extracts.

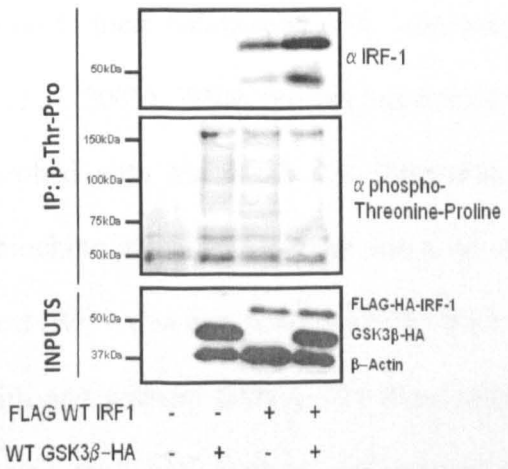

Figure 3.9 Thr^{180} is phosphorylated by GSK3β *in vitro*. HEK293 cells were transfected with 5 μg of FHA-IRF-1 and GSK3β-HA for 48 hours. 6 hours prior to lysis cells were treated with MG132. Protein lysates were immunoprecipitated (1 mg) with pTP Ab and immunoblotted with IRF-1 Ab. Blots were re-probed with p-TP Ab to determine the level of immunoprecipitation. Lysates (10 μg/lane) demonstrate expression of transfected proteins. FHA-IRF-1, GSK3β-HA and actin were probed on a single blot.

3.5. Dual phosphorylation of Thr^{180}/Ser^{184} in HEK293 cells

Many substrates of GSK3β require priming on a + 4 residue to stabilise the interaction between substrate and GSK3β. Ser^{184} was predicted to be a priming residue towards Thr^{180}. Although antibodies that detect p-Ser-Pro are available, there are four S-P pairs in mouse IRF-1, any of which may be phosphorylated. This complicated the study of Ser^{184} phosphorylation. The Thr^{180}/Ser^{184} pair exhibit strong similarity to the Thr^{58}/Ser^{62} pair in c-Myc (see figure 1.14). This pair of residues is known to be phosphorylated by MAPK (Mitogen Activated Protein Kinase) and GSK3β and antibodies are available that detect dual phosphorylated c-Myc. This antibody has recently been shown to recognise a degenerate motif and detects numerous other phosphorylated proteins. The p-T/S antibody also immunoprecipitates numerous other proteins which also contain similar phosphorylation pairs, for example, Zcchc8 and EB1A were discovered as GSK3β substrates due to their recognition and immunoprecipitation with this antibody (Gustafson *et al.* 2005). When protein extracts of HEK293, MRC-5 and H3396 cells were probed with the p-T/S Ab, numerous bands were detected following stringent blocking and washing steps (data not shown). The ability of the p-T/S Abs to detect IRF-1 was then tested in HEK293 extracts expressing wild type eYFP-IRF-1 with and without GSK3β-HA expression (figure 3.10). IRF-1 was immunoprecipitated from cell extracts and immunoblotted with the p-T/S antibody.

A strong increase in IRF-1 phosphorylation was detected when GSK3β-HA was expressed, while the amount of phosphorylation without GSK3β was weak, but detectable. The amount of GSK3β detected in the protein extracts suggests that endogenous GSK3β may be able to phosphorylate IRF-1 at Thr^{180}/Ser^{184}. To determine the specificity of the p-T/S antibody, alanine mutants of each residue singly, and in combination (TA T180A, SA S184A and TS-A T180A / S184A) were co-expressed with GSK3β (3.10). The p-T/S antibody did not react with any of the alanine substitute of IRF-1, proving that this antibody is recognising the Thr^{180}/Ser^{184} pair on eYFP-IRF1.

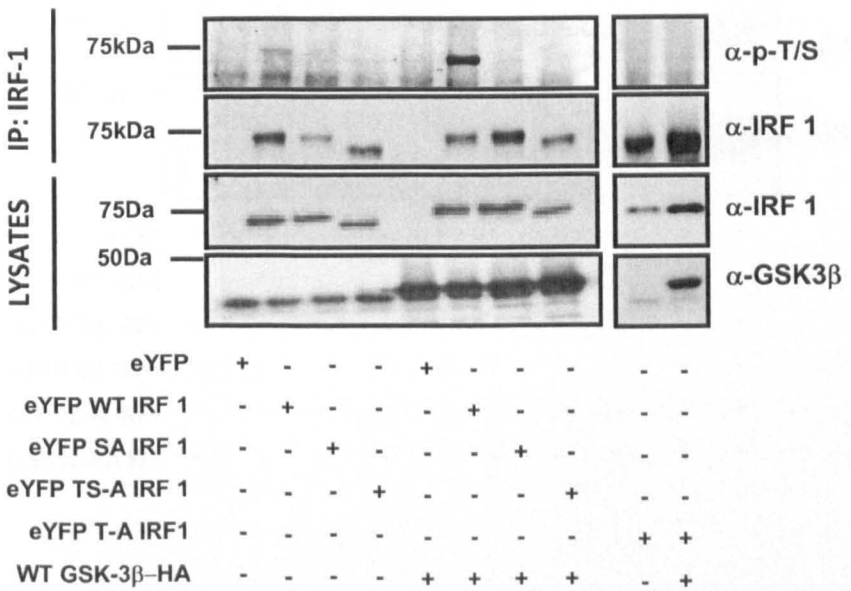

Figure 3.10 eYFP-IRF-1 phosphorylation at Thr^{180}/Ser^{184} is increased by GSK3β. HEK293 cells were transfected with 5 μg of eYFP-IRF-1 and empty vector or GSK3β-HA wild type for 48 hours. Protein extracts (500 μg) were immunoprecipitated with IRF-1 M20 Ab and immunoblotted with the p-T/S Ab. The blot was re-probed with M20 to determine the IP efficiency. 10% protein lysates are shown to indicate expression levels of transfected proteins. (WT wildtype, TA T180A, SA S184A and TS-A T180A/S184A).

Reciprocal IP's were carried out in which eYFP-IRF-1 was immunoprecipitated with the p-T/S antibody (see figure 3.11). In agreement with figure 3.10, eYFP-IRF-1 was phosphorylated when GSK3β was over-expressed, while lower levels of phosphorylation could be detected without GSK3β-HA being expressed. The pT/S Ab was much less able to IP the alanine mutants of IRF-1.

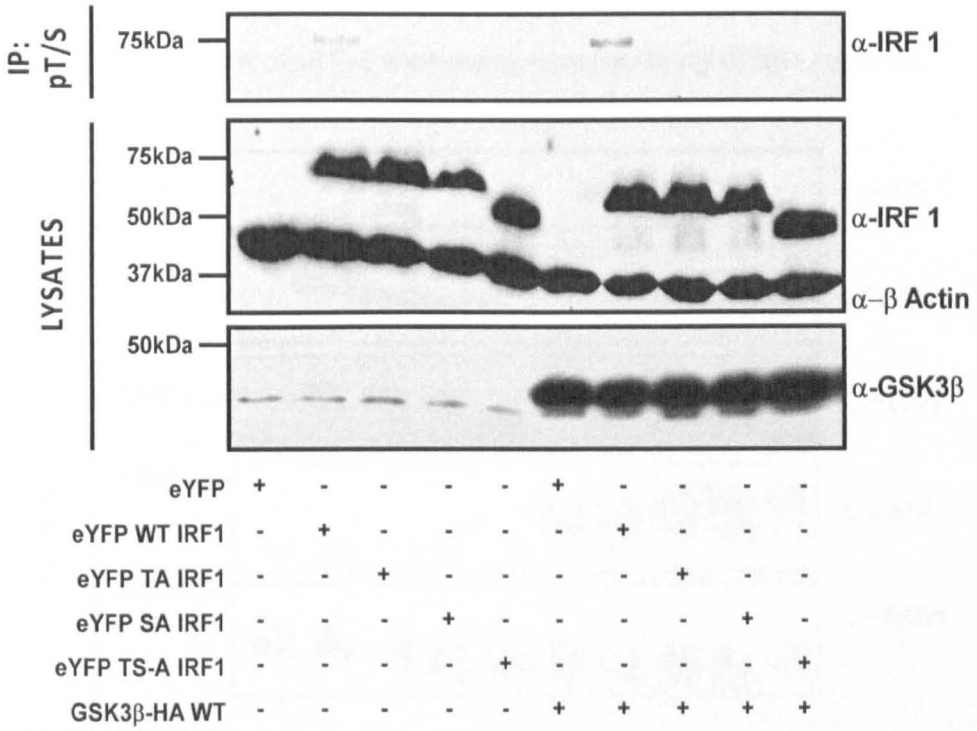

Figure 3.11 eYFP-IRF-1 can be immunoprecipitated by the p-T/S Ab
HEK293 cells were transfected with 5 μg each of eYFP-IRF-1 and empty vector or GSK3β-HA WT for 48 hours. Protein extracts (500 μg) were immunoprecipitated with p-T/S Ab and immunoblotted with the IRF-1 M20. High salt washes were used to remove any non specific interactions of the p-T/S Ab. 10% protein lysates are shown to indicate expression levels of transfected proteins. (WT wildtype, TA T180A, SA S184A and TS-A T180A/S184A).

Figure 3.10 was then repeated, but with the FLAG-IRF-1 in place of eYFP-IRF-1 (see figure 3.11). This was to discount any effect the large YFP protein tag may have had on phosphorylation of IRF-1. The results in figure 3.12 are broadly similar to those in figure 3.10. Increased phosphorylation of FLAG- wild type IRF-1 was detected when GSK3β-HA was expressed, although phosphorylation of wild type FLAG IRF-1 could be more easily detected without increased expression of GSK3β-HA. Additionally, the p-T/S antibody was not able to detect the Alanine substitution of IRF-1 confirming the specificity of this antibody.

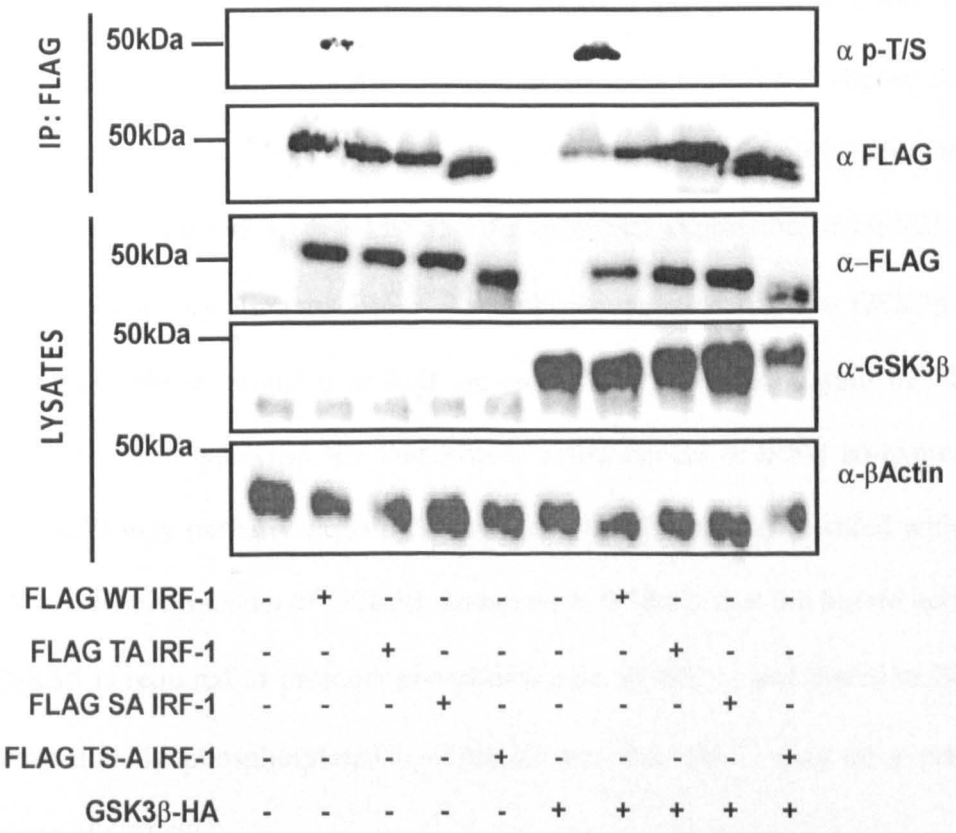

Figure 3.12 FLAG-IRF-1 phosphorylation at Thr^{180}/Ser^{184} is increased by GSK3β. HEK293 cells were transfected with 5 μg of FLAG-IRF-1 and empty vector or GSK3β-HA wild type for 48 hours. Protein extracts (500 μg) were immunoprecipitated with FLAG M2 Ab and immunoblotted with the p-T/S Ab. The blot was re-probed with FLAG to determine the IP efficiency. 10% protein lysates are shown to indicate expression levels of transfected proteins. (WT wildtype, TA T180A, SA S184A and TS-A T180A/S184A).

Next, mutants of GSK3β-HA were tested for their ability to promote phosphorylation of IRF-1. A kinase inactive mutant of GSK3β-HA was tested (K85A). This mutation causes the collapse of the ATP binding pocket, preventing GSK3β from phosphorylating any substrate (Cole *et al.* 2004). A second mutant was employed (R96A) this mutant cannot interact with substrates which contain a negative charge (phosphate ion) on the +4 residue. The R96A mutant has been used by several groups to test substrates for the presence of phosphorylation on a priming residue, and can be used to discriminate between primed and non primed substrates (Cho and Johnson 2003). These mutants, and wild type GSK3β-HA were co-expressed with eYFP and FLAG tagged wild type IRF-1 (figure 3.13). Phosphorylation was detected by immunoblot of IRF-1 immunoprecipitates. In agreement with figures 3.10, 3.11 and 3.12 increased expression of GSK3β-HA promotes phosphorylation of IRF-1. In both experiments, neither GSK3β-HA mutant was able to promote as high an increase in phosphorylation of IRF-1 (compared to wild type GSK3β). Differences in the amount of IRF-1 co-expressed with GSK3β may partially explain the reduced phosphorylation detected with the K85A and R96A mutants of GSK3β, however. It is likely that the kinase activity of GSK3β is required to promote phosphorylation of IRF-1, and therefore IRF-1 is being directly phosphorylated by GSK3β and that Thr^{180} may be a primed substrate of GSK3β.

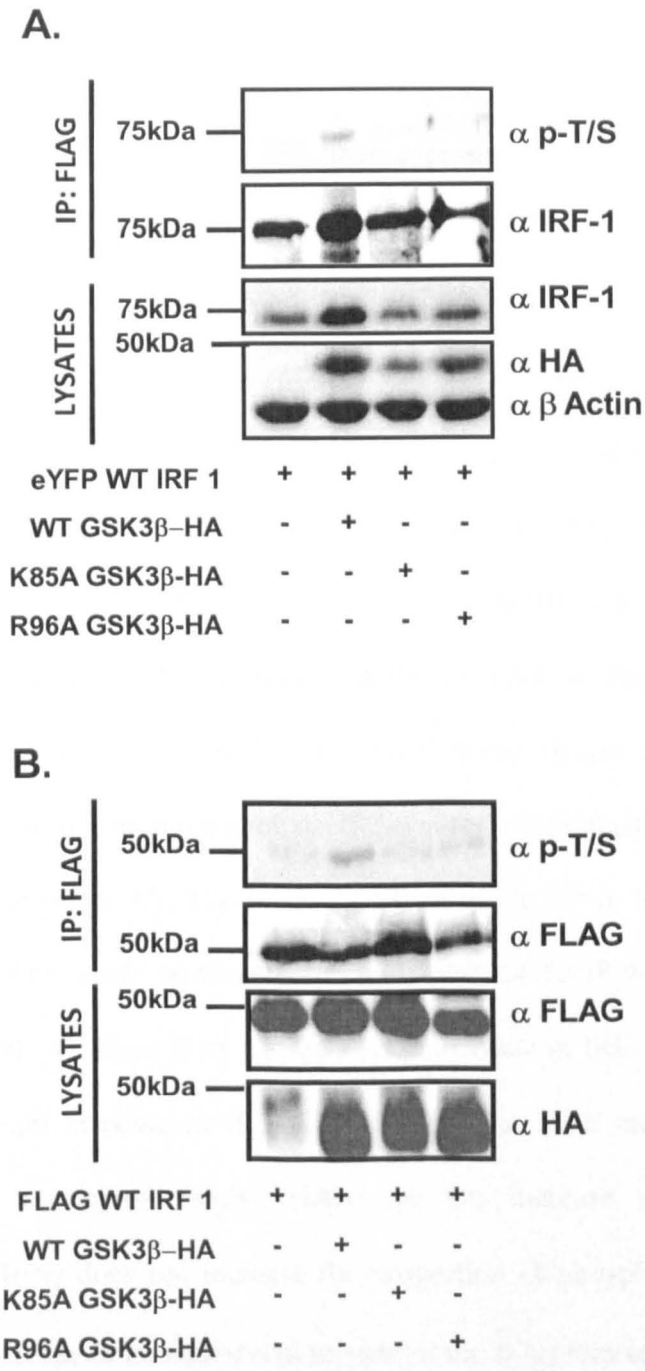

Figure 3.13 Kinase inactive (K85A) and priming (R96A) mutants of GSK3β do not increase IRF-1 phosphorylation at Thr^{180}/Ser^{184}. HEK293 cells expressing 5 μg of IRF-1 and GSK3β-HA were lysed 48 hours post transfection. Lysates were immunoprecipitated with IRF-1 M20 (A) or FLAG (B) and immunoblotted with p-T/S Ab. IP efficiency was tested by blotting with the IP Ab. 10% lysates are shown to illustrate expression of transfected proteins.

3.6 IRF-1 is phosphorylated at Thr^{180}/Ser^{184} in MRC-5 and H3396 cells.

The phosphorylation of IRF-1 was then studied in H3396 and MRC-5 cells without transfecting GSK3β. Both cell lines express IRF-1 at low levels, with IRF-1 migrating at ~50 kDa. To help confirm the identity of immunoprecipitated IRF-1, both cell lines were treated with IFNγ (1000U/mL) for 3 hours to induce high levels of IRF-1 expression (figure 3.13). H3396 cell extracts were immunoprecipitated with the p-T/S Ab, and the eluates probed with IRF-1 C20 Ab. IRF-1 was efficiently immunoprecipitated by the p-T/S Ab, suggesting that in H3396 cells, dual phosphorylation of Thr^{180}/Ser^{184} occurs without the need to increase expression of GSK3β. Similar experiments were carried out in MRC-5 cells, but the IRF-1 C20 Ab (a rabbit polyclonal raised against human IRF-1 C terminus) was used to immunoprecipitate IRF-1 after which phosphorylation was detected using the p-T/S Ab. The levels of IRF-1 are lower in MRC-5 cells; as such almost no IRF-1 could be detected in the lysates, or the IP without treatment with IFNγ. In both cell lines IFNγ causes a large increase in IRF-1 protein levels, with a concomitant increase in IRF-1 phosphorylation. The increase in IRF-1 phosphorylation is approximately relative to the increase in total IRF-1, suggesting that IFNγ does not increase the proportion of phosphorylated IRF-1. Therefore the increase in phosphorylation seen in the IFNγ treated lanes in figure 3.14 is caused by an increase in the total amount of IRF-1 rather than an increase in the proportion of phosphorylated IRF-1. Phosphorylation of IRF-1 does however occur on newly synthesised IRF-1 protein.

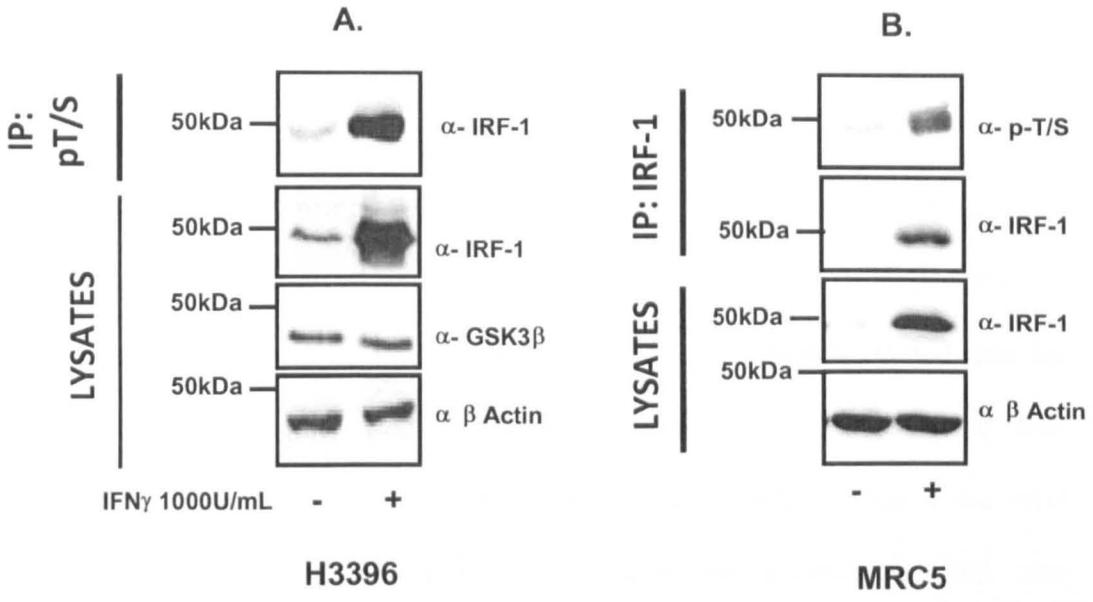

Figure 3.14. IRF-1 is phosphorylated at Thr^{180}/Ser^{184} in human cell lines. H3396 and MRC-5 cells were treated with IFNγ (1000 U/mL) for 3 hours prior to lysis. Extracts (500 μg) of H3396 cells were immunoprecipitated using the p-T/S Ab and immunoblotted with human IRF-1 Ab (C20). MRC-5 extracts (500 μg) were immunoprecipitated with IRF-1 C20 Ab and blotted against p-T/S Ab and IRF-1 C20 Ab (to determine IP efficiency). 10% lysates are shown below IP panels to indicate expression of IRF-1 following IFNγ treatment.

3.7. Proteasome inhibition increases the proportion of phosphorylated IRF-1

IRF-1 is a highly unstable protein with a $t^{1/2}$ (half life) of approximately 30 minutes (Pion *et al.* 2009). Many proteins have been shown to be degraded by the proteasome following phosphorylation by GSK3β, with the phosphorylation serving as a mark for destruction (Xu *et al.* 2009a). Detection of phosphorylated IRF-1 was often found to be problematic, even when protein levels were relatively high. It was postulated that IRF-1 exists in a Thr^{180}/Ser^{184} phosphorylated state for a brief period of time prior to its destruction. It was also noted that phosphorylation of c-Myc at Thr^{58}/Ser^{62} is difficult to detect without the cells being treated with proteasome inhibitors. Experiments in which HEK293 cells were transfected with empty vector or GSK3β-HA with or without MG132 were carried out to determine if IRF-1 phosphorylation was more detectable following proteasome inhibition (3.15). As expected MG132 treatment resulted in an increase in IRF-1 protein levels. The phosphorylation of IRF-1 was barely detectable in DMSO treated cells that expressed empty vector and FLAG-IRF-1, while MG132 increased the detection of phosphorylated IRF-1, although the total level of IRF-1 was also increased. When cells were co-transfected with FLAG-IRF-1 and GSK3β-HA the phosphorylation of IRF-1 at Thr^{180}/Ser^{184} was detected in DMSO treated cells, in agreement with previous figures which showed that increased GSK3β expression enhances the proportion of phosphorylated IRF-1. MG132 treatment more than tripled the proportion of phosphorylated IRF-1, while importantly the increase in total IRF-1 was less than two fold. This suggested that MG132 increased the fraction of phospho-Thr^{180}/Ser^{184} IRF-1 rather than increasing the total IRF-1 levels, in the way that IFNγ increased IRF-1 protein.

Collectively, this suggests that Thr^{180}/Ser^{184} phosphorylated IRF-1 is labile, possibly due to its ability to target IRF-1 for destruction. The levels of GSK3β protein were not increased by proteasome inhibition.

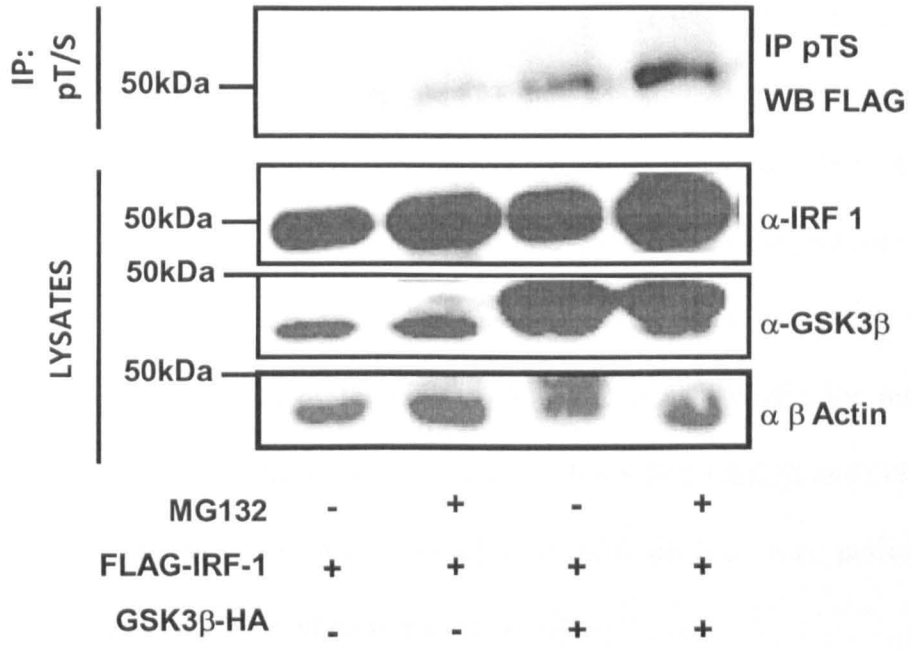

Figure 3.15. Proteasome inhibition increases detection of IRF-1 phosphorylation at Thr^{180}/Ser^{184}. HEK293 cells were transfected with FLAG-IRF-1 and GSK3β-HA (5 μg each,) for 48 hours. 6 hours prior to lysis, cells were treated with 10 μM MG132. Protein lysates (500 μg) were immunoprecipitated with p-T/S Ab and immunoblotted with IRF-1 Ab. 10% lysates are indicated below the IP to demonstrate the expression of relevant proteins.

3.8 IRF-1 and GSK3β-HA interact *in vitro.*

GSK3β has been shown to form relatively stable contacts with a number of its substrates, including NFκB-p65, p53 and E2F1 (Garcia-Alvarez *et al.* 2007; Gong *et al.* 2008; Eom and Jope 2009), during the process of phosphorylation. To confirm that IRF-1 and GSK3β interact with one another an *in vitro* GST pulldown assay (figure 3.16) was performed using wild type GST-IRF-1 and GSK3β that had been *in vitro* transcribed and translated in the presence of [^{35}S] Met (IVT GSK3β). As a control, [^{35}S] GSK3β was incubated with GST. No [^{35}S] GSK3β was pulled down by the GST conjugated beads, showing the interaction does not occur through the GST tag on IRF-1. When IVT GSK3β and GST-IRF-1 were incubated together, the [^{35}S] labelled IVT product was pulled down, suggesting that these two proteins interact *in vitro.*

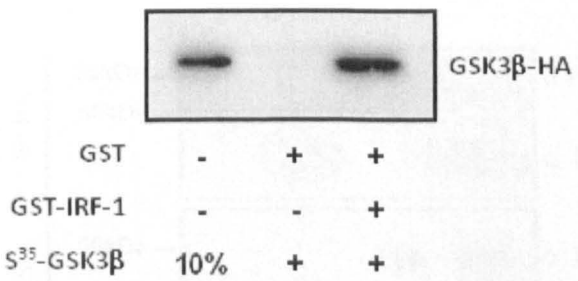

Figure 3.16. GST-IRF-1 and GSK3β-HA interact *in vitro.* *In vitro* GST pulldown assay using approximately 1 μg of GST or GST-IRF-1 conjugated to GSH-sepharose beads. 10% input (0.2 μL) of IVT product is used as a control. Experiment performed by J.Xicluna.

3.9. FLAG-IRF-1 and GSK3β-HA interact *in vivo.*

The *in vitro* conditions used in figure 3.16 poorly reproduce the physiological conditions that occur in a cell. To confirm that IRF-1 and GSK3β interact with one another in cells, co-immunoprecipitations were performed on proteins expressed in HEK293 cells. FLAG-IRF-1 and GSK3β-HA were transfected in HEK293 cells singly and in combination, followed by immunoprecipitation with HA antibody and immunoblot detection using FLAG Ab (figure 3.17). To determine the efficiency of the immunoprecipitation, blots was also probed with HA antibody. As expected, the HA Ab immunoprecipitated a band at ~45 kDa only in lanes that expressed GSK3β-HA. A protein at ~50 kDa was detected when both GSK3β-HA and FLAG-IRF-1 were co-expressed, but not when either protein were expressed alone. The identity of this protein was confirmed using the M20 IRF-1 Ab (data not shown).

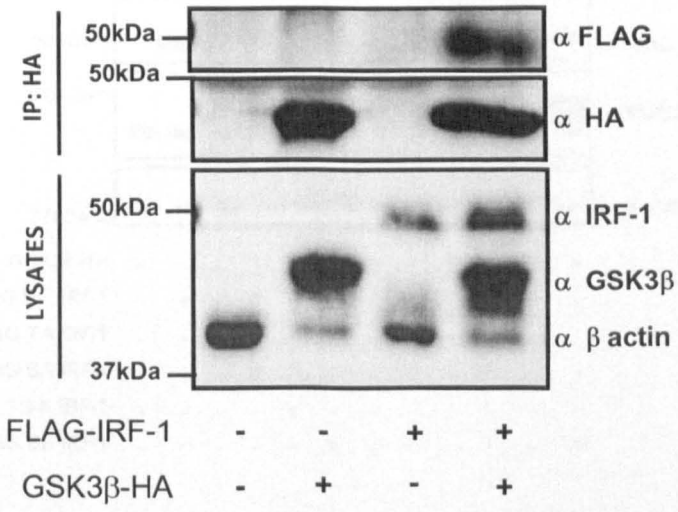

Figure 3.17. FLAG IRF-1 interacts with GSK3β-HA. HEK293 cells transfected with 5 μg of GSK3β-HA and FLAG-IRF-1 (or relevant empty vector) for 48 hours. 1 mg of protein extract was immunoprecipitated with HA Ab, Eluates were subjected to immunoblot against FLAG and HA Ab. Lysates (50 μg) demonstrate expression of transfected proteins.

Next, the interaction between FLAG-IRF-1 and GSK3β-HA was tested further by carrying out a reciprocal co immunoprecipitation using the FLAG Ab to immunoprecipitate proteins that were associated with FLAG-IRF-1 (figure 3.18). In addition to the wild type FLAG-IRF-1, phosphorylation mutants of FLAG-IRF-1 were also tested to determine if the interaction between FLAG-IRF-1 and GSK3β-HA was solely due to phosphorylation at the mutated residues. All of the IRF-1 constructs were capable of co-immunoprecipitating with GSK3β-HA. The interaction between GSK3β and IRF-1 SA, TS-A and SE (S184E) was greater than the wild type or T180A mutant. The interactions generally varied between experiments, although the interaction was always detectable. As expected no GSK3β was immunoprecipitated when no GSK3β-HA was co-transfected.

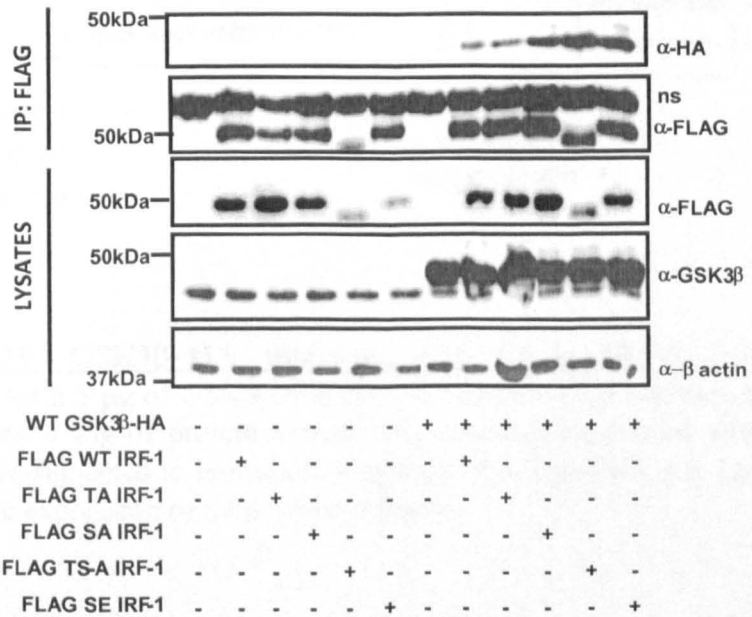

Figure 3.18. GSK3β-HA interacts with FLAG-IRF-1. HEK293 cells transfected with 5 μg of GSK3β-HA and FLAG-IRF-1 plasmid (or relevant empty vector) for 48 hours. 1 mg of protein extract was immunoprecipitated with FLAG Ab, Eluates were subjected to immunoblot against FLAG and HA Ab. Lysates (50 μg) demonstrate expression of transfected proteins. (WT wildtype, TA T180A, SA S184A, TS-A T180A/S184A and SE S184E).

Interactions between the K85A and R96A mutants of GSK3β with IRF-1 were next tested. This was to confirm that the inability of the K85A and R96A mutants to phosphorylate IRF-1 was not due to their inability to form protein-protein interactions. Transfections were carried out as for figure 3.18, but using wild type FLAG-IRF-1 and GSK3β-HA wild type, K85A and R96A. When the FLAG Ab was used to IP IRF-1 from HEK293 cell extracts, all three GSK3β-HA proteins were found to Co-IP with IRF-1. This confirms that GSK3β interacts with IRF-1 independently of phosphorylation.

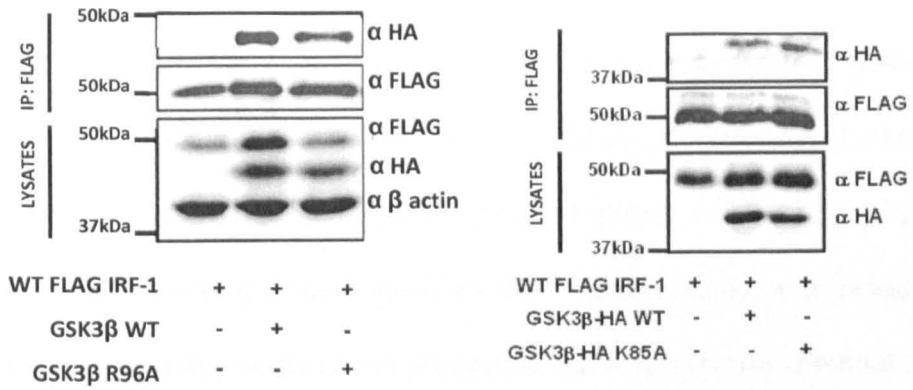

Figure 3.19. GSK3β–HA interacts with FLAG-IRF-1. HEK293 cells transfected with 5 μg of GSK3β-HA and FLAG-IRF-1 (or relevant empty vector) for 48 hours. 1 mg of protein extract was immunoprecipitated with FLAG Ab, Eluates were subjected to immunoblot against FLAG and HA Ab. Lysates (50 μg) demonstrate expression of transfected proteins.

3.10. Discussion

IRF-1 has a predicted molecular weight of 37 kDa, but migrates closer to 50 kDa in a variety of different cell types. This 13kDa discrepancy has been attributed to phosphorylation (and possible other PTMs). This study aimed to identify a phosphorylated residue and the kinase responsible for the modification.

In vitro phosphorylation was the first assay used to demonstrate that IRF-1 is a substrate of GSK3β. Both the wild type and T180A IRF-1 were studied, and both were found to be phosphorylated by GSK3β, suggesting that although IRF-1 is a substrate it probably has more than one residue phosphorylated by GSK3β. This suggests that IRF-1 is a direct target for GSK3β phosphorylation, and that no additional proteins are required for phosphorylation. Additionally it proves that PTMs on IRF-1 are not essential for prior phosphorylation by GSK3β. This seems to be in conflict with the requirement for Ser^{184} phosphorylation to prime Thr^{180}; however the priming increases the interaction but is not always essential. *In vitro* phosphorylation of Bax by GSK3β does not require priming, however *in vivo* it does (Linseman *et al.* 2004). It is most likely that in an *in vivo* setting in which much lower concentrations of GSK3β are encountered by IRF-1, priming compensates, and while *in vitro* the higher concentration of GSK3β and lack of other competing proteins enables phosphorylation. Given that figure 3.4 shows phosphorylation of the T180A mutant, and the GST-S184A mutant was not tested, it is also possible that GSK3β phosphorylated both residues. GST protein alone was not subjected to in vitro phosphorylation, although it has been shown previously not to be a GSK3β substrate. Additionally, later in figure 3.16 it was shown not to interact with GSK3β *in vitro*. To determine if Thr^{180} is a target of

GSK3β, cold *in vitro* kinase assays were used (un labelled ATP followed by immunoblot with phospho antibodies). Phosphorylation of IRF-1 was detected only when GSK3β was incubated with IRF-1, in addition, only the more slowly migrating band was detected as being phosphorylated. The phosphorylation reaction did not result in a complete shift in migration of IRF-1, suggesting the reaction may not have gone to completion. This could be due to the lack of priming on Ser^{184} making the reaction less efficient. It would be interesting to test the SE mutant in these experiments to determine if this increases the proportion of phosphorylated IRF-1. The inability of the p-TP Ab to detect the lower migrating (un-modified) band of IRF-1 confirms that GST-IRF-1 is not phosphorylated in the *E.coli* BL21 cells. GST-IRF-1 also migrated at ~70 kDa which is exactly the expected mass of this protein. It is also matches the data of Upreti & Rath who utilised mouse GST-IRF-1. There is no difference in the migration of the GST-IRF-1 TS-A mutant when expressed in BL21 cells also, while when expressed in mammalian cells the TS-A mutant of IRF-1 migrates as a faster doublet compared to wild type IRF-1 (data not shown). It remains to be determined whether the change in migration of the double mutant TS-A is a result of loss of phosphorylation on Thr^{180}/Ser^{184}, or is caused by other PTMs that are added to IRF-1 as a result of Thr^{180}/Ser^{184} phosphorylation. The differences in apparent molecular weight between IRF-1 expressed in bacteria and mammalian cells is therefore likely to be caused by PTMs. Subsequently it was concluded that, *in vitro* IRF-1 may be phosphorylated on multiple residues, but Thr^{180} was among the modified residues.

To determine if Thr^{180} could be phosphorylated *in vivo*, co-transfections were carried out in HEK293 cells. An increase in phosphorylation was detected when

GSK3β was over-expressed with IRF-1 (figures 3.9-3.13). Phosphorylation on Thr^{180} was also detected in the absence of GSK3β over expression, suggesting that either endogenous GSK3 or another kinase is able to phosphorylate Thr^{180}. It should be noted that MG132 had to be used in order to detect phosphorylation of Thr^{180}; this will be discussed later, but suggested that the Thr^{180} phosphorylated fraction of IRF-1 is sensitive to proteasomal degradation.

Next, dual Thr^{180}/Ser^{184} was assessed to determine if both residues are phosphorylated, to support the theory that phosphorylated Ser^{184} acts as priming site for Thr^{180}. The c-Myc phospho Thr^{58}/Ser^{62} rabbit polyclonal antibody was used for these studies (figures 3.10-3.13). Epitope tagged IRF-1 (eYFP or FLAG constructs) were used rather than untagged IRF-1 for technical reasons. Phosphorylation was detected only on the wild type IRF-1, with an increase being detected when co transfected with GSK3β. The antibody did not cross react with any of the alanine mutants, suggesting that it only detects the phospho-Thr/Ser motif of IRF-1. Additionally the p-T/S Ab was able to immunoprecipitate IRF-1, with more IRF-1 being immunoprecipitated following over-expression of GSK3β, suggesting that increasing cellular GSK3β concentration enhances the amount of phospho-Thr^{180}/Ser^{184} IRF-1 (figure 3.11). Since the Ab only detects dual phosphorylated substrates it is not possible from these studies to determine if the modifications can occur independently of one another, although the previous figures confirmed that Thr^{180} is phosphorylated. The status of Ser^{184} phosphorylation has not been fully studied. It has been reported that similar phosphorylated pairs can be uncoupled from one another. It has been shown that Ser^{62} phosphorylation of c-Myc promotes functions that are completely independent of its ability to promote phosphorylation of Thr^{58} (Benassi *et al.*

2006; Seo *et al.* 2008). It should be considered, that GSK3β is a tightly regulated protein, and is not always available to phosphorylate its nuclear substrates. Consequently phosphorylation of priming residues can have completely independent roles from GSK3β priming.

The dual phosphorylation motif which is recognised by the p-T/S Ab may be quite prevalent in cells, a database search identified over 200 human proteins which also possessed the T/S-P-X-L-S/T-P motif; this could explain the large number of bands detected when the p-T/S Ab is used in immunoblot. Occasionally, when over-expressed alongside GSK3β, a band corresponding to IRF-1 could be detected by the p-T/S Ab in direct immunoblot, however, the large number of other bands made difficult to use directly for these purposes. Consequently IRF-1 always had to be immunoprecipitated in order to isolate it for immunoblot with the p-T/S Ab. The ability of both the p-T-P and p-T/S Abs to immunoprecipitate IRF-1 suggests that the phosphorylated residues were surface exposed. Although small amounts of detergent in the buffers used may have altered surface exposure on the IRF-1 protein. It would be of interest to use buffers without detergents to determine if the phospho Abs are able to IP IRF-1.

A kinase inactive mutant of GSK3β was next used to confirm that the antibodies detected an increase in phosphorylation of IRF-1. When both YFP and FLAG tagged IRF-1 were used, no increase in phosphorylation could be detected. It is notable that there was no decrease in phosphorylation. It is possible that K85A GSK3β does not prevent endogenous GSK3β from phosphorylating IRF-1. Alternatively other kinases (that are not affected by K85A GSK3β) may be able to phosphorylate Thr^{180}. The dual detection of the p-T/S Ab may also explain the

residual phosphorylation detected, as this may be due to the phosphorylation of Ser^{184}. A priming mutant of GSK3β was next used (R96A). This mutation does not prevent GSK3β from phosphorylating its substrates as the kinase domain is unaffected, however, it does not phosphorylate substrates that carry a negative charge on the + 4 residue. This negative charge is usually provided by phosphorylation. In confirmation of the studies with the dual p-T/S Ab, no increase in phosphorylation could be detected when this mutant was expressed with IRF-1. Most likely this is because the Ser^{184} is phosphorylated.

An important consideration for this study was to show that IRF-1 was phosphorylated at Thr^{180} in cells without the need to over-express GSK3β. All of the data previous to figure 3.10 employed mouse IRF-1, and figure 3.10 is the first evidence that human IRF-1 is also phosphorylated at these residues. Figure 3.10 highlights that GSK3β does not need to be over expressed to promote phosphorylation of IRF-1, and most likely a small fraction of IRF-1 will contain the phospho Thr^{180}/Ser^{184} mark. To determine if IRF-1 phosphorylation levels are altered by IFNγ, cells were treated to induce *de novo* IRF-1 protein synthesis. This also served as a control to be sure the immunoprecipitated protein was IRF-1. Other studies (Hu *et al.* 2006 and Tsai *et al.* 2009) have suggested that GSK3β activity is linked to IFNγ, although not yet well understood, it has been shown that IFNγ reduces the inhibitory phosphorylation of GSK3β at Ser^9, thereby making more GSK3β available towards its substrates. It has been suggested that IFNγ transcriptionally regulates one of the phosphatases that removed the inhibitor Ser^9 mark. Additionally GSK3β regulates the activity of STAT transcription factors

which regulate IRF-1 expression in response to IFNγ treatment. The relative amount of IRF-1 phosphorylation was not enhanced by IFNγ treatment, rather the proportion stayed static, with an increase in phospho-IRF-1 being detected following treatment matching an overall increase in IRF-1 total protein expression. Figure 3.14 did show however, that during the 3 hour treatment in which new IRF-1 protein was made, phosphorylation was occurring, suggesting a dynamic process. It would be of interest to determine if the phosphorylation levels of IRF-1 are different in cell lines that are known to be poorly responsive to IRF-1.

These above data shows that IRF-1 is phosphorylated at Thr^{180}/Ser^{184}, but does not conclusively show that GSK3β is responsible for the phosphorylation, although it has been shown that when it is over-expressed in HEK293 cells there is an increase in phosphorylation. Both cell lines express GSK3β protein, although the levels of inhibitory / activation phosphorylation were not accessed. Most likely GSK3β is active and able to phosphorylate IRF-1. Use of siRNA against GSK3β to determine if the level of basal phosphorylation is decreased would have been helpful in confirming that GSK3β is important for this modification. It should be noted that several other kinases were predicted to phosphorylate both residues, and as such knockdown of GSK3β may lead to other kinases compensating. Numerous proteins are subjected to proteasomal degradation following phosphorylation by GSK3β; it was therefore not surprising that MG132 treatment lead to an increase in the phosphorylation state of IRF-1. This is the first evidence that the Thr^{180}/Ser^{184} phosphorylation is a short lived event, most likely because it promotes degradation of IRF-1; therefore Thr^{180}/Ser^{184} phosphorylated

IRF-1 is marked for destruction. Reverse IPs in which IRF-1 was immunoprecipitated and immunoblotted with the p-T/S Ab were also performed and produced similar results to figure 3.11 (data not shown). Previous experiments had confirmed that the relative amount of phosphorylation on these residues was small, when the amount of total IRF-1 was considered. This could be due to the reversibility of the phosphorylation, or the rareness of the modification.

To support the findings that GSK3β phosphorylated IRF-1, the interaction between the two proteins was studied. *In vitro* GST pulldown assays demonstrated that GSK3β interacts with IRF-1 directly. The *in vitro* conditions in which this assay was carried out mostly preclude other proteins serving as adapters or scaffolds in this interaction. One caveat however, is that the rabbit reticulocyte (from which the IVT GSK3β is produced) may contain other proteins that modulate the interaction between IRF-1 and GSK3β. However as phosphorylation occurs between these two purified protein *in vitro* it is more likely the interaction is direct. Figure 3.4 also shows that IRF-1 does not require PTMs to allow the interaction with GSK3β. It is highly unlikely that PTMs will occur on IRF-1, as it was expressed in bacteria, which have a far more restricted repertoire of PTM machinery. These findings also suggest that IRF-1 does not need to be in a DNA bound state to become an interacting partner of GSK3β, although DNA binding may enhance phosphorylation by stabilising the interaction. Use of GST- GSK3β and [^{35}S] Met labelled IRF-1 would have been useful to validate this interaction. To verify the interactions occur in cells, Co-IPs were carried out HEK293 cells. This was because HEK293 cells were used for the phosphorylation studies, and so it was expected that an interaction would occur in these cells. The 12CA5 HA Ab was used for detecting and immunoprecipitating GSK3β-HA to prevent

background GSK3β from interfering with the results. Use of GSK3β Ab may, however have been useful for demonstrating an interaction between endogenous (untagged) GSK3β and IRF-1. When CoIP's were carried out with FLAG or HA Ab, the results showed an interaction between the two proteins which was specific for their co-expression. The interaction also occurred when lower levels of GSK3β was transfected (data not shown) suggesting that the interaction does not come about due excessive amounts of GSK3β being expressed in cells. As expected; all of the IRF-1 mutants were capable of interacting with GSK3β. This confirms that the absence of phosphorylation of the alanine mutants was not caused by a loss of interaction with GSK3β. This also suggests that the interaction between IRF-1 and GSK3β occurs in another region of IRF-1 and is not dependent on the interaction with the GSK3 consensus site. Most kinases possess docking sites that are separate from the target consensus site. These docking sites serve to greatly increase the specificity of the kinases, especially when considering their degenerate consensus motifs (Ubersax and Ferrell 2007). It would be of interest to map the docking site between GSK3β and IRF-1. It could be assumed that mutation of the GSK3β docking site would prevent IRF-1 from being phosphorylated. This could be relevant when considering splice mutants of IRF-1 that are found in certain cancers. Relatively few substrates have had their interaction with GSK3β mapped, although Axin, GBP (GSK3 Binding Protein), LANA (Latency Associated Nuclear Antigen) and NFkB-p65 all interact with via amino acids 262-299 of GSK3β (Farr *et al.* 2000, Ferkey and Kimelman 2002, Fujimuro *et al.* 2005 and Gong *et al.* 2008). Alternatively p53 interacts with amino acids 78-92 of GSK3β (Eom and Jope 2009). Both the GSK3β mutants

used in this study were equally able to interact with IRF-1, confirming that a loss of their catalytic activity is the reason for the reduced phosphorylation, rather than a reduced interaction. It would also be of interest to study if binding of GSK3β also plays a role in IRF-1 activity that is independent of phosphorylation. For example, p53 is phosphorylated by GSK3β, but the interaction also increases acetylation of p53 and as such alters its activity (Eom and Jope 2009). The interaction between GSK3β and E2F1 regulates the activity of the latter to a more significant degree then phosphorylation (Garcia-Alvarez *et al.* 2007).

In conclusion GSK3β phosphorylates IRF-1 at Thr^{180} (and possibly other residues), while the Ser^{184} kinase remains to be identified. The modification occurs in normal and breast cancer cells, but is unstable, potentially because it acts as ubiquitination signal.

Chapter 4.

Phosphorylation of Thr^{180}/Ser^{184} regulates IRF-1 transcriptional activity

4.1. Introduction.

A key aim of this study is to determine the effects of phosphorylation on IRF-1 activity. In this section reporter assays were employed to determine the effects of substitution of the mapped phosphorylation sites on IRF-1 transactivation activity against the TRAIL promoter. To confirm the importance of GSK3β in IRF-1 transcriptional activity, small chemical inhibitors, siRNA and a dominant negative allele (K85A) of GSK3β were used. Collectively these assays show that both Ser^{184} and Thr^{180} are important for IRF-1 activity against the TRAIL promoter and a synthetic multimerised reporter (4X ISRE). Chemical inhibition, siRNA transfection or over-expression of K85A all caused a decrease in IRF-1 transcriptional activity. Interestingly phospho mimetic mutations of IRF-1 (T180D and S184E) did not increase the activity of IRF-1; neither did over-expression of wild type GSK3β or treatment with the PI3K inhibitor wortmannin. Potential mechanisms for this discrepancy are discussed. To confirm the importance of Thr^{180}/Ser^{184} for IRF-1's transcriptional activity, stable cells lines were employed which express wild type or alanine mutant IRF-1 under the control of the Tet repressor. While clones that expressed wild type IRF-1 were able to produce a robust increase in TRAIL mRNA, both T180A and TS-A IRF-1 expressing cells were significantly less capable of producing TRAIL mRNA. In conclusion, the GSK3β-Thr^{180}/Ser^{184} axis is important for IRF-1 dependent transcription of TRAIL.

4.2. Thr^{180} and Ser^{184} are important for IRF-1 transcriptional activity.

IRF-1 brings about most of its functions in the cell through its ability to regulate gene expression at the transcriptional level. Early studies suggested that IRF-1's DBD is essential for IRF-1 anticancer activity (Kirchhoff *et al.* 1993) as such the activity of IRF-1 as a transcription factor were the focus for this work. IRF-1 acts as a positive transcriptional regulator of the TRAIL (TNFα Related Apoptosis Inducing Factor) gene in a number of cell lines in response to IFNα/β/γ, retinoids and HIV infection (Clarke *et al.* 2004, Park *et al.* 2004, Papageorgiou *et al.* 2007, Huang *et al.* 2009). In addition other members of the IRF family are able to regulate TRAIL including IRF-3, IRF-4, IRF-5 and IRF-7 (Kirshner *et al.* 2005, Yoshida *et al.* 2005, Romieu-Mourez *et al.* 2006 and Hu and Barnes 2009). IRF-2 was found to be localised on the TRAIL promoter, but its function is not yet known (Clarke *et al.* 2004) the sites on which IRF family members interact with the TRAIL promoter have also been mapped, allowing a fragment of the promoter to be used in reporter assays (Clarke *et al.* 2004). Significantly, the IRF-1-TRAIL axis has been shown to be important in apoptosis, with TRAIL induction being one of the major mechanisms by which IFN and retinoids (via IRF-1) bring about apoptosis in cancer cells. Consequently the TRAIL promoter was used as the model system in these studies, particularly the minimal region required for IRF-1 dependent transactivation. To study IRF-1 transcriptional activity, reporter assays were employed in Cos7 cells. A region of the TRAIL promoter was fused up-stream of a Luciferase reporter gene. Cos-7 cells were employed due to their ease of transfection and their lack of any endogenous IRF-1 expression. Transactivation of the TRAIL promoter was assayed by an enzyme activity assay for Luciferase protein, which is a product of IRF-1 transactivation of the TRAIL

promoter fragment which controls the expression of the Luciferase gene. Luciferase protein is only produced when IRF-1 binds the reporter plasmid and recruits the relevant coactivators and RNA Pol II.

The contribution of Thr^{180} and Ser^{184} to IRF-1 transcriptional activity was measured using amino acid substitutions (hereafter referred to as mutants) of each residue to alanine singly and in combination. alanine cannot be phosphorylated, but is structurally similar to Thr and Ser and so minimises any structural effects of the substitution. Schematics of the mutants used are given in figure 4.9. Transient transfections were carried out for reporter assays for 24 and 48 hours, with either 100 or 50 ng of pcDNA3.1 IRF-1 wild type, T180A, S184A and TS-A (data not shown). Results were consistent among the two time points and concentrations, but the lower concentration and longer time-point were selected to reduce the toxicity of IRF-1 over-expression and to allow greater time for the Luciferase protein to accumulate.

Consistently the alanine mutants of IRF-1 exhibited lower reporter activity than wild type IRF-1, despite the expression of the mutants and wild type being comparable (figure 4.1). Intriguingly the S184A mutant exhibited the same activity as the T180A mutant. The double TS-A mutant produced the same level of transactivation at either single mutant, suggesting that loss of both residues has the same effect as loss of either single residue. The consequence of phosphate group attachment to Ser/Thr residues is the gain of a negative charge (Ser/Thr residues are uncharged). This gain of negative charge can be mimicked by the substitution of potentially phosphorylated residues with the acidic amino acids aspartic acid (D or Asp) or glutamic acid (E or Glu). These phospho-mimetic

mutants can be regarded as constitutively phosphorylated forms of protein. IRF-1 T180D and S184E were constructed to determine if a negative charge on these residues is important for transcriptional activity (see figure 4.1). Surprisingly both of these mutants demonstrated significantly reduced activity compared to wild type IRF-1, again both mutants were expressed at similar levels to wild type, with no apparent change in molecular weight. To determine if the Thr^{180} and Ser^{184} residues are important for IRF-1 activity on other promoters, a synthetic multimerised ISRE reporter was used. This reporter construct is derived from the histone 4 promoter and contains four tandem copies of an ISRE sequence which is recognised by a number of IRF family members (Xie *et al.* 2001). The higher numbers of binding sites leads to the potential for multiple IRF proteins to act together in synergy, as it has been reported that IRF-1 can homodimerise (Kirchhoff *et al.* 1998) and a number of genes contain multiple IRF binding sites in tandem (see table 1.4). The stochiometry of IRF-1 transactivation on this promoter is potentially quite different to the TRAIL promoter, which contains only two IRF binding sites (an IRF-E and an ISRE).

The reporter activity of wild type and all of the IRF-1 mutants was broadly comparable between the TRAIL and 4X ISRE reporters. As such it is possible that the effects on IRF activity are not confined to the TRAIL promoter and could potentially globally impact the IRF-1 transcriptional programme (figure 4.1).

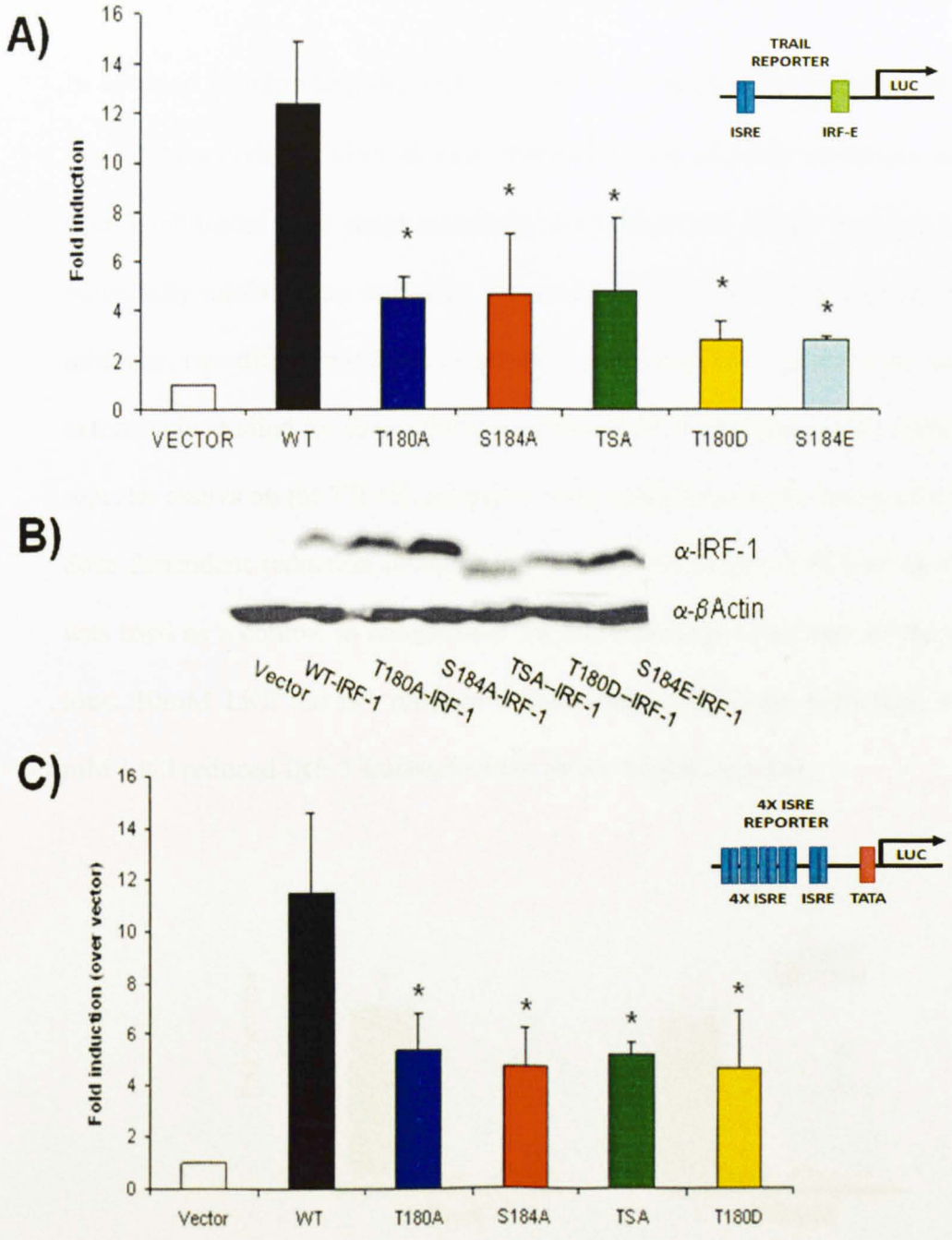

Figure 4.1 Substitution of phosphorylated residues for either alanine or acidic residues severely reduces IRF-1 transcriptional activity. A) Cos7 cells transfected with 50 ng/well IRF-1 expression plasmid, 75 ng/well TRAIL promoter reporter and 5 ng/well βGAL for 48 hours. B). Immunoblot of IRF-1 expression in Cos7 reporter extracts. C). Reporter assay as for A. but using a 4X multimerised ISRE reporter. Schematics for each report are shown in the top right of each figure. Values are expressed as a fold difference between empty vector and IRF-1 expressing cells. Error bars denote standard deviation and * represents significant difference (<0.05) as determined by Students t-test. Values are from three independent experiments carried out in triplicate.

4.3. Inhibition of GSK3 reduces IRF-1 activity on the TRAIL promoter

In addition to inhibiting the ability of IRF-1 to be phosphorylated at Thr^{180} and Ser^{184}, the activity of GSK3β was inhibited by use of small molecule inhibitors. GSK3 inhibitors have equal selectivity for both of the GSK3 isoforms, and can potentially inhibit other enzymes. To account for any effect specific to a certain inhibitor, two different classes of inhibitor were selected. Lithium ions have been extensively studied for their ability to inhibit GSK3 (Martinez *et al.* 2002). When reporter assays on the TRAIL promoter were carried out in the presence of LiCl, a dose dependent reduction in activity was observed (figure 4.2) Sodium Chloride was used as a control to compensate for any effect on osmolarity of the chloride ions. 10mM LiCl did not produce a statistically significant reduction, while 20 mM LiCl reduced IRF-1 transactivation of the TRAIL reporter.

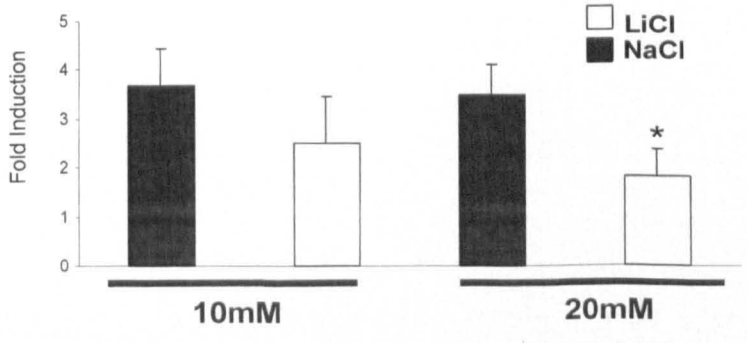

Figure 4.2. GSK3 inhibitor Lithium reduces IRF-1 transcriptional activity on the TRAIL promoter. Cos7 cells transfected with 50 ng/well IRF-1 expression plasmid, 75 ng/well TRAIL promoter reporter and 5 ng/well βGAL for 48 hours. Inhibitor treatments were carried out for 15 hours. All Luciferase values are relative to βGAL expression. Values are expressed as a fold difference between empty vector and IRF-1 expressing cells treated with the same concentration of inhibitor. Error bars denote standard deviation and * represents significant difference (<0.05) as determined by Students t-test. Values are from three independent experiments carried out in triplicate.

The second class of inhibitor used was those based on indirubin (Meijer *et al.* 2003). These compounds are thought to act through the ATP pocket of GSK3β, a region which is not targeted by lithium ions. Two structurally similar inhibitors were used, inhibitor IX (not shown) and inhibitor X (see figure 4.3). Both of these inhibitors promoted a dose responsive reduction of IRF-1 reporter activity on the TRAIL promoter. Inhibitor X exhibited a more potent reproducible inhibition of IRF-1 reporter activity then inhibitor IX. A third compound – Inhibitor VII (Methyl-BIO) was used as a control. Addition of a methyl group greatly reduces the activity of this compound. As expected inhibitor VII had no effect on IRF-1 reporter activity when compared to DMSO control.

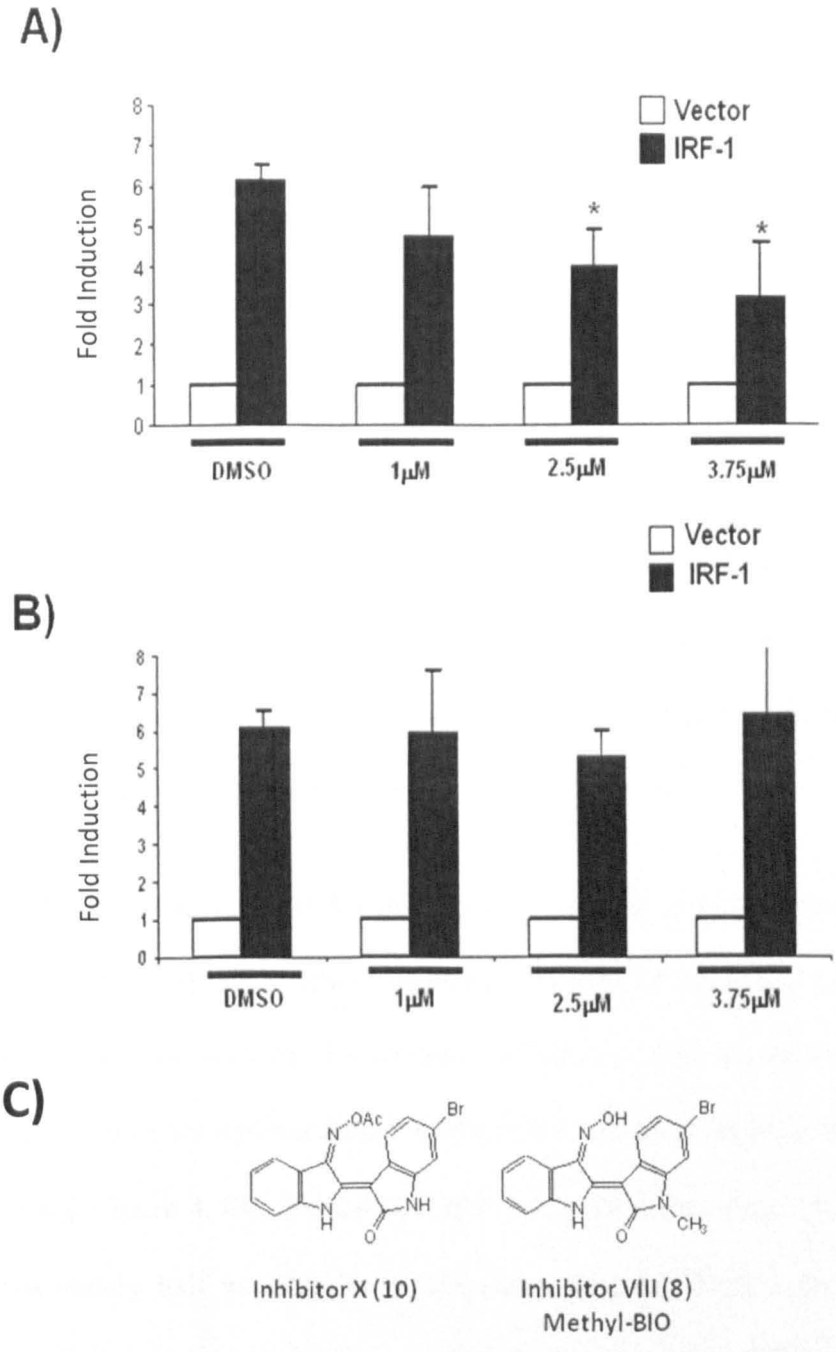

Figure 4.3 GSK3 inhibitor X reduces IRF-1 transcriptional activity on the TRAIL promoter. Cos7 cells transfected with 50 ng/well IRF-1 expression plasmid, 75 ng/well TRAIL promoter reporter and 5 ng/well βGAL for 48 hours. **A)** Treatment with GSK3 inhibitor X, **B)** treatment with GSK3 inhibitor XIV. Inhibitor treatments were carried out for 15 hours. All Luciferase values are relative to βGAL expression. Values are expressed as a fold difference between empty vector and IRF-1 expressing cells treated with the same concentration of inhibitor. The final DMSO concentration was 0.01%. Error bars denote standard deviation and * represents significant difference (<0.05) as determined by Students t-test. Values are from three independent experiments carried out in triplicate. **C)** Structures of inhibitors used.

4.4. Depletion of GSK3β reduces IRF-1 transcriptional activity.

A significant disadvantage of using chemical inhibitors to probe the activity of GSK3β is that they lack specificity, due the structural similarities between CDK and GSK kinases and a certain degree of cross inhibition is unavoidable (Meijer *et al.* 2003). Inhibitors also prevent kinases from phosphorylating their substrates, but do not necessarily prevent physical association with substrates. Chapter 3 established an interaction between GSK3β and IRF-1, to determine if depleting GSK3β protein from cells has a similar effect to inhibiting its catalytic activity, siRNA knockdown was employed. Duplex siRNA oligos that were validated to only target GSK3β were purchased from QIAGEN and used to knockdown GSK3β in MRC-5 cells (see figure 4.4).

MRC-5 cells were selected for these assays because it had already been shown that the mutants of IRF-1 behave identically in MRC-5 as in Cos7 cells in reporter assays (data not shown). Knockdown efficiency was determined in protein extracts used in the reporter assays to check that efficient depletion of GSK3β was occurring (figure 4.4B). Transfected IRF-1 in cells expressing less GSK3β were approximately half as effective at transactivating the TRAIL promoter (figure 4.4A). Activity was expressed as a fold change between cells transfected with empty vector and IRF-1 to cancel out any effects GSK3β siRNA had on basal activity of the TRAIL promoter. However the basal activity was not significantly altered (data now shown).

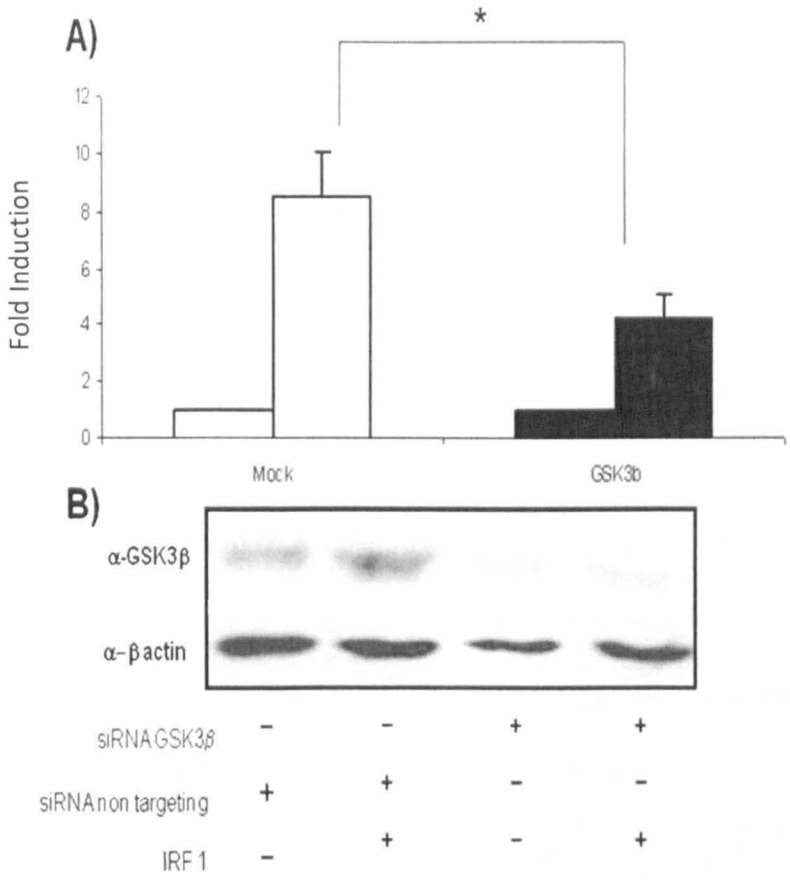

Figure 4.4. siRNA mediated depletion of GSK3β reduces IRF-1 transactivation of the TRAIL promoter. A) MRC-5 cells transfected with 5 nM of either control non targeting siRNA, or GSK3β siRNA for 15 hours followed by transfection with 125 ng of TRAIL reporter, 100 ng of IRF-1 and 20 ng of βGAL expression plasmid for 24 hours. Data is from three experiments carried out in triplicate. Data is shown as fold induction using empty vector. Error bars indicate standard deviation. * Denotes statistical difference (non targeting siRNA v. GSK3β siRNA) as determined by Students t-test (p less than 0.05). **B)** Representative western blot of GSK3β expression in extracts used for reporter assay (20 μg/lane).

4.5 Over-expression of DN (Dominant negative) GSK3β reduces IRF-1 transcriptional activity.

The K85A kinase inactive mutant of GSK3β used in chapter three has also been reported to have dominant negative activity, due to its ability to bind, but not phosphorylate substrates. Potentially, this prevents endogenous GSK3β from phosphorylating substrates. To determine if over-expressed K85A GSK3β was able to reduce IRF-1 activity, it was transfected in reporter assays containing IRF-1. Increasing expression of K85A GSK3β caused a significant reduction in IRF-1s ability to activate the TRAIL reporter. Additionally there was a slight decrease in the basal (vector transfected) levels, suggesting that GSK3β may play a role in the basal activity of the TRAIL promoter (see figure 4.5).

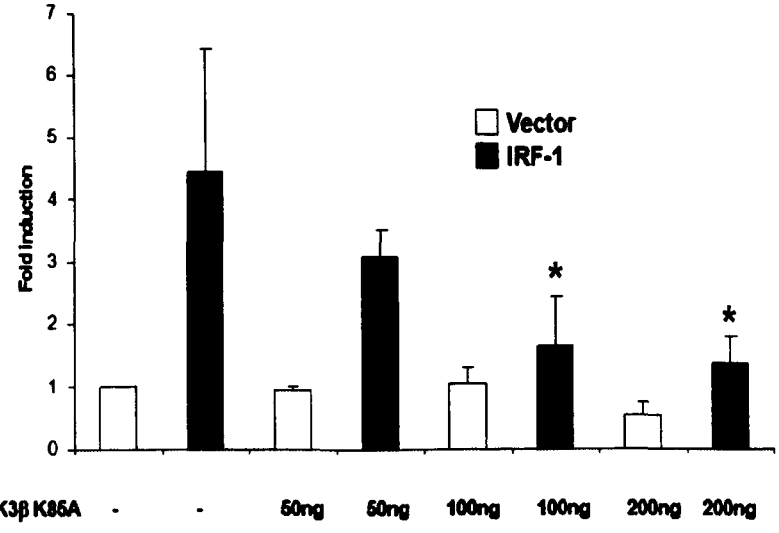

Figure 4.5. Dominant negative (K85A) GSK3β reduces IRF-1 transcriptional activity on the TRAIL promoter. Cos7 cells transfected with 50 ng/well IRF-1 expression plasmid, 75 ng/well TRAIL promoter reporter and 5 ng/well βGAL for 48 hours. A titration of HA-GSK3β K85A between 50 and 200 ng was co-transfected either with empty vector or IRF-1.Values are expressed as a fold difference between empty vector and IRF-1 expressing cells. Error bars denote standard deviation and * represents significant difference (<0.05) between empty vector and GSK3β-HA K85A. Values are from three independent experiments carried out in triplicate.

4.6 Increasing GSK3β activity and protein does not increase IRF-1 activity.

Increased expression of the K85A mutant of GSK3β causes a dose dependent reduction in IRF-1 activity, to determine if wild type GSK3β was able to increase the activity of IRF-1, GSK3β was co-expressed with IRF-1 (figure 4.6). Surprisingly, increased expression of GSK3β did not promote a statistically significant increase in IRF-1 activity. To a small (not significant) degree GSK3β was able to reduce the activity of IRF-1. Titrating GSK3β with IRF-1 at a set concentration also did not enhance the activity of IRF-1 to an appreciable degree. Both IRF-1 and GSK3β proteins were expressed in the cell extracts (data not shown). An alternative strategy was then employed in which rather than increasing the amount of GSK3β protein, the activity of endogenous GSK3β protein was enhanced with wortmannin treatment. Wortmannin is a PI3K (Phosphoinositide 3 Kinase) inhibitor. This leads to reduced activation of PKB/Akt, which in turn leads to a reduction in the phosphorylation of Ser^9 on GSK3β. This has been shown to enhance the activity of GSK3β, by relieving the auto-inhibition of the kinase domain. Titration of wortmannin did not lead to any significant increase in IRF-1 activity (figure 4.7), suggesting that wortmannin does not regulate IRF-1 activity towards the TRAIL promoter. Additionally a mutant of GSK3β which does not possess the auto-inhibitory Ser^9 residue (GSK3β-HA S9A) was also titrated and found to have no significant effect on IRF-1 activity (data not shown).

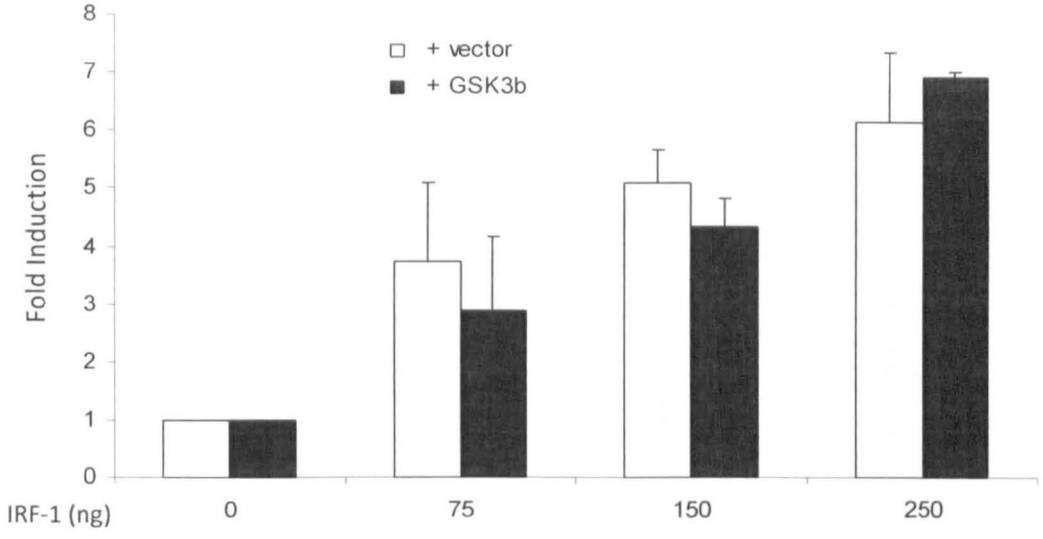

Figure 4.6. GSK3β over-expression does not enhance IRF-1 reporter activity. Cos7 cells transfected with 75, 150 and 250 ng of IRF-1 expression vector, and 150 ng of TRAIL promoter reporter. 10 ng per well of βGAL expression plasmid was used as a transfection control. 75 ng of GSK3β-HA wild type or empty vector were co-transfected with the above plasmids. Transfection was for 48 hours. Values are from three independent experiments carried out in triplicate. Data is expressed as fold increase compared to empty vectors or GSK3β-HA wild type alone (X axis). Error bars denote standard deviation; no statistical significance was detected between vector and GSK3β transfected cells at any concentration.

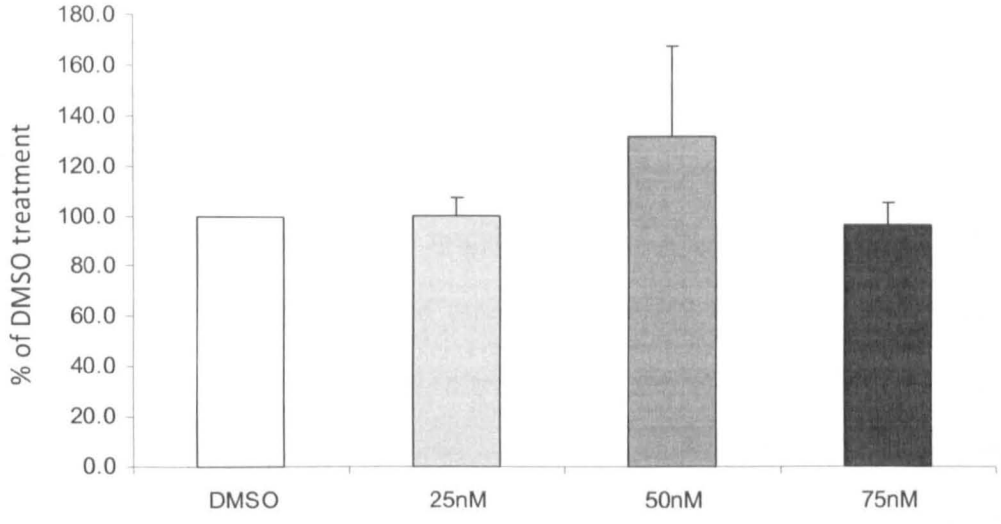

Figure 4.7. Wortmannin does not increase IRF-1 transcriptional activity on the TRAIL promoter. Cos7 cells were transfected with 50 ng IRF-1, 100 ng TRAIL reporter and 5 ng CMV βGAL for 48 hours. 24 hours prior to lysis for the reporter assays, cells were treated with DMSO (0.01%) or the indicated concentration of wortmannin. Induction was determined as a fold increase in Luc expression over empty vector expressing cells treated with the appropriate concentration of inhibitor. Experiments were carried out in triplicate in three independent experiments. Data is expressed as % of vehicle control (0.01% DMSO). Error bars denote standard deviation.

4.7 Thr^{180}/Ser^{184} are required for IRF-1 dependent gene expression in Breast cancer cells

Previously, the activity of the TRAIL promoter reporter has been shown to closely match the activity of IRF-1 on TRAIL mRNA and protein (Clarke *et al.* 2004). To determine if phosphorylation is important for the production of TRAIL mRNA, stable cell lines were generated (see 2.2.8). Stable H3396 Tet-Off cells were employed due to the difficulty in transiently transfecting H3396 cells. It also allows for a relevant cell system to be used in which the IRF-1-TRAIL pathway has been shown to induce apoptosis. Stable clone that express empty vector (VA4, VA7), wild type IRF-1 (WX14, WX3), T180A-IRF-1 (TC5, TG1) or TS-A (TSX2, TSX15) were treated with doxycline for the indicated time period to induce the expression of IRF-1. The cells were then lysed and mRNA extracted. Neither vector clones were able to significantly increase expression of TRAIL mRNA, showing that dox does not induce the cells to produce TRAIL mRNA. As expected the wild type clones were able to produce a robust level of TRAIL mRNA within a short period of time. All of the mutant clones (TC5, TG1, TSX2, and TSX15) were significantly less able to induce the expression of TRAIL mRNA at each time point tested. Without dox treatment none of the clones significantly induced TRAIL mRNA above the levels seen in the empty vector clones. This shows that IRF-1 is responsible for the induction of TRAIL mRNA. The mRNA (not shown) and protein levels of murine IRF-1 were tested to determine if the expression of IRF-1 was comparable. With the exception of TSX15 all of the clones produced near identical levels of IRF-1 protein. The lower level of TSX15 IRF-1 protein is likely attributed to the lower levels of protein blotted (see the actin levels below).

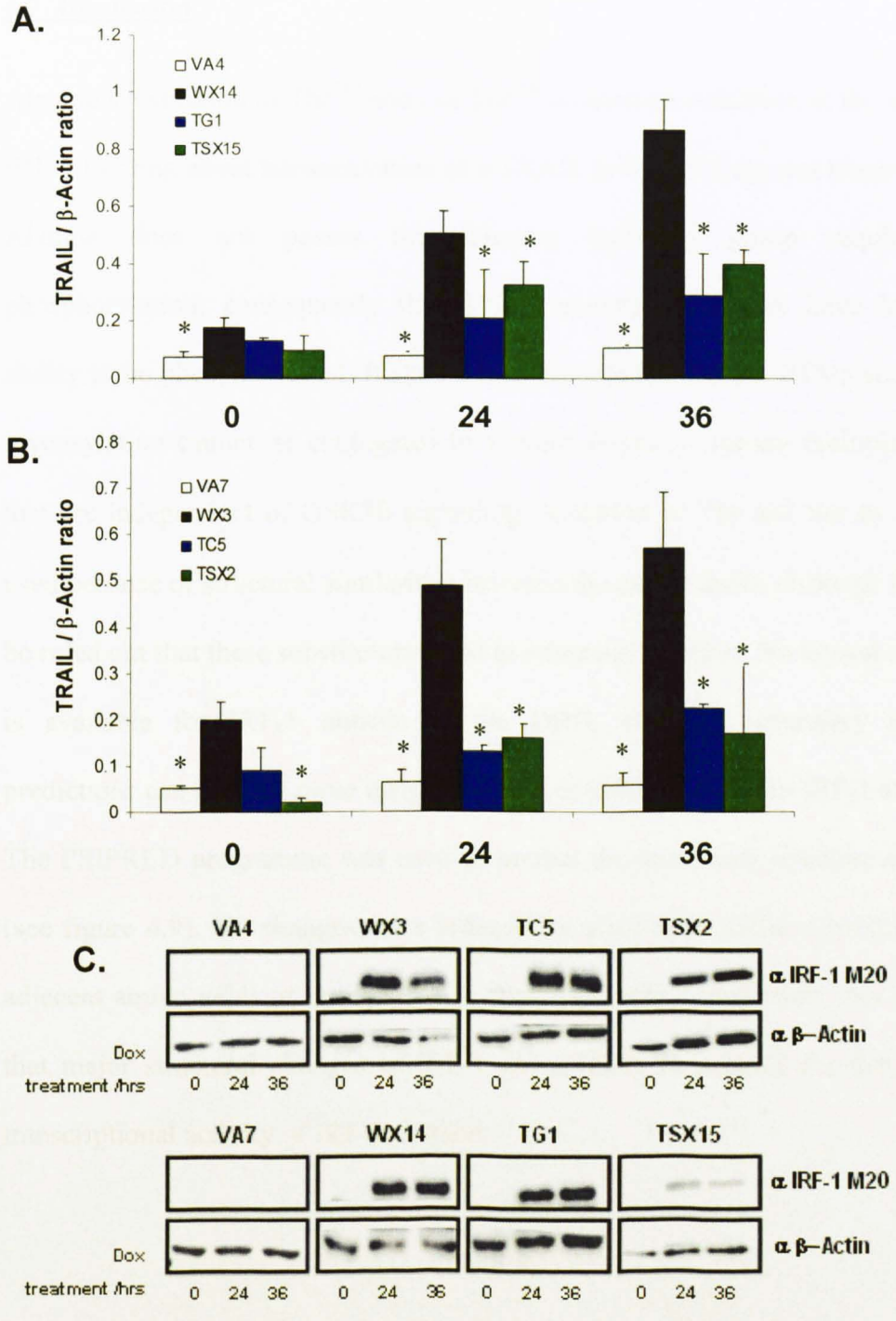

Figure 4.8 TRAIL mRNA expression of H3396 IRF-1 Tet-Off cell lines. Each clone was seeded at $1x10^6$ and treated with 2 μg/mL dox for the indicated time periods. Experiments were carried out in triplicate, with an additional plate being used to check protein. **A).** TRAIL mRNA expression at 0, 24 and 36 hours of dox treatment. TRAIL mRNA levels are expressed as ratio to β-actin mRNA. **B)** As for A, but with different stable cell lines. **C)** 10 μg of protein extract from parallel experiments was immunoblotted against IRF-1 M20 and β-actin to demonstrate expression of induced IRF-1 protein. Data is representative of three experiments carried out in triplicate. Error bars denote standard deviation. * indicate statistically different from the wild type clone. cDNA preparation and QPCR performed by A. Rettino.

4.7. Discussion

Alanine substitution of Thr^{180} and / or Ser^{184} promotes a reduction in the ability of IRF-1 to bring about transactivation of a TRAIL promoter fragment (figure 4.1A). Alanine does not posses the function hydroxyl group required for phosphorylation; consequently the alanine mutants used here have lost their ability to be phosphorylated. It should also be noted that other PTMs such as O-glycosylation cannot be conjugated to alanine, possibly causing multiple effects that are independent of GSK3β signalling. Mutation of Thr and Ser to Ala was used because of structural similarities between the amino acids, although it cannot be ruled out that these substitutions lead to structural changes. No crystal structure is available for IRF-1 outside of the DBD, although secondary structure predictions can provide some insight into the potential changes in IRF-1 structure. The PSIPRED programme was used to predict the secondary structure of IRF-1 (see figure 4.9). No changes were induced by alanine or acidic substitutions, in adjacent amino acids of murine IRF-1. Although only a prediction, this suggests that major structural changes in IRF-1 are unlikely to account for the reduced transcriptional activity of IRF-1 mutants.

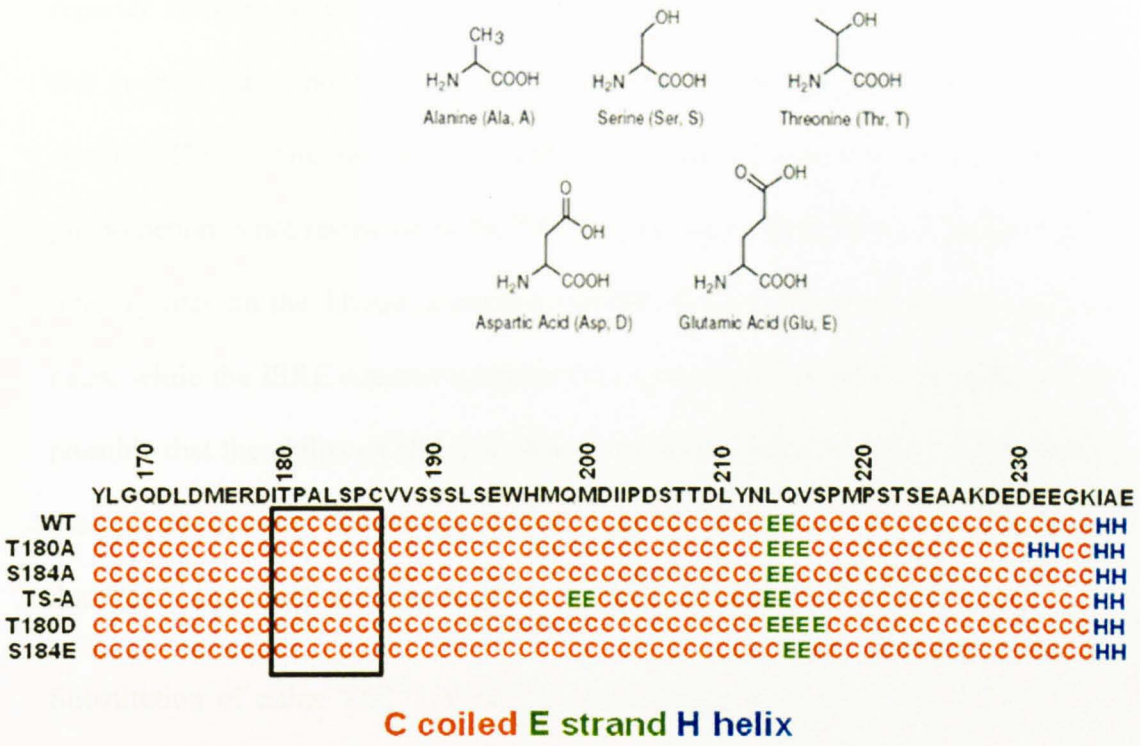

Figure 4.9 Predicted secondary structure of IRF-1 Phosphorylation mutants. Top, diagrams of the amino acids Thr, Ser and the three amino acids used to make phosphorylation mutants. Amino acid sequences of mouse IRF-1 WT, T180A, S184A, TS-A, T180D and S184E were submitted to the PSIPRED (psipred@cs.ucl.ac.uk)

Both the alanine mutants, T180A and S184A behaved almost identically in both reporter systems, as did the double TS-A mutant (see figure 4.1). This suggests that the Ser^{184} does not have a major effect on IRF-1 activity, but acts as a priming site for Thr^{180}. The use of two different reporter constructs proves that this phenomenon is not restricted to the TRAIL promoter. There are two potential IRF binding sites on the TRAIL promoter reporter that are separated by several base pairs, while the ISRE reporter contains four concatermized ISRE sequences. It is possible that the ability of IRF-1 to form conjugates with each other is reduced in the alanine mutants. All of the alanine mutants retain some activity suggesting that Thr^{180} and Ser^{184} are not completely essential for IRF-1 activity.

Substitution of either Thr^{180} or Ser^{184} for acidic residues was not able to rescue their activity (see figure 4.1). Although in other reports acidic residues have been shown to act as phospho-mimics, in some cases they do not behave as expected. It should be noted that although the acidic amino acids carry a negative charge, they cannot be phosphorylated. Phosphorylation is also a dynamic process, and it is possible that the phosphate on Thr^{180} and Ser^{184} is added and removed several times during the lifespan of IRF-1. Phosphorylation can be added to a protein during translation or following translation. Addition of phosphate after the IRF-1 protein is fully folded could have quite different consequences to the presence of acidic residues during translation. Constitutive presence of acidic residues may also promote protein-protein interactions that would not normally occur without phosphorylation.

Lithium modulates a number of TFs activity in reporter assays including, E2F1, β catenin, NFκB, AR, ERα and Rev-erbα (Espada *et al.* 2007, Nowicki *et al.* 2008 Nemeth *et al.* 2002, Wang *et al.* 2004, Mendez and Garcia-Segura 2006 and Yin *et al.* 2006). In reporter assays using the TRAIL promoter, lithium chloride was able to cause a dose dependent reduction in activity. The activity of IRF-1 in vehicle control treated cells was slightly lower in these assays, possible due to the use of NaCl as a control. Osmotic stress may have reduced the activity of IRF-1, use of water (the lithium chloride solvent) allowed for a much greater induction of IRF-1, and a more significant change in reporter activity at lower concentrations of lithium (data not shown). Lithium is a poor inhibitor of GSK3β, with concentrations of 1 mM in the blood of patients being needed for any therapeutic benefit. Lithium is a direct reversible inhibitor of GSK3 with an IC_{50} of 2 mM *in vitro*. Numerous potential mechanisms by which lithium inhibits GSK3 activity have been proposed, although no consensus has yet been reached. Lithium may compete with the Mg^{2+} ion associated with ATP, or it could inhibit the phosphatase responsible for the removal of the inhibitory Ser^{9} modification. Lithium also inhibits a number of other enzymes, including inositol monophosphatase (O'Brien and Klein 2009). Lithium chloride treatment did not alter the abundance of IRF-1 protein in Cos7 or HEK293 cells; it also did not promote a change in IRF-1 localisation in the latter cell type (data not shown).

Modified indirubins that have substantially higher selectivity were used in reporter assays to determine the effect of GSK3 on IRF-1 reporter activity. GSK3 inhibitor IX (6 Bromoindirubin 3'oxime) has an in vitro IC_{50} of 5 nM and inhibits CDK enzymes at between 83 and 10,000nM). Compared to DMSO control inhibitor IX caused a decrease in IRF-1 reporter activity (data not shown). A similar GSK3 inhibitor (inhibitor X – 6 bromoindirubin 3'acetoxime) produced a more significant and consistent decrease in IRF-1 reporter activity. It is not known why Inhibitor X effected a greater reduction in IRF-1 activity then Inhibitor IX. The IC_{50} of Inhibitor X is slightly higher than Inhibitor IX (10 nM compared to 5 nM). Inhibitor X exhibits much greater selectivity towards GSK3 over CDKs (IC50 ranging from 2.4-63 μM). It is possible that the difference in selectivity is responsible for the difference in activity. A control inhibitor was also used; methyl-BIO is a methylated derivative with an IC_{50} towards GSK3β of more than 100 μM. No significant change in IRF-1 activity, compared to DMSO was observed when methyl-BIO was added to cells, suggesting that it is the GSK3 inhibitory activity that is altering IRF-1 function. Dose ranges were used to determine any cytotoxic effects of these inhibitors. It was found that concentrations greater than 5 μM produced a marked decrease in cell growth, while concentrations above 10 μM initiated cell death (data not shown).

Collectively, this data suggest that endogenous GSK3 regulates the activity of IRF-1 while transactivating the TRAIL promoter fragment. The maximal reduction in activity was approximately 50% which is close the reduction in IRF-1 activity following substitution of Thr^{180} for alanine. Should the GSK3 inhibitors have produced a greater reduction in IRF-1 activity then the alanine mutants, it might suggest that other GSK3 phosphorylated sites were

involved in IRF-1 activity. Since this is not the case it could be argued that Thr^{180} is the most important GSK3β acceptor residue in IRF-1.

Knockdown of GSK3β was employed to determine if it was specifically this enzyme that was involved in IRF-1 transactivation of TRAIL. Knockdown of GSK3β promoted a significant reduction in IRF-1 reporter activity compared to the non targeting siRNA. By reducing the GSK3β protein, both the ability to phosphorylate and interact with IRF-1 is reduced. The reduction in IRF-1 activity is similar to the inhibitors, as such it could be postulated that the major effect of GSK3 is brought about by phosphorylation rather than interaction. Knockdown of GSK3β also shows that GSK3α is not able to completely compensate for the loss of GSK3β. The ability of GSK3α to interact with and phosphorylate IRF-1 has not been studied here, but a number of substrates have been shown to be preferentially phosphorylated by only one isoform (Force & Woodgett 2009). A complete knockdown of GSK3β was not achievable, most likely due to the high stability of GSK3β protein. It is possible that the remaining activity in IRF-1 is due to the remaining GSK3β protein. It should also be considered that not all GSK3β protein is available to phosphorylate IRF-1 and so an incomplete loss of GSK3β protein may still have significant effects on IRF-1 activity. Use of exogenously expressed IRF-1 rather than using endogenous IRF-1 (following *de novo* induction with IFNγ) also allowed any effects on IRF-1 induction to be discounted from the action of GSK3. For example, the IFNγ signalling pathway relies on a number of phosphorylation events and transcription factors, many of which could be regulated by GSK3β. A recent report suggest that STATs are regulated by GSK3β, suggesting that GSK3β may alter the ability of IFNγ to

induce functional IRF-1 protein (Tsai *et al.* 2009). Knockdown of GSK3β had no significant effect on basal (empty vector transfected) activation of the TRAIL promoter compared to non targeting siRNA transfection, confirming that GSK3 is not regulating basal transcription factors that promote a small induction of reporter activity in the absence of IRF-1. In addition to use of inhibitors and siRNA a dominant negative mutant of GSK3β was used (K85A). The K85A GSK3β was able to promote a dose dependent reduction in IRF-1 activity. Consequently, GSK3β K85A would appear to act as a dominant negative towards IRF-1 activity.

Figure 4.1 did not show that phosphorylation (or gain of negative charge) increases IRF-1 activity on the TRAIL promoter. As figures 3.9-3.12 demonstrated that increasing GSK3β in cells enhances IRF-1 phosphorylation, and figure 4.1 shows that the phosphorylated residues are needed for activity, the effect of increased wild type GSK3β was assayed. Increasing the concentration of IRF-1 and GSK3β on a 1:1 ratio had no effect of IRF-1 reporter activity, as there was no significant difference between IRF-1 and vector and IRF-1 and GSK3β (figure 4.6). Increasing the concentration of GSK3β, while keeping the IRF-1 concentration static also had no significant effect on IRF-1 activity (data not shown). Numerous combinations of IRF-1 and GSK3β were used in reporter assays, and consistently, no significant increase in activity for IRF-1 was detected. It is possible that increasing the phosphorylation of IRF-1 does not promote increased activity. Potentially proteins that interact with phosphorylated IRF-1 are limiting in these assays, so no increase in activity is detected. It is also possible that increased GSK3β concentration leads to an inappropriate phosphorylation of

IRF-1, either in the wrong cell compartment, at the wrong point in the transcription cycles, or possibly during the cell cycle. Other PTMs throughout the IRF-1 protein may also be needed for full transcriptional activity, the enzymes that supply these additional modifications may be rate limiting. GSK3β may also phosphorylate other proteins that are involved in the IRF-1 dependent transcription activity; as such an indirect mechanism may mask the actual increase in activity. In all experiments the amount of reporter was increased to allow for an increased reporter activity, and titrations of IRF-1 had shown that the reporter activity was in the linear range during these assays (data not shown).

Rather than Overexpression of GSK3β protein, an alternative approach was used to modify the activity of endogenous GSK3β. Figures (4.1-4.4) suggest that the endogenous GSK3 likely plays a role in IRF-1 transcriptional activity, so increasing the activity of GSK3β was performed with the PI3K inhibitor wortmannin. A range of doses were added to reporter assays for 24 hours, but no concentration had an effect on IRF-1 reporter activity. The level of Ser^9 phosphorylation has not been assayed in the Cos7 cells used in this assay, so it possible that the wortmannin treatment did not bring about the decrease in phosphorylation. It is also possible that very little GSK3β is Ser^9 phosphorylated in Cos7 cells. Multiple kinases are known to regulate GSK3β via the Ser^9 modification, so it is possible that other kinases could compensate. The activity of GSK3β is also controlled by localisation, and sequestration into large protein complexes, subsequently treatment by wortmannin may have had little effect on the activity of GSK3β. The data from figure 4.6 also suggest that even if the activity of GSK3β was increased by wortmannin and enhanced phosphorylation

of IRF-1 occurred, this may not increase its reporter activity. These results contrast those of Wang *et al.* 2002, in which wortmannin was shown to enhance TRAIL mRNA expression in colon cancer cells. This group then went on to show that GSK3β regulates TRAIL mRNA expression, as inhibitors of GSK3β prevent TRAIL induction by wortmannin. This study predated the discovery of IRF-1 as a major regulator of TRAIL expression (Wang *et al.* 2002). Collectively these figures suggest that although Thr^{180}/Ser^{184} and phosphorylation are important for IRF-1 activity, these modifications are tightly regulated, as constitutive phosphorylation (acidic mutants) or enhanced phosphorylation (GSK3β over expression) do not promote IRF-1 transcriptional activity. Finally to determine if the reporter assays correlate with mRNA induction, H3396 cells which express IRF-1 following treatment with dox were assayed for their TRAIL mRNA. In a very similar fashion to figure 4.1, neither T180A nor TS-A IRF-1 expressing cells were able to induce as much TRAIL mRNA as wild type clones despite expressing comparable levels of IRF-1 protein. Two clones of each were tested and found to produce similar amounts of TRAIL mRNA. Consequently, the reporter assays predict the outcome of IRF-1 on the full TRAIL promoter. Although not tested here, it is likely that GSK3β inhibitors and siRNA would have similar effect on TRAIL mRNA as TRAIL reporter activity. High sustained induction of IRF-1 is required to efficiently induce TRAIL dependent apoptosis, possible due to the large amounts of TRAIL mRNA (and therefore protein) needed to trigger apoptosis (Clarke *et al.* 2004). As such from this data it is unlikely that the T180A or TS-A mutant would be able to promote apoptosis to a similar degree as wild type IRF-1.

CHAPTER 5

IRF-1 TURNOVER IS REGULATED BY PHOSPHORYLATION

5.1. Introduction

In this chapter, potential mechanisms by which phosphorylation effects IRF-1 function were investigated. The subcellular localisation of IRF-1 was not affected by alanine substitution, GSK3β expression or GSK3β inhibitors (Supplementary figure S3 and data not shown). However, replacement of Thr^{180} and/or Ser^{184} to alanine reduced *in vivo* ubiquitination and promoted an increase in IRF-1 $t_{1/2}$. Conversely phosphomimetic mutants of IRF-1 were more ubiquitinated and less stable. Increasing GSK3β expression destabilised IRF-1, while dominant negative GSK3β stabilised IRF-1. To determine if stability of IRF-1 is responsible for the variation in transactivation, reporter assays using the TRAIL promoter were carried out in the presence of the proteasome inhibitor MG132. While inhibition of the proteasome (and IRF-1 turnover) had no effect on the phosphorylation mutants of IRF-1, wild type IRF-1 activity was greatly reduced. To confirm that IRF-1 ubiquitination/degradation was essential for its transcriptional activity, lysine mutants of IRF-1 that were less ubiquitinated were designed. Lys^{240} and Lys^{255} were identified as potential ubiquitin acceptor residues. K240R and K255R mutants of IRF-1 were less able to transactivate the TRAIL promoter, suggesting that ubiquitination and proteasomal degradation of IRF-1 is regulated by phosphorylation, and are needed for full transcriptional activity.

5.2. Mouse IRF-1 is ubiquitinated

Previous reports have identified human IRF-1 as a ubiquitinated protein (Nakagawa and Yokosawa 2000). To confirm that mouse IRF-1 was also ubiquitinated *in vivo* ubiquitination assays were performed in which murine IRF-1 was co-expressed with FLAG-Ubq (figure 5.1). Transfected cells were either treated with vehicle (DMSO) or the proteasome inhibitor MG132. In concurrence with figure 3.7 the levels of IRF-1 protein are increased following MG132 treatment, suggesting that mouse IRF-1 is degraded through the proteasome. The levels of FLAG-Ubq conjugates are also increased following MG132 treatment showing that ubiquitinated proteins are not stable - due to its ability to act as a tag for protein destruction. FLAG-Ubq migrated as multi-ubiquitin conjugated protein polymers rather than a single band at the predicted 10 kDa. This is due to the integration of FLAG-Ubq onto cellular proteins. When co-immunoprecipitation was carried out using the FLAG Ab to IP FLAG-Ubq, IRF-1 was brought down (figure 5.1A). This confirms that mouse IRF-1 interacts with FLAG-Ubq. The amount of IRF-1 co-immunoprecipitated by FLAG-Ubq was greater following MG132 treatment possibly because of the higher levels of IRF-1 and FLAG-Ubq in the MG132 lysates. Next, an alternative strategy was employed in which FLAG-IRF-1 was co-transfected with HA-Ubq (figure 5.1B). This was due to the inability of the IRF-1 M20 Ab toimmunoprecipitate the poly-ubiquitinated IRF-1 (data not shown). Protein extracts expressing IRF-1 alone, HA-Ubq alone and both in combination with and without MG132 were immunoprecipitated with FLAG Ab, and immunoblotted with HA Ab to detect the poly-ubiquitinated IRF-1. The HA Ab did not detect any immunoprecipitated Ubq conjugated proteins in control extracts containing FLAG-IRF-1 or HA-Ubq alone. Ubq conjugated

proteins could also not be immunoprecipitated by FLAG Ab in DMSO treated cells. A poly-Ubq IRF-1 smear could only be detected in the extracts in which both IRF-1 and Ubq were co-expressed in MG123 treated cells. The protein smear began at approximately 75 kDa and extended to just under 250 kDa. Given the approximate 10 kDa mass of HA-Ubq, this suggests the lowest detected bands are di-ubiquitinated IRF-1 and the highest bands contain approximately twenty ubiquitin conjugates.

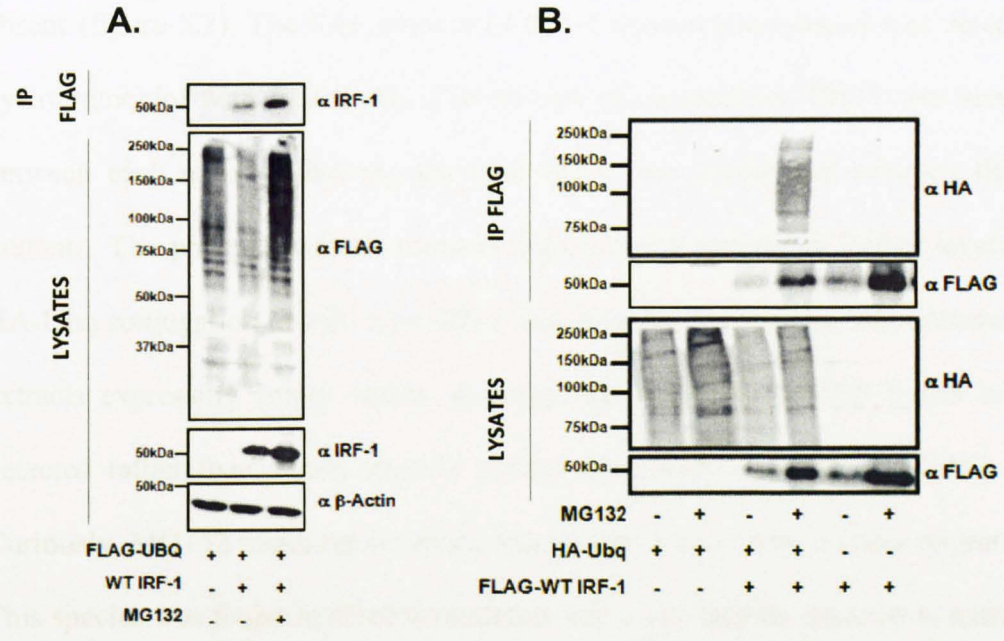

Figure 5.1. Murine IRF-1 ubiquitination is detectable in MG132 treated protein extracts. A) HEK293 cells transfected with 5 µg of mouse IRF-1 and FLAG-ubiquitin or FLAG empty vector for 48 hours. 6 hours prior to lysis cells were treated with DMSO or MG132. Protein lysates (0.5 mg) were immunoprecipitated with FLAG Ab and immunoblotted with IRF-1 M20 Ab. Lysates (10%) are shown to indicate the levels of transfected proteins. **B)** As for **A,** but using HA-Ubq and FLAG-IRF-1 (mouse), IP was performed using FLAG Ab and WB with HA 12CA5 Ab. 10% lysates indicate the expression of transfected proteins.

5.3. IRF-1 phosphorylation mutants show differential ubiquitin conjugation.

To determine if the phosphorylation status of IRF-1 modulates the incorporation of HA-Ubq, the alanine and phospho mimic mutants were expressed in HEK293 cells as for figure 5.1. All protein lysates were from cells treated with MG132, as without MG132 no poly-Ubq IRF-1 could be detected (see figure 5.1). Consistently all of the alanine substitution mutants showed reduced incorporation of HA-Ubq, with the Ubq smears pulled down by the FLAG Ab being fainter or absent (figure 5.2). The total amount of IRF-1 immunoprecipitated was detected by immunoblot with FLAG Ab. The amount of un-modified IRF-1 was similar between each mutant, showing the total IRF-1 was unchanged between IRF-1 mutants. The phosphomimetic mutants demonstrated similar or higher levels of HA-Ubq conjugation to wild type IRF-1. No HA-Ubq conjugation was detected in extracts expressing empty vector, showing that ubiquitinated IRF-1 was being detected rather than a non specific protein immunoprecipitated by FLAG Ab. Curiously, MG132 treatment reveals a second IRF-1 band with a faster migration. This species was found in all of the mutants and could only be detected in extracts from MG132 treated cells. This lower band was detected using FLAG and IRF-1 M20 Ab, confirming its identity as IRF-1. The band migrated slightly above 40 kDa.

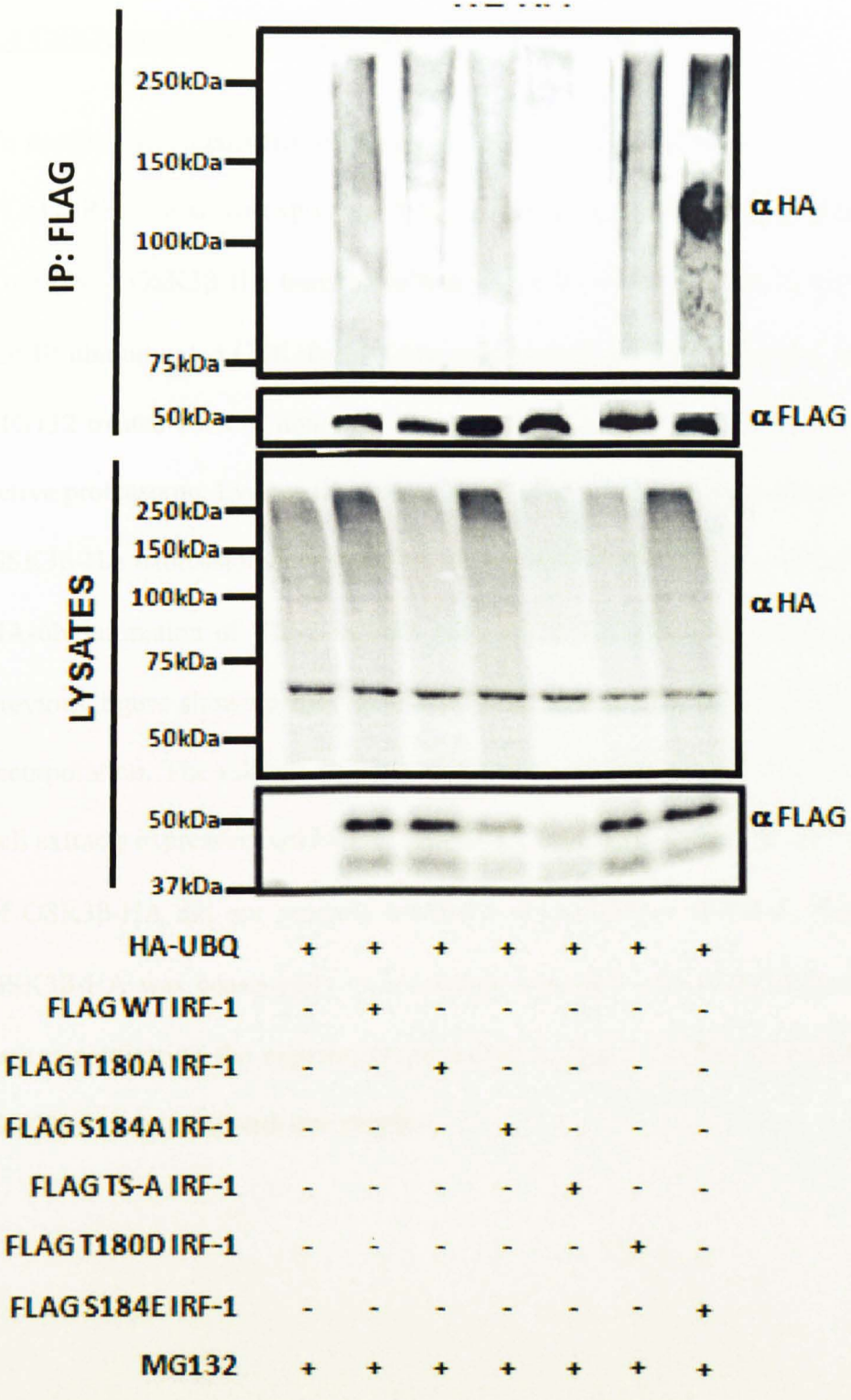

Figure 5.2 Differential ubiquitination of IRF-1 phosphorylation mutants. HEK293 cells were transfected with 2.5 µg of HA-UBQ and 2.5 µg FLAG-IRF-1 for 48 hours. 6 hours prior to lysis cells were treated with 10 µM MG132. Protein lysates (0.5 mg) were immunoprecipitated with FLAG and immunoblotted with HA Ab. Blots were re-probed with FLAG Ab to confirm FLAG-IRF-1 immunoprecipitation. Lower panels (lysates) 10% inputs to demonstrate expression of transfected proteins. (WT wildtype, TA T180A, SA S184A, TS-A T180A/S184A, TD T180D and SE S184E).

5.4 GSK3β modulates incorporation of Ubq onto IRF-1

To confirm the importance of phosphorylation on IRF-1 ubiquitination, wild type FLAG-IRF-1 was co-expressed with HA-Ubq and GSK3β-HA (figure 5.3). Controls of GSK3β-HA transfected with HA-Ubq confirmed that FLAG Ab does not IP ubiquitinated GSK3β-HA (data not shown). All protein lysates were from MG132 treated cells as ubiquitin conjugation could not be detected in cells with active proteasome. Lysates illustrating the levels of transfected proteins show that GSK3β-HA expression does not alter the expression of HA-Ubq or FLAG-IRF-1. HA-ubiquitination of IRF-1 in cells not expressing GSK3β-HA were similar to previous figure showing that increased DNA transfection did not alter HA-Ubq incorporation. The relative amount of HA-Ubq conjugated IRF-1 was greater in cell extracts expressing wild type GSK3β-HA then vector, while the K85A mutant of GSK3β-HA did not promote increased ubiquitination of IRF-1. Additionally GSK3β-HA was consistently co-immunoprecipitated with FLAG-IRF-1 in these assays confirming the experiment presented in figure 3.9 that FLAG-IRF-1 and GSK3β-HA interact with one another.

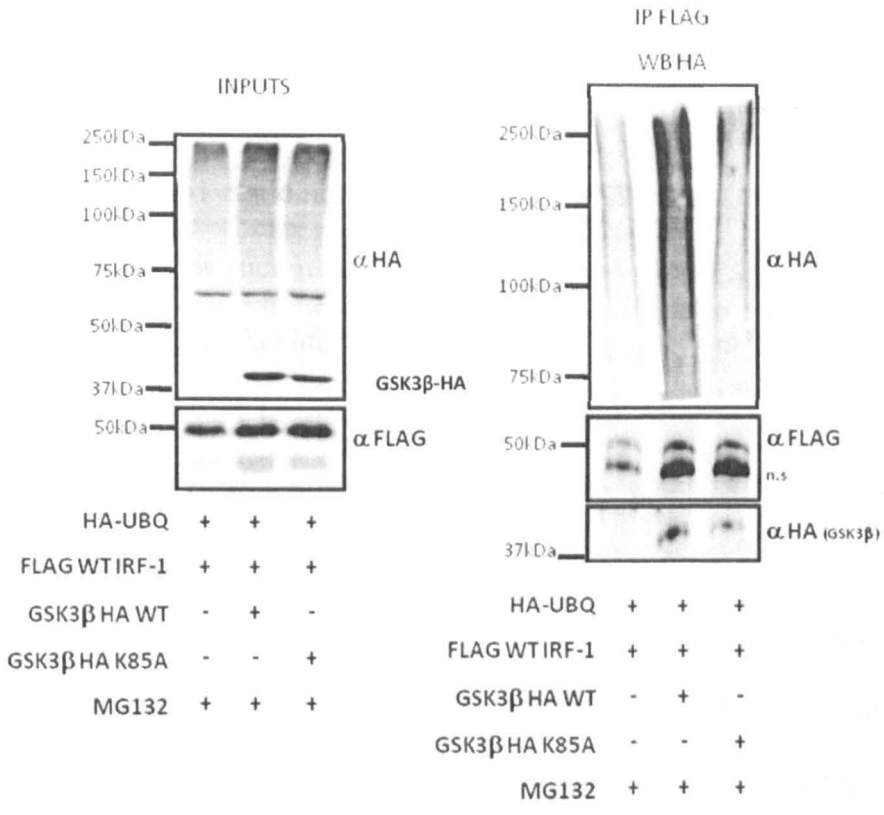

Figure 5.3 GSK3β regulates IRF-1 Ubiquitination. Assays were performed as described in figure 5.2, but with the additional transfection of 2.5 μg of HA empty vector, GSK3β-HA WT or GSK3β-HA K85A. Left panel demonstrates expression of lysates. The band in the HA panel above 37 kDa is GSK3β-HA. Right panel *in vivo* ubiquitination assay with additional co-immunoprecipitation of GSK3β-HA.

5.5. Thr^{180}/Ser^{184} are important for IRF-1 stability

Most forms of poly ubiquitination result in degradation of its substrates. Ubiquitinated IRF-1 could not be detected without the addition of the proteasome inhibitor MG132; as such it is likely that the ubiquitination of IRF-1 is related to its degradation. Cycloheximide (CHX) chases were carried out in MRC-5 cells expressing IRF-1 and its phosphorylation mutants. Addition of CHX to cells results in a block in translation. This prevents any new IRF-1 from being produced in the cells, leaving the remaining IRF-1 to be degraded. Time courses of CHX addition were then carried out to determine the rate of loss of IRF-1 protein. Various concentrations of CHX were tested, but all were found to have the same effect on IRF-1, as such the middle concentration (25 μg/mL) was used. Time points ranging from 15 minutes to 4 hours were tested. In all experiments the amount of wild type IRF-1 decreased 90% by 2 hours and did not decrease any further, to prevent any unwanted side effects of CHX treatment, time points longer than 2 hours were not used. Short time points such as 15 minutes were not used because of the difficulty in preparing protein samples accurately for this time point.

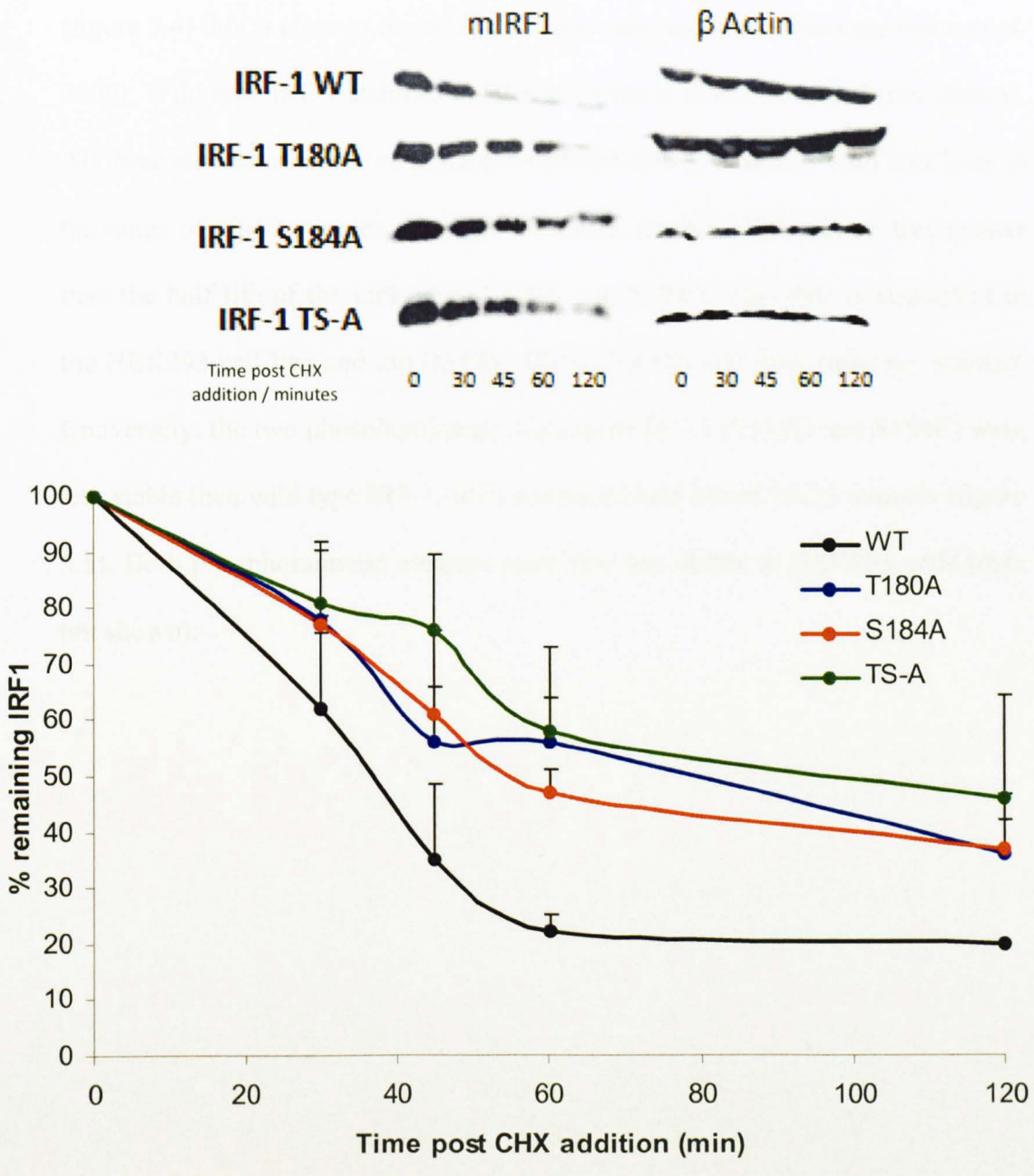

Figure 5.4 IRF-1 Alanine mutants exhibit increased stability. CHX assays were performed on MRC-5 cells transfected with 4 μg of IRF-1. 2.5 μg/mL CHX for the indicated time points. Protein lysates (15 μg) were immunoblotted with IRF-1 M20 and β-actin. IRF-1 protein was divided by β-actin protein to correct for protein loading. Data is expressed as a precentage of the 0 minute time point. CHX time point versus time in minutes. Data is from three independent experiments with each set of extracts being immunoblotted in duplicate. Error bars denote standard deviation. The upper panel is a representative immunoblot of IRF-1 and β-actin. (TS-A T180A/S184A)

wild type IRF-1 was found to have a half life of approximately 35-37 minutes, (figure 5.4) this is close to the other half lives reported in the literature (Pion *et al.* 2009). Wild type IRF-1 stability in HEK293 cells is almost identical (not shown). All three alanine substitution mutants exhibited slower turnover, with half lives in the range of 50-60 minutes. The half life of the double TS-A mutant was greater than the half life of the individual T180A and S184A. This data is consistent in the HEK293 cell line and the H3396 –IRF-1 Tet Off cell lines (data not shown). Conversely, the two phosphomimetic mutants of IRF-1 (T180D and S184E) were less stable then wild type IRF-1, with a reduced half life of 20-25 minutes (figure 5.5). Both phosphomimetic mutants were also less stable in HEK293 cells (data not shown).

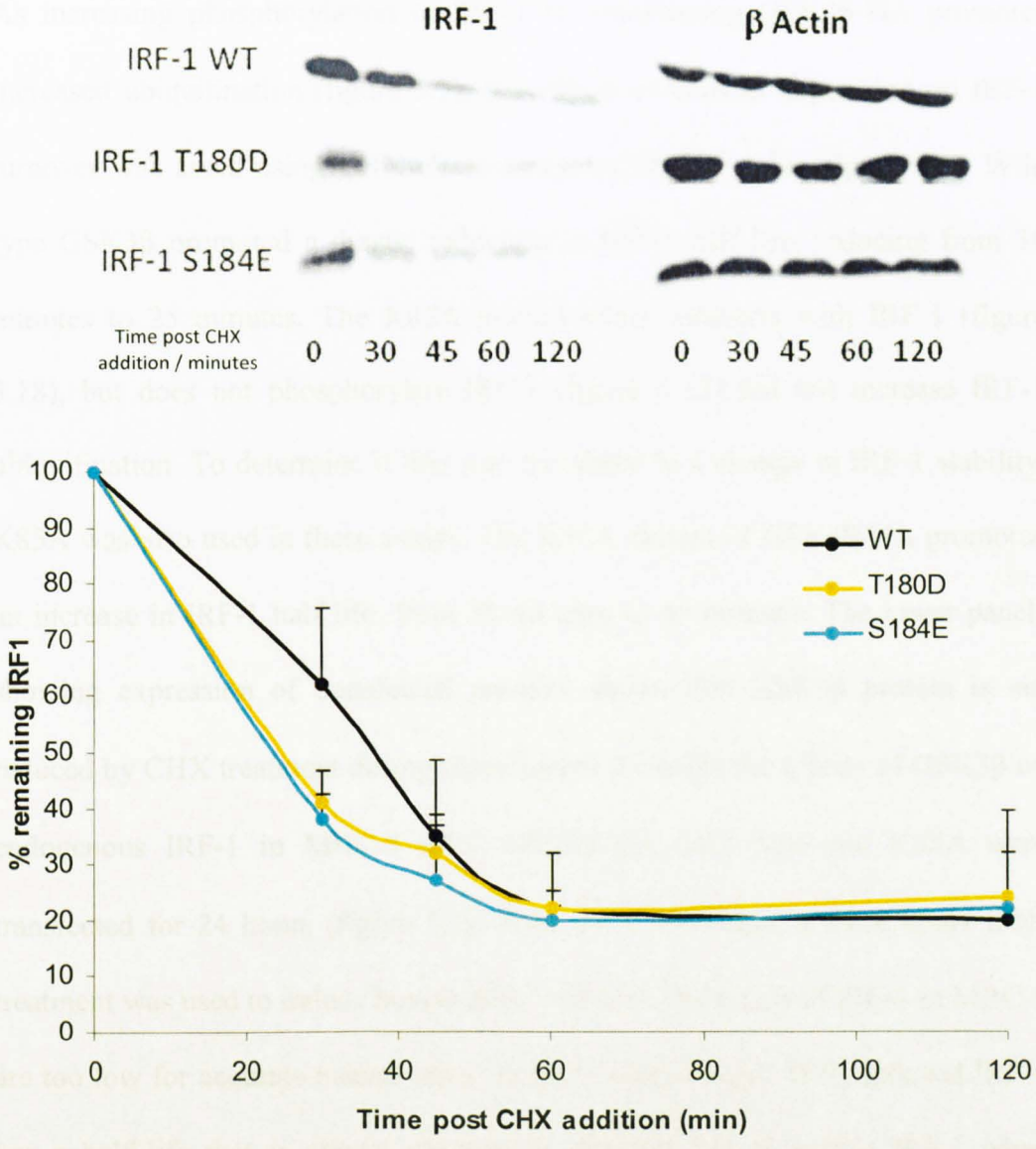

Figure 5.5 IRF-1 phospho-mimic mutants exhibit decreased stability. CHX assays were performed on MRC-5 cells transfected with 4 μg of IRF-1. Cells were treated with 2.5 μg/mL CHX for the indicated time points. Protein lysates (15 μg) were immunoblotted with IRF-1 M20 and β-Actin. IRF-1 protein was divided by β-Actin protein to correct for protein loading. Data is expressed as a precentage of the 0 minute timepoint. Data is from three independent experiments with each set of extracts being immunoblotted in duplicate. Error bars denote standard deviation. The upper panel shows representative immunoblots of IRF-1 and β-Actin.

5.6. GSK3β regulates IRF-1 stability

As increasing phosphorylation of IRF-1 by transfecting GSK3β-HA promotes increased ubiquitination (figure 5.2), the effects of GSK3β expression on IRF-1 turnover was assed using CHX chase assays in MRC-5 cells (figure 5.6). Wild type GSK3β promoted a drastic reduction in IRF-1 half life, reducing from 30 minutes to 25 minutes. The K85A mutant which interacts with IRF-1 (figure 3.18), but does not phosphorylate IRF-1 (figure 3.13) did not increase IRF-1 ubiquitination. To determine if this was translated to a change in IRF-1 stability, K85A was also used in these assays. The K85A mutant of GSK3β-HA promoted an increase in IRF-1 half life, from 30 minutes to 60 minutes. The lower panels showing expression of transfected proteins shows that GSK3β protein is not reduced by CHX treatment during these assays. To study the effects of GSK3β on endogenous IRF-1 in MRC-5 cells, GSK3β-HA wild type and K85A were transfected for 24 hours (figure 5.7). Prior the CHX chase, a three hours IFNγ treatment was used to induce human IRF-1 protein. The levels of IRF-1 in MRC-5 are too low for accurate measurement in CHX chase assays. IFNγ induced IRF-1 has a half life that is almost identical to the half life of mouse IRF-1 when expressed in MRC-5 cells. Wild type GSK3β promoted a very small decrease in IRF-1 stability, with a decrease of 5 minutes in half life. The K85A mutant of GSK3β increased IRF-1 half life by over 10 minutes. Neither the endogenous (lower) or exogenous (upper) GSK3β protein expression were altered by CHX addition.

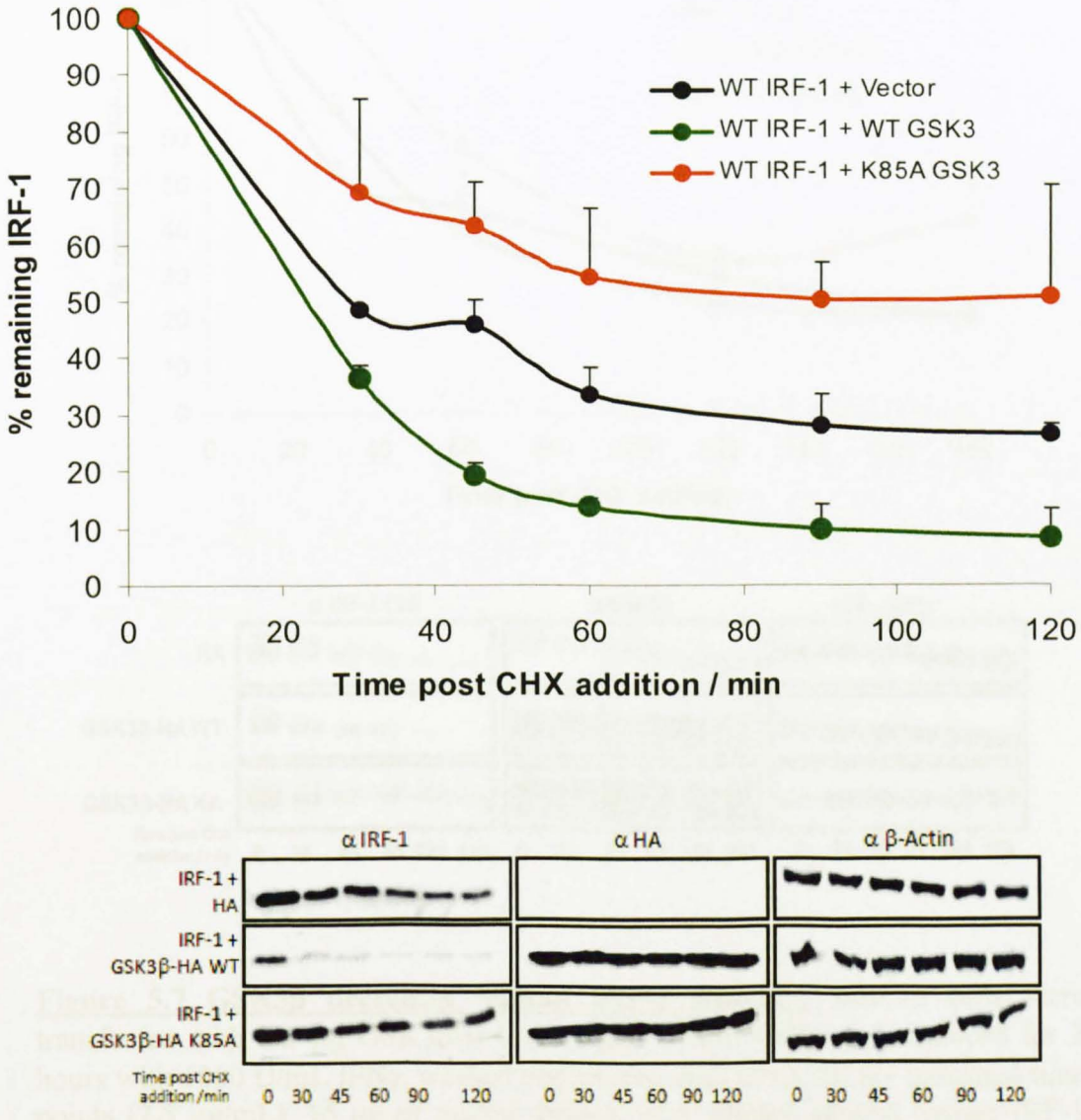

Figure 5.6 GSK3β decreases IRF-1 stability. CHX assays were performed on HEK293 cells transfected with 2.5 μg GSK3β and 2.5 μg IRF-1. Cells were treated with 2.5 μg/mL CHX for the indicated time points. Protein lysates (15 μg) were immunoblotted with IRF-1 M20, HA and β-actin. IRF-1 protein was divided by β-actin protein to correct for protein loading. Data is expressed as a precentage of the 0 minute time point. Data is from three independent experiments with each set of extracts being immunoblotted in duplicate. Error bars denote standard deviation. The lower panel shows representative immunoblots of IRF-1, HA and β-actin.

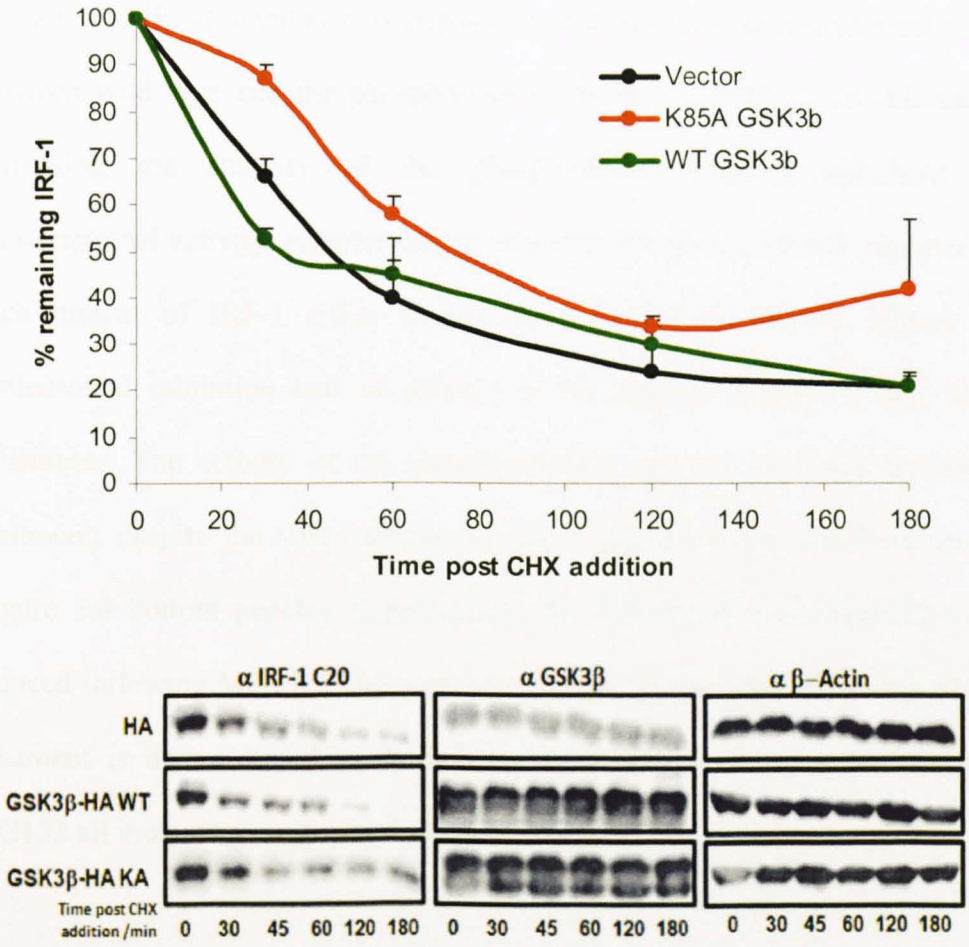

Figure 5.7 GSK3β decreases human IRF-1 stability. MRC-5 cells were transfected with 2.5 μg GSK3β-HA or empty vector. Cells were induced for 3 hours with 1000 U/mL IFNγ, washed and treated with CHX for the indicated time points (2.5 μg/mL). 15 μg of protein lysates were blotted against human IRF-1 (C20), GSK3β and β-actin. Data was calculated as for figure 5.4 onwards. Lower panels, representative immunoblots of IRF-1, GSK3β and β-actin. The 45 minutes time point is not plotted on the graph. Error bars denote standard deviation.

5.7 MG132 inhibits IRF-1 transcriptional activity on the TRAIL promoter

Variation in IRF-1 stability may explain the differences in transcriptional activity between wild type and the phosphorylation mutants of IRF-1. To determine if increasing the stability of the phosphomimic mutants enhanced their transcriptional activity, reporter assays were carried out on TRAIL reporter with each mutant of IRF-1 either treated with DMSO or MG132 (figure 5.8). Proteasomal inhibition had no effect on the activity of any of the alanine substitutes. The activity of the phosphomimics was not increased by MG132 treatment; despite the vast increase in IRF-1 protein levels for these mutants (figure 5.8 bottom panels). Significantly, the activity of wild type IRF-1 was reduced following MG132. The increase in protein expression following MG132 treatment is demonstrated in the western blot below, showing that following MG132 all mutants are expressed at equal levels.

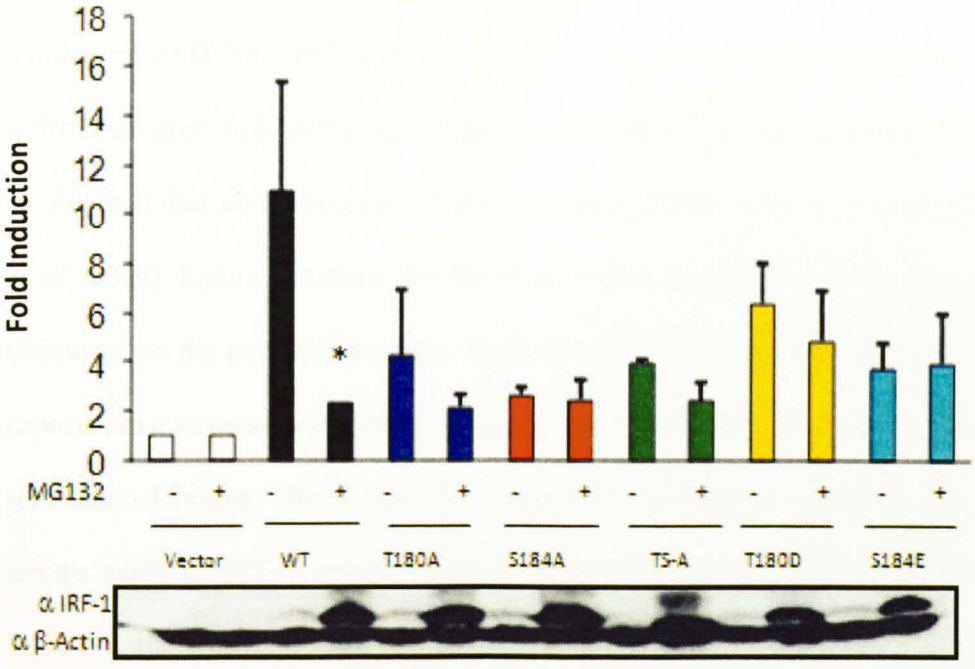

Figure 5.8 MG132 inhibits IRF-1 transcriptional activity. Cos7 cells were transfected with 5 ng βGAL control plasmid, 50 ng IRF-1 and 150 ng TRAIL promoter reporter for 48 hours. 16 hours prior to reporter assay cells were treated with 10 μM MG132 or DMSO (0.01%). Results are expressed as fold induction compared to empty vector transfection for each treatment. Data is from three independent experiments carried out in triplicate. Error bars denote standard error. * signifies significant difference as determine by Students t-test ($p<0.05$). Lower panel immunoblot of IRF-1 (M20) and β-actin from parallel transfected wells. Each lane contains total protein lysates from a single well. (TS-A T180A/S184A).

5.8 Prediction of potential ubiquitin acceptor lysine

To determine if the stability of IRF-1 was important for its transcriptional activity a different approach to the use of proteasome inhibitors was pursued. It has been established that ubiquitination of IRF-1 predominantly leads to degradation (Pion *et al.* 2009). Lysine residues are the major amino acid that can be conjugated to ubiquitin, so the potential acceptor Lys residues were mapped on IRF-1. Previous reports have suggested that IRF-1 degradation occurs through residues in the far C terminus of human IRF-1. The first report by Nakagawa suggested the last 39 amino acids of IRF-1 are required for degradation (Nakagawa and Yokosawa 2000). Later Kim and co-workers suggested that Lys^{275} and Lys^{299} were major ubiquitin acceptor residues. SUMO-1ylation also occurs on these residues and it was noted that SUMO-1ylation of IRF-1 increases the protein half life (Park *et al.* 2007). Work on a series of splicing mutants of human IRF-1 also suggested that the stability of IRF-1 is controlled via the C terminus (Lee *et al.* 2006). To help predict which lysine may be ubiquitinated, two prediction programmes were used, with the amino acid sequences of human and mouse IRF-1 being submitted to the UniPred and UbPred programmes (figure 5.9) only the Lys that are conserved between human and mouse IRF-1 are shown.

A.

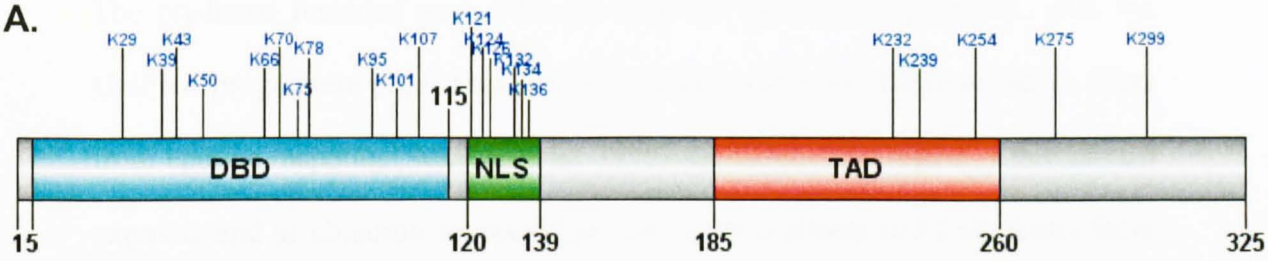

B.

		LYSINE	UniPred	UbPred	Surface Exposed?
DBD	29	IWINKEEMI	NO	NO	NO
	39	QIPWKHAAK	YES	NO	NO
	43	KHAAKHGWD	NO	NO	NO
	50	WDINKDACL	NO	NO	NO
	66	TGRYKAGEK	YES	NO	NO
	70	KAGEKEPDP	YES	NO	NO
	75	EPDPKTWKA	YES	NO	NO
	78	PKTWKANFR	YES	NO	NO
	95	IEEVKDQSR	YES	YES	NO
	101	QSRNKGSSA	YES	NO	NO
NLS	121	RNQRKERKS	NO	NO	YES
	124	RKERKSKSS	NO	NO	YES
	126	ERKSKSSRD	NO	NO	YES
	132	SRDTKSKTK	NO	NO	NO
	134	DTKSKTKRK	NO	NO	NO
	136	KSKTKRKLC	NO	NO	NO
	138	KTKRKLCGD	NO	NO	NO
TAD	232 (233)	DEEGKLPED	YES	YES	YES
	239 (240)	EDIHKLLEQ	YES	YES	YES
	254 (255)	NVDGKGYLL	NO	YES	YES
	275 (276)	DFSCKEEPE	NO*	YES	NO
	299 (300)	FTDLKMNDA	NO	NO	NO

Figure 5.9 Prediction of potential ubiquitin acceptor lysines in IRF-1. A. Schematic diagram of human IRF-1 and its major domains. Location of individual lysine residues is indicated. B) Two ubiquitination prediction programmes (UniPred and UbPred) were used to predict potential Ubq acceptor residues. Only lysine residues which are conserved between human and mouse IRF-1 are illustrated. Indicated Lys residues are highlight in pink. Surface exposure data was from experiments with mouse IRF-1 carried out in Schaper *et al.* 2000. Amino acids in bracket represent the position in murine IRF-1.

The predicted residues were different between the two programmes, with the UniPred programme predicting several residues within the DBD of IRF-1. Data from epitope mapping (Schaper *et al.* 1998) shows that this region is not solvent exposed, and as ubiquitin acceptor Lys need to be available to E2 enzymes, these residues were discounted. Additionally crystal structure data for the IRF-1 DBD also suggested that these residues are all buried in DNA bound mouse IRF-1 (Escalante *et al.* 1998). Neither programmes detected Lys within the NLS of IRF-1, although several Lys residues in this region are known to be solvent exposed. Several predictions were made in the C terminus, which has already been shown to be important for IRF-1 ubiquitination (Nakagawa and Yokosawa 2000). The five C terminal Lys were studies further, with each residue being substituted for arginine, which is structurally and chemically similar to lysine, but cannot undergo ubiquitination (figure 5.10).

5.10. lysine-arginine mutants used in this study. Amino acid sequence of murine IRF-1, with lysine residues indicated in bold. Where lysine residues are substituted for Arg the residue is indicated as a red R.

5.9 Mapping of potential Lys Ubq acceptor residues

Each FLAG-IRF-1 K→R mutant was expressed in HEK293 cells (figure 5.11A). All of the K→R mutants of IRF-1 migrated at 50 kDa. No K→R mutant was found to express at higher levels than wild type IRF-1. When treated with MG132 all of the mutants increased at the protein level. This indicated that all of the K→R mutants were undergoing proteasomal degradation. In addition high molecular weight conjugates of IRF-1 could be detected in MG132 treated cell extracts, these bands could potentially be poly-ubiquitinated IRF-1 (figure 5.11B). The two double mutants (K240/255R and K276/300R) were also not expressed at higher levels than wild type IRF-1, and like the single mutants were sensitive to MG132 and exhibited poly-ubiquitination. To confirm the addition of ubiquitin to each of these K→R mutants, *in vivo* ubiquitination assays were performed (figure 5.12). With the exception of K240R and K255R, all of the K→R mutants exhibited similar levels of ubiquitin incorporation to wild type IRF-1. Ubiquitination appeared to be slightly lower in the K276R mutant; however inputs show that the HA-Ubq was not as highly expressed in those extracts. Next CHX chases in HEK293 cells were performed to determine if the half life of each mutant was affected (figure 5.13). Neither the K300R nor K276R exhibited any change in half life. A small increase in half life was observed in the K233R mutant, while a doubling of half life was observed in the K240R and K255R. This data agrees with figure 5.12 and suggest that while they are not the sole acceptor residues, K240 and K255 are important residues for IRF-1 ubiquitination and degradation. Many substrates are ubiquitinated on multiple residues rather than relying on a single Lys acceptor. To determine if this was the case; the double mutants were subjected the CHX chase (figure 5.14). An increase in half life was

observed in the K276/K300R mutant, although not a very large increase. Joint substitution of K240 and K255 to Arg did not produce any further increase in half life compared to the K240R and K255R single mutants. A triple (K300/276/255R) and quadruple (K300/276/255/240) mutant of IRF-1 was produced. Surprisingly these mutants had a significantly decreased half life compared to wild type IRF-1. It is possible that these substitutions promote misfolding of IRF-1 and cause destruction of the protein. The 3KR and 4KR mutants were also sensitive to MG132 and underwent *in vivo* ubiquitination (data not shown).

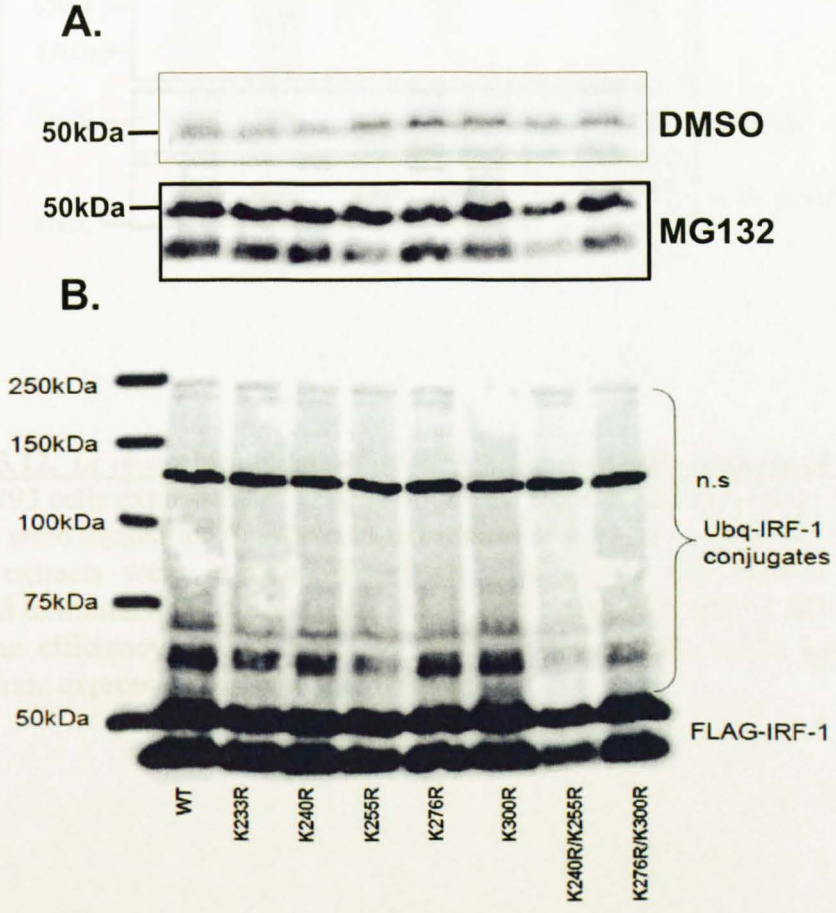

Figure 5.11. IRF-1 K-R substitution mutants expression in HEK293 cells. A) Each mutant was expressed in HEK293 cells (2.5 µg/plate) for 48 hours. Prior to lysis cells were treated with DMSO or 10 µM MG132 for 6 hours. 10 µg of protein extract was subjected to immunoblot with FLAG Ab. B) Longer exposure of MG132 treated extracts reveals the presence of poly-Ubq IRF-1 conjugates.

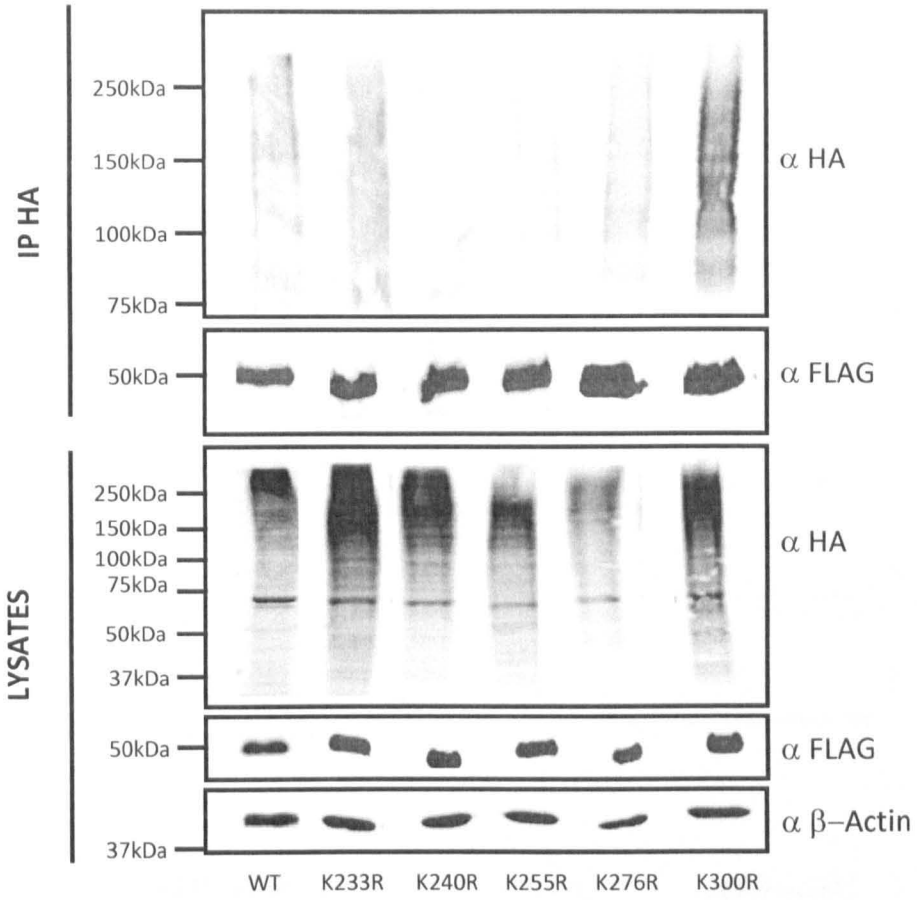

Figure 5.12. *In vivo* ubiquitination of K→R substitution mutants of IRF-1. HEK293 cells expressing FLAG-IRF-1 K→R mutants and HA-Ubq (2.5 μg of each) were treated for 6 hours with 10 μM MG132 prior to lysis. 0.5 mg of protein extracts were immunoprecipitated with FLAG Ab, Eluates were subjected to immunoblot with HA Ab. Blots were re-probed with FLAG Ab to determine efficiency of IRF-1 IP by FLAG. Lower panels (10% Lysates) demonstrate expression of transfected proteins.

A.

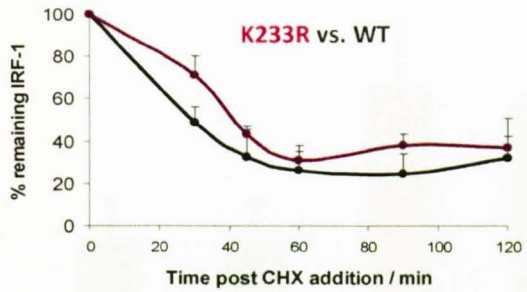

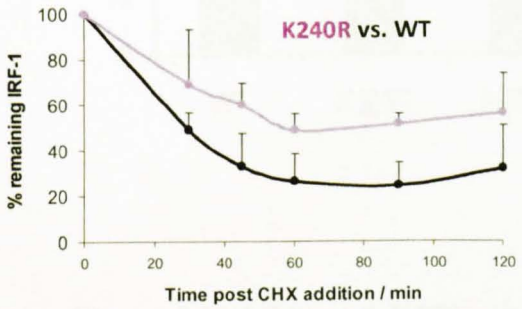

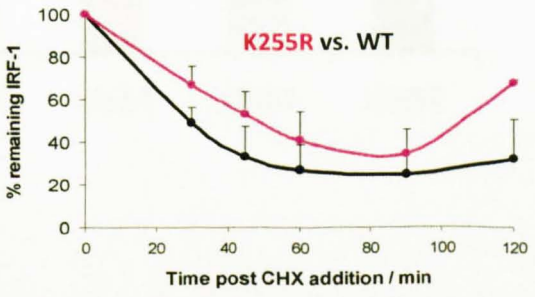

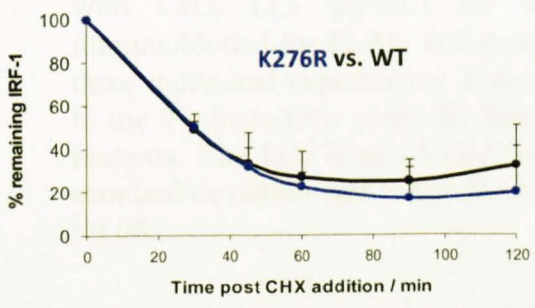

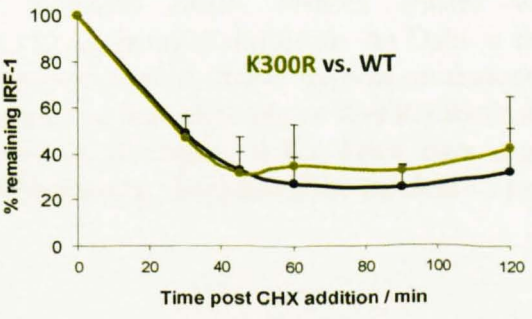

B.

See next page for figure legend.

C.

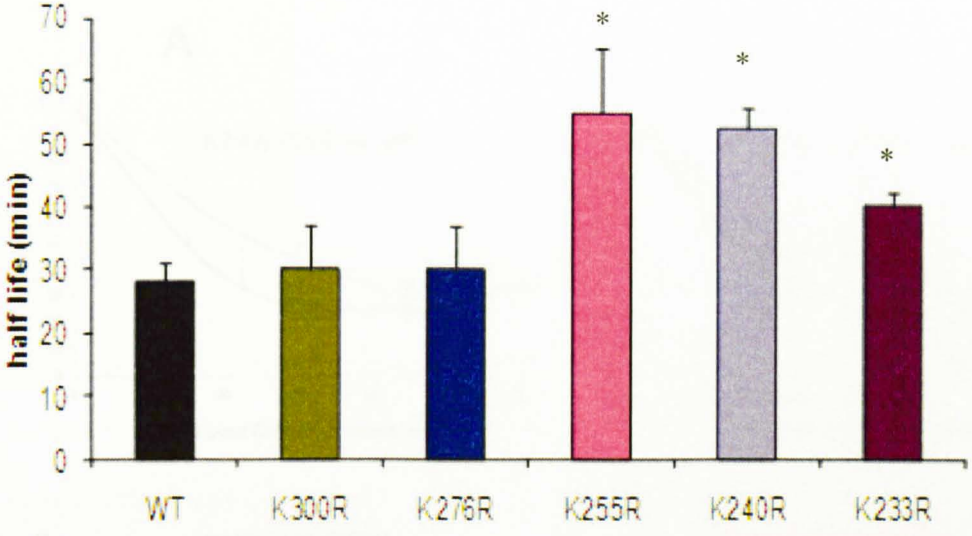

Figure 5.13 K240 and K255 are important for IRF-1 stability. HEK293 cells transfected with 2.5 µg of FLAG-IRF-1 wild type and K→R mutants were chased with CHX (2.5 µg-mL) for the indicated times. Protein lysates were immunoblotted for FLAG and β-actin (10 µg/lane) in duplicate. **A)** Data is from three individual experiments. Data is expressed as % IRF-1 expression compared to the 0 minute time point. **B)** Representative immunoblots of K→R substitution mutants. The half lives of each mutant are indicated in **C).** Error bars denote standard deviation and * significant difference as determined by Students-t test $p < 0.05$.

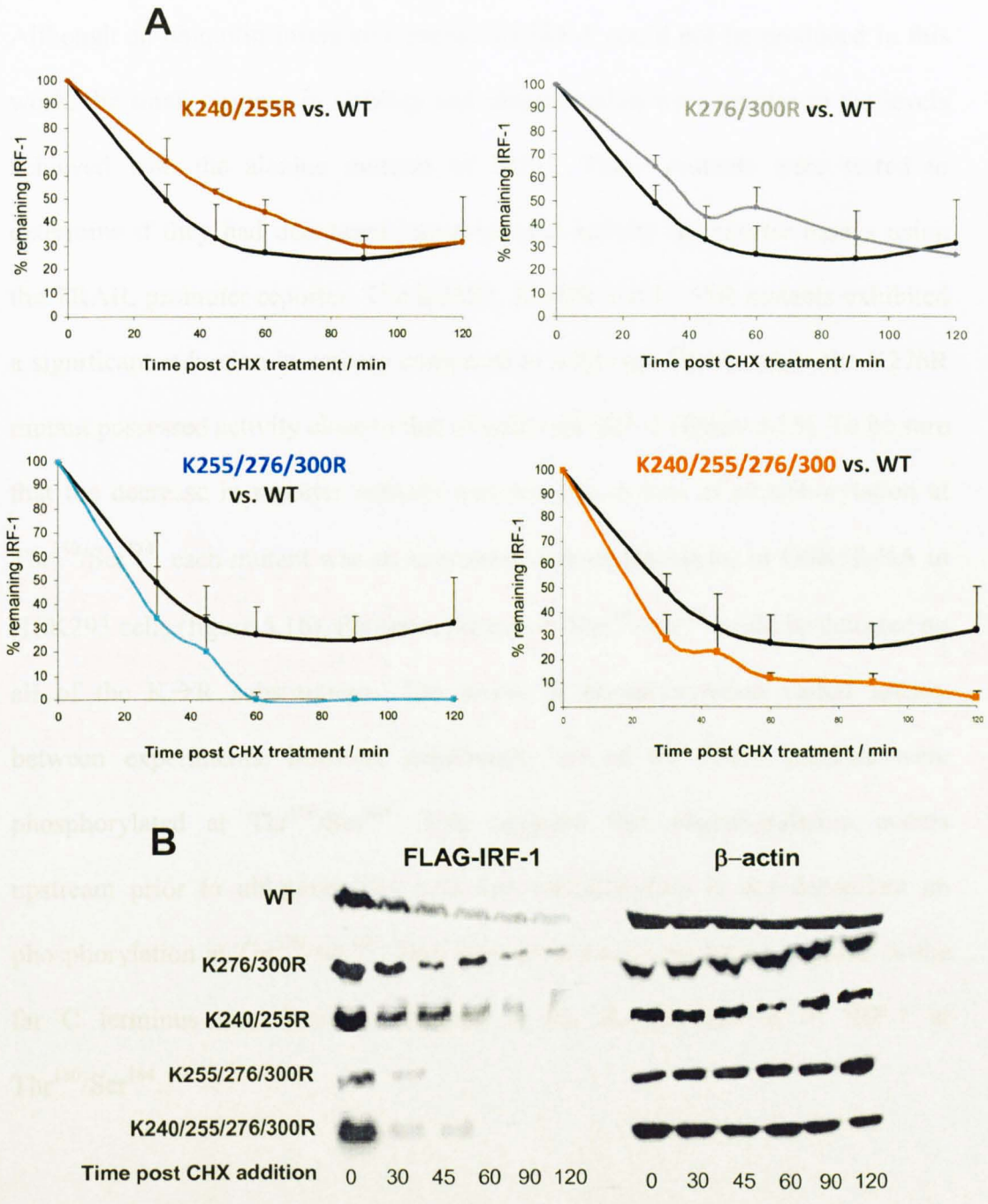

Figure 5.14 Multiple K→R substitutions do not increase IRF-1 stability. HEK293 cells transfected with 2.5 µg of FLAG-IRF-1 WT and KR mutants were chased with CHX (2.5 µg-mL) for the indicated times. Protein lysates were immunoblotted for FLAG and β-Actin (10 µg/lane) in duplicate. Data is from three individual experiments. Data is expressed as % IRF-1 expression compared to the 0 minute time point. B) Representative immunoblots of K→R substitution mutants.

5.10. Full ubiquitination of IRF-1 is needed for transcriptional activity.

Although an ubiquitin insensitive mutant of IRF-1 could not be produced in this work, the small changes in stability and ubiquitination were similar to the levels achieved with the alanine mutants of IRF-1. These mutants were tested to determine if they had decreased transcriptional activity in reporter assays using the TRAIL promoter reporter. The K233R, K240R and K255R mutants exhibited a significant reduction in activity compared to wild type IRF-1, while the K276R mutant possessed activity close to that of wild type IRF-1 (figure 5.15). To be sure that the decrease in reporter activity was not due to loss of phosphorylation at Thr^{180}/Ser^{184}, each mutant was co-expressed with empty vector or GSK3β-HA in HEK293 cells (figure 5.16). Phosphorylation on Thr^{180}/Ser^{184} could be detected on all of the K→R substitutions. The levels of phosphorylation varied greatly between experiments, however consistently all of the K→R mutants were phosphorylated at Thr^{180}/Ser^{184}. This suggests that phosphorylation occurs upstream prior to ubiquitination, and that ubiquitination is not dependent on phosphorylation at Thr^{180}/Ser^{184}. However the status of the lysine residues in the far C terminus may have an impact on the phosphorylation of IRF-1 at Thr^{180}/Ser^{184}.

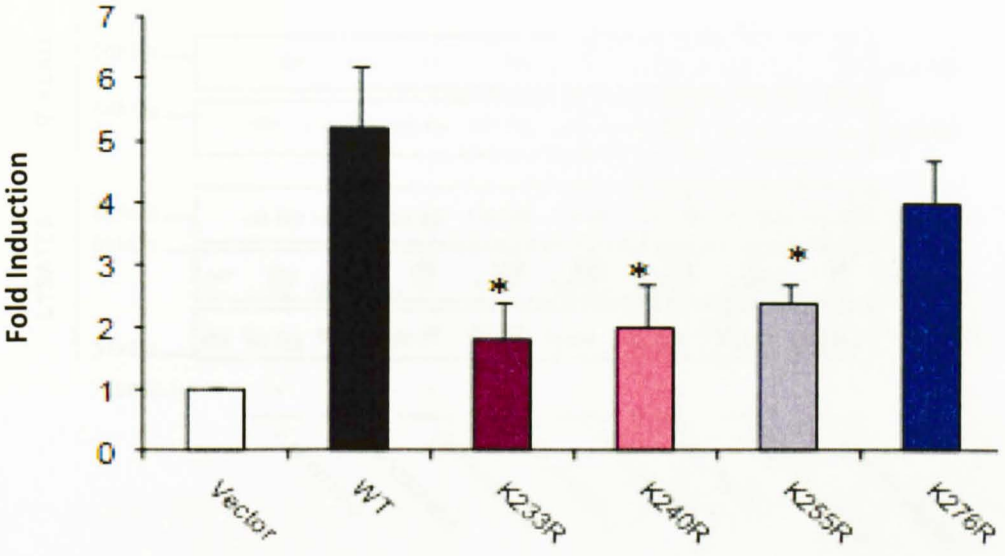

Figure 5.15 Reduced ubiquitination of IRF-1 decreases transcriptional activity. TRAIL reporter assays were carried out in Cos-7 cells transfected with 50 ng FLAG-IRF-1, 75 ng TRAIL reporter promoter and 5 ng βGAL control plasmid. Transfections were carried out for 48 hours. Data is shown as a fold increase in reporter activity compared to empty vector transfected cells. Data is from three independent experiments carried out in triplicate. Error bars denote standard deviation and * denotes statistical significance determined by Student t-test $p>0.05$.

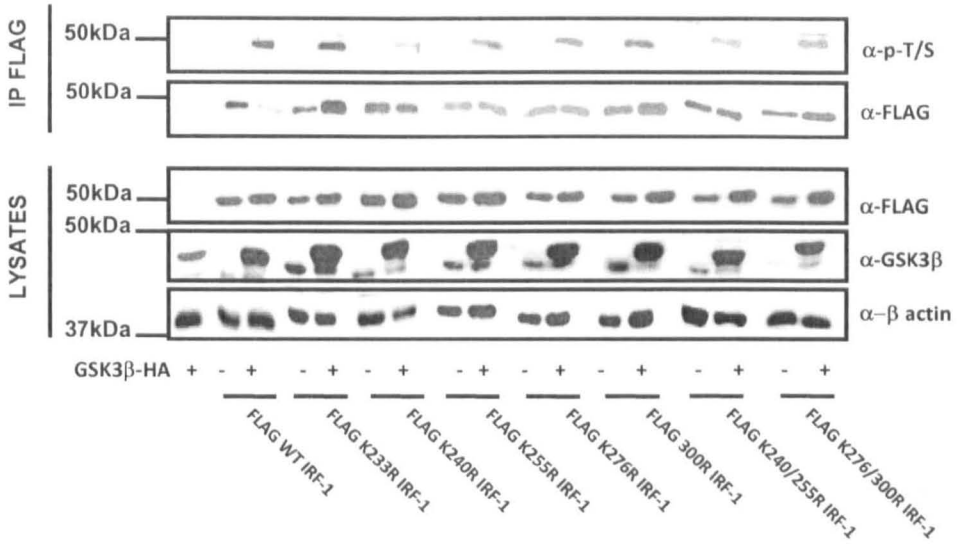

Figure 5.16 K→R mutants of IRF-1 are phosphorylated at Thr^{180}/Ser^{184} in response to GSK3β expression. HEK293 cells were transfected with 5 μg of FLAG-IRF-1 and GSK3β-HA or empty vector for 48 hours. Protein lysates (1 mg) were immunoprecipitated with FLAG Ab and immunoblotted with p-T/S Ab. Blots were stripped and re-probed with FLAG Ab to confirm the presence of IRF-1. Lower panels (5% lysates) demonstrate expression of transfected proteins.

5.11 Discussion

A positive interaction between mouse IRF-1 and human ubiquitin was shown by co-immunoprecipitation (figure 5.1). The interaction only occurred in the presence of MG132 suggesting that this modification quickly promotes degradation. No mono or multi-mono ubiquitination could be detected; rather the poly-ubiquitination was uniform. As such it can be assumed, that like human IRF-1, mouse IRF-1 is primarily poly-ubiquitinated and this ubiquitination promotes degradation through the proteasome. Studies by Pion *et al.* used a mutant of ubiquitin which cannot undergo linkages through its K^{48} residue. A significant loss of ubiquitination was detected when this mutant was used, however some ubiquitination remained. Other chain types such as Lys^{27} have been identified as degradation promoting chains (Komander 2009). Ubiquitin mutants are available in which each potential Lys is mutated to Arg, in addition to mutants that only contain a single ubiquitin conjugating lysine. Use of these mutants would help to discriminate which chain type(s) are most prevalent in IRF-1 ubiquitination. In addition further understanding of the types of ubiquitination occurring would help in the identification of the E3 ligases responsible and the possible effects of the modification of IRF-1 activity. The lack of any detectable ubiquitination in cells with active proteasome suggests that ubiquitin does not play a role in IRF-1 activity that is independent of degradation. Alternatively, such as in the case of SRC-3, monoubiquitination which serves to promote protein-protein interaction is a short lived modification which initiates poly-ubiquitination and therefore destruction (Wu *et al.* 2007). As such mono ubiquitination that is independent of degradation of IRF-1 may be an extremely short lived modification. It is also possible that other non degradative ubiquitin chain types are added to IRF-1, but

are either not highly abundant, or are removed by DUB enzymes making their identification difficult. Particular stimuli may also be needed to promote non degradative ubiquitination of IRF-1 such as viral infection. IRF-1 has not been shown to contain a functional nuclear export signal (NES), and prediction programmes (NetNES1.1) failed to detect a leucine rich NES in either human or mouse IRF-1. It is therefore likely that IRF-1 is imported into the nucleus and degraded by the proteasome in the same compartment.

Although produced from strong viral promoter (CMV) small differences in the protein levels of the alanine and phosphomimic mutants could be detected when lower levels of plasmid were transfected (data not shown). This led to the supposition that Thr^{180} and Ser^{184} may regulate IRF-1 stability through ubiquitination. The considerable precedence in the literature supported a role for GSK3β dependent phosphorylation in ubiquitination (Xu *et al.* 2009a) prompting the study of ubiquitination of the phosphorylation mutants used in this study. As for the wild type IRF-1 no ubiquitination could be detected on any of the mutants without MG132 treatment (not shown). All of the mutants were stabilised by MG132 treatment suggesting a common route of degradation for all of these proteins (figure5.2). The levels of ubiquitination on the alanine mutants were significantly decreased in comparison to wild type IRF-1 in which ubiquitination could be robustly detected. The levels of ubiquitination for the alanine mutant varied from no HA-Ubq incorporation, to 50% of wild type. The total amount of IRF-1 immunoprecipitated in these assays was similar between different mutants showing that the proportion of HA-Ubq-IRF-1 was dependent on the status of Thr^{180} and Ser^{184}. Ser^{184} behaved similarly to Thr^{180} in these assays, as it also does in the reporter assays from chapter four (figure 4.2). In figure 5.3 the TS-A mutant

does not appear to be ubiquitinated at all, although the amount of HA-Ubq in those extracts was less. Generally, the TS-A mutant was ubiquitinated to the same extent as the individual Thr^{180} and Ser^{184} mutants. HA-Ubq was used in these assays as endogenous Ubq is a highly abundant protein, and determining changes in substrate ubiquitination is more problematic. This approach enables the amount of ubiquitin in the cell to be controlled with only the incorporation of HA-Ubq being studied.

In contrast to the alanine mutants, the acidic mutants exhibited HA-ubiquitin incorporation that was similar or greater than wild type (figure 5.2). This inferred that charge on Thr^{180} and Ser^{184} are promoting ubiquitination of IRF-1, as such IRF-1 is likely to be a phosphorylation dependent ubiquitination substrate. To determine if GSK3β dependent phosphorylation was responsible for the increased ubiquitination, wild type and K85A GSK3β were co-transfected in ubiquitination assays with wild type IRF-1. The level of ubiquitination of wild type IRF-1 was increased when wild type GSK3β was co-expressed (figure 5.3). As over-expression of GSK3β promotes an increase in phosphorylation of IRF-1 on Thr^{180} it is likely that this promotes the enhanced ubiquitination. To be sure that this increase was not caused by the interaction with GSK3β rather than the phosphorylation, the K85A mutant was used. Kinase inactive GSK3β was not able to promote an increase in IRF-1 ubiquitination, and sometimes promoted a decrease in ubiquitination. As the kinase inactive mutant of GSK3β does not induce phosphorylation of IRF-1, it could be assumed from this data that phosphorylation, particularly through Thr^{180} is important for ubiquitination.

The relationship between ubiquitination and stability of IRF-1 was confirmed by CHX chases, which enabled monitoring of the half lives of the various IRF-1 mutants. The alanine mutants exhibit decreased ubiquitination and posses longer half lives than wild type (figure 5.5). The TS-A mutant was found to be more stable than the individual mutants in CHX chases carried out HEK293 (not shown) and MRC-5 cells. The reason for the discrepancy is not known as the TS-A mutant was not less ubiquitinated than either single mutant alone. The acidic phosphomimetic mutants demonstrated a clear reduction in stability which was also consistent with their enhanced ubiquitination (figure 5.6). Therefore addition of negative charge on Thr^{180} and Ser^{184} promotes enhanced ubiquitination and turnover of IRF-1.

Collating data from chapter four and this chapter suggested that GSK3β is required for IRF-1 transcriptional activity, but does not increase IRF-1 activity when over-expressed (figure 4.6). However endogenous GSK3β is needed for IRF-1 transcriptional activity as knockdown in MRC-5 cells reduced reporter activity by ~50% (figure 4.4). The alanine substitution mutants of IRF-1 display reduced activity, but increased stability, the K85A mutant of GSK3β -HA provokes a dose dependent reduction in TRAIL reporter activity while it increases IRF-1 half life in CHX assays and does not promote ubiquitination. The phosphomimic mutants of IRF-1 are less transcriptionally active, but are also far less stable, and are more ubiquitinated. Together, this suggests there may be a link between IRF-1 activity and stability. The proteasome is composed of numerous subunits (1.1.7) making a knockdown approach more problematic, however chemical inhibition of the proteasome was possible through the use of MG132. Numerous prior studies have shown that TFs that require proteasome dependent

turnover for activity exhibit reduced reporter activity when cells are treated with MG132. Most of these examples include nuclear receptors including RARα (Retinoic acid receptor α), PR (Progesterone Receptor), AR (Androgen Receptor) and ERα (Estrogen Receptor α), MR (Mineralocorticoid Receptor), RARγ (Retinoid acid Receptor γ) (Gianni *et al.* 2002, Lin *et al.* 2002, Andela and Rosier 2004, Dennis *et al.* 2005 and Tirard *et al.* 2007). The reporter activity was not increased by MG132 in any of the mutants tested, nor was there any change in basal TRAIL promoter activity. The activity of wild type IRF-1 was reduced significantly by MG132 treatment. Western blots of the protein lysates used in the reporter assays show a large increase in protein level for all of the IRF-1 constructs. The amount of reporter plasmid was increased in these experiments to prevent any saturation. Previous experiments have shown that increased concentration of IRF-1 in cells does not lead to a reduction in TRAIL reporter activity, rather the reporter activity plateaus (data not shown). Additionally, much higher levels of human IRF-1 are induced in cells treated with IFNγ or IFNγ + retinoids, but this does not induce an inhibition of TRAIL promoter. High levels of IRF-1 protein are needed to promote a detectable increase in TRAIL mRNA (Clarke *et al.* 2004). This suggests that the decrease in activity is not caused by inhibition of the promoter construct by excess IRF-1. Instead other mechanisms must be responsible for the lack of activity of the stable IRF-1. The levels of βGAL (the transfection internal control) were not significantly altered in the MG132 treated cells confirming a specific effect on transcriptional activity of IRF-1.

A lack of increase in reporter activity in the two phosphomimetic mutants of IRF-1 after MG132 treatment suggests that constitutive phosphorylation or negative charge results in other modifications or changes to IRF-1 which inhibits activity on promoter. Alternatively other modifications that already exist independently of phosphorylation on transcriptionally active IRF-1 inhibit activity when not turned over.

Treatment of cells with MG132 to block the proteasome is highly effective; however, MG132 treatment also activates c-Jun N terminal kinase pathway, and represses NFκB activation, in addition to numerous bystander effects caused by blocking the cells major route of protein destruction. MG132 can consequently initiate cell stress responses which may impact on the ability of IRF-1 to bring about transcription. A more fine tuned approach was used in which mutants of IRF-1 lacking ubiquitin acceptor lysine residues were assayed for their transcriptional activity. While MG132 does not inhibit ubiquitination of IRF-1, it does prevent the degradation, therefore this approach monitored the effects of ubiquitination on IRF-1 activity rather than the effects of degradation.

Prediction of ubiquitin acceptor Lys residues is particularly difficult due to the lack of a strong ubiquitin consensus sequence (Tung and Ho 2008). The reason for this is not fully understood. It is possible that individual ubiquitin E3 ligases each have their lysine preference given the number of E3 ligases in the human genome (up to 600) and the potential for multiple E3 ligases to act on a single substrate this poses many complications. Working from previous biochemical analysis that suggested that IRF-1 degradation predominantly occurred via the far C terminus

of IRF-1 and likely involved K276 and K300 (K275 and K299 in human IRF-1) five residues clustered in the C terminus were studied.

None of the five lysine residues were found to be essential for ubiquitination as substitution of Lys to Arg did not result in a stabilisation. This may suggest that IRF-1 can be ubiquitinated on multiple residues, with other Lys residues substituting when others are made unavailable. Occasionally proteins can be degraded through addition of ubiquitin to an N terminal amino acid that is not a Lys (the N end rule); also rarely ubiquitin has been shown to attach to cysteine residues (Williams *et al.* 2007). However, Lys^{240} and Lys^{255} may be important for ubiquitination as K→R mutants of each resulted in an increase in stability in CHX chase assays, and a decrease in HA-ubq conjugation. However neither protein was completely stable, they were sensitive to MG132 treatment, and high molecular weight conjugates could be detected by western blot in cell extracts treated with MG132, but not DMSO. Together this suggests that loss of Lys^{240} and Lys^{255} does not produce an ubiquitination insensitive species of IRF-1. Multiple mutations also did not yield an insentivive mutant; rather they may have adversely effected the folding of IRF-1 protein. Secondary structure prediction was carried out to determine if any large predicted shifts in secondary structure could be caused by the various K→R substitutions. Although small shifts in helix formation were caused by K→R substitutions, the majority of the predicted changes were small (data not shown). Although without more knowledge of the IRF-1 structure we cannot know the effects of these modifications.

Reporter assays using the TRAIL promoter suggested that even small changes in IRF-1 turnover can bring about large decrease in activity. Both the K240R and

K255R IRF-1 exhibited a marked reduction in activity, similar to the reduction in wild type IRF-1 following MG132 treatment. The K276R mutant that was as stable as the wild type was able to transactivate the TRAIL promoter to the same degree as wild type IRF-1, confirming the importance of ubiquitination / stability on IRF-1 activity. Although not tested in this study, it would be of interest to determine if K→R mutants of IRF-1 have dominant negative activity. This may help build a model for IRF-1 transcriptional activity. For example, it is possible that when treated with MG132, IRF-1 is ubiquitinated but not cleared from the promoter, preventing access to new IRF-1 that is ready to initiate the formation of a new pre-initiation complex. Currently we do not have any data supporting a connection between DNA binding and ubiquitination, as such it is only theoretical that IRF-1 is degraded and removed from the promoter following successful DNA binding. Some studies have utilised IRF-1 lacking its C terminus as dominant negative mutants (Boucker *et al.* 2004). It has been noted that a DNA binding mutant of IRF-1 (YLP) has an increased half life compared to wild type IRF-1 (Eckert *et al.* 2006) this supports the model in which IRF-1 is degraded following DNA binding. The DNA binding domain of IRF-1 has been used as a DN mutant in other works (Schaper *et al.* 1998) it is possible that the IRF-1 DBD binds DNA, but cannot be removed because it lacks the degradation inducing Lys residues; however it also lacks the TAD which may explain some of its DN activity. It would be interesting to determine if IRF-1 DBD mutants are able less ubiquitinated than wild type IRF-1.

It has been observed that for some transcription factors, integrity of their TADs is required to promote ubiquitination and degradation (Poukka *et al.* 2000) (Salghetti *et al.* 2000). Thus the transcriptional activation domain marks a protein

for efficient destruction – the so called suicide / Kamikaze transcription factors (Thomas and Tyers 2000). It is therefore of interest that the three major ubiquitin acceptor Lys reside within the IRF-1 TAD (K233, K240 and K255). Therefore there is a possibility that these residues are important for maintaining the structure of the TAD, rather than being acceptors of ubiquitin. Substitution to arginine may alter the structure of the TAD, reducing the transcriptional activity of IRF-1, which in turn reduces the recruitment of ubiquitin E3 ligases, and degradation of IRF-1. It would be interesting to substitute other non Lys residues in the TAD which disrupts its structure and determine if this impacts IRF-1 ubiquitination / turnover. It might be potentially impossible to disconnect cause and effect from IRF-1 activation and destruction.

Variability in IRF-1 phosphorylation at Thr^{180}/Ser^{184} may be partially responsible for the reduced transcriptional activity of the K→R mutants. However, only the K240R mutant is shown to exhibit reduced phosphorylation, and that was not consistent between experiments. It is more likely that all of the K→R mutants are available to GSK3β mediated phosphorylation of Thr^{180}/Ser^{184}. This suggests that phosphorylation is upstream of ubiquitination and that GSK3β dependent phosphorylation of IRF-1 promotes ubiquitination, which leads to proteasome dependent destruction. This turnover of IRF-1 protein is then required for IRF-1 to fully transactivate the TRAIL promoter. In order to link phosphorylation of IRF-1 to its ubiquitination, a potential E3 ligase (SCF^{Fbxw7}) was identified by literature searches. An interaction of this E3 ligase with phosphorylated IRF-1 and whether it could promote IRF-1 ubiquitination was next investigated.

CHAPTER 6

The SCF^{Fbxw7} ubiquitin E3 Ligase links IRF-1 phosphorylation by GSK3β to ubiquitination/degradation.

6.1. Introduction

A number of E3 ligases have been identified that recognise phosphorylated residues, most notably the SCF family of E3 ligases. SCF E3 ligases use variable Fbox proteins for substrate selection. On closer inspection, the phosphorylated motif of IRF-1 constitutes an Fbxw7 phospho-degron. *In vivo* GST pulldown assays demonstrated an interaction between Fbxw7α and Fbxw7β with IRF-1; this was confirmed by co-immunoprecipitation between HA-Fbxw7 and FLAG-IRF-1. An interaction could not be detected between IRF-1 and a truncated form of Fbxw7α which does not have WD40 repeats (ΔWD40). The interaction between IRF-1 and Fbxw7α was reduced in the T180A mutant but increased in the T180D mutant. This suggests that a negative charge on Thr^{180} strengthens the interaction between IRF-1 and Fbxw7α. Finally, when HA-Fbxw7α is over-expressed in HEK293 cells, it accelerated the rate of degradation of IRF-1. The ΔWD40 mutant; that cannot interact with IRF-1, had no significant effect on turnover. In conclusion phosphorylation of Thr^{180} promotes the interaction with the WD40 repeats of Fbxw7α which in turn promotes ubiquitination and degradation of IRF-1.

6.2. Phosphorylation of Thr^{180} produces a Fbxw7 phospho-degron.

Phosphorylation induced degradation of IRF-1 was examined in the previous chapter, although the E3 ligase responsible was not identified. Phosphorylation increases the affinity of substrate towards a group of E3 ligases termed the SCF family (Skowyra *et al.* 1997). A large number of GSK-3 phosphorylated substrates interact with three SCF E3 ligases, these being $SCF^{Fbxw1/\beta TRCP1}$, $SCF^{Fbxl1/Skp2}$ and SCF^{Fbxw7} (Xu *et al.* 2009a). Although the SCF family is quite large, there are the only three Fbox family members that have been well studied. Recognition motifs known as phospho-degrons have been identified for Fbxw1 and Fbxw7, but Fbxl1 does not have a recognisable phospho-degron so Fbxl1 interactions cannot be predicted from amino acid sequences. The consensus sequence for Fbxw1 is D-pS-G-X-X-(X)-pS. This does not match the amino acids surrounding Thr^{180}, although the consensus for Fbxw7 (L-L-pT-P-X-X-D/E/pT/Ps) closely matches. An alignment of the amino acids surrounding Thr^{180} with other validated Fbxw7 phospho-degrons is given in figure 6.1. The Fbxw7 consensus sequence, requiring L-L prior to the phosphorylated Thr is not well conserved among most substrates. There are no other known E3 ligases that interact with this motif; consequently, Fbxw7 was pursued as a potential phosphorylation dependent ubiquitin E3 ligase for IRF-1.

A.

	-2	-1	•	+1	+2	+3	+4	+5	
c-Myc	L	P	T	P	P	L	S	P	Human Fbxw7
c-Jun	G	E	T	P	P	L	S	P	
SREBP-1	T	L	T	P	P	P	S	D	
Cyclin E	L	L	T	P	P	Q	S	G	
Cyclin E	P	C	S	L	I	P	T	P	
SRC-3	V	H	S	P	M	A	S	S	
PGC1α	P	L	T	P	E	S	P	N	
PGC1α	G	L	T	P	P	T	T	P	
NOTCH-1	F	L	T	P	S	P	E	S	
SV40 T	P	P	T	P	P	P	E	P	
Gcn4	L	P	T	P	V	L	E	D	Yeast cdc4
Far1	P	I	S	P	P	P	S	L	
Cdc6	D	V	T	P	E	S	S	P	
Cdc6	P	L	T	P	Y	T	S	P	
Clb6	I	P	S	P	I	S	E	R	
Clb6	N	L	T	P	H	S	T	N	
Rim-1	P	P	T	P	A	K	T	P	
Rcn-1	L	I	S	P	P	A	S	P	
IRF-1 (human)	A	L	T	P	A	L	S	P	
IRF-1 (mouse)	D	I	T	P	A	L	S	P	
Proposed consensus	L	L	T	P	X	X	D/E/ T/S	X	
% degrons containing residue	22	39	72	94	-	-	94	-	

B.

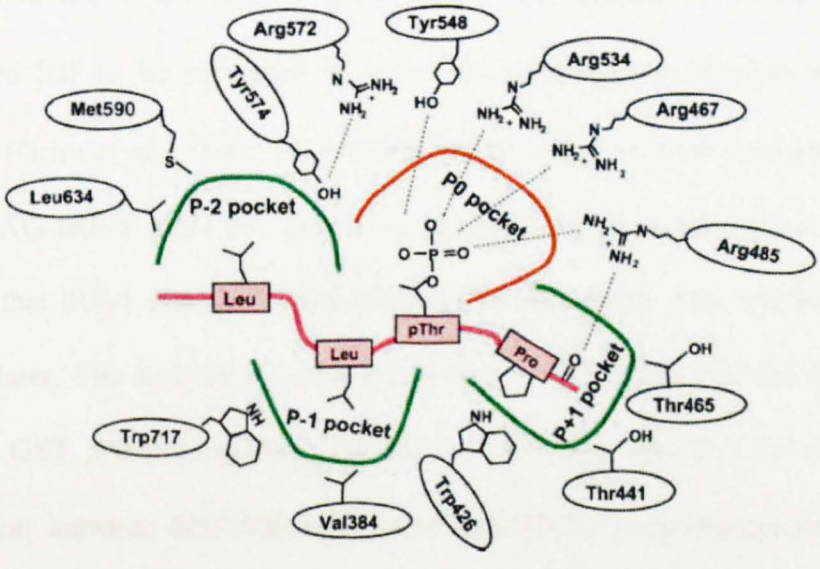

Figure 6.1. Alignment of Fbxw7 phospho-degrons. A) All known Fbxw7 phospho-degrons were aligned against one another. Yeast Fbxw7 (cdc4) substrates are also listed. Substrates of cdc4 which contain multiple sub-optimal phospho-degrons have been omitted. The phosphorylated residues are highlighted in the boxes. The phospho-degron consensus proposed by Orlicky *et al.* 2003 is illustrated, and the precentage of residues which conform to the consensus is shown below. **B)** Diagram of Fbxw7 interaction with a phospho-degron. From Orlicky *et al.* 2003 .

6.3. FLAG-IRF-1 interacts with GST-Fbxw7

To determine if IRF-1 is able to interact with the Fbxw7 subunit of the SCF E3 ligase complex an in *vivo* GST pulldown assay was used. Fbxw7 exists as three isoforms, α, β and γ. The α isoform is the most highly expressed of the three, and is expressed in the nucleus, with the β isoform residing in the cytosol and the γ isoform in the nucleolus (Spruck et al. 2002). IRF-1 is found almost exclusively in the nucleus when over-expressed in HEK293 cells, and has not been shown to be located in nucleoli. However it was decided that all three isoforms would be tested for their interaction with IRF-1. Although very weak; interactions with both the β and γ isoforms were detected (see figure 6.2). The strongest interaction was with the α isoform. This was as expected as the α isoform and IRF-1 are found in the same cell compartment. The β and γ isoform were also expressed at slightly lower levels than the α isoform. In other reports the amount of β and γ plasmid expressed has to be increased to allow for equivalent expression with the α isoform (Grim *et al.* 2008). It is of interest that the β isoform interacted weakly with FLAG-IRF-1, since this isoform is thought to reside in the cytosol. This may suggest that IRF-1 can also be ubiquitinated in the cytosol. This will be discussed further later. The lack of interaction between FLAG-IRF-1 and the GSH beads and the GST protein suggests that this interaction is specific. To confirm the interaction between GST-Fbxw7α and FLAG-IRF-1 a co-immunoprecipitation was carried out with the FLAG Ab (figure 6.3). When both FLAG-IRF-1 and GST-Fbxw7α were co-expressed in HEK293 cells a co-immunoprecipitation occurred, confirming that GST-Fbxw7α interacts with FLAG-IRF-1. No GST

protein was immunoprecipitated by FLAG-IRF-1, and there was no GST-Fbxw7α band in the lanes that contained FLAG-IRF-1 alone.

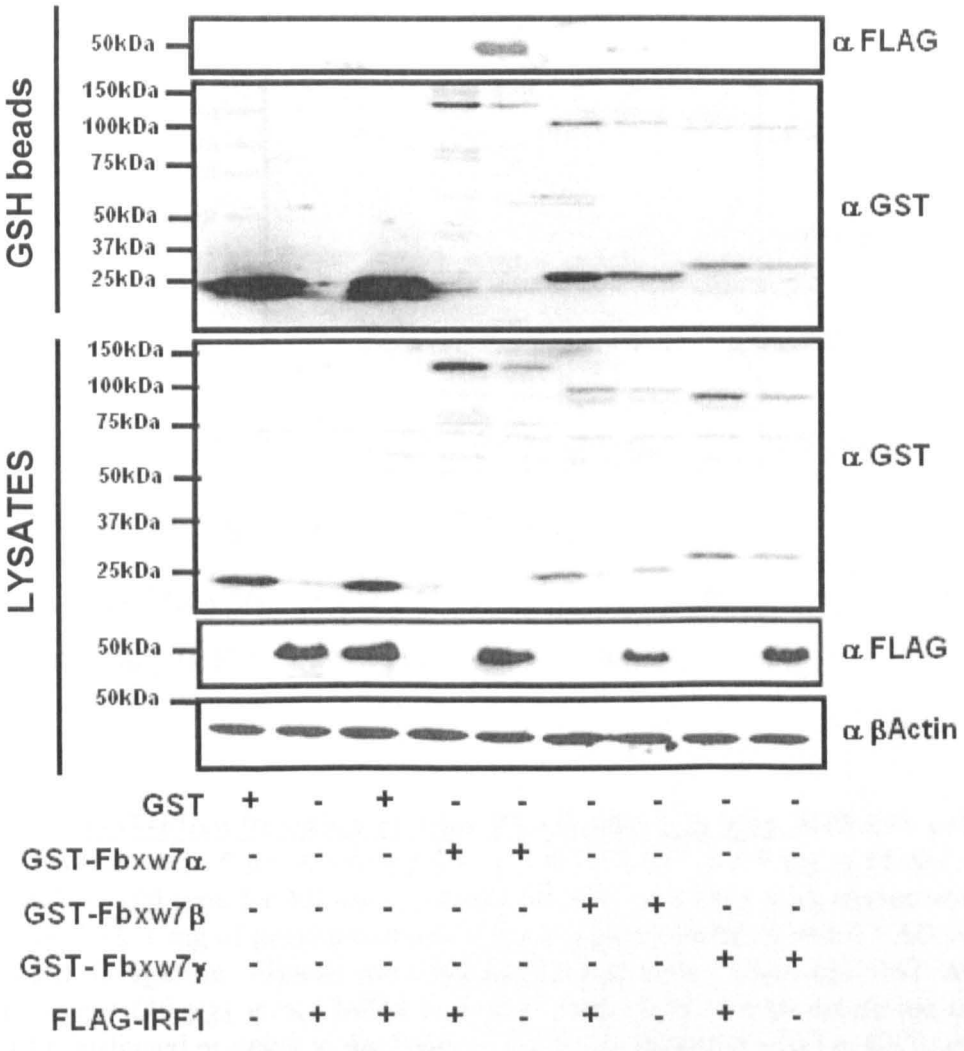

Figure 6.2. FLAG IRF-1 interacts with GST-Fbxw7α and GST-Fbxw7β *in vivo.* HEK293 cells were transfected with 5 μg of either GST or GST-Fbxw7 and 5 μg of FLAG or FLAG-IRF-1 wild type plasmids for 48 hours. 6 hours prior to lysis cells were treated with 10 μM MG132. Protein extracts (0.5 mg) were incubated with GSH- sepharose beads for 3 hours at 4°C. Proteins that were bound to the beads were immunoblotted with GST and FLAG Abs. Protein lysates (20 μg/lane) illustrate the expression of transfected proteins in the lysates.

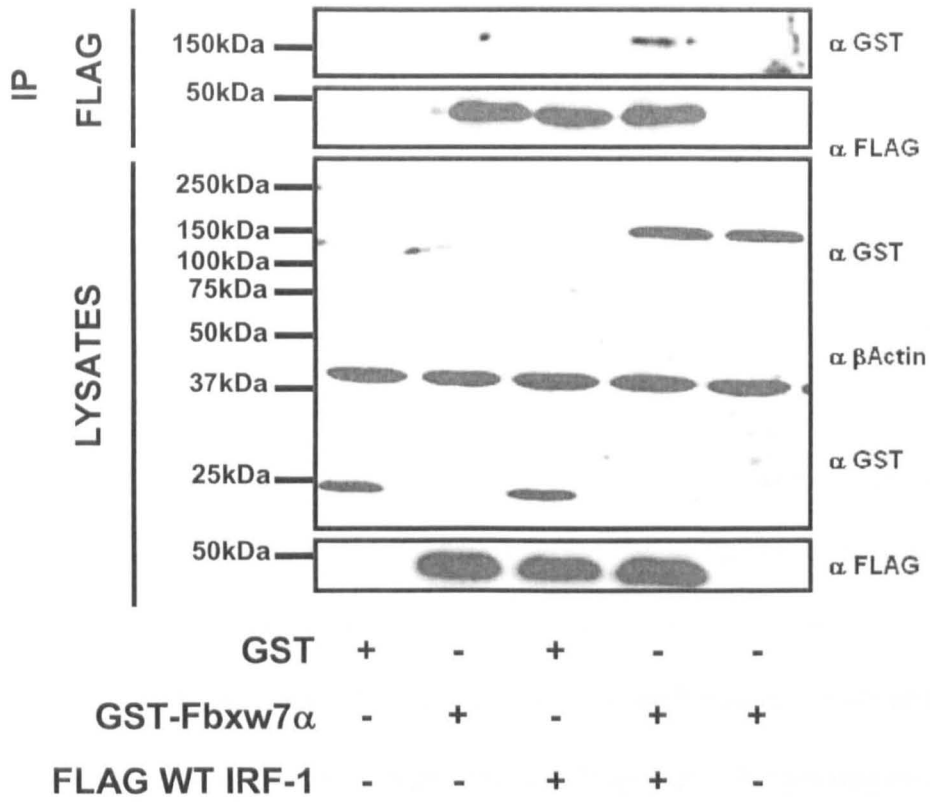

Figure 6.3 GST-Fbxw7α interacts with FLAG-IRF-1 *in vivo.* HEK293 cells were transfected with 5 μg of either GST, or GST-Fbxw7 and 5 μg of FLAG or FLAG-IRF-1 wild type for 48 hours. 6 hours prior to lysis cells were treated with 10 μM MG132. 1 mg of protein extracts was immunoprecipitated with FLAG Ab and Protein G agarose. Eluates were immunoblotted with FLAG and GST Ab. Protein lysates (40 μg) were blotted with GST and FLAG Ab to determine the levels of transfected proteins in the lysates. The lower band (25 kDa) is GST, and the higher bands GST-Fbxw7α.

6.4. FLAG IRF-1 interacts with HA-Fbxw7

The GST protein tag is quite large (~25 kDa) and as such has the potential to interfere with protein-protein interactions. Although the interaction between FLAG-IRF-1 and GST-Fbxw7α was detectable, it was decided to use a smaller epitope tag. Full length Fbxw7α and Fbxw7β were sub cloned into pCMV-HA. Both proteins were expressed in HEK293 cells with and without FLAG-IRF-1 (figure 6.4). The Fbxw7 proteins were immunoprecipitated with the HA Ab, subjected to SDS-PAGE and probed against FLAG. In agreement with figure 6.2 both isoforms co-immunoprecipitated with FLAG-IRF-1. The two isoforms interacted with FLAG-IRF-1 to a similar level, unlike figure 6.2 in which Fbxw7α interacted with IRF-1 more strongly than the β isoform. The interaction between HA-Fbxw7α and FLAG IRF-1 was confirmed by reciprocal co-immunoprecipitation using the FLAG Ab to immunoprecipitate IRF-1 (figure 6.5).

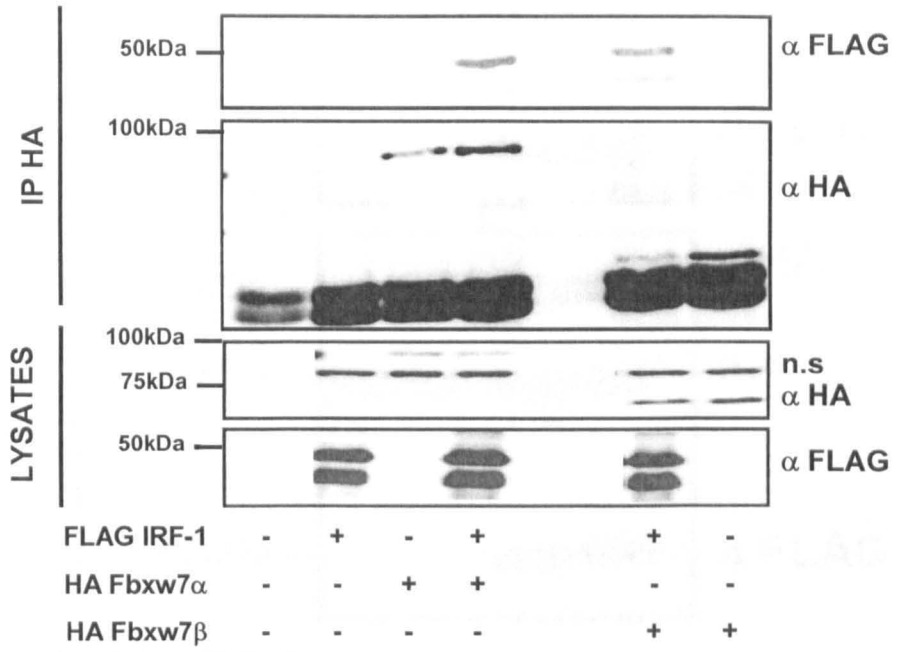

Figure 6.4 FLAG IRF-1 interacts with HA-Fbxw7α and HA-Fbxw7β *in vivo*. HEK293 cells were transfected with 5 μg of HA, or HA-Fbxw7 and 5 μg of FLAG or FLAG-IRF-1 wild type plasmid for 48 hours. 6 hours prior to lysis cells were treated with 10 μM MG132. 1mg of protein extracts were immunoprecipitated with HA Ab and Protein G agarose. Eluates were immunoblotted with HA and FLAG Ab. Protein lysates (40 μg) were blotted with HA and FLAG Ab to determine the levels of the transfected proteins in lysates.

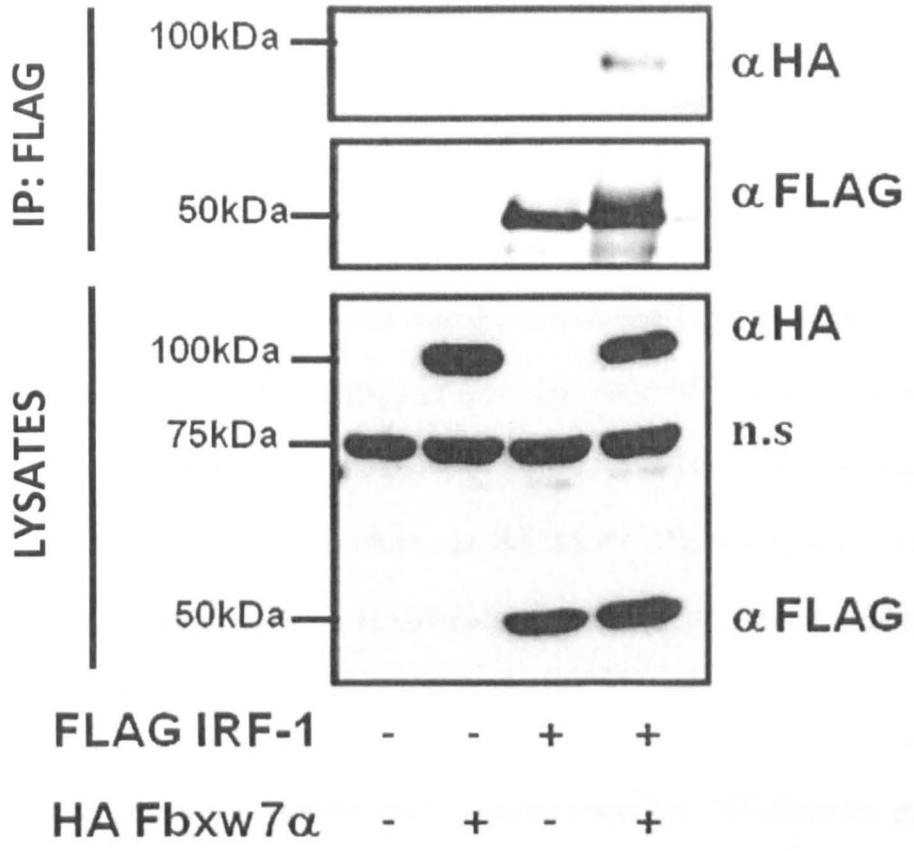

Figure 6.5 HA-Fbxw7α interacts with wild type FLAG IRF-1 *in vivo.* HEK29.3 cells were transfected with 5 μg of either HA or HA-Fbxw7α and 5 μg of FLAG or FLAG-IRF-1 wild type plasmid for 48 hours. 6 hours prior to lysis, cells were treated with 10 μM MG132. 1mg of protein lysates was immunoprecipitated with HA Ab and Protein G agarose. Eluates were immunoblotted with HA and FLAG Ab. Protein lysates (40 μg) were blotted with HA and FLAG Ab to determine the levels of the transfected proteins in lysates.

6.5. Interaction between FLAG-IRF-1 and HA-Fbxw7 is dependent on the WD40 repeats of Fbxw7 and IRF-1 Thr^{180}.

The previous data confirms that Fbxw7α and IRF-1 interact with each other, but does not link the interaction to phosphorylation of IRF-1 at Thr^{180}. To address this, HA-Fbxw7α was co-expressed with the T180A and T180D mutants of IRF-1 in addition to wild type IRF-1 (figures 6.6). The HEK293 protein extracts were then subjected to immunoprecipitation with FLAG Ab and co-immunoprecipitated Fbxw7α was detected by immunoblot with the HA Ab. The wild type FLAG-IRF-1 was immunoprecipitated with HA-Fbxw7α confirming the interaction between these proteins.

The T180A mutant consistently immunoprecipitated less HA-Fbxw7α protein. Fbxw7α has a preference for phosphorylated threonine residues, and therefore implicates Thr^{180} as a potential docking site for Fbxw7α. The interaction between these two proteins is however detectable, suggesting that Fbxw7α can interact with other residues beside Thr^{180} (figure 6.6A). The ability of Fbxw7 to form homo and heterodimers may also allow the formation of multiple contacts with sub-optimal phospho-degrons. In these experiments HA-Fbxw7α is over-expressed at higher then physiological levels, this may promote the formation of dimers, which may not be able to form in normal conditions. When lower levels of Fbxw7α were co-transfected with FLAG-IRF-1 the interaction between T180A IRF-1 and HA-Fbxw7α was not detectable (figure 6.6B).

The importance of Thr^{180} is highlighted by the interaction between the FLAG T180D mutant and HA-Fbxw7α. Consistently this interaction was significantly

stronger than the interaction between wild type IRF-1 and HA-Fbxw7α. This suggests that either more T180D IRF-1 is interacting with HA-Fbxw7α or that the interaction is stronger. Phosphorylation (and therefore addition of a negative charge) of Thr residues has been shown to greatly increase the interaction between the WD40 domain of Fbxw7α and its substrates The great majority of phosphorylation specific interactions between Fbxw7α and its substrates occur through the WD40 repeats. A truncation mutant of HA-Fbxw7α was made (aa 1-373) which removed all eight WD40 repeats. This truncated Fbxw7α retains its Fbox, dimerisation domain and NLS, and subsequently can be recruited to the SCF E3 ligase complex, but cannot interact with substrates (Welcker *et al.* 2004). As expected the interaction between FLAG-IRF-1 wild type and HA-Fbxw7α ΔWD40 is not detectable, thus indicating that the WD40 repeats interact with IRF-1 (figure 6.6A).

A.

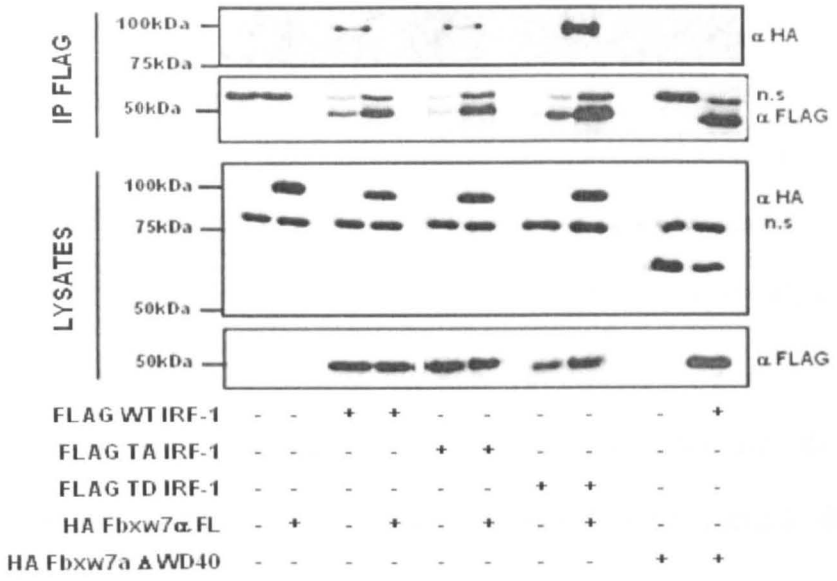

B.

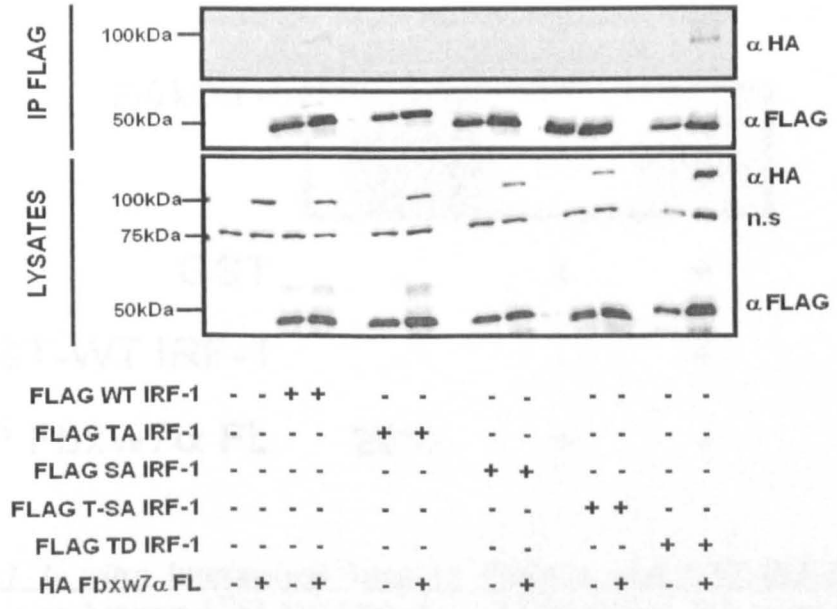

Figure 6.6. Importance of IRF-1 Thr^{180} and the WD40 repeats of Fbxw7α for interaction *in vivo*. **A).** HEK293 cells were transfected with 7.5 μg of empty (HA), HA-Fbxw7α FL or HA-Fbxw7α ΔWD40 expression plasmid with 2.5 μg of FLAG-IRF-1 plasmids – WT (wild type), TA (T180A), and TD (T180D) for 48 hours. 6 hours prior to lysis, cells were treated with 10 μM MG132. 1 mg of protein extract was immunoprecipitated with FLAG M2 Ab using Protein-G agarose beads. Eluates were probed with HA and FLAG. Lysates (40 μg) were blotted with FLAG and HA Ab to determine expression levels of transfected proteins. **B).** As for A) but with the exception that 5 μg of HA-Fbxw7α and 5 μg of FLAG-IRF-1 were used. In addition the SA (S184A) and TS-A (S184A and T180A/S184A) mutants were included.

6.6. GST-IRF-1 interacts weakly with Fbxw7α *in vitro*

To determine if IRF-1 and Fbxw7α interact directly, an *in vitro* GST pulldown assay was used. Fbxw7α was in vitro transcribed and translated in the presence of [^{35}S] methionine and mixed with GST-IRF-1 (figure 6.7). In agreement with previous data, an interaction between the two proteins was identified, as GST-IRF-1 pulled down the [^{35}S] Met labelled Fbxw7α. No interaction was visible in the GST only lane, showing that the interaction is occurring through IRF-1, not the GST tag. The interaction was quite weak – perhaps 5% (compared to the 20% input).

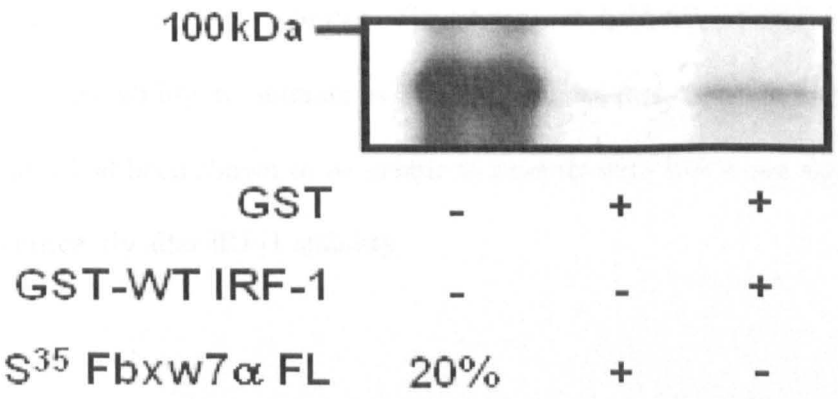

Figure 6.7 *In vitro* interactions between Fbxw7α and GST-IRF-1. GST pulldown assay between [^{35}S] Met-Fbxw7α and GST-IRF-1. 20% input lane of [^{35}S] Met-Fbxw7α is to demonstrate relative quantity.

6.7. Over-expression of HA-Fbxw7α increases IRF-1 turnover in HEK293 cells.

To date, the only known function of Fbxw7α is to act as a substrate recruitment module for the SCF E3 ligase complex. This recruitment in turn brings about ubiquitination, and subsequent proteasomal degradation of its substrates. To determine if the interaction with Fbxw7α brings about degradation of IRF-1, CHX chases were performed (fig. 6.8) in HEK293 cells co-transfected with either empty vector (HA), full length Fbxw7α (FL) or the truncation mutant lacking the WD40 repeats (ΔWD40). The half life of IRF-1 when Fbxw7α FL is expressed was approximately 20-25 minutes, while IRF-1 transfected with empty HA vector had a half life of 35-40 minutes. The change in half life of IRF-1 is directly related to its ability to interact with Fbxw7α, as the ΔWD40 mutant (which previously had been shown to be unable to interact with IRF-1 see figure 6.6) did not significantly alter IRF-1 stability.

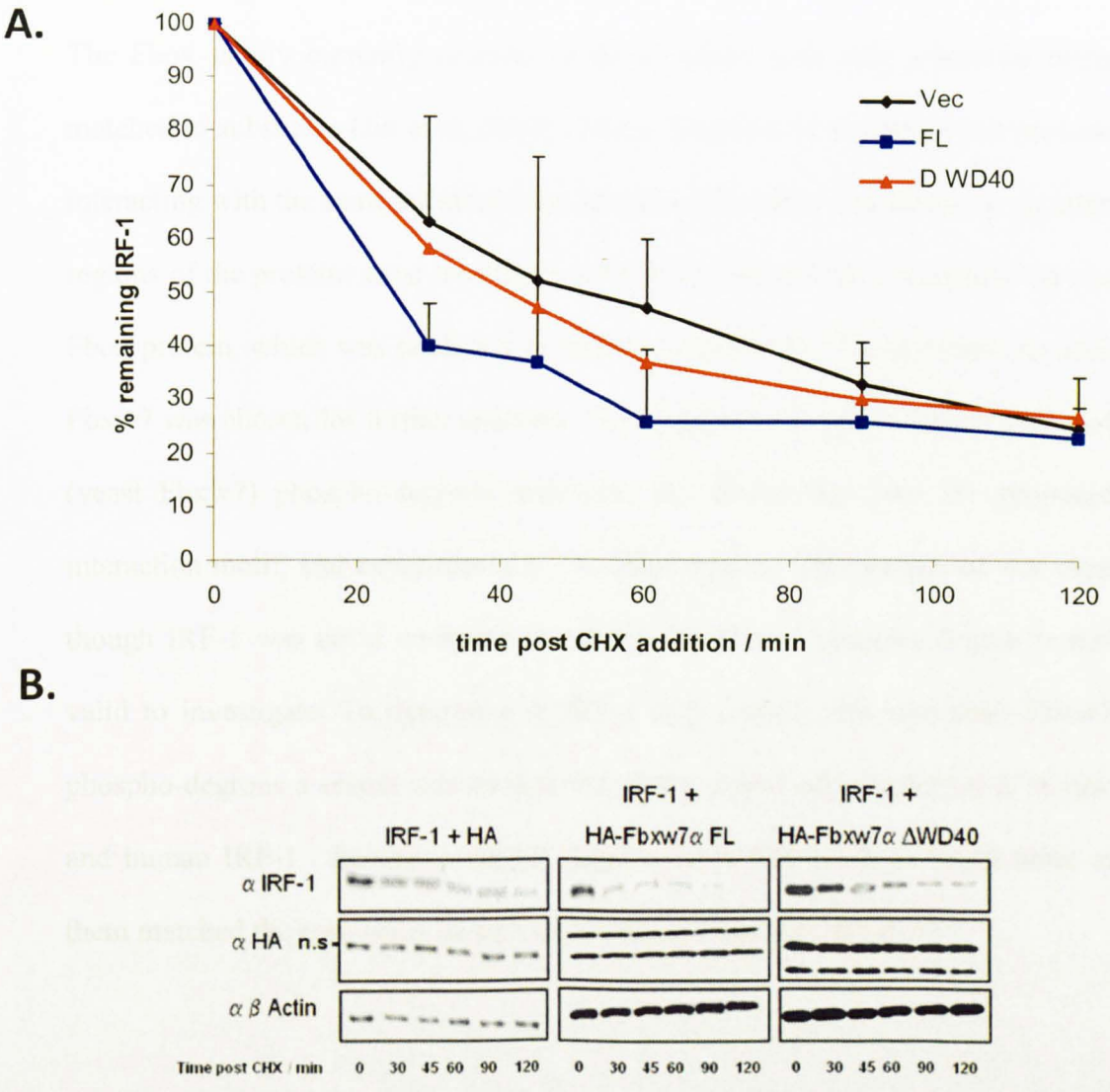

Figure 6.8 Over-expression of HA-Fbxw7α increases IRF-1 turnover. HEK293 cells were seeded on six well plates and transfected with 2.5 µg of HA, HA-Fbxw7α or HA-Fbxw7 ΔWD40 with 2.5 µg of FLAG-IRF-1 wild type. 24 hours post transfection, cells were treated with CHX at 25 µg/mL for the indicated times. Extracts were made and immunoblotted (15 ug) against FLAG, HA and β-actin. **A)** Precentage remaining IRF-1 (as determined according to chapter five) plotted against time from three independent experiments carried out in duplicate. **B)** Representative Immunoblots.

6.8 Discussion

The Fbox family currently consists of 68 members with only a handful being matched to substrates (Jin et al. 2004). Many examples of multiple Fbox proteins interacting with the same substrate (sometimes on the same consensus, or on other regions of the protein) exist (see figure 6.9). It was decided to concentrate on one Fbox protein, which was predicted to interact with the Thr^{180} consensus. As such Fbxw7 was chosen for further analysis. The alignment of known Fbxw7 and cdc4 (yeast Fbxw7) phospho-degrons highlights the divergence from the proposed interaction motif, and experimentally validated regions. This suggested that even though IRF-1 was not a complete match for the Fbxw7 phospho-degron it was valid to investigate. To determine if IRF-1 may contain any secondary Fbxw7 phospho-degrons a search was carried out on the amino acid sequences of mouse and human IRF-1. Several potential degrons were identified, although none of them matched the consensus as well as the degron surrounding Thr^{180}.

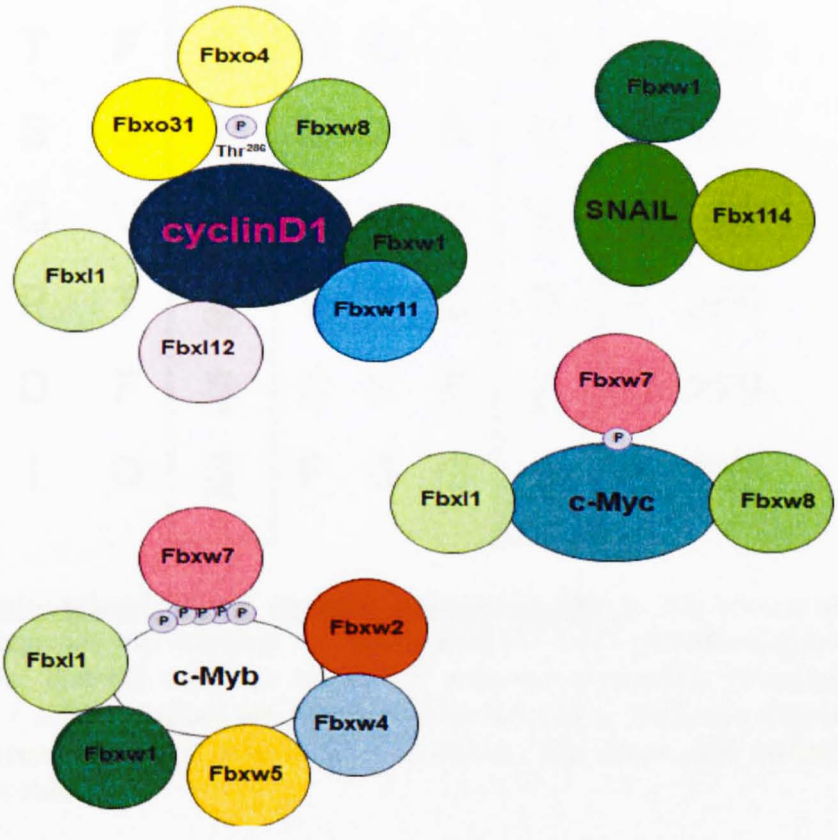

Figure 6.9. Multiple Fbox proteins can interact with the same substrate. Cartoon illustration of known Fbox-substrate interactions. CyclinD1 interacts with three different Fbox proteins via the same phospho-degron (Santra *et al.* 2009, Lin *et al.* 2006 and Okabe *et al.* 2006). Additional Fbox protein interact with Cyclin D1 independently of this degron (Skaar *et al.* 2009). SNAIL interacts with Fbxw1 following phosphorylation by GSK3β, while it can also interact with Fbxl14 independently of GSK3 phosphorylation (Katoh 2006). Fbxw7 interacts with c-Myb via multiple phosphorylated residues, but a screen of Fbox proteins identified five other interactions not involving the phosphorylated residues (Kanei-Ishii *et al.* 2008). Phosphorylation of Thr^{58} by GSK3β on c-Myc induces an interaction with Fbxw7, but Fbxl1 and Fbxw8 bind other regions of c-Myc (Welcker *et al.* 2004, Kim *et al.* 2003b and Koch *et al.* 2007). It is likely that individual substrate-Fbox interactions are induced by specific signalling events and that an Fbox proteins can compensate for one another. For example, Fbxw1 and Fbxw11 are highly homologous proteins that recognise overlapping substrates.

146	T	F	S	D	G	L	S	S	*155*
153	S	S	T	L	P	D	D	H	*162*
213	Q	V	S	P	M	P	S	T	*221*
248	P	T	S	V	Y	G	D	F	*256*
271	D	F	S	C	K	E	E	D	*279*
251	I	D	S	P	G	G	S	I	*259*

Figure 6.10. Sub-optimal Fbxw7 phospho-degrons in IRF-1. The mouse and human IRF-1 sequence was searched for other potential Fbxw7 phospho-degrons, particularly those that did not fully match the proposed consensus. Potentially phosphorylated / acidic residues are highlighted in the boxes. Only the degrons conserved between human and mouse IRF-1 is shown. The amino acid numbers are shown either side.

As predicted, an interaction between IRF-1 and Fbxw7 could be detected in co-transfected HEK293 extracts (figure 6.2-6.5). This interaction could be demonstrated by reciprocal co-IP. An interaction between endogenous IRF-1 and Fbxw7 could not be demonstrated because of the lack of sensitive antibodies against Fbxw7. The preference for an interaction with the Fbxw7α isoform was not surprising considering they reside in the same cell compartment. The interaction between HA-Fbxw7β and FLAG-IRF-1 was as strong as HA-Fbxw7α in figure 6.4, which contrasted with figure 6.2. It is likely that the higher expression of HA-Fbxw7β compared to GST-Fbxw7β may account for this. It is possible that under the experimental conditions used GST-Fbxw7β or HA-Fbxw7β also locates into the nucleus. Fbxw7β may also be able to locate to the

nucleus in the form of heterodimers with Fbxw7α or Fbxw7γ as this has been reported in the literature (Zhang and Koepp 2006).

The WD40 repeats which are required for phosphorylation dependent interactions are identical between the three isoforms of Fbxw7 as such the phosphorylation interaction domain is common to all isoforms (see figure 6.11). It is also feasible that IRF-1 can be phosphorylated outside the nucleus, consequently becoming a substrate for the cytosolic HA-Fbxw7β. It has not been discounted that phosphorylation at Thr^{180} occurs away from DNA and the nucleus, and also that it has roles in protein turnover that are not coupled to transcription. Several reports suggest that the Fbxw7β isoform is differentially expressed to the Fbxw7α isoform. The β isoform is not found in as many cell types as the α isoform, and is not as highly expressed as the α isoform. In a more physiological context it is possible that Fbxw7β has a minimal effect on IRF-1 turnover, and the interaction observed is an artefact of protein over expression. For this reason, the interaction between IRF-1 and Fbxw7α was studied in more detail.

The GST-Fbxw7γ did not interact significantly with FLAG-IRF-1 even though the amount of GST-Fbxw7γ protein was similar to Fbxw7β. This is most likely due to the restricted nucleolar localisation of Fbxw7γ. It has never been reported that IRF-1 locates to the nucleoli and direct fluorescence microscopy of YFP-IRF-1 in HEK293 cells suggests that IRF-1 is excluded from the nucleoli (data not shown).

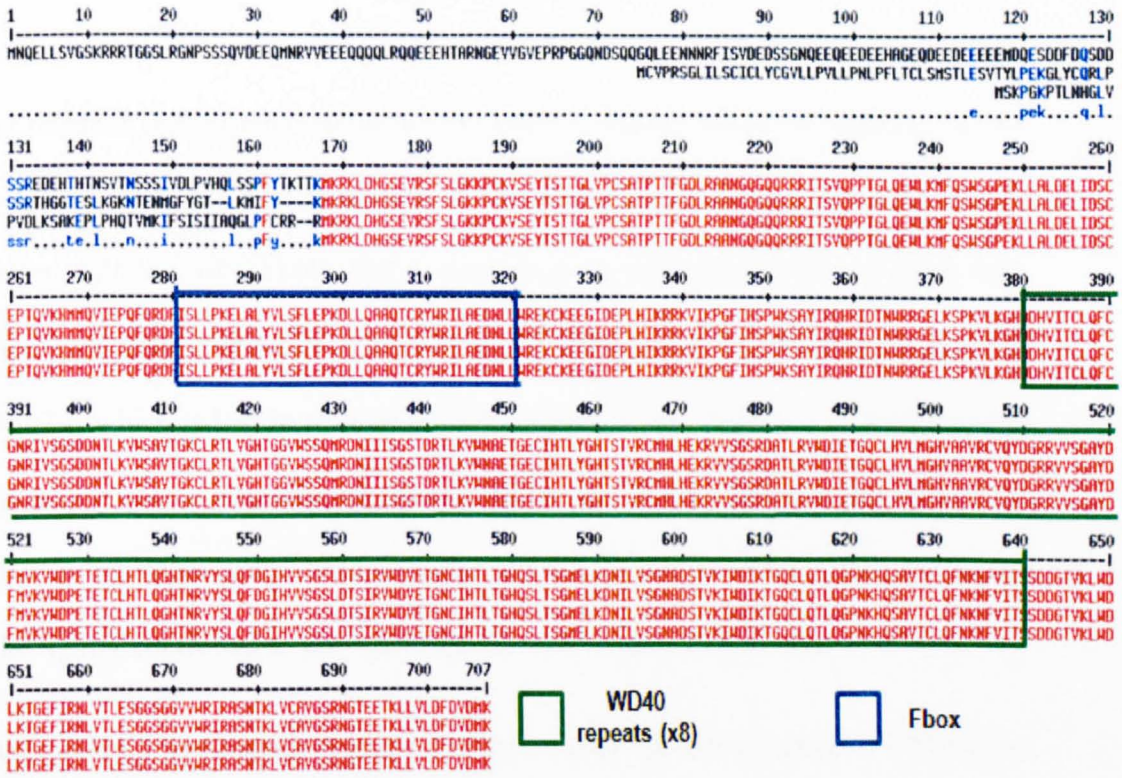

Figure 6.11 Amino acid alignment between Fbxw7α, Fbxw7β and Fbxw7γ. Amino acid sequences for (top to bottom) Fbxw7a/β/γ (also known as Fbxw isoforms 1/2/3) were aligned against one another using the Mutalign programme (http://bioinfo.genotoul.fr/multalin/multalin.html). The Fbox and WD40 repeats are highlighted in boxes. The bottom line indicates the consensus alignment between the three isoforms.

Reciprocal co-immunoprecipitation using the FLAG tag to precipitate IRF-1 demonstrated that HA-Fbxw7α interacts with FLAG-IRF1. To further probe the interaction between IRF-1 and HA-Fbxw7α the T180A and T180D mutants of IRF-1 were used. As expected the interaction between T180A IRF-1 and HA-Fbxw7α was reduced suggesting that Thr^{180} is important in making contact with Fbxw7α. To demonstrate that addition of a negative charge in place of Thr^{180} regulates association with IRF-1, the T180D mutant was immunoprecipitated with HA-Fbxw7α. Consistently this mutant precipitated more HA-Fbxw7a than the

wild type IRF-1 (figure 6.6). Fbxw7α makes contact with its phospho-threonine via three conserved arginine residues (see figure 6.1) the positive charge of the Arg residues makes contacts with the negative charge which is supplied by the phosphate, or in this case aspartic acid. The increased association may explain the shorter half life of T180D IRF-1 compared to wild type IRF-1 (figure 5.5). Phosphomimetic mutants of Notch have been shown to restore interaction with Fbxw7α, which is lost in alanine mutants (O'Neill *et al.* 2007). It is also possible that inappropriate interaction between IRF-1 and Fbxw7 reduces the activity of IRF-1 on its target genes. This suggests that the GSK3 phosphorylation signal has to be tightly controlled to prevent inappropriate degradation of IRF-1.

It is important to consider that the T180A mutant can still interact with Fbxw7α, which suggests that Thr^{180} is not completely essential for the interaction. This could be for several reasons. Chapter 3 established that IRF-1 is most likely dual phosphorylated at Ser^{184} and Thr^{180}, although Fbxw7α is reported to prefer Thr over Ser residues (Welcker *et al.* 2004), the phospo-Ser^{184} itself could form a Fbxw7 phospho degron (A L S P C A) as it contains a Leu residue and Pro residue before and after the phosphorylated Ser respectively. The S184A and S184E mutant were both tested for their interaction with HA-Fbxw7α and were found to behave exactly as their Thr counterparts. However, this could be due to the priming effect on Thr^{180} rather than being direct interactions themselves. The double TS-A mutant was also tested for its interaction and was also found to have a very weak residual interaction with HA-Fbxw7α (data not shown). This suggests that another residue is involved in this interaction. Some Fbxw7α interacting partners contain multiple phospho-degrons including PGC1α and

Cyclin E (Welcker and Clurman 2008). It is possible that the same phenomenon occurs with IRF-1, and a list of potential sites is given in figure 6.11. It is also possible that IRF-1 makes stabilising contacts elsewhere on the Fbxw7α protein; these interactions may be independent of phosphorylation. When lower levels of Fbxw7α were used (5 μg rather than 7.5 μg) the interaction was weaker between HA-Fbxw7α and wild type IRF-1 as well as T180D IRF-1, but the interaction was completely lost with FLAG T180A, S184A and TS-A IRF-1. The lower level of HA-Fbxw7α is most likely more similar to the physiological levels of Fbxw7α. Consequently the interaction between T180A IRF-1 and Fbxw7α may be a result of abnormally high levels of Fbxw7α in cells. Deletion mapping of IRF-1 with HA-Fbxw7α interactions may be of use in studying this. Mutation of either Leu^{179} or Pro^{183} could also be used to determine the role of these residues in Fbxw7α interaction. Fbxw7α can form dimers which make contact with non phosphorylated residues that are not part of recognisable consensus (Zhang and Koepp 2006) potentially making any residue a possible contact. The over-expression of HA-Fbxw7α may promote the formation of these dimers, and as such the remaining interaction may not be physiological. Mutations in the dimerisation domain of Fbxw7α or Fbxw7β could be used to determine if dimerisation is required for interaction with the T180A mutant of IRF-1. It should also be noted that phosphorylated IRF-1 is most likely not a homogenous species, but rather a mix of different forms of phosphorylated IRF-1 and as such there may be a fraction that is highly phosphorylated on numerous residues, offering a stronger interaction with Fbxw7α. A direct interaction between GSK3 and Fbxw7α has never been identified, but interaction between the SCF and HIPK1

has been demonstrated in the case of c-Myb (Kanei-Ishii *et al.* 2008). These interactions help stabilise the newly phosphorylated substrate with the SCF^{Fbxw7} complex. Chapter 3 showed that the alanine mutants are equally able to interact with GSK3β, should GSK3β be able to interact with Fbxw7α, an indirect interaction may occur.

To further define the interaction between IRF-1 and Fbxw7α, truncation of the Fbxw7α WD40 repeats was carried out. Loss of the WD40 repeats should render Fbxw7α incapable of interacting with substrates. When co-expressed with FLAG IRF-1, no co-immunoprecipitation of ΔWD40 HA-Fbxw7α occurred. This suggests that Fbxw7α uses its WD40 repeats to interact with IRF-1. A mutant of Fbxw7α encompassing just the WD40 repeats and the very far C terminus was constructed but expression of the protein could not be detected in protein extracts. This mutant would have been used to demonstrate that only the WD40 repeats are required for the interaction with IRF-1. All the interactions were assayed in the presence of MG132 to block the proteasome and prevent degradation of the newly ubiquitinated IRF-1. It was assumed that following interaction with Fbxw7α, IRF-1 is rapidly poly-ubiquitinated and degraded, and as such the interaction would not be detectable without the addition of MG132. It would be intriguing to determine if this interaction can be detected in the absence of MG132. The interaction studies here is between murine IRF-1 and human Fbxw7α, the phospho-degron is almost identical between human ad mouse IRF-1, suggesting that the interaction is also likely to be conserved. An interaction could be detected between GST-IRF-1 [^{35}S] Met Fbxw7α; suggesting that an interaction can occur without phosphorylation of IRF-1. However as this was not an entirely *in vitro*

interaction it is also possible that other components (from the rabbit reticulocyte lysates - RRL) are allowing an indirect interaction to occur. It has been noted that other components of the SCF complex are present in RRL and so it is possible that this interaction is occurring with other SCF components. Future experiments will need to be conducted to confirm tha *in vitro* phosphorylation of GST-IRF-1 enhance the interaction with Fbxw7α directly. The interaction between SREBP1 and Fbxw7α was found to be very weak *in vitro,* but was significantly increased by addition of oligonucleotides containing SREBP1 binding sites, while a DBD mutant of SREBP1 was less able to interact with Fbxw7α (Punga *et al.* 2006). Therefore it is possible that DNA binding is needed to enhance the interaction between IRF-1 and Fbxw7α *in vitro.* Phosphorylation could occur directly between GSK3β and IRF-1 *in vitro* without DNA present (figure 3.3) although it is feasible that phosphorylation may be more efficient with DNA bound IRF-1. The binding of IRF-1 to DNA could also aid phosphorylation / ubiquitination by immobilising IRF-1.

CHX chase assays demonstrated that Fbxw7α was able to promote an increase in IRF-1 turnover (figure 6.8), and that this depended on its ability to interact with IRF-1, as the ΔWD40 mutant had no effect. In a similar manner to the phospho-mimic mutants it was not possible to cause a larger decrease in IRF-1 stability, possibly because it is already an unstable protein that is readily degraded in HEK293 cells by alternative pathways. In addition Fbxw7α alone cannot promote degradation of IRF-1, but requires the other components of the SCF complex and the E2 enzyme. Since none of these proteins were over-expressed in combination it is possible that they were limiting factors in IRF-1 degradation. In addition it

has already been shown that only a small fraction of IRF-1 is phosphorylated by GSK3β, if the interaction between IRF-1 and Fbxw7 is dependent on phosphorylation by GSK3β this could also have been limiting. It would be interesting to determine if combined over-expression of Fbxw7α and GSK3β promotes synergistic degradation of IRF-1. The K85A mutant of GSK3β could also be used to determine if it prevents the Fbxw7α dependent acceleration of IRF-1 turnover. It is most likely that other E3 ligases play a role in IRF-1 turnover, and subsequently increasing the expression of a single E3 component may only have a small overall effect, especially when phosphorylation may be limiting. It can also not be ruled out that phosphatases and de-ubiquitinases may hinder the GSK3β-Fbxw7α pathway of IRF-1 degradation. Another method of determining the importance of Fbxw7α would be to deplete endogenous Fbxw7α in cells to determine if it plays a role in IRF-1 turnover. MEF cell lines that do not express Fbxw7α could also be used to determine if IRF-1 stability is greater than wild type cells. A number of cancer cell lines contain inactivating mutations in Fbxw7α (Strohmaier *et al.* 2001). It would be interesting to determine if IRF-1 half life is different in these cells, and if rescuing Fbxw7α expression increases IRF-1 turnover. A less specific approach for determining of SCF complexes are involved in IRF-1 stability could be to use dominant negative mutants of Cul-1. These mutants cannot interact with Skp1, and so form truncated SCF complexes which cannot associate with substrates (Sundqvist *et al.* 2005). Dominant negative Cul-1 is disadvantageous due to the effects it has on all SCF complexes rather than just the $SCF^{Fbxw7\alpha}$ complex. It would however show that SCF is required for turnover, especially as multiple Fbox proteins may play a role in IRF-1 turnover.

Additionally dominant negative mutants of the other Cul proteins (Cul-2/3/4/5) could be used to asses if other multisubunit E3 ligase complexes regulate IRF-1 degradation. In conclusion, an interaction between IRF-1 Thr^{180} (at least partially) and the WD40 repeats of Fbxw7α is promoted by GSK3β dependent phosphorylation. The interaction promotes increased turnover of IRF-1 which explains the phosphorylation dependent turnover of IRF-1 established in chapter five.

Chapter 7: Conclusions and future work

7.1 Conclusions

Twenty years after the initial characterisation of IRF-1 as a phospho-protein (Pine and Darnell 1989) no single amino acid – kinase pair has been described *in vivo*. Other members of the IRF family, particularly IRF-3 and IRF-7 have been extensively studied in the context of post translational modifications. Multiple kinases, acetyl-transferases, phosphatases and ubiquitin E3 ligases have been matched to other IRFs (see figure 7.1), while knowledge of IRF-1 PTMs lags far behind. This thesis set out to identify a kinase and the amino acid(s) it phosphorylates, but also to reveal a functional consequence of the modification. Consequently GSK3β was identified as an IRF-1 kinase, which phosphorylated Thr^{180}. This pathway was shown to be important for IRF-1 transcriptional activity against an important pro-apoptotic target gene (TRAIL) both in reporter assays, and in breast cancer cells.

Phosphorylation was then found to modulate the stability of IRF-1 protein. The stability of IRF-1 proved to be crucial for its transcriptional activity, as stabilised IRF-1 was a less effective transcriptional activator. The missing link between phosphorylation and ubiquitination was then identified as the $SCF^{Fbxw7\alpha}$ ubiquitin E3 ligase, which specifically recognises phosphorylated substrates. This work has identified the first *in vivo* phosphorylation event of IRF-1 by GSK3β. It is also the first evidence for an interaction between IRF-1 and an ubiquitin E3 ligase. Collectively by identifying a novel kinase for IRF-1, I have been able to describe a molecular pathway by which phosphorylation initiates ubiquitination and degradation of IRF-1, a process required for IRF-1 to be able to transactivate the TRAIL promoter.

IRF	Phosphorylation	Acetylation	Ubiquitination	Glutathionation	Prolyl Isomerisation	SUMOylation	ISG-15ylation
IRF-1	✓					✓	
IRF-2	✓	✓				✓	
IRF-3	✓			✓	✓	✓	✓
IRF-4							
IRF-5	✓		✓				
IRF-6							
IRF-7	✓	✓	✓			✓	
IRF-8	✓						
IRF-9		✓					

Figure 7.1. Mapped PTMs in IRF family members. Only the PTMs matched to a residue *in vivo* are included here, however IRF-4 is known to be prolyl isomerised, IRF-8 is ubiquitinated, IRF-2 is phosphorylated, and IRF-1 is acetylated. All sites were acquired from the phosphosite database (www.phosphosite.org).

Several questions remain to be answered from this work. Although it has highlighted the importance of turnover in transcriptional activity, little is known about the mechanism by which IRF-1 degradation modulates transcription. The signalling pathways that initiate phosphorylation also need to be elucidated. The global effects of phosphorylation on the IRF-1 transcriptional programme need to be studied further. Most importantly the phenotypic effects of this modification on IRF-1 in human disease remains to be uncovered. This is summarised in figure 7.2

Does phosphorylation of IRF-1 at Thr^{180}/Ser^{184} modulate other protein-protein interactions?

Chapter 6 confirms that phosphorylation of Thr^{180}/Ser^{184} modulates the interaction between IRF-1 and the Fbox protein Fbxw7α; however, other protein-protein interactions may occur following the phosphorylation of these residues. As discussed in chapter six, it is possible that other Fbox proteins are able to recognise the Fbxw7 phospho-degron; as such multiple Fbox proteins could be recruited to phosphorylated IRF-1. The WD40 repeats of Fbxw7α are responsible for phosphorylation dependent interactions with substrates, which would suggest that only other Fbxw proteins would be candidates for the interaction with IRF-1. Indeed, during preliminary experiments several additional Fbxw proteins were shown to interact with IRF-1 by *in vivo* GST pulldown assays, it is not known however, if these proteins are recognising the Thr^{180}/Ser^{184} motif, or another phosphorylation site on IRF-1. In the case of phosphorylated Thr^{286} of Cyclin D1, different classes of Fbox protein interact, one WD40 containing (Fbxw8) and two with other domains (Fbxo31 and Fbxo4). Each Fbox protein interacts with Cyclin D1 under different conditions; consequently different Fbox proteins may interact with IRF-1 depending on the cellular environment (Santra *et al.* 2009, Lin *et al.* 2006 and Okabe *et al.* 2006).

Phosphorylation of T-P and S-P motifs also produces an interaction motif for the proline isomerase Pin1. The interaction between substrate and Pin1 occurs through the WW motif, which recognises phosphorylated T/S followed by proline. The Pro residue is consequently isomerised into its trans confirmation. This change has significant structural effects on the protein. In the case of c-Myc,

phosphorylation of Ser^{62} by ERK1/2 primes phosphorylation of Thr^{58} by GSK3β, this in turn leads to the recruitment of Pin1 to phosphorylated Thr^{58}. Pin1 isomerises Pro^{59}, and promotes interaction with the phosphatase PP2A (Protein Phosphatase 2A). This leads to removal of the phosphate on Ser^{62}. Fbxw7 is then able to interact with c-Myc and bring about its ubiquitination. Consequently, Pin1 is needed to edit the phosphorylation of c-Myc, making it available for destruction (Yeh *et al.* 2004). c-Myc could appear to be alone in its requirement for the removal of the phosphorylated priming site, as other Fbxw7 substrates are able to interact when both residues are phosphorylated. Phosphorylation of SRC-3 (later shown to be via GSK3β) promotes interaction and proline isomerisation by Pin1. This step is important for SRC-3-nuclear receptor interactions (Yi *et al.* 2005). It would be of interest to test if Pin1 interacts and isomerises IRF-1, by interacting with either Thr^{180} or Ser^{184}, as both are flanked by Pro residues. Given the presence of the PxLxP motif, it would be especially interesting to determine if this modulates interactions with other proteins (such as the MYND domain proteins).

In addition to WW and WD40 motifs, numerous other phospho-threonine and phospho-serine motifs are found in the proteome, further increasing the number of potential interacting partners for phosphorylated IRF-1 (see table 1.2). A proteomic screen using the aanine versus wild type mutants of IRF-1 would help elucidate the importance of these residues in protein-protein interactions. Identification of proteins that are recruited to phosphorylated IRF-1 may be of use in exploring the requirement for phosphorylation for IRF-1 transcriptional activity. Although ubiquitination and degradation are likely important for IRF-1 activity, it cannot be discounted that phosphorylation affects IRF-1 roles in the cell in a mechanism that is independent of recruiting ubiquitin E3 ligases. For

example, MafA phosphorylation by GSK3β promotes an interaction with PCAF,. This interaction protects MafA from proteasomal degradation, yet phosphorylation increases MafA degradation. Hence phosphorylation can promote interactions with coactivators, while also marking the protein for destruction. The authors suggest that PCAF physically blocks access to E3 ligases, but disengagement of PCAF leaves phosphorylated MafA vulnerable to degradation, and therefore termination of its transcriptional activity (Rocques *et al.* 2007). It is also possible that PCAF acetylates the ubiquitin acceptor lysines on MafA, and that de-acetylation of MafA is needed for its degradation via an E3 ligase that recognises phosphorylated MafA. IRF-1 is known to interact with the KAT enzymes CBP, p300, PCAF, SRC-2 and GCN5 (see table 1.5), and it would be of interest to determine if phosphorylation modulates the interaction between IRF-1 and these KAT enzymes, particularly if these enzymes are able to acetylate ubiquitin acceptor lysines in IRF-1.

Although not studied here, the interaction between the IRF-1 PxLxP motif and MYND domain proteins could be perturbed or enhanced by phosphorylation of Thr^{180}/Ser^{184}. Many of the MYND domain proteins act as transcriptional repressors or adapters for transcriptional repressor complexes (BS69, RACK7, DEAF-1, and ETO). A subgroup of SET domain methyltransferases is also equipped with MYND domains (SMYD1-5). Some of these methyltransferases are transcriptional repressors, while SMYD3 is a transcriptional activator, possibly through its interaction with RNA Pol II (Hamamoto *et al.* 2004). SMYD3 is also reported to act as a transcriptional coactivator of ERα (Kim *et al.* 2009). It would be of interest to determine if IRF-1 interacts with SMYD family members, partly because these proteins have established roles in transcription, but

additionally because they are methyltransferases. As such an interaction could lead to methylation of IRF-1, a modification that has not yet been shown to occur on any IRF protein. Very little is known about PxLxP motifs, and the range of proteins to which they interact, and it is possible a far greater range of proteins interact with IRF-1 through this motif, other than MYND domain proteins. Thr^{180}/Ser^{184} also resides within the heterodimerisation (IAD) domain of IRF-1 (aa 164-219). This domain regulates the interaction between IRF-1 and IRF-8. This interaction is not likely to have been significant in these studies as IRF-8 is not expressed in any of the cell types used, however it is not known if other IRF proteins (e.g. IRF-5 which is more widely expressed) also interact with this domain. Consequently phosphorylation could alter heterodimerisation between IRF-1 and other IRFs.

Is the phosphorylation and ubiquitination of IRF-1 reversible?

Increasing evidence suggests that PTMs are not static, but rather are constantly being removed or edited throughout the lifetime of a protein. It is possible that phosphorylation of IRF-1 at Thr^{180}/Ser^{184} is reversible; which may explain the relatively low levels of phosphorylation of IRF-1 at these residues. Due to the requirement for phosphorylation on IRF-1 for degradation, de-phosphorylation may promote stabilisation of IRF-1. This could in turn lead to reduction in IRF-1 transcriptional activity towards the TRAIL promoter, although it is not known what effects this would have on other IRF-1 target genes. It is difficult to predict which phosphatase will interact with IRF-1. The most suitable method of determining which phosphatases can antagonise Thr^{180}/Ser^{184} phosphorylation would be to screen a selection of proteins for their ability to reduce IRF-1

phosphorylation. This method has been successfully used to determine which phosphatase was responsible for the removal of the GSK3β phosphorylation on SRC-3 (Li *et al.* 2008). As expected these phosphatases increased SRC-3 stability, and reduced the ability of SRC-3 to interact with nuclear receptors, leading to a reduction in SRC-3 transcriptional activity. No phosphatases have been shown to interact with IRF-1, however the tyrosine phosphatases SHP1 (Protein tyrosine Phosphatase 1) decreases IRF-1 phosphorylation at Tyr^{109} (Kautz *et al.* 2001). Phosphorylation is a relatively simple on/off modification, unlike ubiquitination which occurs in chains and further complication arises from the diversity of chain types depending on the internal Lys used in chain formation. As such DUB enzymes may simply remove ubiquitin from IRF-1, or edit the ubiquitin chain types on IRF-1. Increasing evidence suggests that chain types may regulate protein-protein interactions, as so may have drastic effects on IRF-1 activity. Popov *et al.* identified USP28 (Ubiquitin Specific Protease 28) as a c-Myc DUB, intriguingly USP28 is associated with Fbxw7α and Fbxw7γ (but not Fbxw7β), and is recruited to c-Myc along with Fbxw7α (Popov *et al.* 2007). Although paradoxical it has been shown that a large number of ubiquitin E3 ligases are found in association with DUB enzymes. As expected, USP28 has oncogenic activity and is over-expressed in a number of cancers. USP28 is also involved in the DNA damage response, de-ubiquitinating a number of proteins involved in the p53 pathway (Zhang *et al.* 2006). IRF-1 protein is stabilised following DNA damage (Pamment *et al.* 2002), it would be of interest to determine if USP28 reduces IRF1-1 turnover, and why IRF-1 needs to be stabilised during DNA damage.

What are the transcriptional effects of IRF-1 phosphorylation/ubiquitination?

Loss or reduction in phosphorylation of Thr^{180}/Ser^{184} was found to result in a reduction in reporter activity. This suggests that phosphorylation of IRF-1 at Thr^{180}/Ser^{184} is not essential for its DNA binding, as this was the first critical step in IRF-1 transactivation - DBD mutants of IRF-1 cannot transactivate the TRAIL promoter (Eckert *et al.* 2006). It is however possible that loss of phosphorylation reduces the strength or duration of protein-DNA interaction. Studies using EMSA and ChIP would help establish if phosphorylation is important for IRF-1-DNA interactions *in vitro* and *in vivo* respectively. Given that alanine phosphorylation mutants of IRF-1 are more stable, it is possible that the strength of interaction between IRF-1 and the TRAIL promoter could be greater. FRAP (Fluorescence Recovery After Photo-bleaching) could be utilised to determine if IRF-1 mobility is effected by its phosphorylation. Although it has not been demonstrated, it could also be possible that phosphorylation alters the physical characteristics of the DBD, possibly changing its DNA recognition and hence the promoters it recognises.

GSK3β phosphorylates many proteins involved in transcription. Several GSK3β substrates are known to interact with IRF-1, including NFκB p50/p65, C/EBPα, HIF1α, GRα, p53 and STAT-1 (see table 1.5). Consequently GSK3β may phosphorylate IRF-1 and its TF partners at the same time; it is also possible that IRF-1 recruits GSK3β to promoters, allowing phosphorylation of other proteins. Microarray studies on GSK3β phosphorylation resistant mutants of BCL-3, MafA and GRα (Viatour *et al.* 2004, Rocques *et al.* 2007 and Galliher-Beckley *et al.* 2008) have shown not all of the target genes for these transcriptional regulators

are sensitive to the phosphorylation status. In fact phosphorylation only affected a small subset of Bcl-3 target genes, while it had a much more profound effect on GRα transcriptional programme. In this study selection of a sensitive target gene may fortuitous. For example one study on MafA activity following GSK3β dependent phosphorylation concluded that GSK3β does not alter MafA transcriptional activity, while another study suggests it is important for MafA dependent transcription. The divergence between these two studies was that the first used reporter assays based on the insulin promoter, which was transactivated equally by wild type and phosphorylation mutants, while the other study used a multimerised synthetic reporter that was highly sensitive to phosphorylation of MafA. The two groups also used different cell lines (Han *et al.* 2007)and Rocques *et al.* 2007).

Phosphorylation by a single kinase through certain residues is unlikely to have a completely global effect on transcriptional activity. This is most likely due to the variability in composition and structure of each promoter. Additionally transcription factors will have different degrees of requirement on each promoter, so loss of activity may only have a small effect on genes in which other transcription factors can compensate. It is most likely that the IRF-1 gene programme would not be completely reliant on IRF-1 phosphorylation. This could be because IRF-1 is undergoing other modifications which may be able to override the Thr^{180}/Ser^{184} phosphorylation. IRF-1 alanine mutants were not completely stable; and thus other pathways are capable of degrading IRF-1 protein. In addition, although the phosphorylation of IRF-1 may be involved in several interesting protein-protein interactions, other interactions will occur independently.

One of the most compelling reasons to carry out transcriptional profiling of IRF-1 and its phosphorylation mutants is that it may shed light on how IRF-1 selects its target genes. Several distinct roles are played by IRF-1, but it is not likely that IRF-1 will cause all of these responses to occur at the same time. Accumulating evidence suggests that IRF-1 can select between causing cell cycle pausing, or apoptosis, (Prost *et al.* 1998 and Bouker *et al.* 2005). The potential for this phosphorylation-ubiquitination pathway to act as a transcriptional switch is worth investigating. Transcriptional profiling would also give us a better understanding of the impact phosphorylation has on IRF-1 activity. The only gene tested here is TRAIL, so it would be useful to know if other important IRF-1 targets also require IRF-1 turnover for their transcription. The apparent drugability of this pathway would depend on which pathways phosphorylated IRF-1 regulates. Recent work has suggested that GSK3β is involved in inflammation, although the mechanisms of this action are usually attributed to GSK3β phosphorylation of NFκB proteins. Many inflammatory genes are co-regulated by NFκB and IRF-1 proteins. A table of genes that are known IRF-1 transcriptional targets, whose expression is modulated by GSK3β, is given below.

Gene	Effect of IRF-1	Effect of GSK3β	Reference
CD95	↑	↑	Beurel *et al.* 2004
ICAM	↑	↑	Gotschel *et al.* 2008
IL-12p35	↑	↑	Rodionova *et al.* 2007
IL-12p40	↑	↑	Martin *et al.* 2005
iNOS	↑	↑	Gotschel *et al.* 2008 & Yuskaitis and Jope 2009
RANTES	↑	↑	Wang *et al.* 2009 & Gong *et al.* 2005
TRAIL	↑	↑	Wang *et al.* 2002
VCAM	↑	↑	Eto *et al.* 2005

Table 7.1. Genes that are co-regulated by IRF-1 and GSK3β. Reported instances of IRF-1 target gene expression being altered by GSK3β inhibition, knockdown or absence in knockout mice.

Does phosphorylation offer a therapeutic route to regulating IRF-1 activity?

Clinically, IRF-1 expression is druggable, due to its induction by IFNs and retinoids. Evidence suggests that IRF-1 is an important cellular mediator of these agents in human diseases (see 1.4.1-1.4.5). Presently little is known about the control of IRF-1 activity post translation, pursuing inhibitors of IRF-1 activity could therefore be of use in a number of diseases associated with inappropriate IRF-1 action – most of these are inflammatory conditions, although IRF-1 is also required for HIV replication (Sgarbanti *et al.* 2008 and Remoli *et al.* 2006). GSK3β inhibitors are currently being investigated for their roles in cancer, diabetes and bi-polar disorder (Martinez *et al.* 2002). The anti-inflammatory actions of some of these inhibitors has been attributed to their action of NFκB, however IRF-1 is well known to co-operate with NFκB family members in the induction of genes, consequently GSK3β inhibitors may act on both IRF-1 and NFκB.

Is Fbxw7α a novel coactivator of IRF-1?

It has not been fully established if Fbxw7α is a direct a coactivator of IRF-1 transcriptional activity. Knockdown of Fbxw7α was not carried out to determine its effects on IRF-1 activity. However, mutation of either Thr^{180} or Ser^{184} to alanine reduces the interaction between Fbxw7α and IRF-1, and consequently IRF-1 transcriptional activity;.

This would infer that Fbxw7α acts as a coactivator of IRF-1 on the TRAIL promoter. Fbxw7α serves as a coactivator of SRC-3 by promoting multi-mono ubiquitination which may be involved in protein-protein interactions with nuclear receptors (Wu *et al.* 2007). Consequently Fbxw7a may serve as a coactivator of IRF-1 by modulating its stability. A number of ubiquitin E3 ligases act as co-activators towards their substrate TFs. HectH3 promotes K^{63} linked ubiquitination of c-Myc, which is required for interaction with p300, this interaction is needed for c-Myc transcriptional activity on a subset of promoters (Adhikary *et al.* 2005). Another ubiquitin E3, Skp2 also acts as a co-activator of c-Myc function by promoting degradation (von der Lehr *et al.* 2003) RNF6 (RING Finger 6) promotes ubiquitination of AR (Androgen Receptor) via K^6 and K^{27} linkages. Depletion of RNF6 or substitution of the ubiquitinated Lys residues results in an alteration in the AR transcriptional programme. Ubiquitination of AR was found to be essential for its promoter recruitment and its interaction with the co-activator ARA54 (AR Associated Protein 54), which contains ubiquitin interaction domains *(Xu et al. 2009b). A number of RING finger ubiquitin ligases serve as co-activators of transcription factors, including RNF4, RNF8, RNF25 and RNF31* (Takano *et al.* 2004; Perry *et al.* 2008 and Ehrlund *et al.* 2009) Further

experiments are needed to determine how Fbxw7α regulates IRF-1 activity, whether through regulating IRF-1 abundance or ubiquitin dependent protein interactions with the transcriptional machinery. Fbxw7 is also mutated in a number of cancers (Welcker and Clurman 2008) and therefore it would be interesting to determine if IRF-1 is active in these cancers.

Is Ser^{184} essential for IRF-1 activity?

Perhaps neglected in this study, Ser^{184} nether-the-less deserves further study. The indication that it is required for Thr^{180} phosphorylation suggests that Ser^{184} phosphorylation is critical for IRF-1 activity. Although the two alanine and phosphomimic mutants appear to phenocopy one another in a number of assays, it is important not to discard Ser^{184} phosphorylation as merely a priming event. The signalling up-stream of the Ser^{184} kinase will likely have major effects on the IRF-1 transcriptional programme. It should also be considered that the activity of Ser^{184} has only been studied in the context of the TRAIL promoter and a synthetic construct. Other promoters could therefore be dependent on the phosphorylation of Ser^{184} completely independently of its ability to prime Thr^{180} phosphorylation. As mentioned elsewhere, GSK3β is a tightly controlled kinase, and presence of a priming mark on a substrate does not necessarily pre-requisite Thr^{180} phosphorylation. Studies on c-Myc have suggested that Ser^{62} phosphorylation is required for directing c-Myc towards promoters involved in the clearance of free radicals. Loss of Thr^{58} phosphorylation (through use of alanine mutants) had no effect on c-Myc recruitment or activity on these promoters. This opens up the possibility that Ser^{184} phosphorylation could be involved in targeting IRF-1 to

certain promoters, and Thr^{180} phosphorylation promotes clearance from these promoters.

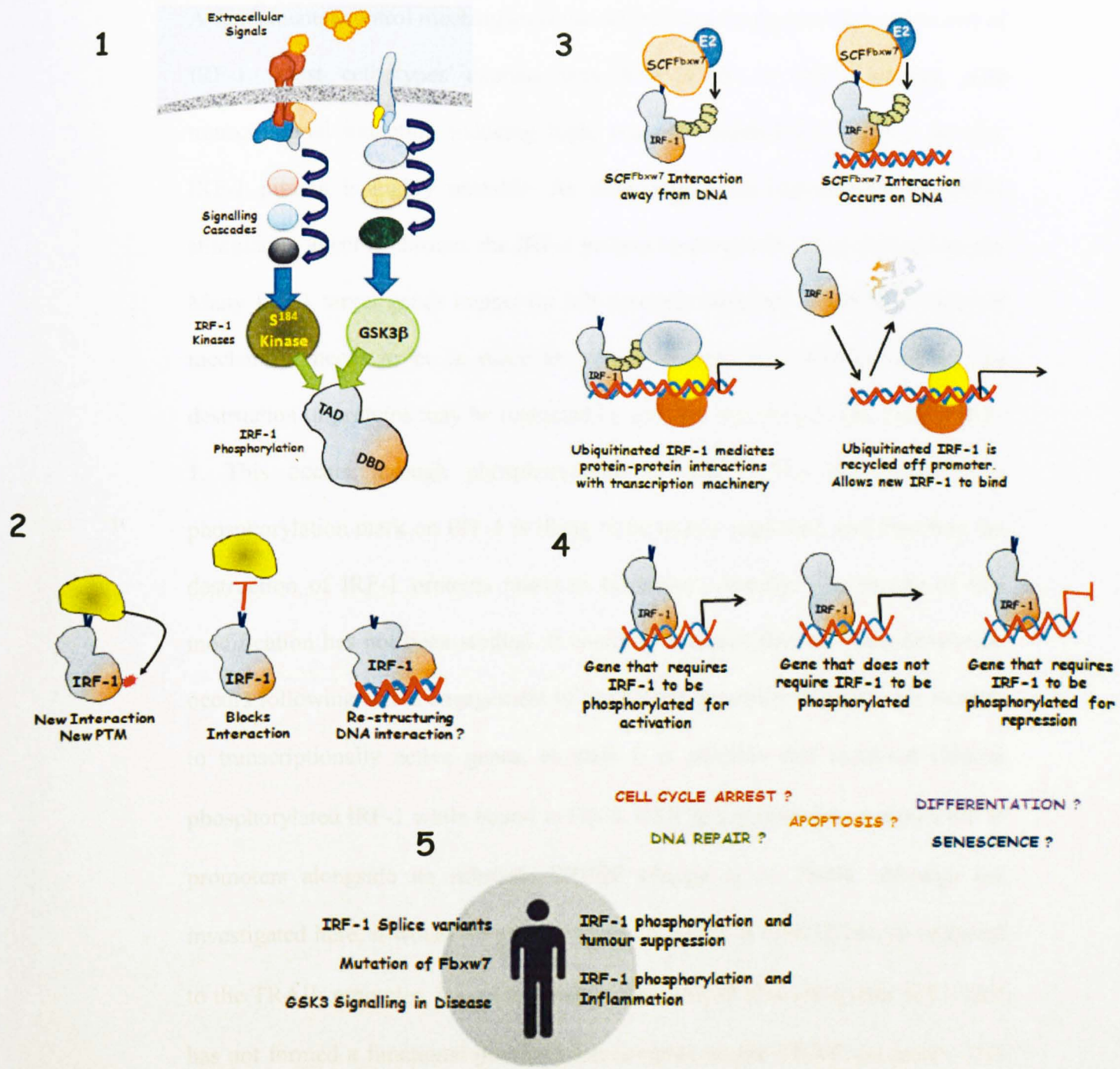

Figure 7.2. Further work on the IRF-1 phosphorylation-ubiquitination axis
1) The signalling pathways that regulate the IRF-1 kinases, and the potential for extra-cellular stimuli to regulate IRF-1 phosphorylation. 2) Effect of phosphorylation / ubiquitination on protein-protein interactions and structure / DNA binding. Phosphorylation has been shown not to effect IRF-1 localisation. 3) Subcellular location of IRF-1 during phosphorylation and ubiquitination. 4) Effects of IRF-1 phosphorylation on the transcription cycle, and the specificity of this event in determining promoter selection. Thus potentially affecting the IRF-1 transcriptional programme. 5) The effects of IRF-1 phosphorylation in human disease, does this pathway offer a route for therapeutic intervention in IRF-1 activity?

A fundamental control mechanism is the cell's ability to regulate the expression of IRF-1. Most cell types express very low levels of IRF-1 protein, with transcriptional induction inducing high, transient expression of IRF-1 protein. IRF-1 protein is highly unstable. As such, unless the exposure to the IRF-1 stimulating agent is chronic, the IRF-1 protein levels quickly drop to basal levels. Many IRF-1 target genes impact on cell survival, therefore an effective shut-off mechanism needs to be in place to prevent chronic activation of IRF-1. The destruction of proteins may be regulated by cellular signalling in the case of IRF-1. This occurs through phosphorylation of Thr^{180}. The acquisition of a phosphorylation mark on IRF-1 is likely to be tightly regulated, and therefore the destruction of IRF-1 proteins needs to be timed correctly. The timing of this modification has not been studied. It could be assumed that the phosphorylation occurs following active engagement of the TRAIL promoter. Kinases can localise to transcriptionally active genes, as such it is possible that localised GSK3β phosphorylated IRF-1 while bound to DNA. GSK3β has been detected by ChIP at promoters alongside its substrate SREBP (Punga *et al.* 2006), although not investigated here, it would be interesting to determine if GSK3β can be recruited to the TRAIL promoter. It is also possible that GSK3β phosphorylates IRF-1 that has not formed a functional pre-initiation complex on the TRAIL promoter. This would cause it to be cleared away, allowing new IRF-1 to be recruited and re-start complex assembly. Given the number and complexity of proteins that need to be recruited to promoters, and the stringent controls placed on transcription it could be possible that such mechanisms are in place to regulate IRF-1. It would also explain why increasing GSK3β expression/activity does not increase TRAIL transactivation, since GSK3β only promotes clearance of aberrant IRF-1. A third

potential mechanism is that GSK3β phosphorylation occurs on IRF-1 not bound to promoters, and rather controls local concentration of IRF-1. Overly high concentrations of IRF-1 in the vicinity of promoters may interfere with other proteins gaining access to the DNA. Phosphorylation also allows specific protein-protein interactions. One such interaction has been shown in this study (Fbxw7α), however it cannot be discounted that other interactions occur through Thr^{180}/Ser^{184}. The ability of the K→R mutants to be phosphorylated (figure 5.16), at Thr^{180}/Ser^{184}, but exhibited reduced activity on the TRAIL promoter (figure 5.15) suggests that the main activity of Thr^{180} is in promoting ubiquitination of lysine acceptor residues. Therefore this work has identified phosphorylation dependent degradation of IRF-1 as being crucial for its transcriptional activity.

IRF-1 plays essential roles in terms of tumour suppression and immune defence, but IRF-1 expression can also be extremely detrimental to cells. This in part explains the molecular "short leash" which IRF-1 is kept on by various control pathways. While IRF-$1^{-/-}$ mice may be severely immune-compromised and more prone to tumour development, they are resistant to experimentally induced diabetes, colitis, sepsis, arthritis, thyroiditis, allergic encephalomyelitis, arteritis, lupus and graft rejection (Baron *et al.* 2004, Streetz *et al.* 2001, Jaruga *et al.* 2004 , Tsung *et al.* 2006 , Siegmund *et al.* 2004, Gysemans *et al.* 2009 Nakazawa *et al.* 2001, Tada *et al.* 1997, Tani *et al.* 2002 , Afrouzian *et al.* 2002, Cordoba *et al.* 2006 and Reilly *et al.* 2006). Additionally excessive levels of IRF-1 can be found in biopsies of celiac disease, brain haemorrhage and chrohns disease (De Stefano *et al.* 2006, Paschen *et al.* 1998 and Clavell *et al.* 2000). Clearly, when IRF-1 expression is not properly controlled it can lead to severe pathological defects. It is highly likely that the ability of IRF-1 to regulate

TRAIL expression would need to be tightly regulated. Although TRAIL posses a selective preference for promoting cell death in cancer cells, it is also able to promote cell death in normal tissue also, as such this pro-apoptotic death ligand needs to be expressed in a controlled manner (Koschny *et al.* 2007).

CHAPTER 8: SUPPLEMENTARY DATA

S1 Testing H3396-TetR clones.

To determine expression level of the TetR protein in transfected H3396 cells, immunoblots were carried out against TetR. All ten clones expressed TetR at the expected molecular weight of 25 kDa. The ratio of TetR to β-actin was calculated to compensate for protein loading. Clones D5, D10, C6, D6, E4, G2 and E8 were expanded further, however C6, D5, E4 and E8 were the only clones to survive. The activity of the TetR was measured by a pcDNA4-TO-Luc reporter. In this system, upon transfection the Luc reporter is repressed by the TetR protein within the cells. Treatment with dox relieves the repression by altering the structure of the TetR protein, allowing Luc expression. The fold change (de-repression) between untreated and dox treated is then measured. All clones except E8 exhibited de-repression. Clone E4 was chosen for stable transfection with pcDNA4-TO-IRF-1.

S2 Testing H3396-TetR – IRF-1 clones.

Immunoblots of mouse IRF-1 (M20) expression in the stable cell lines is shown in figure S2. The levels of IRF-1 protein were corrected for actin expression, and the fold was used to choose which cell lines to continue growing. Clones that failed to express IRF-1, or expressed IRF-1 without dox treatment were discarded.

S3 Localisation of YFP-IRF-1 in Cos and HEK293 cells.

The localisation of YFP tagged IRF-1 was investigated in Cos7 and HEK293 cells. All IRF-1 constructs were expressed diffusely throughout the nucleus.

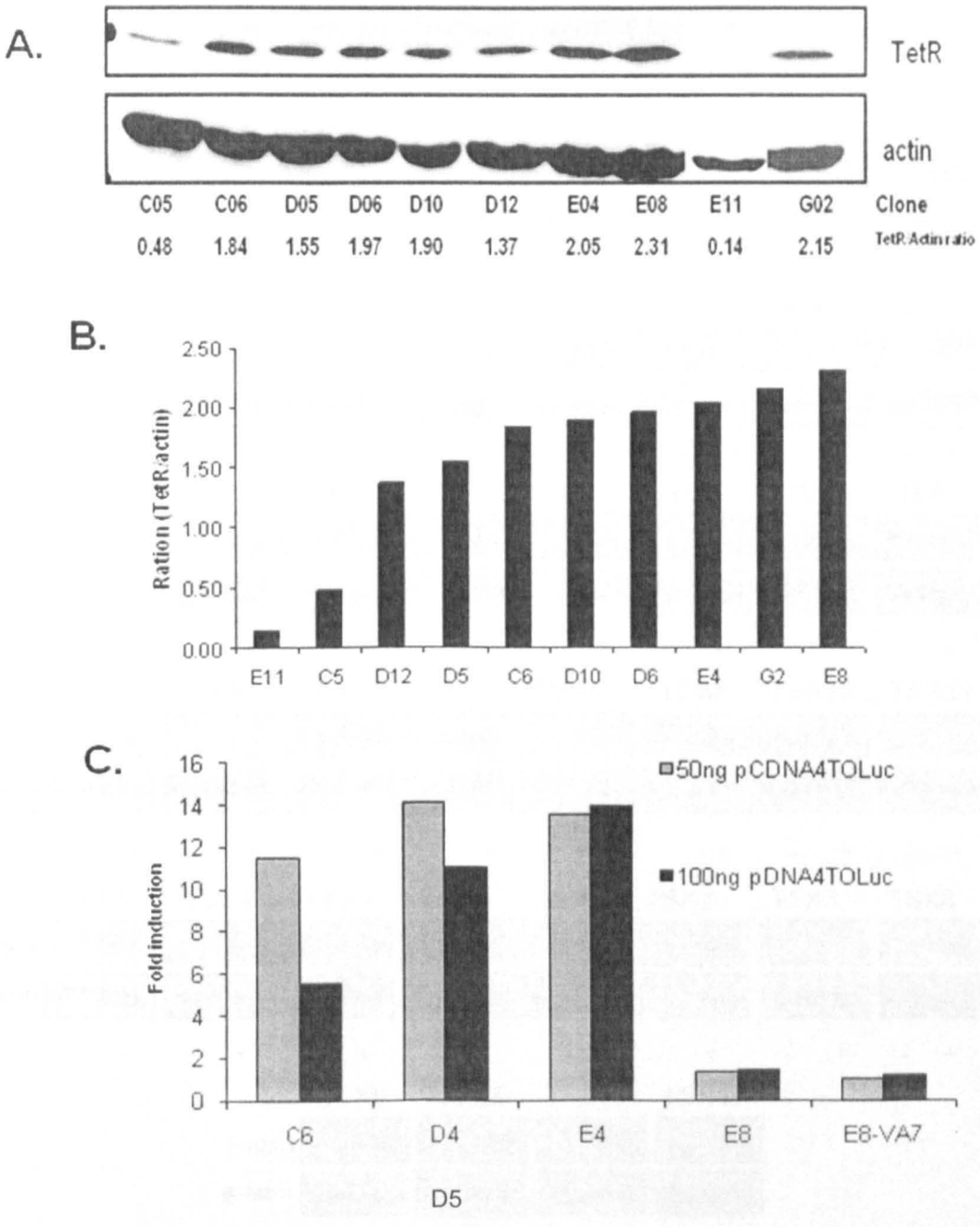

Figure S1. Testing and selection of TetR H3396 cell lines. ***(A)*** Immunoblot (20 μg/lane) of TetR and β-actin expression in extracts from TetR expressing clones. The ratio between TetR and β-actin is given below each clone name. The expression ratio is illustrated in **(B). (C)** pcDNA4-TO-Luc de-repression reporter. 4 clones were transfected with either 50 (grey) or 100 ng pcDNA4-TO-Luc and treated with 1 μg/μL dox or vehicle for 24 hours. Bars indicate the fold induction between vehicle and dox.

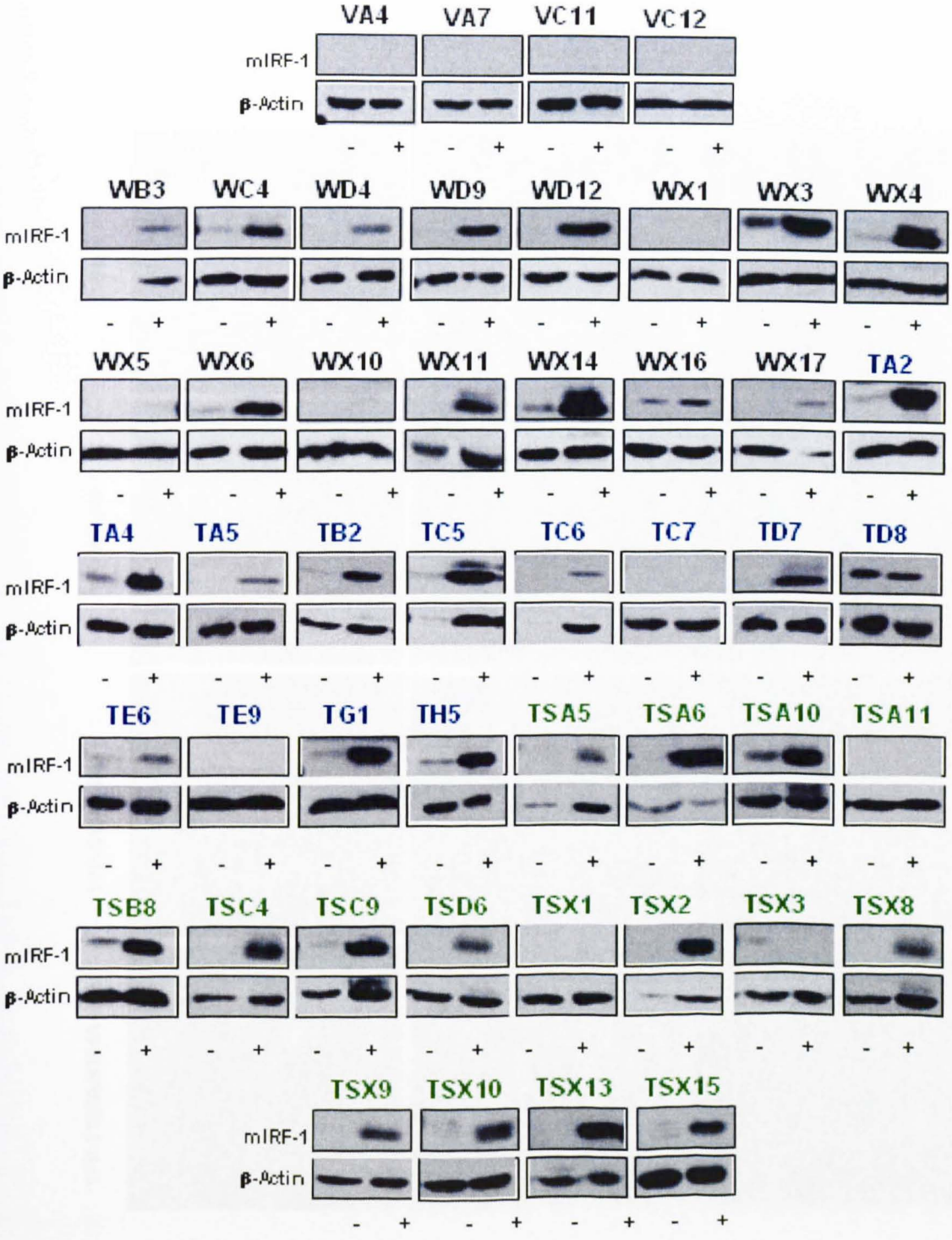

Figure S2. Expression of mIRF-1 following dox treatment. 48 clones were induced with dox at 2 μg/mL or blank media for 24 hours and lysed. Immunoblots against IRF-1 and β actin were performed to determine induction efficiency. – denotes blank media and + indicates dox treatment.

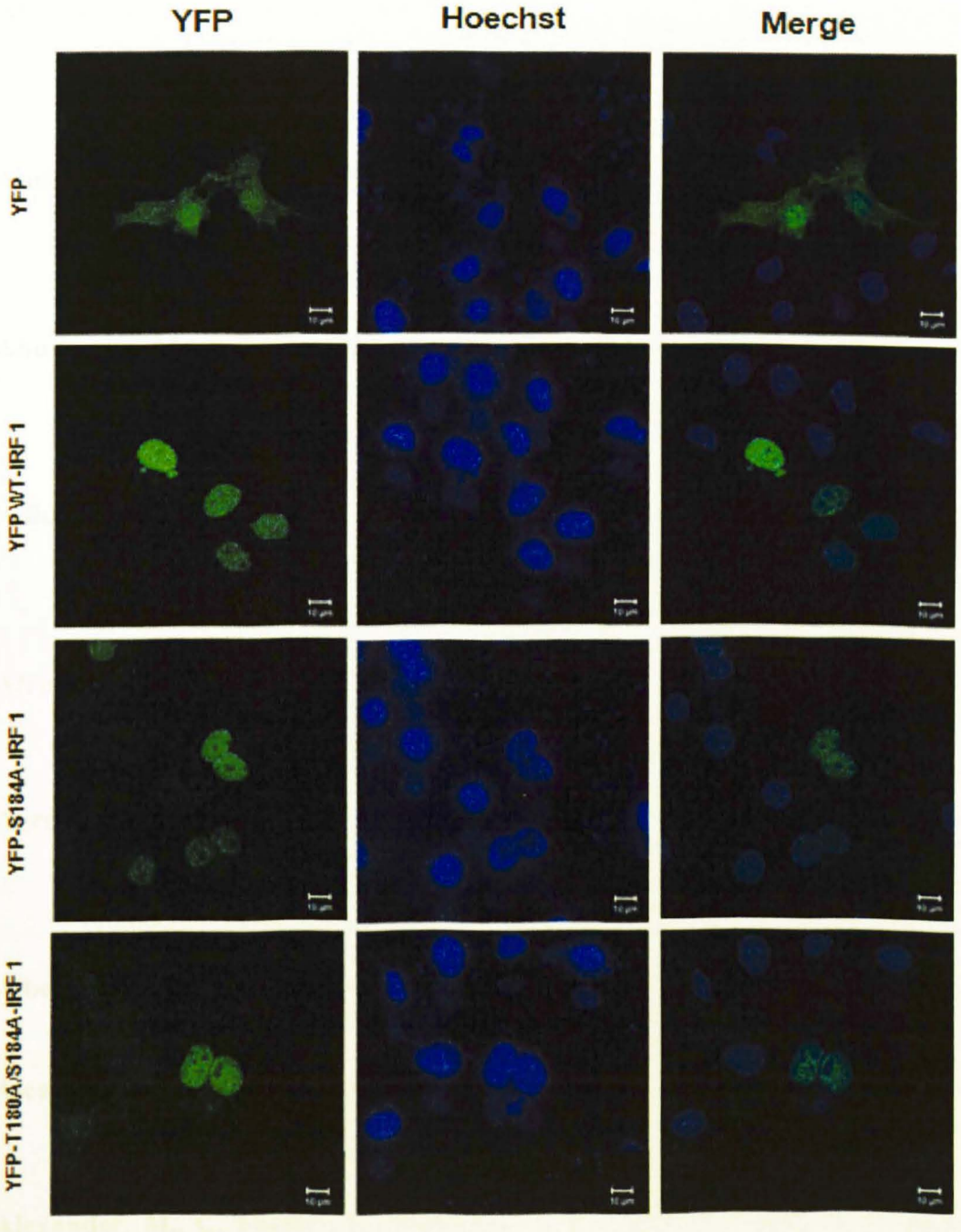

Figure S3 Localisation of various YFP-IRF-1 constructs in Cos-1 cells. Direct fluorescence (YFP) of the proteins indicated at the left are shown in green. DNA staining (Hoechst) is shown in blue and a merged image to illustrate the transfection efficiencies are presented. Measure bar represents 10μm.

References

Abarca-Heidemann, K., S. Friederichs, T. Klamp, U. Boehm, L. A. Guethlein and B. Ortmann (2002). Regulation of the expression of mouse TAP-associated glycoprotein (tapasin) by cytokines. *Immunol Lett* **83**(3): 197-207.

Abdollahi, A., K. A. Lord, B. Hoffman-Liebermann and D. A. Liebermann (1991). Interferon regulatory factor 1 is a myeloid differentiation primary response gene induced by interleukin 6 and leukemia inhibitory factor: role in growth inhibition. *Cell Growth Differ* **2**(8): 401-7.

Abu-Farha, M., J. P. Lambert, A. S. Al-Madhoun, F. Elisma, I. S. Skerjanc and D. Figeys (2008). The tale of two domains: proteomics and genomics analysis of SMYD2, a new histone methyltransferase. *Mol Cell Proteomics* **7**(3): 560-72.

Adhikary, S., F. Marinoni, A. Hock, E. Hulleman, N. Popov, R. Beier, S. Bernard, M. Quarto, M. Capra, S. Goettig, U. Kogel, M. Scheffner, et al. (2005). The ubiquitin ligase HectH9 regulates transcriptional activation by Myc and is essential for tumor cell proliferation. *Cell* **123**(3): 409-21.

Afrouzian, M., V. Ramassar, J. Urmson, L. F. Zhu and P. F. Halloran (2002). Transcription factor IRF-1 in kidney transplants mediates resistance to graft necrosis during rejection. *J Am Soc Nephrol* **13**(5): 1199-209.

Agresti, C., A. Bernardo, N. Del Russo, G. Marziali, A. Battistini, F. Aloisi, G. Levi and E. M. Coccia (1998). Synergistic stimulation of MHC class I and IRF-1 gene expression by IFN-gamma and TNF-alpha in oligodendrocytes. *Eur J Neurosci* **10**(9): 2975-83.

Alberts B, Johnson A, Lewis J, Raff M, Roberts K and Walter P (2002). Molecular biology of the cell 4th edition, Garland science.

Alcantara, F. F., H. Tang and A. McLachlan (2002). Functional characterization of the interferon regulatory element in the enhancer 1 region of the hepatitis B virus genome. *Nucleic Acids Res* **30**(9): 2068-75.

Alexander, M., C. Forster, K. Sugimoto, H. B. Clark, S. Vogel, M. E. Ross and C. Iadecola (2003). Interferon regulatory factor-1 immunoreactivity in neurons and inflammatory cells following ischemic stroke in rodents and humans. *Acta Neuropathol* **105**(5): 420-4.

Aly, S., J. Mages, N. Reiling, U. Kalinke, T. Decker, R. Lang and S. Ehlers (2008). Mycobacteria-induced granuloma necrosis depends on IRF-1. *J Cell Mol Med*.

Andela, V. B. and R. N. Rosier (2004). The proteosome inhibitor MG132 attenuates retinoic acid receptor trans-activation and enhances trans-repression of nuclear factor kappaB. Potential relevance to chemo-preventive interventions with retinoids. *Mol Cancer* **3**: 8.

Andersen, P., M. W. Pedersen, A. Woetmann, M. Villingshoj, M. T. Stockhausen, N. Odum and H. S. Poulsen (2008). EGFR induces expression of IRF-1 via STAT1 and STAT3 activation leading to growth arrest of human cancer cells. *Int J Cancer* **122**(2): 342-9.

Ansieau, S. and A. Leutz (2002). The conserved Mynd domain of BS69 binds cellular and oncoviral proteins through a common PXLXP motif. *J Biol Chem* **277**(7): 4906-10.

Arany, I., K. J. Grattendick, W. E. Whitehead, I. A. Ember and S. K. Tyring (2003a). A functional interferon regulatory factor-1 (IRF-1)-binding site in the upstream regulatory region (URR) of human papillomavirus type 16. *Virology* **310**(2): 280-6.

Arany, I., W. E. Whitehead, I. A. Ember and S. K. Tyring (2003b). Dose-dependent activation of p21WAF1 transcription by all-trans-acid in cervical squamous carcinoma cells. *Anticancer Res* **23**(1A): 495-7.

Au, W. C., P. A. Moore, W. Lowther, Y. T. Juang and P. M. Pitha (1995). Identification of a member of the interferon regulatory factor family that binds to the interferon-stimulated response element and activates expression of interferon-induced genes. *Proc Natl Acad Sci U S A* **92**(25): 11657-61.

Au, W. C. and P. M. Pitha (2001). Recruitment of multiple interferon regulatory factors and histone acetyltransferase to the transcriptionally active interferon a promoters. *J Biol Chem* **276**(45): 41629-37.

Azimi, N., K. M. Shiramizu, Y. Tagaya, J. Mariner and T. A. Waldmann (2000). Viral activation of interleukin-15 (IL-15): characterization of a virus-inducible element in the IL-15 promoter region. *J Virol* **74**(16): 7338-48.

Bahram, F., N. von der Lehr, C. Cetinkaya and L. G. Larsson (2000). c-Myc hot spot mutations in lymphomas result in inefficient ubiquitination and decreased proteasome-mediated turnover. *Blood* **95**(6): 2104-10.

Bai, C., P. Sen, K. Hofmann, L. Ma, M. Goebl, J. W. Harper and S. J. Elledge (1996). SKP1 connects cell cycle regulators to the ubiquitin proteolysis machinery through a novel motif, the F-box. *Cell* **86**(2): 263-74.

Baker, M. S., X. Chen, A. R. Rotramel, J. J. Nelson and D. B. Kaufman (2003). Interferon regulatory factor-1 down-regulates cytokine-induced IP-10 expression in pancreatic islets. *Surgery* **134**(2): 134-41.

Barnes, B. J., A. E. Field and P. M. Pitha-Rowe (2003). Virus-induced heterodimer formation between IRF-5 and IRF-7 modulates assembly of the IFNA enhanceosome in vivo and transcriptional activity of IFNA genes. *J Biol Chem* **278**(19): 16630-41.

Baron, R. M., I. M. Carvajal, X. Liu, R. O. Okabe, L. E. Fredenburgh, A. A. Macias, Y. H. Chen, K. Ejima, M. D. Layne and M. A. Perrella (2004). Reduction of nitric oxide synthase 2 expression by distamycin A improves survival from endotoxemia. *J Immunol* **173**(6): 4147-53.

Benassi, B., M. Fanciulli, F. Fiorentino, A. Porrello, G. Chiorino, M. Loda, G. Zupi and A. Biroccio (2006). c-Myc phosphorylation is required for cellular response to oxidative stress. *Mol Cell* **21**(4): 509-19.

Benedito, A. B., M. Lehtinen, R. Massol, U. G. Lopes, T. Kirchhausen, A. Rao and A. Bonni (2005). The transcription factor NFAT3 mediates neuronal survival. *J Biol Chem* **280**(4): 2818-25.

Berger, S. L. (2002). Histone modifications in transcriptional regulation. *Curr Opin Genet Dev* **12**(2): 142-8.

Beurel, E., M. Kornprobst, M. J. Blivet-Van Eggelpoel, C. Ruiz-Ruiz, A. Cadoret, J. Capeau and C. Desbois-Mouthon (2004). GSK-3beta inhibition by lithium confers resistance to chemotherapy-induced apoptosis through the repression of CD95 (Fas/APO-1) expression. *Exp Cell Res* **300**(2): 354-64.

Bhandare, R., G. Damera, A. Banerjee, J. R. Flammer, S. Keslacy, I. Rogatsky, R. A. Panettieri, Y. Amrani and O. Tliba (2009). Glucocorticoid Receptor Interacting Protein-1 Restores glucocorticoid Responsiveness in Steroid-resistant Airway Structural Cells. *Am J Respir Cell Mol Biol.*

Bijur, G. N. and R. S. Jope (2003). Glycogen synthase kinase-3 beta is highly activated in nuclei and mitochondria. *Neuroreport* **14**(18): 2415-9.

Blanco, J. C., C. Contursi, C. A. Salkowski, D. L. DeWitt, K. Ozato and S. N. Vogel (2000). Interferon regulatory factor (IRF)-1 and IRF-2 regulate interferon gamma-dependent cyclooxygenase 2 expression. *J Exp Med* **191**(12): 2131-44.

Book McAlexander, M. and L. Yu-Lee (2001a). Prolactin activation of IRF-1 transcription involves changes in histone acetylation. *FEBS Lett* **488**(1-2): 91-4.

Book McAlexander, M. and L. Y. Yu-Lee (2001b). Sp1 is required for prolactin activation of the interferon regulatory factor-1 gene. *Mol Cell Endocrinol* **184**(1-2): 135-41.

Bouker, K. B., T. C. Skaar, D. S. Harburger, R. B. Riggins, D. R. Fernandez, A. Zwart and R. Clarke (2007). The A4396G polymorphism in interferon regulatory factor 1 is frequently expressed in breast cancer cell lines. *Cancer Genet Cytogenet* **175**(1): 61-4.

Bouker, K. B., T. C. Skaar, R. B. Riggins, D. S. Harburger, D. R. Fernandez, A. Zwart, A. Wang and R. Clarke (2005). Interferon regulatory factor-1 (IRF-1) exhibits tumor suppressor activities in breast cancer associated with caspase activation and induction of apoptosis. *Carcinogenesis* **26**(9): 1527-35.

Boultwood, J., C. Fidler, S. Lewis, A. MacCarthy, H. Sheridan, S. Kelly, D. Oscier, V. J. Buckle and J. S. Wainscoat (1993). Allelic loss of IRF1 in myelodysplasia and acute myeloid leukemia: retention of IRF1 on the 5q- chromosome in some patients with the 5q- syndrome. *Blood* **82**(9): 2611-6.

Brass, A. L., A. Q. Zhu and H. Singh (1999). Assembly requirements of PU.1-Pip (IRF-4) activator complexes: inhibiting function in vivo using fused dimers. *EMBO J* **18**(4): 977-91.

Brucet, M., L. Marques, C. Sebastian, J. Lloberas and A. Celada (2004). Regulation of murine Tap1 and Lmp2 genes in macrophages by interferon gamma is mediated by STAT1 and IRF-1. *Genes Immun* **5**(1): 26-35.

Burysek, L., W. S. Yeow, B. Lubyova, M. Kellum, S. L. Schafer, Y. Q. Huang and P. M. Pitha (1999). Functional analysis of human herpesvirus 8-encoded viral interferon regulatory factor 1 and its association with cellular interferon regulatory factors and p300. *J Virol* **73**(9): 7334-42.

Calhoun, E. S., J. B. Jones, R. Ashfaq, V. Adsay, S. J. Baker, V. Valentine, P. M. Hempen, W. Hilgers, C. J. Yeo, R. H. Hruban and S. E. Kern (2003). BRAF and FBXW7 (CDC4, FBW7, AGO, SEL10) mutations in distinct subsets of pancreatic cancer: potential therapeutic targets. *Am J Pathol* **163**(4): 1255-60.

Casano, F. J., A. M. Rolando, J. S. Mudgett and S. M. Molineaux (1994). The structure and complete nucleotide sequence of the murine gene encoding interleukin-1 beta converting enzyme (ICE). *Genomics* **20**(3): 474-81.

Casciano, I., A. De Ambrosis, M. Croce, G. Pagnan, A. Di Vinci, G. Allemanni, B. Banelli, M. Ponzoni, M. Romani and S. Ferrini (2004). Expression of the caspase-8 gene in neuroblastoma cells is regulated through an essential interferon-sensitive response element (ISRE). *Cell Death Differ* **11**(1): 131-4.

Cavalli, L. R., R. B. Riggins, A. Wang, R. Clarke and B. R. Haddad (2009). Frequent loss of heterozygosity at the interferon regulatory factor-1 gene locus in breast cancer. *Breast Cancer Res Treat.*

Cho, J. H. and G. V. Johnson (2003). Glycogen synthase kinase 3beta phosphorylates tau at both primed and unprimed sites. Differential impact on microtubule binding. *J Biol Chem* **278**(1): 187-93.

Cho, Y. C., H. J. Kim, Y. J. Kim, K. Y. Lee, H. J. Choi, I. S. Lee and B. Y. Kang (2008). Differential anti-inflammatory pathway by xanthohumol in IFN-gamma and LPS-activated macrophages. *Int Immunopharmacol* **8**(4): 567-73.

Chou, T. Y., G. W. Hart and C. V. Dang (1995). c-Myc is glycosylated at threonine 58, a known phosphorylation site and a mutational hot spot in lymphomas. *J Biol Chem* **270**(32): 18961-5.

Chow, W. A., J. J. Fang and J. K. Yee (2000). The IFN regulatory factor family participates in regulation of Fas ligand gene expression in T cells. *J Immunol* **164**(7): 3512-8.

Ciccaglione, A. R., E. Stellacci, C. Marcantonio, V. Muto, M. Equestre, G. Marsili, M. Rapicetta and A. Battistini (2007). Repression of interferon regulatory factor 1 by hepatitis C virus core protein results in inhibition of antiviral and immunomodulatory genes. *J Virol* **81**(1): 202-14.

Clarke, N., A. M. Jimenez-Lara, E. Voltz and H. Gronemeyer (2004). Tumor suppressor IRF-1 mediates retinoid and interferon anticancer signaling to death ligand TRAIL. *EMBO J* **23**(15): 3051-60.

Clavell, M., H. Correa-Gracian, Z. Liu, R. Craver, R. Brown, E. Schmidt-Sommerfeld, J. Udall, Jr., A. Delgado and E. Mannick (2000). Detection of interferon regulatory factor-1 in lamina propria mononuclear cells in Crohn's disease. *J Pediatr Gastroenterol Nutr* **30**(1): 43-7.

Coccia, E. M., E. Stellacci, M. Valtieri, B. Masella, T. Feccia, G. Marziali, J. Hiscott, U. Testa, C. Peschle and A. Battistini (2001). Ectopic expression of interferon regulatory factor-1 potentiates granulocytic differentiation. *Biochem J* **360**(Pt 2): 285-94.

Cole, A., S. Frame and P. Cohen (2004). Further evidence that the tyrosine phosphorylation of glycogen synthase kinase-3 (GSK3) in mammalian cells is an autophosphorylation event. *Biochem J* **377**(Pt 1): 249-55.

Colonna, M. (2007). TLR pathways and IFN-regulatory factors: to each its own. *Eur J Immunol* **37**(2): 306-9.

Connett, J. M., L. Badri, T. J. Giordano, W. C. Connett and G. M. Doherty (2005). Interferon regulatory factor 1 (IRF-1) and IRF-2 expression in breast cancer tissue microarrays. *J Interferon Cytokine Res* **25**(10): 587-94.

Conte, E., L. Manzella, A. Zeuner, G. Cocchiaro, C. Conticello, L. Zammataro, C. G. Messina, R. De Maria and A. Messina (2003). Involvement of interferon regulatory factor-1 in monocyte CD95 expression and CD95-mediated apoptosis. *Cell Death Differ* **10**(5): 615-7.

Coppola, D., V. Parikh, D. Boulware and G. Blanck (2009). Substantially reduced expression of PIAS1 is associated with colon cancer development. *J Cancer Res Clin Oncol* **135**(9): 1287-91.

De Ambrosis, A., I. Casciano, M. Croce, G. Pagnan, L. Radic, B. Banelli, A. Di Vinci, G. Allemanni, G. P. Tonini, M. Ponzoni, M. Romani and S. Ferrini (2007). An interferon-sensitive response element is involved in constitutive caspase-8 gene expression in neuroblastoma cells. *Int J Cancer* **120**(1): 39-47.

De Creus, A., K. Van Beneden, F. Stevenaert, V. Debacker, J. Plum and G. Leclercq (2002). Developmental and functional defects of thymic and epidermal V gamma 3 cells in IL-15-deficient and IFN regulatory factor-1-deficient mice. *J Immunol* **168**(12): 6486-93.

Deng, W. G. and K. K. Wu (2003). Regulation of inducible nitric oxide synthase expression by p300 and p50 acetylation. *J Immunol* **171**(12): 6581-8.

Dennis, A. P., D. M. Lonard, Z. Nawaz and B. W. O'Malley (2005). Inhibition of the 26S proteasome blocks progesterone receptor-dependent transcription through failed recruitment of RNA polymerase II. *J Steroid Biochem Mol Biol* **94**(4): 337-46.

Deshaies, R. J. and C. A. Joazeiro (2009). RING domain E3 ubiquitin ligases. *Annu Rev Biochem* **78**: 399-434.

Detjen, K. M., K. Farwig, M. Welzel, B. Wiedenmann and S. Rosewicz (2001). Interferon gamma inhibits growth of human pancreatic carcinoma cells via caspase-1 dependent induction of apoptosis. *Gut* **49**(2): 251-62.

Diehl, J. A., M. Cheng, M. F. Roussel and C. J. Sherr (1998). Glycogen synthase kinase-3beta regulates cyclin D1 proteolysis and subcellular localization. *Genes Dev* **12**(22): 3499-511.

Doble, B. W. and J. R. Woodgett (2003). GSK-3: tricks of the trade for a multi-tasking kinase. *J Cell Sci* **116**(Pt 7): 1175-86.

Doherty, G. M., L. Boucher, K. Sorenson and J. Lowney (2001). Interferon regulatory factor expression in human breast cancer. *Ann Surg* **233**(5): 623-9.

Dornan, D., M. Eckert, M. Wallace, H. Shimizu, E. Ramsay, T. R. Hupp and K. L. Ball (2004). Interferon regulatory factor 1 binding to p300 stimulates DNA-dependent acetylation of p53. *Mol Cell Biol* **24**(22): 10083-98.

Drew, P. D., G. Franzoso, K. G. Becker, V. Bours, L. M. Carlson, U. Siebenlist and K. Ozato (1995a). NF kappa B and interferon regulatory factor 1 physically interact and synergistically induce major histocompatibility class I gene expression. *J Interferon Cytokine Res* **15**(12): 1037-45.

Drew, P. D., G. Franzoso, L. M. Carlson, W. E. Biddison, U. Siebenlist and K. Ozato (1995b). Interferon regulatory factor-2 physically interacts with NF-kappa B in vitro and inhibits NF-kappa B induction of major histocompatibility class I and beta 2-microglobulin gene expression in transfected human neuroblastoma cells. *J Neuroimmunol* **63**(2): 157-62.

Dror, N., M. Alter-Koltunoff, A. Azriel, N. Amariglio, J. Jacob-Hirsch, S. Zeligson, A. Morgenstern, T. Tamura, H. Hauser, G. Rechavi, K. Ozato and B. Z. Levi (2007). Identification of IRF-8 and IRF-1 target genes in activated macrophages. *Mol Immunol* **44**(4): 338-46.

Duncan, G. S., H. W. Mittrucker, D. Kagi, T. Matsuyama and T. W. Mak (1996). The transcription factor interferon regulatory factor-1 is essential for natural killer cell function in vivo. *J Exp Med* **184**(5): 2043-8.

Eason, D. D., C. LeBron, D. Coppola, L. C. Moscinski, S. Livingston, E. T. Sutton and G. Blanck (2003). Development of CD30+ lymphoproliferative disease in mice lacking interferon regulatory factor-1. *Oncogene* **22**(40): 6166-76.

Eckert, M., S. E. Meek and K. L. Ball (2006). A novel repressor domain is required for maximal growth inhibition by the IRF-1 tumor suppressor. *J Biol Chem* **281**(32): 23092-102.

Ehrlund, A., E. H. Anthonisen, N. Gustafsson, N. Venteclef, K. Robertson Remen, A. E. Damdimopoulos, A. Galeeva, M. Pelto-Huikko, E. Lalli, K. R. Steffensen, J. A. Gustafsson and E. Treuter (2009). E3 ubiquitin ligase RNF31 cooperates with DAX-1 in transcriptional repression of steroidogenesis. *Mol Cell Biol* **29**(8): 2230-42.

Elser, B., M. Lohoff, S. Kock, M. Giaisi, S. Kirchhoff, P. H. Krammer and M. Li-Weber (2002). IFN-gamma represses IL-4 expression via IRF-1 and IRF-2. *Immunity* **17**(6): 703-12.

Eom, T. Y. and R. S. Jope (2009). GSK3 beta N-terminus binding to p53 promotes its acetylation. *Mol Cancer* **8**: 14.

Erickson, L., G. Crews, F. Pan, O. Fisniku, M. S. Jang, C. Wynn, M. Kobayashi and H. Jiang (2004). Unique gene expression profiles of heart allograft rejection in the interferon regulatory factor-1-deficient mouse. *Transpl Immunol* **13**(3): 169-75.

Escalante, C. R., J. Yie, D. Thanos and A. K. Aggarwal (1998). Structure of IRF-1 with bound DNA reveals determinants of interferon regulation. *Nature* **391**(6662): 103-6.

Etienne-Manneville, S. and A. Hall (2003). Cdc42 regulates GSK-3beta and adenomatous polyposis coli to control cell polarity. *Nature* **421**(6924): 753-6.

Eto, M., A. Kouroedov, F. Cosentino and T. F. Luscher (2005). Glycogen synthase kinase-3 mediates endothelial cell activation by tumor necrosis factor-alpha. *Circulation* **112**(9): 1316-22.

Ewing, R. M., P. Chu, F. Elisma, H. Li, P. Taylor, S. Climie, L. McBroom-Cerajewski, M. D. Robinson, L. O'Connor, M. Li, R. Taylor, M. Dharsee, et al. (2007). Large-scale mapping of human protein-protein interactions by mass spectrometry. *Mol Syst Biol* **3**: 89.

Farr, G. H., 3rd, D. M. Ferkey, C. Yost, S. B. Pierce, C. Weaver and D. Kimelman (2000). Interaction among GSK-3, GBP, axin, and APC in Xenopus axis specification. *J Cell Biol* **148**(4): 691-702.

Ferkey, D. M. and D. Kimelman (2002). Glycogen synthase kinase-3 beta mutagenesis identifies a common binding domain for GBP and Axin. *J Biol Chem* **277**(18): 16147-52.

Fiol, C. J., J. S. Williams, C. H. Chou, Q. M. Wang, P. J. Roach and O. M. Andrisani (1994). A secondary phosphorylation of CREB341 at Ser129 is required for the cAMP-mediated control of gene expression. A role for glycogen synthase kinase-3 in the control of gene expression. *J Biol Chem* **269**(51): 32187-93.

Flodstrom, M. and D. L. Eizirik (1997). Interferon-gamma-induced interferon regulatory factor-1 (IRF-1) expression in rodent and human islet cells precedes nitric oxide production. *Endocrinology* **138**(7): 2747-53.

Foss, G. S. and H. Prydz (1999). Interferon regulatory factor 1 mediates the interferon-gamma induction of the human immunoproteasome subunit multicatalytic endopeptidase complex-like 1. *J Biol Chem* **274**(49): 35196-202.

Fragale, A., L. Gabriele, E. Stellacci, P. Borghi, E. Perrotti, R. Ilari, A. Lanciotti, A. L. Remoli, M. Venditti, F. Belardelli and A. Battistini (2008). IFN regulatory factor-1 negatively regulates CD4+ CD25+ regulatory T cell differentiation by repressing Foxp3 expression. *J Immunol* **181**(3): 1673-82.

Frame, S. and P. Cohen (2001). GSK3 takes centre stage more than 20 years after its discovery. *Biochem J* **359**(Pt 1): 1-16.

Frontini, M., M. Vijayakumar, A. Garvin and N. Clarke (2009). A ChIP-chip approach reveals a novel role for transcription factor IRF1 in the DNA damage response. *Nucleic Acids Res* **37**(4): 1073-85.

Fujii, Y., T. Shimizu, M. Kusumoto, Y. Kyogoku, T. Taniguchi and T. Hakoshima (1999). Crystal structure of an IRF-DNA complex reveals novel DNA recognition and cooperative binding to a tandem repeat of core sequences. *EMBO J* **18**(18): 5028-41.

Fujimuro, M., J. Liu, J. Zhu, H. Yokosawa and S. D. Hayward (2005). Regulation of the interaction between glycogen synthase kinase 3 and the Kaposi's sarcoma-associated herpesvirus latency-associated nuclear antigen. *J Virol* **79**(16): 10429-41.

Fujita, T., Y. Kimura, M. Miyamoto, E. L. Barsoumian and T. Taniguchi (1989). Induction of endogenous IFN-alpha and IFN-beta genes by a regulatory transcription factor, IRF-1. *Nature* **337**(6204): 270-2.

Gabriele, L., A. Fragale, P. Borghi, P. Sestili, E. Stellacci, M. Venditti, G. Schiavoni, M. Sanchez, F. Belardelli and A. Battistini (2006). IRF-1 deficiency skews the differentiation of dendritic cells toward plasmacytoid and tolerogenic features. *J Leukoc Biol* **80**(6): 1500-11.

Galliher-Beckley, A. J., J. G. Williams, J. B. Collins and J. A. Cidlowski (2008). Glycogen synthase kinase 3beta-mediated serine phosphorylation of the human glucocorticoid receptor redirects gene expression profiles. *Mol Cell Biol* **28**(24): 7309-22.

Galon, J., C. Sudarshan, S. Ito, D. Finbloom and J. J. O'Shea (1999). IL-12 induces IFN regulating factor-1 (IRF-1) gene expression in human NK and T cells. *J Immunol* **162**(12): 7256-62.

Gao, J., M. Senthil, B. Ren, J. Yan, Q. Xing, J. Yu, L. Zhang and J. H. Yim (2009). IRF-1 transcriptionally upregulates PUMA, which mediates the mitochondrial apoptotic pathway in IRF-1-induced apoptosis in cancer cells. *Cell Death Differ.*

Garcia-Alvarez, G., V. Ventura, O. Ros, R. Aligue, J. Gil and A. Tauler (2007). Glycogen synthase kinase-3beta binds to E2F1 and regulates its transcriptional activity. *Biochim Biophys Acta* **1773**(3): 375-82.

Gianni, M., A. Bauer, E. Garattini, P. Chambon and C. Rochette-Egly (2002). Phosphorylation by p38MAPK and recruitment of SUG-1 are required for RA-induced RAR gamma degradation and transactivation. *EMBO J* **21**(14): 3760-9.

Giatromanolaki, A., M. I. Koukourakis, K. Ritis, K. Mimidis and E. Sivridis (2004). Interferon regulatory factor-1 (IRF-1) suppression and derepression during endometrial tumorigenesis and cancer progression. *Cytokine* **26**(4): 164-8.

Girdlestone, J., M. Isamat, D. Gewert and C. Milstein (1993). Transcriptional regulation of HLA-A and -B: differential binding of members of the Rel and IRF families of transcription factors. *Proc Natl Acad Sci U S A* **90**(24): 11568-72.

Giroux, M., M. Schmidt and A. Descoteaux (2003). IFN-gamma-induced MHC class II expression: transactivation of class II transactivator promoter IV by IFN regulatory factor-1 is regulated by protein kinase C-alpha. *J Immunol* **171**(8): 4187-94.

Glenn, K. A., R. F. Nelson, H. M. Wen, A. J. Mallinger and H. L. Paulson (2008). Diversity in tissue expression, substrate binding, and SCF complex formation for a lectin family of ubiquitin ligases. *J Biol Chem* **283**(19): 12717-29.

Gobin, S. J., P. Biesta and P. J. Van den Elsen (2003). Regulation of human beta 2-microglobulin transactivation in hematopoietic cells. *Blood* **101**(8): 3058-64.

Gobin, S. J., M. van Zutphen, A. M. Woltman and P. J. van den Elsen (1999). Transactivation of classical and nonclassical HLA class I genes through the IFN-stimulated response element. *J Immunol* **163**(3): 1428-34.

Goenka, S., J. Youn, L. M. Dzurek, U. Schindler, L. Y. Yu-Lee and M. Boothby (1999). Paired Stat6 C-terminal transcription activation domains required both for inhibition of an IFN-responsive promoter and trans-activation. *J Immunol* **163**(9): 4663-72.

Gong, R., A. Rifai and L. D. Dworkin (2005). Activation of PI3K-Akt-GSK3beta pathway mediates hepatocyte growth factor inhibition of RANTES expression in renal tubular epithelial cells. *Biochem Biophys Res Commun* **330**(1): 27-33.

Gong, R., A. Rifai, Y. Ge, S. Chen and L. D. Dworkin (2008). Hepatocyte growth factor suppresses proinflammatory NFkappaB activation through GSK3beta inactivation in renal tubular epithelial cells. *J Biol Chem* **283**(12): 7401-10.

Gotschel, F., C. Kern, S. Lang, T. Sparna, C. Markmann, J. Schwager, S. McNelly, F. von Weizsacker, S. Laufer, A. Hecht and I. Merfort (2008). Inhibition of GSK3 differentially modulates NF-kappaB, CREB, AP-1 and beta-catenin signaling in hepatocytes, but fails to promote TNF-alpha-induced apoptosis. *Exp Cell Res* **314**(6): 1351-66.

Graham, R. R., S. V. Kozyrev, E. C. Baechler, M. V. Reddy, R. M. Plenge, J. W. Bauer, W. A. Ortmann, T. Koeuth, M. F. Gonzalez Escribano, B. Pons-Estel, M. Petri, M. Daly, et al. (2006). A common haplotype of interferon regulatory factor 5 (IRF5) regulates splicing and expression and is associated with increased risk of systemic lupus erythematosus. *Nat Genet* **38**(5): 550-5.

Green, W. B., M. L. Slovak, I. M. Chen, M. Pallavicini, J. L. Hecht and C. L. Willman (1999). Lack of IRF-1 expression in acute promyelocytic leukemia and in a subset of acute myeloid leukemias with del(5)(q31). *Leukemia* **13**(12): 1960-71.

Grim, J. E., M. P. Gustafson, R. K. Hirata, A. C. Hagar, J. Swanger, M. Welcker, H. C. Hwang, J. Ericsson, D. W. Russell and B. E. Clurman (2008). Isoform- and cell cycle-dependent substrate degradation by the Fbw7 ubiquitin ligase. *J Cell Biol* **181**(6): 913-20.

Guo, Z., S. Garg, K. M. Hill, L. Jayashankar, M. R. Mooney, M. Hoelscher, J. M. Katz, J. M. Boss and S. Sambhara (2005). A distal regulatory region is required for constitutive and IFN-beta-induced expression of murine TLR9 gene. *J Immunol* **175**(11): 7407-18.

Gupta, S., D. Xia, M. Jiang, S. Lee and A. B. Pernis (1998). Signaling pathways mediated by the TNF- and cytokine-receptor families target a common cis-element of the IFN regulatory factor 1 promoter. *J Immunol* **161**(11): 5997-6004.

Gustafson, M. P., M. Welcker, H. C. Hwang and B. E. Clurman (2005). Zcchc8 is a glycogen synthase kinase-3 substrate that interacts with RNA-binding proteins. *Biochem Biophys Res Commun* **338**(3): 1359-67.

Gysemans, C., H. Callewaert, F. Moore, M. Nelson-Holte, L. Overbergh, D. L. Eizirik and C. Mathieu (2009). Interferon regulatory factor-1 is a key transcription factor in murine beta cells under immune attack. *Diabetologia*.

Hamamoto, R., Y. Furukawa, M. Morita, Y. Iimura, F. P. Silva, M. Li, R. Yagyu and Y. Nakamura (2004). SMYD3 encodes a histone methyltransferase involved in the proliferation of cancer cells. *Nat Cell Biol* **6**(8): 731-40.

Han, S. I., S. Aramata, K. Yasuda and K. Kataoka (2007). MafA stability in pancreatic beta cells is regulated by glucose and is dependent on its constitutive phosphorylation at multiple sites by glycogen synthase kinase 3. *Mol Cell Biol* **27**(19): 6593-605.

Harada, H., T. Fujita, M. Miyamoto, Y. Kimura, M. Maruyama, A. Furia, T. Miyata and T. Taniguchi (1989). Structurally similar but functionally distinct factors, IRF-1 and IRF-2, bind to the same regulatory elements of IFN and IFN-inducible genes. *Cell* **58**(4): 729-39.

Harada, H., M. Kitagawa, N. Tanaka, H. Yamamoto, K. Harada, M. Ishihara and T. Taniguchi (1993). Anti-oncogenic and oncogenic potentials of interferon regulatory factors-1 and -2. *Science* **259**(5097): 971-4.

Harada, H., T. Kondo, S. Ogawa, T. Tamura, M. Kitagawa, N. Tanaka, M. S. Lamphier, H. Hirai and T. Taniguchi (1994). Accelerated exon skipping of IRF-1 mRNA in human myelodysplasia/leukemia; a possible mechanism of tumor suppressor inactivation. *Oncogene* **9**(11): 3313-20.

Harada, H., K. Willison, J. Sakakibara, M. Miyamoto, T. Fujita and T. Taniguchi (1990). Absence of the type I IFN system in EC cells: transcriptional activator (IRF-1) and repressor (IRF-2) genes are developmentally regulated. *Cell* **63**(2): 303-12.

Hartmann-Petersen, R., M. Seeger and C. Gordon (2003). Transferring substrates to the 26S proteasome. *Trends Biochem Sci* **28**(1): 26-31.

Hartwell, L. H. (1973). Three additional genes required for deoxyribonucleic acid synthesis in Saccharomyces cerevisiae. *J Bacteriol* **115**(3): 966-74.

Heery, D. M., E. Kalkhoven, S. Hoare and M. G. Parker (1997). A signature motif in transcriptional co-activators mediates binding to nuclear receptors. *Nature* **387**(6634): 733-6.

Heinz, S., V. Haehnel, M. Karaghiosoff, L. Schwarzfischer, M. Muller, S. W. Krause and M. Rehli (2003). Species-specific regulation of Toll-like receptor 3 genes in men and mice. *J Biol Chem* **278**(24): 21502-9.

Hobart, M., V. Ramassar, N. Goes, J. Urmson and P. F. Halloran (1997). IFN regulatory factor-1 plays a central role in the regulation of the expression of class I and II MHC genes in vivo. *J Immunol* **158**(9): 4260-9.

Hochhaus, A., X. H. Yan, A. Willer, R. Hehlmann, M. Y. Gordon, J. M. Goldman and J. V. Melo (1997). Expression of interferon regulatory factor (IRF) genes and response to interferon-alpha in chronic myeloid leukaemia. *Leukemia* **11**(7): 933-9.

Hoeflich, K. P., J. Luo, E. A. Rubie, M. S. Tsao, O. Jin and J. R. Woodgett (2000). Requirement for glycogen synthase kinase-3beta in cell survival and NF-kappaB activation. *Nature* **406**(6791): 86-90.

Holtschke, T., J. Lohler, Y. Kanno, T. Fehr, N. Giese, F. Rosenbauer, J. Lou, K. P. Knobeloch, L. Gabriele, J. F. Waring, M. F. Bachmann, R. M. Zinkernagel, et al. (1996). Immunodeficiency and chronic myelogenous leukemia-like syndrome in mice with a targeted mutation of the ICSBP gene. *Cell* **87**(2): 307-17.

Honda, K. and T. Taniguchi (2006a). IRFs: master regulators of signalling by Toll-like receptors and cytosolic pattern-recognition receptors. *Nat Rev Immunol* **6**(9): 644-58.

Honda, K. and T. Taniguchi (2006b). Toll-like receptor signaling and IRF transcription factors. *IUBMB Life* **58**(5-6): 290-5.

Hook, S. S., A. Orian, S. M. Cowley and R. N. Eisenman (2002). Histone deacetylase 6 binds polyubiquitin through its zinc finger (PAZ domain) and copurifies with deubiquitinating enzymes. *Proc Natl Acad Sci U S A* **99**(21): 13425-30.

Horiuchi, M., H. Yamada, M. Akishita, M. Ito, K. Tamura and V. J. Dzau (1999). Interferon regulatory factors regulate interleukin-1beta-converting enzyme expression and apoptosis in vascular smooth muscle cells. *Hypertension* **33**(1): 162-6.

Hu, G. and B. J. Barnes (2009). IRF-5 is a mediator of the death receptor-induced apoptotic signaling pathway. *J Biol Chem* **284**(5): 2767-77.

Hu, X., P. K. Paik, J. Chen, A. Yarilina, L. Kockeritz, T. T. Lu, J. R. Woodgett and L. B. Ivashkiv (2006). IFN-gamma suppresses IL-10 production and synergizes with TLR2 by regulating GSK3 and CREB/AP-1 proteins. *Immunity* **24**(5): 563-74.

Huang, Y., A. Walstrom, L. Zhang, Y. Zhao, M. Cui, L. Ye and J. C. Zheng (2009). Type I interferons and interferon regulatory factors regulate TNF-related apoptosis-inducing ligand (TRAIL) in HIV-1-infected macrophages. *PLoS One* **4**(4): e5397.

Hughes-Davies, L., D. Huntsman, M. Ruas, F. Fuks, J. Bye, S. F. Chin, J. Milner, L. A. Brown, F. Hsu, B. Gilks, T. Nielsen, M. Schulzer, et al. (2003). EMSY links the BRCA2 pathway to sporadic breast and ovarian cancer. *Cell* **115**(5): 523-35.

Hunter, T. (2007). The age of crosstalk: phosphorylation, ubiquitination, and beyond. *Mol Cell* **28**(5): 730-8.

Hurgin, V., D. Novick and M. Rubinstein (2002). The promoter of IL-18 binding protein: activation by an IFN-gamma -induced complex of IFN regulatory factor 1 and CCAAT/enhancer binding protein beta. *Proc Natl Acad Sci U S A* **99**(26): 16957-62.

Hurley, J. H., S. Lee and G. Prag (2006). Ubiquitin-binding domains. *Biochem J* **399**(3): 361-72.

Iadecola, C., C. A. Salkowski, F. Zhang, T. Aber, M. Nagayama, S. N. Vogel and M. E. Ross (1999). The transcription factor interferon regulatory factor 1 is expressed after cerebral ischemia and contributes to ischemic brain injury. *J Exp Med* **189**(4): 719-27.

Ingraham, C. R., A. Kinoshita, S. Kondo, B. Yang, S. Sajan, K. J. Trout, M. I. Malik, M. Dunnwald, S. L. Goudy, M. Lovett, J. C. Murray and B. C. Schutte (2006). Abnormal skin, limb and craniofacial morphogenesis in mice deficient for interferon regulatory factor 6 (Irf6). *Nat Genet* **38**(11): 1335-40.

Iwase, S., Y. Furukawa, J. Kikuchi, S. Saito, M. Nakamura, R. Nakayama, J. Horiguchi-Yamada and H. Yamada (1999). Defective binding of IRFs to the initiator element of interleukin-1beta-converting enzyme (ICE) promoter in an interferon-resistant Daudi subline. *FEBS Lett* **450**(3): 263-7.

Jackson, M., S. E. Howie, R. Weller, E. Sabin, J. A. Hunter and R. C. McKenzie (1999). Psoriatic keratinocytes show reduced IRF-1 and STAT-1alpha activation in response to gamma-IFN. *FASEB J* **13**(3): 495-502.

Jarosinski, K. W. and P. T. Massa (2002). Interferon regulatory factor-1 is required for interferon-gamma-induced MHC class I genes in astrocytes. *J Neuroimmunol* **122**(1-2): 74-84.

Jaruga, B., F. Hong, W. H. Kim and B. Gao (2004). IFN-gamma/STAT1 acts as a proinflammatory signal in T cell-mediated hepatitis via induction of multiple chemokines and adhesion molecules: a critical role of IRF-1. *Am J Physiol Gastrointest Liver Physiol* **287**(5): G1044-52.

Ji, H., T. B. Ball, J. Kimani and F. A. Plummer (2004). Novel interferon regulatory factor-1 polymorphisms in a Kenyan population revealed by complete gene sequencing. *J Hum Genet* **49**(10): 528-35.

Jia, W. and Q. Guo (2008). Gene structures and promoter characteristics of interferon regulatory factor 1 (IRF-1), IRF-2 and IRF-7 from snakehead Channa argus. *Mol Immunol* **45**(8): 2419-28.

Jiang, X., M. Norman, L. Roth and X. Li (2004). Protein-DNA array-based identification of transcription factor activities regulated by interaction with the glucocorticoid receptor. *J Biol Chem* **279**(37): 38480-5.

Jin, J., T. Cardozo, R. C. Lovering, S. J. Elledge, M. Pagano and J. W. Harper (2004). Systematic analysis and nomenclature of mammalian F-box proteins. *Genes Dev* **18**(21): 2573-80.

Jope, R. S. and G. V. Johnson (2004). The glamour and gloom of glycogen synthase kinase-3. *Trends Biochem Sci* **29**(2): 95-102.

Kadam, S. and B. M. Emerson (2003). Transcriptional specificity of human SWI/SNF BRG1 and BRM chromatin remodeling complexes. *Mol Cell* **11**(2): 377-89.

Kanazawa, N., M. Kurosaki, N. Sakamoto, N. Enomoto, Y. Itsui, T. Yamashiro, Y. Tanabe, S. Maekawa, M. Nakagawa, C. H. Chen, S. Kakinuma, S. Oshima, et al. (2004). Regulation of hepatitis C virus replication by interferon regulatory factor 1. *J Virol* **78**(18): 9713-20.

Kanei-Ishii, C., T. Nomura, T. Takagi, N. Watanabe, K. I. Nakayama and S. Ishii (2008). Fbxw7 acts as an E3 ubiquitin ligase that targets c-Myb for nemo-like kinase (NLK)-induced degradation. *J Biol Chem* **283**(45): 30540-8.

Kano, S., K. Sato, Y. Morishita, S. Vollstedt, S. Kim, K. Bishop, K. Honda, M. Kubo and T. Taniguchi (2008). The contribution of transcription factor IRF1 to the interferon-gamma-interleukin 12 signaling axis and TH1 versus TH-17 differentiation of CD4+ T cells. *Nat Immunol* **9**(1): 34-41.

Kariko, K., H. Ni, J. Capodici, M. Lamphier and D. Weissman (2004). mRNA is an endogenous ligand for Toll-like receptor 3. *J Biol Chem* **279**(13): 12542-50.

Karlsen, A. E., D. Pavlovic, K. Nielsen, J. Jensen, H. U. Andersen, F. Pociot, T. Mandrup-Poulsen, D. L. Eizirik and J. Nerup (2000). Interferon-gamma induces interleukin-1 converting enzyme expression in pancreatic islets by an interferon regulatory factor-1-dependent mechanism. *J Clin Endocrinol Metab* **85**(2): 830-6.

Katoh, M. (2006). Cross-talk of WNT and FGF signaling pathways at GSK3beta to regulate beta-catenin and SNAIL signaling cascades. *Cancer Biol Ther* **5**(9): 1059-64.

Kautz, B., R. Kakar, E. David and E. A. Eklund (2001). SHP1 protein-tyrosine phosphatase inhibits gp91PHOX and p67PHOX expression by inhibiting interaction of PU.1, IRF1, interferon consensus sequence-binding protein, and CREB-binding protein with homologous Cis elements in the CYBB and NCF2 genes. *J Biol Chem* **276**(41): 37868-78.

Kim, E. J., J. M. Lee, S. E. Namkoong, S. J. Um and J. S. Park (2002). Interferon regulatory factor-1 mediates interferon-gamma-induced apoptosis in ovarian carcinoma cells. *J Cell Biochem* **85**(2): 369-80.

Kim, E. J., C. H. Park, J. S. Park and S. J. Um (2003a). Functional dissection of the transactivation domain of interferon regulatory factor-1. *Biochem Biophys Res Commun* **304**(2): 253-9.

Kim, E. J., J. S. Park and S. J. Um (2008). Ubc9-mediated sumoylation leads to transcriptional repression of IRF-1. *Biochem Biophys Res Commun* **377**(3): 952-6.

Kim, H., K. Heo, J. H. Kim, K. Kim, J. Choi and W. An (2009). Requirement of histone methyltransferase SMYD3 for estrogen receptor-mediated transcription. *J Biol Chem* **284**(30): 19867-77.

Kim, J. W., Q. Q. Tang, X. Li and M. D. Lane (2007). Effect of phosphorylation and S-S bond-induced dimerization on DNA binding and transcriptional activation by C/EBPbeta. *Proc Natl Acad Sci U S A* **104**(6): 1800-4.

Kim, L. and A. R. Kimmel (2000). GSK3, a master switch regulating cell-fate specification and tumorigenesis. *Curr Opin Genet Dev* **10**(5): 508-14.

Kim, S. Y., A. Herbst, K. A. Tworkowski, S. E. Salghetti and W. P. Tansey (2003b). Skp2 regulates Myc protein stability and activity. *Mol Cell* **11**(5): 1177-88.

Kirchhoff, S. and H. Hauser (1999). Cooperative activity between HER oncogenes and the tumor suppressor IRF-1 results in apoptosis. *Oncogene* **18**(25): 3725-36.

Kirchhoff, S., F. Schaper and H. Hauser (1993). Interferon regulatory factor 1 (IRF-1) mediates cell growth inhibition by transactivation of downstream target genes. *Nucleic Acids Res* **21**(12): 2881-9.

Kirchhoff, S., F. Schaper, A. Oumard and H. Hauser (1998). In vivo formation of IRF-1 homodimers. *Biochimie* **80**(8-9): 659-64.

Kirchhoff, S., T. Sebens, S. Baumann, A. Krueger, R. Zawatzky, M. Li-Weber, E. Meinl, F. Neipel, B. Fleckenstein and P. H. Krammer (2002). Viral IFN-regulatory factors inhibit activation-induced cell death via two positive regulatory IFN-regulatory factor 1-dependent domains in the CD95 ligand promoter. *J Immunol* **168**(3): 1226-34.

Kirshner, J. R., A. Y. Karpova, M. Kops and P. M. Howley (2005). Identification of TRAIL as an interferon regulatory factor 3 transcriptional target. *J Virol* **79**(14): 9320-4.

Ko, J., A. Gendron-Fitzpatrick, T. A. Ficht and G. A. Splitter (2002). Virulence criteria for Brucella abortus strains as determined by interferon regulatory factor 1-deficient mice. *Infect Immun* **70**(12): 7004-12.

Koch, H. B., R. Zhang, B. Verdoodt, A. Bailey, C. D. Zhang, J. R. Yates, 3rd, A. Menssen and H. Hermeking (2007). Large-scale identification of c-MYC-associated proteins using a combined TAP/MudPIT approach. *Cell Cycle* **6**(2): 205-17.

Komander, D. (2009). The emerging complexity of protein ubiquitination. *Biochem Soc Trans* **37**(Pt 5): 937-53.

Konan, K. V. and M. W. Taylor (1996). Importance of the two interferon-stimulated response element (ISRE) sequences in the regulation of the human indoleamine 2,3-dioxygenase gene. *J Biol Chem* **271**(32): 19140-5

Kondo, S., B. C. Schutte, R. J. Richardson, B. C. Bjork, A. S. Knight, Y. Watanabe, E. Howard, R. L. de Lima, S. Daack-Hirsch, A. Sander, D. M. McDonald-McGinn, E. H. Zackai, et al. (2002). Mutations in IRF6 cause Van der Woude and popliteal pterygium syndromes. *Nat Genet* **32**(2): 285-9.

Koschny, R., H. Walczak and T. M. Ganten (2007). The promise of TRAIL--potential and risks of a novel anticancer therapy. *J Mol Med* **85**(9): 923-35.

Kram, A., L. Li, R. D. Zhang, D. S. Yoon, J. Y. Ro, D. Johnston, H. B. Grossman, S. Scherer and B. Czerniak (2001). Mapping and genome sequence analysis of chromosome 5 regions involved in bladder cancer progression. *Lab Invest* **81**(7): 1039-48.

Kroef, M. J., M. W. Bolk, R. Willemze and J. E. Landegent (1994). Absence of loss of heterozygosity of the IRF1 gene in some patients with a 5q31 deletion. *Blood* **83**(8): 2382.

Kroger, A., A. Dallugge, S. Kirchhoff and H. Hauser (2003). IRF-1 reverts the transformed phenotype of oncogenically transformed cells in vitro and in vivo. *Oncogene* **22**(7): 1045-56.

Kroger, A., D. Ortmann, T. U. Krohne, L. Mohr, H. E. Blum, H. Hauser and M. Geissler (2001). Growth suppression of the hepatocellular carcinoma cell line Hepa1-6 by an activatable interferon regulatory factor-1 in mice. *Cancer Res* **61**(6): 2609-17.

Kroger, A., A. Stirnweiss, J. E. Pulverer, K. Klages, M. Grashoff, J. Reimann and H. Hauser (2007). Tumor suppression by IFN regulatory factor-1 is mediated by transcriptional down-regulation of cyclin D1. *Cancer Res* **67**(7): 2972-81.

Kular, R. K., F. Yehiely, K. U. Kotlo, Z. M. Cilensek, R. Bedi and L. P. Deiss (2009). GAGE, an antiapoptotic protein binds and modulates the expression of nucleophosmin/B23 and interferon regulatory factor 1. *J Interferon Cytokine Res* **29**(10): 645-55.

Kuroboshi, H., T. Okubo, K. Kitaya, T. Nakayama, N. Daikoku, S. Fushiki and H. Honjo (2003). Interferon regulatory factor-1 expression in human uterine endometrial carcinoma. *Gynecol Oncol* **91**(2): 354-8.

la Sala, A., J. He, L. Laricchia-Robbio, S. Gorini, A. Iwasaki, M. Braun, G. S. Yap, A. Sher, K. Ozato and B. Kelsall (2009). Cholera toxin inhibits IL-12 production and CD8alpha+ dendritic cell differentiation by cAMP-mediated inhibition of IRF8 function. *J Exp Med* **206**(6): 1227-35.

Lallemand, C., B. Blanchard, M. Palmieri, P. Lebon, E. May and M. G. Tovey (2007). Single-stranded RNA viruses inactivate the transcriptional activity of p53 but induce NOXA-dependent apoptosis via post-translational modifications of IRF-1, IRF-3 and CREB. *Oncogene* **26**(3): 328-38.

Lang, C., M. Algner, N. Beinert, U. Gross and C. G. Luder (2006). Diverse mechanisms employed by Toxoplasma gondii to inhibit IFN-gamma-induced major histocompatibility complex class II gene expression. *Microbes Infect* **8**(8): 1994-2005.

Le Stunff, C. and P. Rotwein (1998). Growth hormone stimulates interferon regulatory factor-1 gene expression in the liver. *Endocrinology* **139**(3): 859-66.

Lechleitner, S., J. Gille, D. R. Johnson and P. Petzelbauer (1998). Interferon enhances tumor necrosis factor-induced vascular cell adhesion molecule 1 (CD106) expression in human endothelial cells by an interferon-related factor 1-dependent pathway. *J Exp Med* **187**(12): 2023-30.

Lee, A. H., J. H. Hong and Y. S. Seo (2000). Tumour necrosis factor-alpha and interferon-gamma synergistically activate the RANTES promoter through nuclear factor kappaB and interferon regulatory factor 1 (IRF-1) transcription factors. *Biochem J* **350 Pt 1**: 131-8.

Lee, E. J., M. Jo, J. Park, W. Zhang and J. H. Lee (2006). Alternative splicing variants of IRF-1 lacking exons 7, 8, and 9 in cervical cancer. *Biochem Biophys Res Commun* **347**(4): 882-8.

Lee, J. H., T. Chun, S. Y. Park and S. B. Rho (2008). Interferon regulatory factor-1 (IRF-1) regulates VEGF-induced angiogenesis in HUVECs. *Biochim Biophys Acta* **1783**(9): 1654-62.

Lee, Y. J., S. W. Kang, J. K. Song, H. J. Baek, H. J. Choi, Y. D. Bae, H. J. Ryu, E. Y. Lee, E. B. Lee and Y. W. Song (2007). Associations between interferon regulatory factor-1 polymorphisms and Behcet's disease. *Hum Immunol* **68**(9): 770-8.

Lefebvre, S., M. Antoine, S. Uzan, M. McMaster, J. Dausset, E. D. Carosella and P. Paul (2002). Specific activation of the non-classical class I histocompatibility HLA-G antigen and expression of the ILT2 inhibitory receptor in human breast cancer. *J Pathol* **196**(3): 266-74.

Li, C., Y. Y. Liang, X. H. Feng, S. Y. Tsai, M. J. Tsai and B. W. O'Malley (2008). Essential phosphatases and a phospho-degron are critical for regulation of SRC-3/AIB1 coactivator function and turnover. *Mol Cell* **31**(6): 835-49.

Li, X., S. Leung, S. Qureshi, J. E. Darnell, Jr. and G. R. Stark (1996). Formation of STAT1-STAT2 heterodimers and their role in the activation of IRF-1 gene transcription by interferon-alpha. *J Biol Chem* **271**(10): 5790-4.

Liang, M. H. and D. M. Chuang (2007). Regulation and function of glycogen synthase kinase-3 isoforms in neuronal survival. *J Biol Chem* **282**(6): 3904-17.

Lin, H. K., S. Altuwaijri, W. J. Lin, P. Y. Kan, L. L. Collins and C. Chang (2002). Proteasome activity is required for androgen receptor transcriptional activity via regulation of androgen receptor nuclear translocation and interaction with coregulators in prostate cancer cells. *J Biol Chem* **277**(39): 36570-6.

Lin, R. and J. Hiscott (1999). A role for casein kinase II phosphorylation in the regulation of IRF-1 transcriptional activity. *Mol Cell Biochem* **191**(1-2): 169-80.

Lin, R., A. Mustafa, H. Nguyen, D. Gewert and J. Hiscott (1994). Mutational analysis of interferon (IFN) regulatory factors 1 and 2. Effects on the induction of IFN-beta gene expression. *J Biol Chem* **269**(26): 17542-9.

Linseman, D. A., B. D. Butts, T. A. Precht, R. A. Phelps, S. S. Le, T. A. Laessig, R. J. Bouchard, M. L. Florez-McClure and K. A. Heidenreich (2004). Glycogen synthase kinase-3beta phosphorylates Bax and promotes its mitochondrial localization during neuronal apoptosis. *J Neurosci* **24**(44): 9993-10002.

Lipford, J. R. and R. J. Deshaies (2003). Diverse roles for ubiquitin-dependent proteolysis in transcriptional activation. *Nat Cell Biol* **5**(10): 845-50.

Liu, J. and X. Ma (2006). Interferon regulatory factor 8 regulates RANTES gene transcription in cooperation with interferon regulatory factor-1, NF-kappaB, and PU.1. *J Biol Chem* **281**(28): 19188-95.

Liu, J., Z. Xiang and X. Ma (2004). Role of IFN regulatory factor-1 and IL-12 in immunological resistance to pathogenesis of N-methyl-N-nitrosourea-induced T lymphoma. *J Immunol* **173**(2): 1184-93.

Liu, M. Y. and L. M. Khachigian (2009). Histone deacetylase-1 is enriched at the platelet-derived growth factor-D promoter in response to interleukin-1beta and forms a cytokine-inducible gene-silencing complex with NF-kappab p65 and interferon regulatory factor-1. *J Biol Chem* **284**(50): 35101-12.

Liu, Y., W. Chen, J. Gaudet, M. D. Cheney, L. Roudaia, T. Cierpicki, R. C. Klet, K. Hartman, T. M. Laue, N. A. Speck and J. H. Bushweller (2007). Structural basis for recognition of SMRT/N-CoR by the MYND

domain and its contribution to AML1/ETO's activity. *Cancer Cell* **11**(6): 483-97.

Lowney, J. K., L. D. Boucher, P. E. Swanson and G. M. Doherty (1999). Interferon regulatory factor-1 and -2 expression in human melanoma specimens. *Ann Surg Oncol* **6**(6): 604-8.

Luo, X. M. and A. C. Ross (2006). Retinoic acid exerts dual regulatory actions on the expression and nuclear localization of interferon regulatory factor-1. *Exp Biol Med (Maywood)* **231**(5): 619-31.

Machida, K., K. Tsukiyama-Kohara, S. Sekiguch, E. Seike, S. Tone, Y. Hayashi, Y. Tobita, Y. Kasama, M. Shimizu, H. Takahashi, C. Taya, H. Yonekawa, et al. (2009). Hepatitis C virus and disrupted interferon signaling promote lymphoproliferation via type II CD95 and interleukins. *Gastroenterology* **137**(1): 285-96, 296 e1-11.

Majumder, S., L. Z. Zhou, P. Chaturvedi, G. Babcock, S. Aras and R. M. Ransohoff (1998). p48/STAT-1alpha-containing complexes play a predominant role in induction of IFN-gamma-inducible protein, 10 kDa (IP-10) by IFN-gamma alone or in synergy with TNF-alpha. *J Immunol* **161**(9): 4736-44.

Mannick, E. E., R. L. Cote, J. R. Schurr, H. S. Krowicka, G. D. Sloop, A. Zapata-Velandia, H. Correa, B. Ruiz, R. Horswell, J. J. Lentz, P. Byrne, M. M. Gastanaduy, et al. (2005). Altered phenotype of dextran sulfate sodium colitis in interferon regulatory factor-1 knock-out mice. *J Gastroenterol Hepatol* **20**(3): 371-80.

Manzella, L., E. Conte, G. Cocchiaro, E. Guarniera, B. Sciacca, C. Bonaiuto, F. Stagno and A. Messina (1999). Role of interferon regulatory factor 1 in monocyte/macrophage differentiation. *Eur J Immunol* **29**(9): 3009-16.

Manzella, L., R. Gualdi, D. Perrotti, N. C. Nicolaides, G. Girlando, M. A. Giuffrida, A. Messina and B. Calabretta (2000). The interferon regulatory factors 1 and 2 bind to a segment of the human c-myb first intron: possible role in the regulation of c-myb expression. *Exp Cell Res* **256**(1): 248-56.

Maratheftis, C. I., P. E. Bolaraki, S. Giannouli, E. K. Kapsogeorgou, H. M. Moutsopoulos and M. Voulgarelis (2006). Aberrant alternative splicing of interferon regulatory factor-1 (IRF-1) in myelodysplastic hematopoietic progenitor cells. *Leuk Res* **30**(9): 1177-86.

Marecki, S., C. J. Riendeau, M. D. Liang and M. J. Fenton (2001). PU.1 and multiple IFN regulatory factor proteins synergize to mediate transcriptional activation of the human IL-1 beta gene. *J Immunol* **166**(11): 6829-38.

Marsili, G., A. L. Remoli, M. Sgarbanti and A. Battistini (2004). Role of acetylases and deacetylase inhibitors in IRF-1-mediated HIV-1 long terminal repeat transcription. *Ann N Y Acad Sci* **1030**: 636-43.

Martin, M., K. Rehani, R. S. Jope and S. M. Michalek (2005). Toll-like receptor-mediated cytokine production is differentially regulated by glycogen synthase kinase 3. *Nat Immunol* **6**(8): 777-84.

Martinez, A., A. Castro, I. Dorronsoro and M. Alonso (2002). Glycogen synthase kinase 3 (GSK-3) inhibitors as new promising drugs for diabetes, neurodegeneration, cancer, and inflammation. *Med Res Rev* **22**(4): 373-84.

Maser, R. S., B. Choudhury, P. J. Campbell, B. Feng, K. K. Wong, A. Protopopov, J. O'Neil, A. Gutierrez, E. Ivanova, I. Perna, E. Lin, V. Mani, et al. (2007). Chromosomally unstable mouse tumours have genomic alterations similar to diverse human cancers. *Nature* **447**(7147): 966-71.

Masumi, A., I. M. Wang, B. Lefebvre, X. J. Yang, Y. Nakatani and K. Ozato (1999). The histone acetylase PCAF is a phorbol-ester-inducible coactivator of the IRF family that confers enhanced interferon responsiveness. *Mol Cell Biol* **19**(3): 1810-20.

Matikainen, S., T. Ronni, M. Hurme, R. Pine and I. Julkunen (1996). Retinoic acid activates interferon regulatory factor-1 gene expression in myeloid cells. *Blood* **88**(1): 114-23.

Matikainen, S., T. Sareneva, T. Ronni, A. Lehtonen, P. J. Koskinen and I. Julkunen (1999). Interferon-alpha activates multiple STAT proteins and upregulates proliferation-associated IL-2Ralpha, c-myc, and pim-1 genes in human T cells. *Blood* **93**(6): 1980-91.

Matsuoka, S., Y. Oike, I. Onoyama, A. Iwama, F. Arai, K. Takubo, Y. Mashimo, H. Oguro, E. Nitta, K. Ito, K. Miyamoto, H. Yoshiwara, et al. (2008). Fbxw7 acts as a critical fail-safe against premature loss of hematopoietic stem cells and development of T-ALL. *Genes Dev* **22**(8): 986-91.

Matsuyama, T., T. Kimura, M. Kitagawa, K. Pfeffer, T. Kawakami, N. Watanabe, T. M. Kundig, R. Amakawa, K. Kishihara, A. Wakeham and et al. (1993). Targeted disruption of IRF-1 or IRF-2 results in abnormal type I IFN gene induction and aberrant lymphocyte development. *Cell* **75**(1): 83-97.

McElligott, D. L., J. A. Phillips, C. A. Stillman, R. J. Koch, D. E. Mosier and M. V. Hobbs (1997). CD4+ T cells from IRF-1-deficient mice exhibit altered patterns of cytokine expression and cell subset homeostasis. *J Immunol* **159**(9): 4180-6.

Meijer, L., M. Flajolet and P. Greengard (2004). Pharmacological inhibitors of glycogen synthase kinase 3. *Trends Pharmacol Sci* **25**(9): 471-80.

Mendes-da-Silva, P., A. Moreira, J. Duro-da-Costa, D. Matias and C. Monteiro (2000). Frequent loss of heterozygosity on chromosome 5 in non-small cell lung carcinoma. *Mol Pathol* **53**(4): 184-7.

Mendez, P. and L. M. Garcia-Segura (2006). Phosphatidylinositol 3-kinase and glycogen synthase kinase 3 regulate estrogen receptor-mediated transcription in neuronal cells. *Endocrinology* **147**(6): 3027-39.

Meraro, D., S. Hashmueli, B. Koren, A. Azriel, A. Oumard, S. Kirchhoff, H. Hauser, S. Nagulapalli, M. L. Atchison and B. Z. Levi (1999). Protein-protein and DNA-protein interactions affect the activity of lymphoid-specific IFN regulatory factors. *J Immunol* **163**(12): 6468-78.

Merika, M., A. J. Williams, G. Chen, T. Collins and D. Thanos (1998). Recruitment of CBP/p300 by the IFN beta enhanceosome is required for synergistic activation of transcription. *Mol Cell* **1**(2): 277-87.

Mild, G. C., G. E. Schmahl, P. Shayan and C. M. Niemeyer (1999). Expression of interferon regulatory factor 1 and 2 in hematopoietic cells of children with juvenile myelomonocytic leukemia. *Leuk Lymphoma* **35**(5-6): 507-11.

Miyamoto, M., T. Fujita, Y. Kimura, M. Maruyama, H. Harada, Y. Sudo, T. Miyata and T. Taniguchi (1988). Regulated expression of a gene encoding a nuclear factor, IRF-1, that specifically binds to IFN-beta gene regulatory elements. *Cell* **54**(6): 903-13.

Mohideen, F., A. D. Capili, P. M. Bilimoria, T. Yamada, A. Bonni and C. D. Lima (2009). A molecular basis for phosphorylation-dependent SUMO conjugation by the E2 UBC9. *Nat Struct Mol Biol* **16**(9): 945-52.

Momose, I., M. Terashima, Y. Nakashima, M. Sakamoto, H. Ishino, T. Nabika, Y. Hosokawa and Y. Tanigawa (2000). Phorbol ester synergistically increases interferon regulatory factor-1 and inducible nitric oxide synthase induction in interferon-gamma-treated RAW 264.7 cells. *Biochim Biophys Acta* **1498**(1): 19-31.

Moriyama, Y., S. Nishiguchi, A. Tamori, N. Koh, Y. Yano, S. Kubo, K. Hirohashi and S. Otani (2001). Tumor-suppressor effect of interferon regulatory factor-1 in human hepatocellular carcinoma. *Clin Cancer Res* **7**(5): 1293-8.

Morris, A. C., G. W. Beresford, M. R. Mooney and J. M. Boss (2002). Kinetics of a gamma interferon response: expression and assembly of CIITA promoter IV and inhibition by methylation. *Mol Cell Biol* **22**(13): 4781-91.

Moschonas, A., M. Kouraki, P. G. Knox, E. Thymiakou, D. Kardassis and A. G. Eliopoulos (2008). CD40 induces antigen transporter and immunoproteasome gene expression in carcinomas via the coordinated action of NF-kappaB and of NF-kappaB-mediated de novo synthesis of IRF-1. *Mol Cell Biol* **28**(20): 6208-22.

Murata, S., H. Yashiroda and K. Tanaka (2009). Molecular mechanisms of proteasome assembly. *Nat Rev Mol Cell Biol* **10**(2): 104-15.

Muratani, M. and W. P. Tansey (2003). How the ubiquitin-proteasome system controls transcription. *Nat Rev Mol Cell Biol* **4**(3): 192-201.

Nakagawa, K. and H. Yokosawa (2000). Degradation of transcription factor IRF-1 by the ubiquitin-proteasome pathway. The C-terminal region governs the protein stability. *Eur J Biochem* **267**(6): 1680-6.

Nakagawa, K. and H. Yokosawa (2002). PIAS3 induces SUMO-1 modification and transcriptional repression of IRF-1. *FEBS Lett* **530**(1-3): 204-8.

Nakazawa, T., J. Satoh, K. Takahashi, Y. Sakata, F. Ikehata, Y. Takizawa, S. I. Bando, T. Housai, Y. Li, C. Chen, T. Masuda, S. Kure, et al. (2001). Complete suppression of insulitis and diabetes in NOD mice lacking interferon regulatory factor-1. *J Autoimmun* **17**(2): 119-25.

Namiki, S., T. Nakamura, S. Oshima, M. Yamazaki, Y. Sekine, K. Tsuchiya, R. Okamoto, T. Kanai and M. Watanabe (2005). IRF-1 mediates upregulation of LMP7 by IFN-gamma and concerted expression of immunosubunits of the proteasome. *FEBS Lett* **579**(13): 2781-7.

Narayan, V., M. Eckert, A. Zylicz, M. Zylicz and K. L. Ball (2009). Cooperative regulation of the interferon regulatory factor-1 tumor suppressor protein by core components of the molecular chaperone machinery. *J Biol Chem* **284**(38): 25889-99.

Negishi, H., Y. Fujita, H. Yanai, S. Sakaguchi, X. Ouyang, M. Shinohara, H. Takayanagi, Y. Ohba, T. Taniguchi and K. Honda (2006). Evidence for licensing of IFN-gamma-induced IFN regulatory factor 1 transcription factor by MyD88 in Toll-like receptor-dependent gene induction program. *Proc Natl Acad Sci U S A* **103**(41): 15136-41.

Neish, A. S., M. A. Read, D. Thanos, R. Pine, T. Maniatis and T. Collins (1995). Endothelial interferon regulatory factor 1 cooperates with NF-kappa B as a transcriptional activator of vascular cell adhesion molecule 1. *Mol Cell Biol* **15**(5): 2558-69.

Nguyen, J., P. Knapnougel, P. Lesavre and B. Bauvois (2005). Inhibition of matrix metalloproteinase-9 by interferons and TGF-beta1 through distinct signalings accounts for reduced monocyte invasiveness. *FEBS Lett* **579**(25): 5487-93.

Nhu, Q. M., N. Cuesta and S. N. Vogel (2006). Transcriptional regulation of lipopolysaccharide (LPS)-induced Toll-like receptor (TLR) expression in murine macrophages: role of interferon regulatory factors 1 (IRF-1) and 2 (IRF-2). *J Endotoxin Res* **12**(5): 285-95.

Nikcevich, K. M., J. F. Piskurich, R. P. Hellendall, Y. Wang and J. P. Ting (1999). Differential selectivity of CIITA promoter activation by IFN-gamma and IRF-1 in astrocytes and macrophages: CIITA promoter activation is not affected by TNF-alpha. *J Neuroimmunol* **99**(2): 195-204.

Nozawa, H., E. Oda, S. Ueda, G. Tamura, C. Maesawa, T. Muto, T. Taniguchi and N. Tanaka (1998). Functionally inactivating point mutation in the tumor-suppressor IRF-1 gene identified in human gastric cancer. *Int J Cancer* **77**(4): 522-7.

O'Brien, W. T. and P. S. Klein (2009). Validating GSK3 as an in vivo target of lithium action. *Biochem Soc Trans* **37**(Pt 5): 1133-8.

O'Neill, C. F., S. Urs, C. Cinelli, A. Lincoln, R. J. Nadeau, R. Leon, J. Toher, C. Mouta-Bellum, R. E. Friesel and L. Liaw (2007). Notch2 signaling induces apoptosis and inhibits human MDA-MB-231 xenograft growth. *Am J Pathol* **171**(3): 1023-36.

Ogasawara, S., G. Tamura, C. Maesawa, Y. Suzuki, K. Ishida, N. Satoh, N. Uesugi, K. Saito and R. Satodate (1996). Common deleted region on the long arm of chromosome 5 in esophageal carcinoma. *Gastroenterology* **110**(1): 52-7.

Ogata-Kawata, H., K. Yamada, M. Uesaka-Yoshino, N. Kagawa and K. Miyamoto (2007). BS69, a corepressor interacting with ZHX1, is a bifunctional transcription factor. *Front Biosci* **12**: 1911-26.

Okabe, H., S. H. Lee, J. Phuchareon, D. G. Albertson, F. McCormick and O. Tetsu (2006). A critical role for FBXW8 and MAPK in cyclin D1 degradation and cancer cell proliferation. *PLoS One* **1**: e128.

Olson, B. L., M. B. Hock, S. Ekholm-Reed, J. A. Wohlschlegel, K. K. Dev, A. Kralli and S. I. Reed (2008). SCFCdc4 acts antagonistically to the PGC-1alpha transcriptional coactivator by targeting it for ubiquitin-mediated proteolysis. *Genes Dev* **22**(2): 252-64.

Orlicky, S., X. Tang, A. Willems, M. Tyers and F. Sicheri (2003). Structural basis for phosphodependent substrate selection and orientation by the SCFCdc4 ubiquitin ligase. *Cell* **112**(2): 243-56.

Oshima, S., T. Nakamura, S. Namiki, E. Okada, K. Tsuchiya, R. Okamoto, M. Yamazaki, T. Yokota, M. Aida, Y. Yamaguchi, T. Kanai, H. Handa, et al. (2004). Interferon regulatory factor 1 (IRF-1) and IRF-2 distinctively up-regulate gene expression and production of interleukin-7 in human intestinal epithelial cells. *Mol Cell Biol* **24**(14): 6298-310.

Ostendorff, H. P., R. I. Peirano, M. A. Peters, A. Schluter, M. Bossenz, M. Scheffner and I. Bach (2002). Ubiquitination-dependent cofactor exchange on LIM homeodomain transcription factors. *Nature* **416**(6876): 99-103.

Ougolkov, A. V., N. D. Bone, M. E. Fernandez-Zapico, N. E. Kay and D. D. Billadeau (2007). Inhibition of glycogen synthase kinase-3 activity leads to epigenetic silencing of nuclear factor kappaB target genes and induction of apoptosis in chronic lymphocytic leukemia B cells. *Blood* **110**(2): 735-42.

Palombella, V. J., O. J. Rando, A. L. Goldberg and T. Maniatis (1994). The ubiquitin-proteasome pathway is required for processing the NF-kappa B1 precursor protein and the activation of NF-kappa B. *Cell* **78**(5): 773-85.

Pamment, J., E. Ramsay, M. Kelleher, D. Dornan and K. L. Ball (2002). Regulation of the IRF-1 tumour modifier during the response to genotoxic stress involves an ATM-dependent signalling pathway. *Oncogene* **21**(51): 7776-85.

Papageorgiou, A., C. P. Dinney and D. J. McConkey (2007). Interferon-alpha induces TRAIL expression and cell death via an IRF-1-dependent mechanism in human bladder cancer cells. *Cancer Biol Ther* **6**(6): 872-9.

Park, J., K. Kim, E. J. Lee, Y. J. Seo, S. N. Lim, K. Park, S. B. Rho, S. H. Lee and J. H. Lee (2007). Elevated level of SUMOylated IRF-1 in tumor cells interferes with IRF-1-mediated apoptosis. *Proc Natl Acad Sci U S A* **104**(43): 17028-33.

Park, J. S., E. J. Kim, H. J. Kwon, E. S. Hwang, S. E. Namkoong and S. J. Um (2000). Inactivation of interferon regulatory factor-1 tumor suppressor protein by HPV E7 oncoprotein. Implication for the E7-mediated immune evasion mechanism in cervical carcinogenesis. *J Biol Chem* **275**(10): 6764-9.

Park, S. Y., J. W. Seol, Y. J. Lee, J. H. Cho, H. S. Kang, I. S. Kim, S. H. Park, T. H. Kim, J. H. Yim, M. Kim, T. R. Billiar and D. W. Seol (2004). IFN-gamma enhances TRAIL-induced apoptosis through IRF-1. *Eur J Biochem* **271**(21): 4222-8.

Paschen, W., C. Gissel, S. Althausen and J. Doutheil (1998). Changes in interferon-regulatory factor-1 mRNA levels after transient ischemia in rat brain. *Neuroreport* **9**(14): 3147-51.

Pelzer, C., I. Kassner, K. Matentzoglu, R. K. Singh, H. P. Wollscheid, M. Scheffner, G. Schmidtke and M. Groettrup (2007). UBE1L2, a novel E1 enzyme specific for ubiquitin. *J Biol Chem* **282**(32): 23010-4.

Penninger, J. M., C. Sirard, H. W. Mittrucker, A. Chidgey, I. Kozieradzki, M. Nghiem, A. Hakem, T. Kimura, E. Timms, R. Boyd, T. Taniguchi, T. Matsuyama, et al. (1997). The interferon regulatory transcription factor IRF-1 controls positive and negative selection of CD8+ thymocytes. *Immunity* **7**(2): 243-54.

Peralta, R. C., A. G. Casson, R. N. Wang, S. Keshavjee, M. Redston and B. Bapat (1998). Distinct regions of frequent loss of heterozygosity of chromosome 5p and 5q in human esophageal cancer. *Int J Cancer* **78**(5): 600-5.

Perry, J. J., J. A. Tainer and M. N. Boddy (2008). A SIM-ultaneous role for SUMO and ubiquitin. *Trends Biochem Sci* **33**(5): 201-8.

Pflugheber, J., B. Fredericksen, R. Sumpter, Jr., C. Wang, F. Ware, D. L. Sodora and M. Gale, Jr. (2002). Regulation of PKR and IRF-1 during hepatitis C virus RNA replication. *Proc Natl Acad Sci U S A* **99**(7): 4650-5.

Pine, R. and J. E. Darnell, Jr. (1989). In vivo evidence of interaction between interferon-stimulated gene factors and the interferon-stimulated response element. *Mol Cell Biol* **9**(8): 3533-7.

Pion, E., V. Narayan, M. Eckert and K. L. Ball (2009). Role of the IRF-1 enhancer domain in signalling polyubiquitination and degradation. *Cell Signal* **21**(10): 1479-87.

Pirhonen, J., J. Siren, I. Julkunen and S. Matikainen (2007). IFN-alpha regulates Toll-like receptor-mediated IL-27 gene expression in human macrophages. *J Leukoc Biol* **82**(5): 1185-92.

Pizzoferrato, E., Y. Liu, A. Gambotto, M. J. Armstrong, M. T. Stang, W. E. Gooding, S. M. Alber, S. H. Shand, S. C. Watkins, W. J. Storkus and J. H. Yim (2004). Ectopic expression of interferon regulatory factor-1 promotes human breast cancer cell death and results in reduced expression of survivin. *Cancer Res* **64**(22): 8381-8.

Popov, N., M. Wanzel, M. Madiredjo, D. Zhang, R. Beijersbergen, R. Bernards, R. Moll, S. J. Elledge and M. Eilers (2007). The ubiquitin-specific protease USP28 is required for MYC stability. *Nat Cell Biol* **9**(7): 765-74.

Porta, C., R. Hadj-Slimane, M. Nejmeddine, M. Pampin, M. G. Tovey, L. Espert, S. Alvarez and M. K. Chelbi-Alix (2005). Interferons alpha and gamma induce p53-dependent and p53-independent apoptosis, respectively. *Oncogene* **24**(4): 605-15.

Poukka, H., U. Karvonen, O. A. Janne and J. J. Palvimo (2000). Covalent modification of the androgen receptor by small ubiquitin-like modifier 1 (SUMO-1). *Proc Natl Acad Sci U S A* **97**(26): 14145-50.

Preisler, H. D., S. Perambakam, B. Li, W. T. Hsu, P. Venugopal, S. Creech, S. Sivaraman and N. Tanaka (2001). Alterations in IRF1/IRF2 expression in acute myelogenous leukemia. *Am J Hematol* **68**(1): 23-31.

Prost, S., C. O. Bellamy, D. S. Cunningham and D. J. Harrison (1998). Altered DNA repair and dysregulation of p53 in IRF-1 null hepatocytes. *FASEB J* **12**(2): 181-8.

Punga, T., M. T. Bengoechea-Alonso and J. Ericsson (2006). Phosphorylation and ubiquitination of the transcription factor sterol regulatory element-binding protein-1 in response to DNA binding. *J Biol Chem* **281**(35): 25278-86.

Quelo, I., O. Akhouayri, J. Prud'homme and R. St-Arnaud (2004). GSK3 beta-dependent phosphorylation of the alpha NAC coactivator regulates its nuclear translocation and proteasome-mediated degradation. *Biochemistry* **43**(10): 2906-14.

Rahat, M. A., I. Chernichovski and N. Lahat (2001). Increased binding of IFN regulating factor 1 mediates the synergistic induction of CIITA by IFN-gamma and tumor necrosis factor-alpha in human thyroid carcinoma cells. *Int Immunol* **13**(11): 1423-32.

Ramsauer, K., M. Farlik, G. Zupkovitz, C. Seiser, A. Kroger, H. Hauser and T. Decker (2007). Distinct modes of action applied by transcription factors STAT1 and IRF1 to initiate transcription of the IFN-gamma-inducible gbp2 gene. *Proc Natl Acad Sci U S A* **104**(8): 2849-54.

Reid, G., M. R. Hubner, R. Metivier, H. Brand, S. Denger, D. Manu, J. Beaudouin, J. Ellenberg and F. Gannon (2003). Cyclic, proteasome-mediated turnover of unliganded and liganded ERalpha on responsive promoters is an integral feature of estrogen signaling. *Mol Cell* **11**(3): 695-707.

Reilly, C. M., S. Olgun, D. Goodwin, R. M. Gogal, Jr., A. Santo, J. W. Romesburg, S. A. Ahmed and G. S. Gilkeson (2006). Interferon regulatory factor-1 gene deletion decreases glomerulonephritis in MRL/lpr mice. *Eur J Immunol* **36**(5): 1296-308.

Reinehr, R., B. Gorg, A. Hongen and D. Haussinger (2004). CD95-tyrosine nitration inhibits hyperosmotic and CD95 ligand-induced CD95 activation in rat hepatocytes. *J Biol Chem* **279**(11): 10364-73.

Reis, L. F., H. Ruffner, G. Stark, M. Aguet and C. Weissmann (1994). Mice devoid of interferon regulatory factor 1 (IRF-1) show normal expression of type I interferon genes. *EMBO J* **13**(20): 4798-806.

Remoli, M. E., V. Gafa, E. Giacomini, M. Severa, R. Lande and E. M. Coccia (2007). IFN-beta modulates the response to TLR stimulation in human

DC: involvement of IFN regulatory factor-1 (IRF-1) in IL-27 gene expression. *Eur J Immunol* **37**(12): 3499-508.

Rocques, N., N. Abou Zeid, K. Sii-Felice, L. Lecoin, M. P. Felder-Schmittbuhl, A. Eychene and C. Pouponnot (2007). GSK-3-mediated phosphorylation enhances Maf-transforming activity. *Mol Cell* **28**(4): 584-97.

Rodionova, E., M. Conzelmann, E. Maraskovsky, M. Hess, M. Kirsch, T. Giese, A. D. Ho, M. Zoller, P. Dreger and T. Luft (2007). GSK-3 mediates differentiation and activation of proinflammatory dendritic cells. *Blood* **109**(4): 1584-92.

Romieu-Mourez, R., M. Solis, A. Nardin, D. Goubau, V. Baron-Bodo, R. Lin, B. Massie, M. Salcedo and J. Hiscott (2006). Distinct roles for IFN regulatory factor (IRF)-3 and IRF-7 in the activation of antitumor properties of human macrophages. *Cancer Res* **66**(21): 10576-85.

Ronco, L. V., A. Y. Karpova, M. Vidal and P. M. Howley (1998). Human papillomavirus 16 E6 oncoprotein binds to interferon regulatory factor-3 and inhibits its transcriptional activity. *Genes Dev* **12**(13): 2061-72.

Ruiz-Ruiz, C., C. Ruiz de Almodovar, A. Rodriguez, G. Ortiz-Ferron, J. M. Redondo and A. Lopez-Rivas (2004). The up-regulation of human caspase-8 by interferon-gamma in breast tumor cells requires the induction and action of the transcription factor interferon regulatory factor-1. *J Biol Chem* **279**(19): 19712-20.

Saito, H., S. Tada, K. Wakabayashi, N. Nakamoto, M. Takahashi, M. Nakamura, H. Ebinuma and H. Ishii (2002). The detection of IRF-1 promoter polymorphisms and their possible contribution to T helper 1 response in chronic hepatitis C. *J Interferon Cytokine Res* **22**(6): 693-700.

Sale, E. M. and G. J. Sale (2008). Protein kinase B: signalling roles and therapeutic targeting. *Cell Mol Life Sci* **65**(1): 113-27.

Salghetti, S. E., M. Muratani, H. Wijnen, B. Futcher and W. P. Tansey (2000). Functional overlap of sequences that activate transcription and signal ubiquitin-mediated proteolysis. *Proc Natl Acad Sci U S A* **97**(7): 3118-23.

Sanceau, J., D. D. Boyd, M. Seiki and B. Bauvois (2002). Interferons inhibit tumor necrosis factor-alpha-mediated matrix metalloproteinase-9 activation via interferon regulatory factor-1 binding competition with NF-kappa B. *J Biol Chem* **277**(38): 35766-75.

Sanceau, J., J. Hiscott, O. Delattre and J. Wietzerbin (2000). IFN-beta induces serine phosphorylation of Stat-1 in Ewing's sarcoma cells and mediates apoptosis via induction of IRF-1 and activation of caspase-7. *Oncogene* **19**(30): 3372-83.

Sanceau, J., T. Kaisho, T. Hirano and J. Wietzerbin (1995). Triggering of the human interleukin-6 gene by interferon-gamma and tumor necrosis factor-alpha in monocytic cells involves cooperation between interferon regulatory factor-1, NF kappa B, and Sp1 transcription factors. *J Biol Chem* **270**(46): 27920-31.

Sanda, T., S. Iida, S. Kayukawa and R. Ueda (2007). Induction of class II major histocompatibility complex expression in human multiple myeloma cells by retinoid. *Haematologica* **92**(1): 115-20.

Sato, M., H. Suemori, N. Hata, M. Asagiri, K. Ogasawara, K. Nakao, T. Nakaya, M. Katsuki, S. Noguchi, N. Tanaka and T. Taniguchi (2000). Distinct and essential roles of transcription factors IRF-3 and IRF-7 in response to viruses for IFN-alpha/beta gene induction. *Immunity* **13**(4): 539-48.

Saura, M., C. Zaragoza, C. Bao, A. McMillan and C. J. Lowenstein (1999). Interaction of interferon regulatory factor-1 and nuclear factor kappaB during activation of inducible nitric oxide synthase transcription. *J Mol Biol* **289**(3): 459-71.

Schaper, F., S. Kirchhoff, G. Posern, M. Koster, A. Oumard, R. Sharf, B. Z. Levi and H. Hauser (1998). Functional domains of interferon regulatory factor I (IRF-1). *Biochem J* **335 (Pt 1)**: 147-57.

Schlomann, U., S. Rathke-Hartlieb, S. Yamamoto, H. Jockusch and J. W. Bartsch (2000). Tumor necrosis factor alpha induces a metalloprotease-disintegrin, ADAM8 (CD 156): implications for neuron-glia interactions during neurodegeneration. *J Neurosci* **20**(21): 7964-71.

Schmitz, F., A. Heit, S. Guggemoos, A. Krug, J. Mages, M. Schiemann, H. Adler, I. Drexler, T. Haas, R. Lang and H. Wagner (2007). Interferon-regulatory-factor 1 controls Toll-like receptor 9-mediated IFN-beta production in myeloid dendritic cells. *Eur J Immunol* **37**(2): 315-27.

Schwartz, A. L. and A. Ciechanover (2009). Targeting proteins for destruction by the ubiquitin system: implications for human pathobiology. *Annu Rev Pharmacol Toxicol* **49**: 73-96.

Seet, B. T., I. Dikic, M. M. Zhou and T. Pawson (2006). Reading protein modifications with interaction domains. *Nat Rev Mol Cell Biol* **7**(7): 473-83.

Senaldi, G., C. L. Shaklee, J. Guo, L. Martin, T. Boone, T. W. Mak and T. R. Ulich (1999). Protection against the mortality associated with disease models mediated by TNF and IFN-gamma in mice lacking IFN regulatory factor-1. *J Immunol* **163**(12): 6820-6.

Seo, H. R., J. Kim, S. Bae, J. W. Soh and Y. S. Lee (2008). Cdk5-mediated phosphorylation of c-Myc on Ser-62 is essential in transcriptional activation of cyclin B1 by cyclin G1. *J Biol Chem* **283**(23): 15601-10.

Sgarbanti, M., A. Borsetti, N. Moscufo, M. C. Bellocchi, B. Ridolfi, F. Nappi, G. Marsili, G. Marziali, E. M. Coccia, B. Ensoli and A. Battistini (2002). Modulation of human immunodeficiency virus 1 replication by interferon regulatory factors. *J Exp Med* **195**(10): 1359-70.

Sgarbanti, M., A. L. Remoli, G. Marsili, B. Ridolfi, A. Borsetti, E. Perrotti, R. Orsatti, R. Ilari, L. Sernicola, E. Stellacci, B. Ensoli and A. Battistini (2008). IRF-1 is required for full NF-kappaB transcriptional activity at the human immunodeficiency virus type 1 long terminal repeat enhancer. *J Virol* **82**(7): 3632-41.

Shaffer, A. L., N. C. Emre, P. B. Romesser and L. M. Staudt (2009). IRF4: Immunity. Malignancy! Therapy? *Clin Cancer Res* **15**(9): 2954-61.

Shema, E., I. Tirosh, Y. Aylon, J. Huang, C. Ye, N. Moskovits, N. Raver-Shapira, N. Minsky, J. Pirngruber, G. Tarcic, P. Hublarova, L. Moyal, et al. (2008). The histone H2B-specific ubiquitin ligase RNF20/hBRE1 acts as a putative tumor suppressor through selective regulation of gene expression. *Genes Dev* **22**(19): 2664-76.

Shen, Y., M. Xia, J. Zhang, L. Xu, J. Yang, A. Chen, F. Miao, S. Ferrone and W. Xie (2009). IRF-1 and p65 mediate upregulation of constitutive HLA-A antigen expression by hepatocellular carcinoma cells. *Mol Immunol* **46**(10): 2045-53.

Shi, Y., Y. B. Zhang, Z. Zhao, J. Jiang, Q. Y. Zhang and J. F. Gui (2008). Molecular characterization and subcellular localization of Carassius auratus interferon regulatory factor-1. *Dev Comp Immunol* **32**(2): 134-46.

Shin, J. H., S. M. Kang, Y. S. Kim, D. H. Shin, J. Chang and S. K. Kim (2005). Identification of tumor suppressor loci on the long arm of chromosome 5 in pulmonary large cell neuroendocrine carcinoma. *Chest* **128**(4): 2999-3003.

Siegmund, B., J. A. Sennello, H. A. Lehr, G. Senaldi, C. A. Dinarello and G. Fantuzzi (2004). Frontline: interferon regulatory factor-1 as a protective gene in intestinal inflammation: role of TCR gamma delta T cells and interleukin-18-binding protein. *Eur J Immunol* **34**(9): 2356-64.

Sims, R. J., 3rd, E. K. Weihe, L. Zhu, S. O'Malley, J. V. Harriss and P. D. Gottlieb (2002). m-Bop, a repressor protein essential for cardiogenesis, interacts with skNAC, a heart- and muscle-specific transcription factor. *J Biol Chem* **277**(29): 26524-9.

Skaar, J. R., V. D'Angiolella, J. K. Pagan and M. Pagano (2009). SnapShot: F Box Proteins II. *Cell* **137**(7): 1358, 1358 e1.

Skowyra, D., K. L. Craig, M. Tyers, S. J. Elledge and J. W. Harper (1997). F-box proteins are receptors that recruit phosphorylated substrates to the SCF ubiquitin-ligase complex. *Cell* **91**(2): 209-19.

Sowa, M. E., E. J. Bennett, S. P. Gygi and J. W. Harper (2009). Defining the human deubiquitinating enzyme interaction landscape. *Cell* **138**(2): 389-403.

Spruck, C. H., H. Strohmaier, O. Sangfelt, H. M. Muller, M. Hubalek, E. Muller-Holzner, C. Marth, M. Widschwendter and S. I. Reed (2002). hCDC4 gene mutations in endometrial cancer. *Cancer Res* **62**(16): 4535-9.

Stevens, A. M. and L. Y. Yu-Lee (1992). The transcription factor interferon regulatory factor-1 is expressed during both early G1 and the G1/S transition in the prolactin-induced lymphocyte cell cycle. *Mol Endocrinol* **6**(12): 2236-43.

Streetz, K., B. Fregien, J. Plumpe, K. Korber, S. Kubicka, G. Sass, S. C. Bischoff, M. P. Manns, G. Tiegs and C. Trautwein (2001). Dissection of the intracellular pathways in hepatocytes suggests a role for Jun kinase and IFN regulatory factor-1 in Con A-induced liver failure. *J Immunol* **167**(1): 514-23.

Strohmaier, H., C. H. Spruck, P. Kaiser, K. A. Won, O. Sangfelt and S. I. Reed (2001). Human F-box protein hCdc4 targets cyclin E for proteolysis and is mutated in a breast cancer cell line. *Nature* **413**(6853): 316-22.

Su, Z. Z., D. Sarkar, L. Emdad, P. M. Barral and P. B. Fisher (2007). Central role of interferon regulatory factor-1 (IRF-1) in controlling retinoic acid inducible gene-I (RIG-I) expression. *J Cell Physiol* **213**(2): 502-10.

Sun, Q. H., J. P. Peng and H. F. Xia (2006). IFNgamma pretreatment sensitizes human choriocarcinoma cells to etoposide-induced apoptosis. *Mol Hum Reprod* **12**(2): 99-105.

Sundqvist, A., M. T. Bengoechea-Alonso, X. Ye, V. Lukiyanchuk, J. Jin, J. W. Harper and J. Ericsson (2005). Control of lipid metabolism by phosphorylation-dependent degradation of the SREBP family of transcription factors by SCF(Fbw7). *Cell Metab* **1**(6): 379-91.

Takano, Y., S. Adachi, M. Okuno, Y. Muto, T. Yoshioka, R. Matsushima-Nishiwaki, H. Tsurumi, K. Ito, S. L. Friedman, H. Moriwaki, S. Kojima and Y. Okano (2004). The RING finger protein, RNF8, interacts with retinoid X receptor alpha and enhances its transcription-stimulating activity. *J Biol Chem* **279**(18): 18926-34.

Takaoka, A., T. Tamura and T. Taniguchi (2008). Interferon regulatory factor family of transcription factors and regulation of oncogenesis. *Cancer Sci* **99**(3): 467-78.

Takaoka, A., H. Yanai, S. Kondo, G. Duncan, H. Negishi, T. Mizutani, S. Kano, K. Honda, Y. Ohba, T. W. Mak and T. Taniguchi (2005). Integral role of IRF-5 in the gene induction programme activated by Toll-like receptors. *Nature* **434**(7030): 243-9.

Tamura, G., S. Ogasawara, S. Nishizuka, K. Sakata, C. Maesawa, Y. Suzuki, M. Terashima, K. Saito and R. Satodate (1996a). Two distinct regions of deletion on the long arm of chromosome 5 in differentiated adenocarcinomas of the stomach. *Cancer Res* **56**(3): 612-5.

Tamura, T., S. Ueda, M. Yoshida, M. Matsuzaki, H. Mohri and T. Okubo (1996b). Interferon-gamma induces Ice gene expression and enhances cellular susceptibility to apoptosis in the U937 leukemia cell line. *Biochem Biophys Res Commun* **229**(1): 21-6.

Tanaka, N., M. Ishihara, M. S. Lamphier, H. Nozawa, T. Matsuyama, T. W. Mak, S. Aizawa, T. Tokino, M. Oren and T. Taniguchi (1996). Cooperation of the tumour suppressors IRF-1 and p53 in response to DNA damage. *Nature* **382**(6594): 816-8.

Tanaka, N., M. Ishihara and T. Taniguchi (1994). Suppression of c-myc or fosB-induced cell transformation by the transcription factor IRF-1. *Cancer Lett* **83**(1-2): 191-6.

Tanaka, N., T. Kawakami and T. Taniguchi (1993). Recognition DNA sequences of interferon regulatory factor 1 (IRF-1) and IRF-2, regulators of cell growth and the interferon system. *Mol Cell Biol* **13**(8): 4531-8.

Tang, X., S. Orlicky, Z. Lin, A. Willems, D. Neculai, D. Ceccarelli, F. Mercurio, B. H. Shilton, F. Sicheri and M. Tyers (2007). Suprafacial orientation of the SCFCdc4 dimer accommodates multiple geometries for substrate ubiquitination. *Cell* **129**(6): 1165-76.

Tansey, W. P. (2001). Transcriptional activation: risky business. *Genes Dev* **15**(9): 1045-50.

Ten, R. M., V. Blank, O. Le Bail, P. Kourilsky and A. Israel (1993). Two factors, IRF1 and KBF1/NF-kappa B, cooperate during induction of MHC class I gene expression by interferon alpha beta or Newcastle disease virus. *C R Acad Sci III* **316**(5): 496-501.

Tendler, D. S., C. Bao, T. Wang, E. L. Huang, E. A. Ratovitski, D. A. Pardoll and C. J. Lowenstein (2001). Intersection of interferon and hypoxia signal transduction pathways in nitric oxide-induced tumor apoptosis. *Cancer Res* **61**(9): 3682-8.

Testa, U., E. Stellacci, E. Pelosi, P. Sestili, M. Venditti, R. Orsatti, A. Fragale, E. Petrucci, L. Pasquini, F. Belardelli, L. Gabriele and A. Battistini (2004). Impaired myelopoiesis in mice devoid of interferon regulatory factor 1. *Leukemia* **18**(11): 1864-71.

Tetzlaff, M. T., W. Yu, M. Li, P. Zhang, M. Finegold, K. Mahon, J. W. Harper, R. J. Schwartz and S. J. Elledge (2004). Defective cardiovascular development and elevated cyclin E and Notch proteins in mice lacking the Fbw7 F-box protein. *Proc Natl Acad Sci U S A* **101**(10): 3338-45.

Thomas, D. and M. Tyers (2000). Transcriptional regulation: Kamikaze activators. *Curr Biol* **10**(9): R341-3.

Thomas, V., S. Samanta, C. Wu, N. Berliner and E. Fikrig (2005). Anaplasma phagocytophilum modulates gp91phox gene expression through altered interferon regulatory factor 1 and PU.1 levels and binding of CCAAT displacement protein. *Infect Immun* **73**(1): 208-18.

Tirard, M., O. F. Almeida, P. Hutzler, F. Melchior and T. M. Michaelidis (2007). Sumoylation and proteasomal activity determine the transactivation properties of the mineralocorticoid receptor. *Mol Cell Endocrinol* **268**(1-2): 20-9.

Tnani, M. and B. A. Bayard (1999). Evidence for IRF-1-dependent gene expression deficiency in interferon unresponsive HepG2 cells. *Biochim Biophys Acta* **1451**(1): 59-72.

Tomita, Y., V. Bilim, N. Hara, T. Kasahara and K. Takahashi (2003). Role of IRF-1 and caspase-7 in IFN-gamma enhancement of Fas-mediated apoptosis in ACHN renal cell carcinoma cells. *Int J Cancer* **104**(4): 400-8.

Tsai, C. C., J. I. Kai, W. C. Huang, C. Y. Wang, Y. Wang, C. L. Chen, Y. T. Fang, Y. S. Lin, R. Anderson, S. H. Chen, C. W. Tsao and C. F. Lin (2009). Glycogen synthase kinase-3beta facilitates IFN-gamma-induced STAT1 activation by regulating Src homology-2 domain-containing phosphatase 2. *J Immunol* **183**(2): 856-64.

Tsunematsu, R., K. Nakayama, Y. Oike, M. Nishiyama, N. Ishida, S. Hatakeyama, Y. Bessho, R. Kageyama, T. Suda and K. I. Nakayama (2004). Mouse Fbw7/Sel-10/Cdc4 is required for notch degradation during vascular development. *J Biol Chem* **279**(10): 9417-23.

Tsung, A., M. T. Stang, A. Ikeda, N. D. Critchlow, K. Izuishi, A. Nakao, M. H. Chan, G. Jeyabalan, J. H. Yim and D. A. Geller (2006). The transcription factor interferon regulatory factor-1 mediates liver damage during ischemia-reperfusion injury. *Am J Physiol Gastrointest Liver Physiol* **290**(6): G1261-8.

Tung, C. W. and S. Y. Ho (2008). Computational identification of ubiquitylation sites from protein sequences. *BMC Bioinformatics* **9**: 310.

Tzoanopoulos, D., M. Speletas, K. Arvanitidis, C. Veiopoulou, S. Kyriaki, G. Thyphronitis, P. Sideras, G. Kartalis and K. Ritis (2002). Low expression of interferon regulatory factor-1 and identification of novel

exons skipping in patients with chronic myeloid leukaemia. *Br J Haematol* **119**(1): 46-53.

Ubersax, J. A. and J. E. Ferrell, Jr. (2007). Mechanisms of specificity in protein phosphorylation. *Nat Rev Mol Cell Biol* **8**(7): 530-41.

Uchijima, M., E. Raz, D. A. Carson, T. Nagata and Y. Koide (2001). Identification of immunostimulatory DNA-induced genes by suppression subtractive hybridization. *Biochem Biophys Res Commun* **286**(4): 688-91.

Umegaki, N., K. Tamai, H. Nakano, R. Moritsugu, T. Yamazaki, K. Hanada, I. Katayama and Y. Kaneda (2007). Differential regulation of karyopherin alpha 2 expression by TGF-beta1 and IFN-gamma in normal human epidermal keratinocytes: evident contribution of KPNA2 for nuclear translocation of IRF-1. *J Invest Dermatol* **127**(6): 1456-64.

Upreti, M., S. Kumar and P. C. Rath (2004). Replacement of 198MQMDII203 of mouse IRF-1 by 197IPVEVV202 of human IRF-1 abrogates induction of IFN-beta, iNOS, and COX-2 gene expression by IRF-1. *Biochem Biophys Res Commun* **314**(3): 737-44.

Upreti, M. and P. C. Rath (2005). Expression and DNA binding activity of the recombinant interferon regulatory factor-1 (IRF-1) of mouse. *Mol Biol Rep* **32**(2): 103-16.

Viatour, P., E. Dejardin, M. Warnier, F. Lair, E. Claudio, F. Bureau, J. C. Marine, M. P. Merville, U. Maurer, D. Green, J. Piette, U. Siebenlist, et al. (2004). GSK3-mediated BCL-3 phosphorylation modulates its degradation and its oncogenicity. *Mol Cell* **16**(1): 35-45.

Vila-del Sol, V., C. Punzon and M. Fresno (2008). IFN-gamma-induced TNF-alpha expression is regulated by interferon regulatory factors 1 and 8 in mouse macrophages. *J Immunol* **181**(7): 4461-70.

von der Lehr, N., S. Johansson, S. Wu, F. Bahram, A. Castell, C. Cetinkaya, P. Hydbring, I. Weidung, K. Nakayama, K. I. Nakayama, O. Soderberg, T. K. Kerppola, et al. (2003). The F-box protein Skp2 participates in c-Myc proteosomal degradation and acts as a cofactor for c-Myc-regulated transcription. *Mol Cell* **11**(5): 1189-200.

von Mikecz, A. (2006). The nuclear ubiquitin-proteasome system. *J Cell Sci* **119**(Pt 10): 1977-84.

Wakefield, J. G., D. J. Stephens and J. M. Tavare (2003). A role for glycogen synthase kinase-3 in mitotic spindle dynamics and chromosome alignment. *J Cell Sci* **116**(Pt 4): 637-46.

Wang, I. M., J. C. Blanco, S. Y. Tsai, M. J. Tsai and K. Ozato (1996). Interferon regulatory factors and TFIIB cooperatively regulate interferon-responsive promoter activity in vivo and in vitro. *Mol Cell Biol* **16**(11): 6313-24.

Wang, J., Y. Peng, Y. W. Sun, H. He, S. Zhu, X. An, M. Li, M. C. Lin, B. Zou, H. H. Xia, B. Jiang, A. O. Chan, et al. (2006). All-trans retinoic acid induces XAF1 expression through an interferon regulatory factor-1 element in colon cancer. *Gastroenterology* **130**(3): 747-58.

Wang, Q., X. Wang, A. Hernandez, M. R. Hellmich, Z. Gatalica and B. M. Evers (2002). Regulation of TRAIL expression by the phosphatidylinositol 3-kinase/Akt/GSK-3 pathway in human colon cancer cells. *J Biol Chem* **277**(39): 36602-10.

Wang, Y., W. C. Huang, C. Y. Wang, C. C. Tsai, C. L. Chen, Y. T. Chang, J. I. Kai and C. F. Lin (2009). Inhibiting glycogen synthase kinase-3 reduces endotoxaemic acute renal failure by down-regulating inflammation and renal cell apoptosis. *Br J Pharmacol* **157**(6): 1004-13.

Watanabe, N., J. Sakakibara, A. G. Hovanessian, T. Taniguchi and T. Fujita (1991). Activation of IFN-beta element by IRF-1 requires a posttranslational event in addition to IRF-1 synthesis. *Nucleic Acids Res* **19**(16): 4421-8.

Watanabe, Y., O. Suzuki, T. Haruyama and T. Akaike (2003). Interferon-gamma induces reactive oxygen species and endoplasmic reticulum stress at the hepatic apoptosis. *J Cell Biochem* **89**(2): 244-53.

Watson, G. A., P. E. Queiroz de Oliveira, M. T. Stang, M. J. Armstrong, W. E. Gooding, S. F. Kuan, J. H. Yim and S. J. Hughes (2006). Ad-IRF-1 induces apoptosis in esophageal adenocarcinoma. *Neoplasia* **8**(1): 31-7.

Weake, V. M. and J. L. Workman (2008). Histone ubiquitination: triggering gene activity. *Mol Cell* **29**(6): 653-63.

Wei, W., J. Jin, S. Schlisio, J. W. Harper and W. G. Kaelin, Jr. (2005). The v-Jun point mutation allows c-Jun to escape GSK3-dependent recognition and destruction by the Fbw7 ubiquitin ligase. *Cancer Cell* **8**(1): 25-33.

Welcker, M. and B. E. Clurman (2007). Fbw7/hCDC4 dimerization regulates its substrate interactions. *Cell Div* **2**: 7.

Welcker, M. and B. E. Clurman (2008). FBW7 ubiquitin ligase: a tumour suppressor at the crossroads of cell division, growth and differentiation. *Nat Rev Cancer* **8**(2): 83-93.

Welcker, M., A. Orian, J. Jin, J. E. Grim, J. W. Harper, R. N. Eisenman and B. E. Clurman (2004). The Fbw7 tumor suppressor regulates glycogen synthase kinase 3 phosphorylation-dependent c-Myc protein degradation. *Proc Natl Acad Sci U S A* **101**(24): 9085-90.

White, L. C., K. L. Wright, N. J. Felix, H. Ruffner, L. F. Reis, R. Pine and J. P. Ting (1996). Regulation of LMP2 and TAP1 genes by IRF-1 explains the paucity of CD8+ T cells in IRF-1-/- mice. *Immunity* **5**(4): 365-76.

Williams, C., M. van den Berg, R. R. Sprenger and B. Distel (2007). A conserved cysteine is essential for Pex4p-dependent ubiquitination of the peroxisomal import receptor Pex5p. *J Biol Chem* **282**(31): 22534-43.

Willman, C. L., C. E. Sever, M. G. Pallavicini, H. Harada, N. Tanaka, M. L. Slovak, H. Yamamoto, K. Harada, T. C. Meeker, A. F. List and et al. (1993). Deletion of IRF-1, mapping to chromosome 5q31.1, in human leukemia and preleukemic myelodysplasia. *Science* **259**(5097): 968-71.

Woodgett, J. R. (1990). Molecular cloning and expression of glycogen synthase kinase-3/factor A. *EMBO J* **9**(8): 2431-8.

Wormald, S., D. J. Hilton, G. K. Smyth and T. P. Speed (2006). Proximal genomic localization of STAT1 binding and regulated transcriptional activity. *BMC Genomics* **7**: 254.

Wu, R. C., Q. Feng, D. M. Lonard and B. W. O'Malley (2007). SRC-3 coactivator functional lifetime is regulated by a phospho-dependent ubiquitin time clock. *Cell* **129**(6): 1125-40.

Xie, R., A. J. van Wijnen, C. van Der Meijden, M. X. Luong, J. L. Stein and G. S. Stein (2001). The cell cycle control element of histone H4 gene transcription is maximally responsive to interferon regulatory factor pairs IRF-1/IRF-3 and IRF-1/IRF-7. *J Biol Chem* **276**(21): 18624-32.

Xie, R. L., S. Gupta, A. Miele, D. Shiffman, J. L. Stein, G. S. Stein and A. J. van Wijnen (2003). The tumor suppressor interferon regulatory factor 1 interferes with SP1 activation to repress the human CDK2 promoter. *J Biol Chem* **278**(29): 26589-96.

Xu, C., N. G. Kim and B. M. Gumbiner (2009a). Regulation of protein stability by GSK3 mediated phosphorylation. *Cell Cycle* **8**(24): 4032-9.

Xu, K., H. Shimelis, D. E. Linn, R. Jiang, X. Yang, F. Sun, Z. Guo, H. Chen, W. Li, X. Kong, J. Melamed, S. Fang, et al. (2009b). Regulation of androgen receptor transcriptional activity and specificity by RNF6-induced ubiquitination. *Cancer Cell* **15**(4): 270-82.

Xu, Y., J. A. Harton and B. D. Smith (2008). CIITA mediates interferon-gamma repression of collagen transcription through phosphorylation-dependent interactions with co-repressor molecules. *J Biol Chem* **283**(3): 1243-56.

Yamagata, K., H. Daitoku, Y. Takahashi, K. Namiki, K. Hisatake, K. Kako, H. Mukai, Y. Kasuya and A. Fukamizu (2008). Arginine methylation of FOXO transcription factors inhibits their phosphorylation by Akt. *Mol Cell* **32**(2): 221-31.

Yang, C. H., L. Wei, S. R. Pfeffer, Z. Du, A. Murti, W. J. Valentine, Y. Zheng and L. M. Pfeffer (2007). Identification of CXCL11 as a STAT3-dependent gene induced by IFN. *J Immunol* **178**(2): 986-92.

Yang, C. S., C. Yu, H. C. Chuang, C. W. Chang, G. D. Chang, T. P. Yao and H. Chen (2005). FBW2 targets GCMa to the ubiquitin-proteasome degradation system. *J Biol Chem* **280**(11): 10083-90.

Yang, W. H., J. E. Kim, H. W. Nam, J. W. Ju, H. S. Kim, Y. S. Kim and J. W. Cho (2006). Modification of p53 with O-linked N-acetylglucosamine regulates p53 activity and stability. *Nat Cell Biol* **8**(10): 1074-83.

Yang, X. J. and E. Seto (2008). Lysine acetylation: codified crosstalk with other posttranslational modifications. *Mol Cell* **31**(4): 449-61.

Yeh, E., M. Cunningham, H. Arnold, D. Chasse, T. Monteith, G. Ivaldi, W. C. Hahn, P. T. Stukenberg, S. Shenolikar, T. Uchida, C. M. Counter, J. R. Nevins, et al. (2004). A signalling pathway controlling c-Myc degradation that impacts oncogenic transformation of human cells. *Nat Cell Biol* **6**(4): 308-18.

Yi, P., R. C. Wu, J. Sandquist, J. Wong, S. Y. Tsai, M. J. Tsai, A. R. Means and B. W. O'Malley (2005). Peptidyl-prolyl isomerase 1 (Pin1) serves as a coactivator of steroid receptor by regulating the activity of phosphorylated steroid receptor coactivator 3 (SRC-3/AIB1). *Mol Cell Biol* **25**(21): 9687-99.

Yie, J., K. Senger and D. Thanos (1999). Mechanism by which the IFN-beta enhanceosome activates transcription. *Proc Natl Acad Sci U S A* **96**(23): 13108-13.

Yim, J. H., S. J. Wu, M. J. Casey, J. A. Norton and G. M. Doherty (1997). IFN regulatory factor-1 gene transfer into an aggressive, nonimmunogenic sarcoma suppresses the malignant phenotype and enhances immunogenicity in syngeneic mice. *J Immunol* **158**(3): 1284-92.

Yoshida, K., K. Yamamoto, T. Kohno, N. Hironaka, K. Yasui, C. Kojima, H. Mukae, J. Kadota, S. Suzuki, K. Honma, S. Kohno and T. Matsuyama (2005). Active repression of IFN regulatory factor-1-mediated transactivation by IFN regulatory factor-4. *Int Immunol* **17**(11): 1463-71.

Yost, C., M. Torres, J. R. Miller, E. Huang, D. Kimelman and R. T. Moon (1996). The axis-inducing activity, stability, and subcellular distribution of beta-catenin is regulated in Xenopus embryos by glycogen synthase kinase 3. *Genes Dev* **10**(12): 1443-54.

Yuskaitis, C. J. and R. S. Jope (2009). Glycogen synthase kinase-3 regulates microglial migration, inflammation, and inflammation-induced neurotoxicity. *Cell Signal* **21**(2): 264-73.

Zhang, D., K. Zaugg, T. W. Mak and S. J. Elledge (2006). A role for the deubiquitinating enzyme USP28 in control of the DNA-damage response. *Cell* **126**(3): 529-42.

Zhang, S., K. Thomas, J. C. Blanco, C. A. Salkowski and S. N. Vogel (2002). The role of the interferon regulatory factors, IRF-1 and IRF-2, in LPS-induced cyclooxygenase-2 (COX-2) expression in vivo and in vitro. *J Endotoxin Res* **8**(5): 379-88.

Zhang, W. and D. M. Koepp (2006). Fbw7 isoform interaction contributes to cyclin E proteolysis. *Mol Cancer Res* **4**(12): 935-43.

Zhou, Y., S. Wang, A. Gobl and K. Oberg (2000). The interferon-alpha regulation of interferon regulatory factor 1 (IRF-1) and IRF-2 has therapeutic implications in carcinoid tumors. *Ann Oncol* **11**(6): 707-14.

Zhu, Y., B. Singh, S. Hewitt, A. Liu, B. Gomez, A. Wang and R. Clarke (2006). Expression patterns among interferon regulatory factor-1, human X-box binding protein-1, nuclear factor kappa B, nucleophosmin, estrogen receptor-alpha and progesterone receptor proteins in breast cancer tissue microarrays. *Int J Oncol* **28**(1): 67-76.

Ziegler-Heitbrock, L., M. Lotzerich, A. Schaefer, T. Werner, M. Frankenberger and E. Benkhart (2003). IFN-alpha induces the human IL-10 gene by recruiting both IFN regulatory factor 1 and Stat3. *J Immunol* **171**(1): 285-90.

Zimring, J. C., S. Goodbourn and M. K. Offermann (1998). Human herpesvirus 8 encodes an interferon regulatory factor (IRF) homolog that represses IRF-1-mediated transcription. *J Virol* **72**(1): 701-7.

1.6.1. Glycogen Synthase Kinase 3

Glycogen Synthase Kinase 3 is a ubiquitously expressed serine / threonine kinase. GSK3 exits as two isoforms (α/β) encoded by separate genes. GSK3α/β exhibit very high homology in their kinase domains, but are divergent elsewhere (Woodgett 1990). Studies in mice devoid of each isoform suggest specific functions, as the GSK3α is not able to compensate for the loss of GSK3β, leading to early embryonic lethality. The $GSK3\alpha^{-/-}$ mice are viable, but demonstrate a different phenotype to the $GSK3\beta^{-/-}$ mice. The regulation and substrate specificity of the two isoforms is also divergent (Liang and Chuang 2007).

GSK3 regulates the activity of a number of its substrates, many of which are crucial regulator of cell physiology. As such the activity of GSK3 is under tight control. Most of the control is exerted post-translationally. The best studied regulatory modification of GSK3 is phosphorylation of Ser^{9} in GSK3β and Ser^{21} in GSK3α. Phosphorylation of these residues promotes the formation of a pseudosubstrate, which blocks the kinase domain of GSK3 and prevents phosphorylation of substrates A number of kinases have been shown to phosphorylate $Ser^{9/21}$, including PKA, PKB, and PKC as such signalling cascades are able to regulate the activity of GSK3 (Frame and Cohen 2001). Tyrosine phosphorylation of Tyr^{216} (GSK3β) and Tyr^{279} (GSK3α) has the opposite effect and is important for the kinase activity of GSK3. It is not yet known which kinases modulate tyrosine phosphorylation of GSK3 (Frame and Cohen 2001). In addition to post translational modification, protein-protein interactions with GSK3 also regulate its activity. During Wnt signalling, interaction with FRAT (Frequently Rearranged in T cell Lymphoma) prevents GSK3β from